

THE MINOR PLANET BULLETIN

BULLETIN OF THE MINOR PLANETS SECTION OF THE ASSOCIATION OF LUNAR AND PLANETARY OBSERVERS

VOLUME 51, NUMBER 4, A.D. 2024 OCTOBER-DECEMBER

299.

LIGHTCURVE FOR KORONIS FAMILY MEMBER (1482) SEBASTIANA

Dimitrios-Vasileios Zora, Devin Ramos, Francis P. Wilkin
 Union College
 807 Union St., Schenectady, NY 12308
 zorad@union.edu

(Received: 2024 July 10 Revised: 2024 August 7)

We present a lightcurve for (1482) Sebastiana observed in R in 2023 October. Our measured period of 10.484 ± 0.006 h agrees with the previously measured 10.489 ± 0.003 h (Slivan et al., 2008).

(1482) Sebastiana was chosen to continue our study of Koronis family objects, in order to improve the sample completeness (Slivan et al., 2023). It was listed as a target of interest for shape/spin solutions on the koronisfamily.com webtool (Slivan, 2003) and has a definitive published period of 10.489 ± 0.003 h (Slivan et al., 2008).

Sebastiana was observed at the Union College Observatory (UCO) in Schenectady, totaling four observation sessions that span most of the published period. UCO houses a 20" (0.5-m) Ritchey-Chretien reflector. We captured our images using an SBIG STXL 11002 CCD camera with 4008×2672 9- μ m pixels using an R filter. The details of each night are outlined in Table I.

UT date 2023	α (°)	Data Span (h)	Exp. Time (s)
Oct 3	5.8	6.8	240
Oct 13	2.0	1.6	240
Oct 24	3.1	1.5	180
Oct 25	3.6	1.9	180

Table I: Nightly observing information. Columns are: UT date at lightcurve mid-time, solar phase angle α , data span and image exposure time.

Sebastiana increased and then decreased in mean apparent brightness over time. This is due to the solar phase angle, which reached a minimum during our observation period, as reflected by the solar phase angle in Table II. The minimum was on UT 2023 October 18.

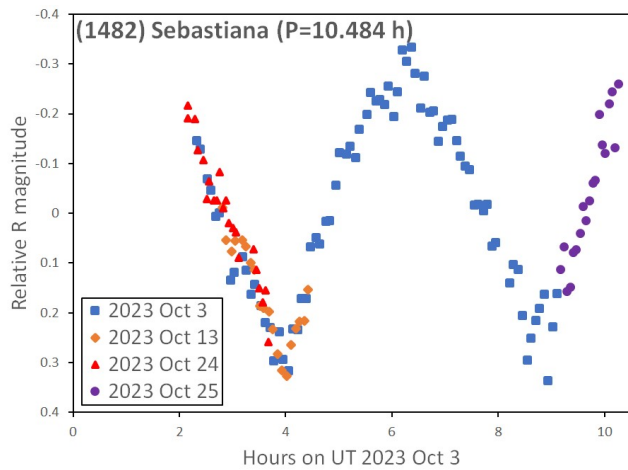
We performed photometry with *AstroImageJ* (Collins et al., 2017). In order to fold the data in a single lightcurve we corrected for light travel time, unit distance and solar phase angle using ephemerides from JPL Horizons (JPL, 2024).

To ascertain the period of Sebastiana, we started from the published result of 10.489 ± 0.003 h (Slivan et al., 2008), which unambiguously allows us to determine the number of half-turns, so that the local minima on the first two nights can be associated. Using the data from the nights of October 3, 13 and 24, we adjusted the period so that it better fits our data, with a result of 10.484 ± 0.006 h. This value agrees with the previously published period. Afterwards, we adjusted these three nights vertically so they produce a self-consistent composite.

However, the night of October 25 was more challenging to place vertically, considering that there are no overlapping UCO data to compare it to. In order to correctly shift this night for presentation purposes, we used the publicly available data of the Asteroid Terrestrial-impact Last Alert System (ATLAS) database (Tonry et al., 2018). These data were obtained from the W68 observatory between UT 2023 July 1 and UT 2023 November 13, in the *o* filter (orange, 560-820 nm). This dataset went through the same corrections as the UCO data. The ATLAS data were used as a template to shift magnitude values from the individual night to produce our final composite lightcurve. The ATLAS data are not shown.

Number	Name	yyyy mm/dd	Phase	L_{PAB}	B_{PAB}	Period(h)	P.E.	Amp	A.E.	Grp
1482	Sebastiana	2023 10/3-10/25	*5.8, 3.6	23	-3	10.484	0.006	0.65	0.03	Kor

Table II. Observing circumstances and results. The phase angle is given for the first and last date. If preceded by an asterisk, the phase angle reached an extremum during the period. L_{PAB} and B_{PAB} are the approximate phase angle bisector longitude/latitude at mid-date (see Harris et al., 1984). Grp is the asteroid family/group (Warner et al., 2009).



Acknowledgments

We thank Dr. S. Slivan for his helpful suggestions and N. Das and L. McLaughlin for assistance with the observations.

References

Collins, K.A.; Kielkopf, J.F.; Stassun, K.G.; Hessman, F.V. (2017). "AstroImageJ: Image Processing and Photometric Extraction for Ultra-precise Astronomical Light Curves." *Astronomical Journal* **153**, 77-89.

Harris, A.W.; Young, J.W.; Scaltriti, F.; Zappala, V. (1984). "Lightcurves and phase relations of the asteroids 82 Alkmene and 444 Gyptis." *Icarus* **57**, 251-258.

JPL (2024). "Horizons System." <https://ssd.jpl.nasa.gov/horizons/app.html#/>

Slivan, S.M. (2003). "A Web-based tool to calculate observability of Koronis program asteroids." *Minor Planet Bull.* **30**, 71-72.

Slivan, S.M.; Binzel, R.P.; Boroumand, S.C.; Pan, M.W.; Simpson, C.M.; Tanabe, J.T.; Villastrigo, R.M.; Yen, L.L.; Ditteon, R.P.; Pray, D.P.; Stephens, R.D. (2008). "Rotation rates in the Koronis family, complete to $H \approx 11.2$." *Icarus* **195**, 226-276.

Slivan, S.M.; Hosek Jr., M.; Kurzner, M.; Sokol, A.; Maynard, S.; Payne, A.V.; Radford, A.; Springmann, A.; Binzel, R.P.; Wilkin, F.P.; Mailhot, E.A.; Midkiff, A.H.; Russell, A.; Stephens, R.D.; Gardiner, V.; Reichart, D.E.; Haislip, J.; LaCluyze, A.; Behrend, R.; Roy, R. (2023). "Spin vectors in the Koronis family: IV. Completing the sample of its largest members after 35 years of study." *Icarus* **394**, A115397.

Tonry, J.L.; Denneau, L.; Heinze, A.N.; Stalder, B.; Smith, K.W.; Smartt, S.J.; Stubbs, C.W.; Weiland, H.J.; Rest, A. (2018). "ATLAS: A High-cadence All-sky Survey System." *PASP* **130**, 064505.

Warner, B.D.; Harris, A.W.; Pravec, P. (2009). "The Asteroid Lightcurve Database." *Icarus* **202**, 134-146. <http://www.minorplanet.info/lightcurvedatabase.html>

LIGHTCURVE AND ROTATION PERIOD FOR 1417 WALINSKIA

Melissa Hayes-Gehrke, Juan Placido-Reyes,
Daniel Villano-Herrera, Ava Lombardo, Kaela Coil,
Jonathan Kitching, Brendan Bauer, James van Doorn,
Daniel Bravo-Palacio, Cyann Jordanel, Alyssa Mazzone,
Eric Jiang, Elizabeth Bonilla
University of Maryland, College Park, Maryland, 20742 USA
mhayesge@umd.edu

Stephen M. Brincat
Flarestar Observatory
San Gwann SGN 3160, MALTA

Charles Galdies
Institute of Earth Systems, University of Malta,
Msida MSD 2080, MALTA
Znith Astronomy Observatory, Naxxar, MALTA
charles.galdies@um.edu.mt

(Received: 2024 June 3)

Photometric observations of asteroid 1417 Walinskia were conducted from 2024 April 02 to 2024 April 16. The aim of the observations was to determine both the rotation period and the lightcurve of 1417 Walinskia. The rotation period found was: $16.5316 \text{ h} \pm 0.0132 \text{ h}$.

1417 Walinskia is a main-belt asteroid that was first observed on 1937 April 01 by Karl Reinmuth in Heidelberg, Germany. Walinskia has a diameter of 16.874 km and an absolute magnitude of 11.27. The asteroid has a semimajor axis of 2.973 AU, an eccentricity of 0.078, and an orbital period of 5.13 years (JPL, 2016).

Dr. Charles Galdies observed 1417 Walinskia from 2024 March 06 to 2024 March 07 at the Znith Astronomy Observatory using Sequence Generator Pro service. The software was used to remotely control a telescope located in Naxxar, Malta (Znith Astronomy Observatory, 2024). All images taken of 1417 Walinskia were completed with a 360-s exposure time.

Students at the University of Maryland observed 1417 Walinskia from 2024 April 02 to 2024 April 16 using the iTelescope service. The software was used to remotely control a telescope located in the Great Basin Desert in Utah, USA (iTelescope Support Document, 2024). All images taken of 1417 Walinskia were completed with a 300-s exposure time and taken in sets of 5 images at a time.

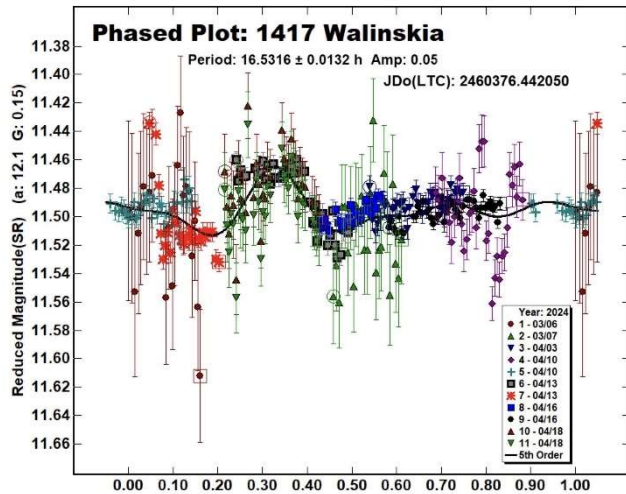
Dr. Stephen Brincat observed the asteroid on 2024 April 18 at the Flarestar Observatory using the Sequence Generator Pro service. The software was used to remotely control a telescope located in San Gwann, Malta (Flarestar, 2024). All images taken of 1417 Walinskia were completed with a 300-s exposure time.

The data were processed by the University of Maryland authors using the *MPO Canopus* software (Warner, 2019), which helped us determine the differential magnitude of the asteroid by utilizing comparison stars and aperture photometry.

Number	Name	yyyy mm/dd	Phase	L _{PAB}	B _{PAB}	Period(h)	P.E.	Amp	A.E.	Grp
1417	Walinskia	2024 4/02-4/16	*4.5, 5.8	196.7	10.2	16.5316	0.0132	0.05	0.05	MBA

Table I. Observing circumstances and results. The phase angle is given for the first and last date. If preceded by an asterisk, the phase angle reached an extrema during the period. L_{PAB} and B_{PAB} are the approximate phase angle bisector longitude/latitude at mid-date range (see Harris et al., 1984). Grp is the asteroid family/group (Warner et al., 2009).

Previous observations of 1417 Walinskia have presented differing results. A look into the Asteroid Lightcurve Database shows an observation from Behrend (2018web) of the asteroid with a listed period of 2.93 h (Warner et al, 2009). Another observation from Fornas et al. (2023) reported that no period was observable for 1417 Walinskia. In our observations, we found a period of $16.5316 \text{ h} \pm 0.0132 \text{ h}$.



This period was obtained by finding the joint zero points for all nights of observations and conducting a Fourier analysis on all nights of data. Despite generating this period, we are not certain about the validity of the period due to how noisy the lightcurve obtained is and the overall shape of it. The lightcurve only has a single peak before shortening to an almost horizontal line. Using a smaller period for the data yielded a more horizontal lightcurve akin to those for spherical asteroids, which were not convincing for 1417 Walinskia. As such we settled on a period of 16.5316 h, although we do recommend further observations into the asteroid before fully confirming its rotation period.

Acknowledgements

The University of Maryland authors would like to thank the Department of Astronomy of the University of Maryland, College Park for making funding possible for using iTelescope. The authors would also like to credit the creators of the *MPO Canopus* (Warner, 2019) and *DS9* platforms which were used for image-viewing and lightcurve analysis.

References

- Behrend, R. (2018web, January 18). Courbes de rotation d'astéroïdes et de comètes, Cdr Courbes de Luminosité d'étoiles variables régulières, *CDL*. CdR&CdL: Courbe de rotation et luminosité d'astéroïdes, de comètes et d'étoiles variables. <https://obswww.unige.ch/~behrend/page4cou.html#001417>
- Fornas, G.; Huet, F.; Arce, E.; Fornas, A. (2023). "Lightcurve Analysis for Sixteen Main-Belt Asteroids." *The Minor Planet Bulletin* **50**, 183–188. <https://ui.adsabs.harvard.edu/abs/2023MPBu...50..183F/abstract>
- Flarestar. (2024). *Flarestar Observatory-MPC:171*. Weebly. <https://flarestar.weebly.com/observatory.html>
- Harris, A.W.; Young, J.W.; Scaltriti, F.; Zappala, V. (1984). "Lightcurves and phase relations of asteroids 82 Alkmene and 444 Gyptis." *Icarus* **57**, 251-258.
- iTelescope Support Document (2024). *Telescope 21*. Support. <https://support.itelescope.net/support/solutions/articles/231906-telescope-21>
- JPL (2016). Small Body Database Search Engine. http://ssd.jpl.nasa.gov/sbdb_query.cgi
- Warner, B.D.; Harris, A.W.; Pravec, P. (2009). "The Asteroid Lightcurve Database." *Icarus* **202**, 134-146. Updated 2016 Sep. <https://minorplanet.info/php/lcdbsummaryquery.php>
- Warner, B.D. (2019). MPO Software, MPO Canopus v 10.8.6.20. Bdw Publishing, <http://minorplanetobserver.com>
- Znith Astronomy Observatory (2024). *Znith Astronomy Observatory. Malta*. Blogspot. <https://znith-observatory.blogspot.com/>

**LIGHTCURVE AND ROTATION PERIOD OF
1238 PREDAPPIA**

Frederick Pilcher
Organ Mesa Observatory (G50)
4438 Organ Mesa Loop
Las Cruces, NM 88011 USA
fpilcher35@gmail.com

Jesús Delgado Casal
Observatorio Nuevos Horizontales (Z73)
Calle Hermanos Quintero 17
Camas (Sevilla - SPAIN) CP 41900

Julian Oey
Blue Mountains Observatory (Q68)
94 Rawson Pde. Leura, NSW, AUSTRALIA

(Received: 2024 May 21 Revised: 2024 June 11)

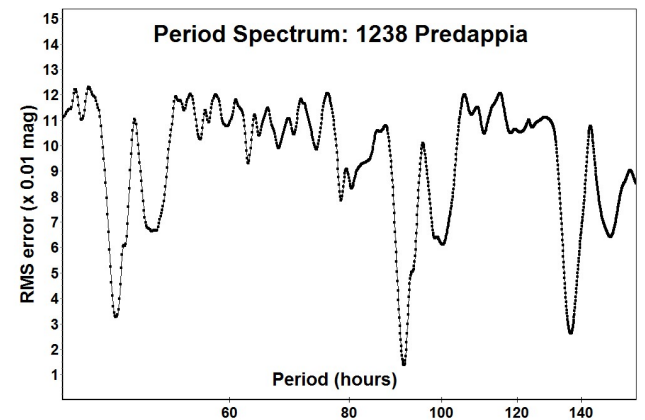
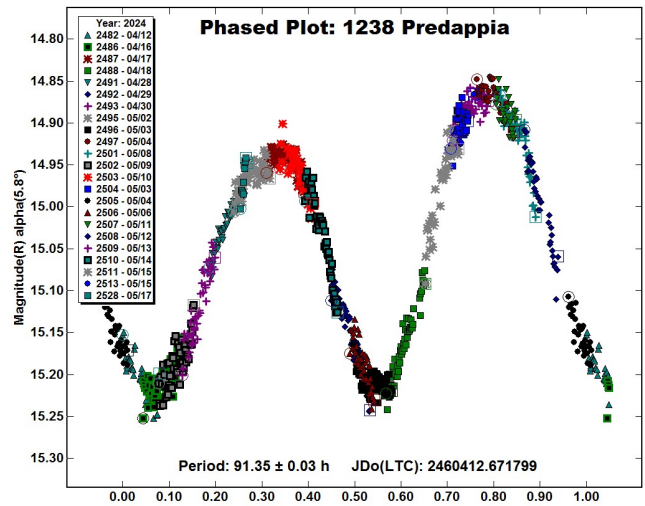
For 1238 Predappia we find a synodic rotation period of 91.35 ± 0.03 hours, amplitude 0.36 ± 0.03 magnitudes near celestial longitude 212° .

The observations by Pilcher to produce the results reported in this paper were made at the Organ Mesa Observatory with a Meade 35-cm LX200 GPS Schmidt-Cassegrain, SBIG STL-1001E CCD, 60 to 120 second exposures, unguided, clear filter. Observations by Delgado are with an 11-inch Celestron Schmidt-Cassegrain, Atik 4.14 EX CCD, 60 to 120 second exposures. Observations by Oey are with a 0.35-m f/5.9 Schmidt-Cassegrain, SBIG STT 1603 CCD, 120 second exposures.

Image measurement and lightcurve construction were with *MPO Canopus* software with calibration star magnitudes for solar colored stars from the CMC15 catalog reduced to the Cousins R band. To reduce the number of data points on the lightcurves and make them easier to read, data points have been binned in sets of 3 with maximum time difference 5 minutes.

1238 Predappia. The Asteroid Lightcurve Database (Warner et al., 2009) lists two previous rotation period determinations. Warner (2006) found a period of 8.94 hours, amplitude 0.03 magnitudes, phase angle bisector celestial longitude 125° . Hayes-Gehrke et al. (2015) published a period of 6.13 hours, amplitude 0.05 magnitudes near phase angle bisector celestial longitude 175° , and state that their data are insufficient to claim their 6.13-hour period is definitive.

New observations obtained on 22 sessions 2024 Apr. 12 - May 17 near celestial longitude 212° provide an excellent fit to an asymmetric bimodal lightcurve with synodic period 91.35 ± 0.03 hours and amplitude 0.36 ± 0.03 magnitudes. The period spectrum between 40 hours and 160 hours shows the available data can satisfy no period other than 91.35 hours.



Discussion: The 8.9-hour period by Warner and the very uncertain 6.13-hour period by Hayes-Gehrke et al. are now definitively ruled out. The 0.03 magnitude amplitude found by Warner (2006) at celestial longitude 125° is informative. The amplitude found in the current study near celestial longitude 212° , approximately a right angle from 125° , is much greater. Hence celestial longitude 125° is at near polar aspect and celestial longitude 212° is at near equatorial aspect and 0.36 magnitudes is close to the maximum amplitude possible.

References

Harris, A.W.; Young, J.W.; Scaltriti, F.; Zappala, V. (1984). "Lightcurves and phase relations of the asteroids 82 Alkmene and 444 Gyptis." *Icarus* **57**, 251-258.

Hayes-Gehrke, M.N.; Chuchuva, D.; Kumthekar, A.; Modica, A.; Higgins, A.; Gmurezyk, B.; Garcia, W.; Argueta, L.; Litz, P. (2015). "Lightcurve analysis for 1238 Predappia." *Minor Planet Bull.* **42**, 240.

Number	Name	yyyy/mm/dd	Phase	L _{PAB}	B _{PAB}	Period(h)	P.E	Amp	A.E.
1238	Predappia	2024/04/12-2024/05/17	* 5.9 - 10.4	212.5	5.0	91.35	0.03	0.36	0.03

Table I. Observing circumstances and results. The phase angle is given for the first and last date. Preceded by an asterisk indicates the phase angle reached a minimum during the period. L_{PAB} and B_{PAB} are the approximate phase angle bisector longitude and latitude at mid-date range (see Harris et al., 1984).

Warner, B.D. (2006). "Asteroid lightcurve analysis at the Palmer Divide Observatory - late 2005 and early 2006." *Minor Planet Bull.* **33**, 58-62.

Warner, B.D.; Harris, A.W.; Pravec, P. (2009). "The Asteroid Lightcurve Database." *Icarus* **202**, 134-146. Updated 2023 Oct. <http://www.minorplanet.info/lightcurvedatabase.html>

AN APPEAL FOR PHOTOMETRIC OBSERVATIONS OF 887 ALINDA

Frederick Pilcher
Organ Mesa Observatory (G50)
4438 Organ Mesa Loop
Las Cruces, NM 88011 USA
fpilcher35@gmail.com

(Received: 2024 July 5)

The Amor-type minor planet 887 Alinda will be brighter than magnitude 15 for six months 2024 October through 2025 March, during which interval it will travel about 1/3 of the way across the sky, becoming brightest 2025 January 13 at magnitude 9.0. Lightcurves obtained through this interval will enable reliable determinations of rotation period, spin axis, possible tumbling behavior, and shape.

This writer is pleased to announce an extended close approach of the Amor-type minor planet to Earth 2024 October - 2025 March, its first since 1975. Throughout this six-month interval this object will be magnitude 15.0 or brighter, becoming brightest 2025 January 13 at magnitude 9.0. Photometric observations throughout the full six-month interval during which time the object moves prograde in right ascension from 3h to 11h, should be sufficient to enable reliable and accurate determinations of its rotation period, spin axis, shape, and possible tumbling behavior. A five-day geocentric ephemeris is included to enable observers to plan observations. This writer also volunteers to collect all observations made at the coming close approach and make them available to interested workers for detailed analysis.

There are two previously published rotation periods, neither definitive. Dunlap and Taylor (1979) based on lightcurves obtained in the years 1973-1974 obtained a period of 73.97 hours. Behrend (2020web) based on lightcurves obtained in the year 2020 obtained a period of 28.41 hours. We hope that observations obtained early in the coming apparition will provide an approximate but definitive rotation period that can be reported to all participating observers to plan subsequent observations.

Elements from: (MPCORB)
File prepared: 2011 Sept. 13
Planet: 887 Alinda

DATE	ET	RA (2000)	DEC (2000)	Mv	Sun	Earth	Phase	Elon
2024-Sep-26	0.0	2h 56.75m	- 6° 29.6'	15.2	1.571	0.675	25.3	138.0
2024-Oct- 1	0.0	3h 1.54m	- 7° 38.4'	14.9	1.533	0.622	24.5	140.5
2024-Oct- 6	0.0	3h 5.88m	- 8° 54.4'	14.7	1.495	0.572	23.9	142.8
2024-Oct-11	0.0	3h 9.75m	-10° 16.8'	14.4	1.458	0.525	23.3	144.6
2024-Oct-16	0.0	3h 13.16m	-11° 44.6'	14.1	1.422	0.482	23.1	146.0
2024-Oct-21	0.0	3h 16.09m	-13° 16.4'	13.9	1.386	0.441	23.2	146.7
2024-Oct-26	0.0	3h 18.55m	-14° 50.4'	13.7	1.351	0.404	23.8	146.8
2024-Oct-31	0.0	3h 20.58m	-16° 24.0'	13.5	1.316	0.370	24.8	146.2
2024-Nov- 5	0.0	3h 22.27m	-17° 53.9'	13.3	1.283	0.338	26.3	144.9
2024-Nov-10	0.0	3h 23.79m	-19° 16.5'	13.1	1.252	0.309	28.3	143.2
2024-Nov-15	0.0	3h 25.36m	-20° 28.1'	13.0	1.221	0.282	30.6	141.1
2024-Nov-20	0.0	3h 27.23m	-21° 24.8'	12.8	1.193	0.257	33.1	138.8
2024-Nov-25	0.0	3h 29.70m	-22° 2.1'	12.7	1.167	0.232	35.6	136.5
2024-Nov-30	0.0	3h 33.18m	-22° 14.2'	12.5	1.143	0.210	38.1	134.4
2024-Dec- 5	0.0	3h 38.22m	-21° 54.4'	12.3	1.121	0.188	40.2	132.7
2024-Dec-10	0.0	3h 45.52m	-20° 53.6'	12.1	1.103	0.167	41.7	131.8
2024-Dec-15	0.0	3h 55.94m	-18° 59.3'	11.8	1.087	0.146	42.4	131.9
2024-Dec-20	0.0	4h 10.54m	-15° 52.1'	11.4	1.075	0.127	41.6	133.5
2024-Dec-25	0.0	4h 30.72m	-11° 2.6'	11.0	1.067	0.110	38.8	137.2
2024-Dec-30	0.0	4h 58.26m	- 3° 54.2'	10.4	1.062	0.095	33.1	143.8
2025-Jan- 4	0.0	5h 34.92m	+ 5° 52.0'	9.8	1.061	0.085	24.3	153.7
2025-Jan- 9	0.0	6h 21.00m	+17° 19.8'	9.2	1.063	0.082	13.7	165.2
2025-Jan-14	0.0	7h 13.39m	+27° 57.5'	9.0	1.069	0.087	8.6	170.7
2025-Jan-19	0.0	8h 5.35m	+35° 35.2'	9.6	1.079	0.098	13.8	164.8
2025-Jan-24	0.0	8h 50.30m	+40° 1.7'	10.3	1.092	0.115	19.2	158.5
2025-Jan-29	0.0	9h 25.40m	+42° 12.3'	10.8	1.109	0.136	22.6	154.4
2025-Feb- 3	0.0	9h 51.21m	+43° 1.1'	11.3	1.129	0.159	24.3	151.9
2025-Feb- 8	0.0	10h 9.66m	+43° 2.5'	11.7	1.151	0.185	24.9	150.5
2025-Feb-13	0.0	10h 22.69m	+42° 35.7'	12.0	1.176	0.212	25.0	149.8
2025-Feb-18	0.0	10h 31.85m	+41° 50.9'	12.4	1.203	0.242	24.8	148.9
2025-Feb-23	0.0	10h 38.33m	+40° 53.6'	12.7	1.232	0.274	24.5	148.9
2025-Feb-28	0.0	10h 43.03m	+39° 46.8'	13.0	1.263	0.308	24.3	148.3
2025-Mar- 5	0.0	10h 46.67m	+38° 32.4'	13.3	1.295	0.344	24.3	147.4
2025-Mar-10	0.0	10h 49.72m	+37° 12.3'	13.6	1.328	0.383	24.5	146.3
2025-Mar-15	0.0	10h 52.51m	+35° 48.1'	13.9	1.363	0.424	24.9	144.8
2025-Mar-20	0.0	10h 55.26m	+34° 21.1'	14.1	1.398	0.468	25.4	143.0
2025-Mar-25	0.0	10h 58.10m	+32° 52.2'	14.4	1.435	0.516	26.0	140.9
2025-Mar-30	0.0	11h 1.14m	+31° 22.3'	14.7	1.471	0.566	26.7	138.6
2025-Apr- 4	0.0	11h 4.45m	+29° 51.9'	15.0	1.509	0.619	27.3	136.2

References

Behrend, R. (2020web). Observatoire de Geneve web site. http://obswww.unige.ch/~behrend/page_cou.html

Dunlap, J.L.; Taylor, R.C. (1979). "Minor planets and related objects. XXVII. Lightcurves for 887 Alinda." *Astron. J.* **84**, 273-279.

Warner, B.D.; Harris, A.W.; Pravec, P. (2009). "The Asteroid Lightcurve Database." *Icarus* **202**, 134-146. Updated 2023 June. <http://www.minorplanet.info/lightcurvedatabase.html>

ROTATION PERIOD OF KORONIS FAMILY MEMBER (2811) STŘEMCHOVÍ, INCLUDING A DISCUSSION OF PERIOD ERROR ESTIMATION

Stephen M. Slivan, August D. Berne, Macy P. Brennan,
Jayna R. Ekelmann, Lucy C. Gray, Elizabeth H. Jackson,
Parimala A. Rajesh, Elaine M. Sheffield
Massachusetts Institute of Technology
Dept. of Earth, Atmospheric, and Planetary Sciences
77 Mass. Ave. Rm. 54-424, Cambridge, MA 02139
slivan@mit.edu

(Received: 2024 July 14)

Lightcurve observations of (2811) Střemchoví during its 2024 apparition yield a determination of its synodic rotation period 3.2488 ± 0.0007 h, in agreement with previously published results. The period uncertainty estimation is discussed.

Koronis family member (2811) Střemchoví was observed as part of a program to extend the study sample of rotation properties of the family's brightest objects (Slivan et al., 2023) to smaller sizes. An unambiguous rotation period 3.249 ± 0.002 h has been reported by Benishek (2018) based on densely-sampled lightcurves recorded on two consecutive nights, and corroborated by analyses of photometric survey data sparsely sampled in time (Chang et al., 2014; Waszczak et al., 2015; Erasmus et al., 2020). The new data reported here record lightcurves from a previously unobserved viewing aspect, and yield an improved determination of the rotation period from dedicated observations.

Střemchoví was observed in 2024 using telescopes at the MIT Wallace Astrophysical Observatory (WAO) in Westford, MA; nightly observing information is summarized in Table I and the instrumentation is detailed in Table II. Image processing and measurement procedures were as described by Slivan et al. (2008) using synthetic aperture sizes informed by Howell (1989).

The new observations on 6 nights over a 22-day interval (Fig. 1) yield a best-fit derived synodic period of 3.2488 ± 0.0007 h, which is consistent with the previously published periods.

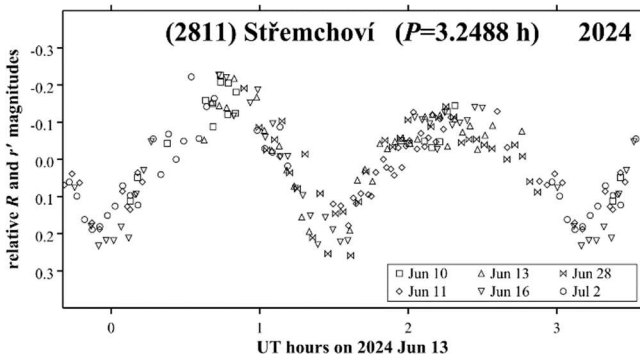


Figure 1. Folded composite lightcurve of (2811) Střemchoví during its 2024 apparition, light-time corrected, showing one rotation period plus the earliest and latest 10% repeated. The legend gives the UT dates of the observations. These relative photometry data have been shifted in brightness to form a self-consistent composite.

The remainder of this paper discusses the error estimate for the period, motivated in part by the importance of the synodic period uncertainty for constraining an object's sidereal period (Slivan,

2012; 2013). The approach used here to estimate the error is derived from the relationship that directly determines a period P by dividing a time interval Δt between two observations of some repeating lightcurve feature by the number of rotations n_{rot} that occurred during that interval. The corresponding period error $\sigma(P)$ is calculated from the time interval error $\sigma(\Delta t)$ as

$$\sigma(P) = \sigma(\Delta t) / n_{\text{rot}}. \quad (\text{Eq. 1})$$

Consideration of Eq. 1 identifies information helpful in choosing which observations of which repeating lightcurve feature are best suited for estimating the period error. For example, because a larger number of rotations in the denominator reduces the period error, using observations separated by a longer interval for more rotations is preferable to observations over a shorter interval, all else being equal.

In the numerator, the interval error $\sigma(\Delta t)$ is related not only to the photometric noise level of the observations, but also to the slope of the repeating lightcurve feature, because overlapping folded observations that exhibit a larger brightness change per unit time are more sensitive to period error. For a given rotation count, minimizing the interval error minimizes the period error, so both a steeper slope and a lower level of photometric noise are desirable.

Here the calculation of $\sigma(\Delta t)$ involves modeling the composite lightcurve shape using a Fourier series as described by Slivan et al. (2024). However, instead of filtering the model to locate epochs, here the unfiltered model is used to estimate the slopes of the lightcurve brightness changes between the extrema, and to estimate brightness uncertainties for the lightcurve observations. A brightness uncertainty for each lightcurve is estimated as the RMS residual error with respect to the model, first subtracting from each observed lightcurve point the model value at the corresponding rotation phase, and then calculating the standard deviation of the resulting set of differences. Dividing these brightness errors $\sigma(m_n)$ for both lightcurves by the slope k of the lightcurve at the overlap gives the errors in time $\sigma(t_n)$, which each produce the same reduction in self-consistency of the slope feature in the folded composite lightcurve as would be produced by the corresponding error in brightness:

$$\sigma(t_n) = \sigma(m_n) / k. \quad (\text{Eq. 2})$$

These are combined in quadrature to calculate the interval error $\sigma(\Delta t)$ for Eq. 1:

$$\sigma^2(\Delta t) = \sigma^2(t_1) + \sigma^2(t_2). \quad (\text{Eq. 3})$$

In the composite lightcurve of the 2024 data (Fig. 1) the best-observed slope features are the decreasing brightness near 1.1 h and the increasing brightness near 1.8 h. As is summarized in Table III, Part A, the earlier feature has the steeper slope while the later feature has observations farther apart in time, with both features yielding the same estimated period error of 0.0007 h.

In order to meaningfully compare our period error with the result by Benishek (2018), we retrieved the 2018 observations from the ALCDEF database to independently estimate the period error. The earliest and latest observations of the decreasing brightness near 1.3 h on the composite (Fig. 2) yield a period error of 0.004 h (Table III, Part B), double the error that was originally reported. We conclude that, despite the greater noise of the 2024 data, the larger number of elapsed rotations during the new observations dominates for a significantly improved synodic period precision.

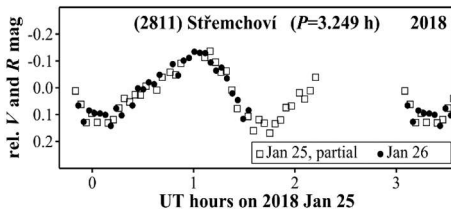


Figure 2. Similar to Fig. 1 but for the 2018 data from Benishek (2018), showing for the Jan 25 data only the first of the 2.5 rotations recorded during that session.

UT date	α	Tel.	Int.	Span
2024	($^{\circ}$)	ID	(s)	(h)
Jun 10.2	9.3	WAO-1, 4	180	2.1
Jun 11.2	9.7	WAO-1, 4	180	2.9
Jun 13.1	10.3	WAO-1	180	3.0
Jun 16.1	11.3	WAO-1	180	2.8
Jun 28.1	14.6	WAO-4	180	2.0
Jul 02.1	15.5	WAO-4	180	1.5

Table I: Nightly observing information, with rows grouped by lunation. Columns are: UT date at lightcurve mid-time, solar phase angle α , telescope ID (Table II), filter(s) used (R , Cousins R ; r , Sloan r), image integration time, and lightcurve duration.

Tel. ID	Dia. (m)	Camera	FOV ($'$)	Bin	Blk. avg.	Scale ($''/px$)
WAO-1	0.36	CMOS QHY268M	21 \times 14	1 \times 1	5 \times 5	1.00
WAO-4	0.36	CCD SBIG STL-1001	21 \times 21	1 \times 1	-	1.25

Table II: Telescopes and cameras information. Columns are: telescope ID (WAO-1, shed pier #1 Celestron C14; WAO-4, shed pier #4 Celestron C14), telescope diameter, camera, detector field of view, binning for camera readout, block averaging when used to rebin images after processing, and image scale for photometry.

Loc (h)	Slope (mag/h)	t1 (UT d)	$\sigma(m1)$ (mag)	t2 (UT d)	$\sigma(m2)$ (mag)	n rot	$\sigma(P)$ (h)
Part A: 2024 lightcurves, Fig. 1							
1.1	0.83	Jun 13.18	0.041	Jun 28.08	0.052	110	0.0007
1.8	0.67	Jun 11.18	0.028	Jun 28.10	0.052	125	0.0007
Part B: 2018 lightcurves, Fig. 2							
1.3	0.72	Jan 24.79	0.020	Jan 26.14	0.021	10	0.0041

Table III: Lightcurve slope features for period error determination. Columns are: feature location on graph time axis, feature slope, approximate start of time interval (light-time corrected) and brightness uncertainty, approximate end of time interval (light-time corrected) and brightness uncertainty, number of rotations elapsed during the interval, and period error result. Slopes and brightness errors were determined using a fourth-order Fourier series model of the composite lightcurve. Note that in this context the interval start and end times need only be precise enough to calculate the integer number of elapsed rotations; here the slope features' mid-times were estimated to the nearest 0.1 h by visual inspection.

Number	Name	yyyy mm/dd	Phase	L_{PAB}	B_{PAB}	Period(h)	P.E.	Amp	A.E.
2811	Střemchovi	2024 06/10-07/02	9.3,15.5	236	-1	3.2488	0.0007	0.35	0.06

Table IV. Observing circumstances and results. Solar phase angle is given for the first and last dates. L_{PAB} and B_{PAB} are the approximate phase angle bisector longitude/latitude at mid-date range.

Acknowledgments

We thank Dr. Michael Person and Timothy Brothers for allocation of telescope time at Wallace, and for observer instruction and support. The student observers were supported by a grant from MIT's Undergraduate Research Opportunities Program. This work uses data obtained from the Asteroid Lightcurve Data Exchange Format (ALCDEF) database, which is supported by funding from NASA grant 80NSSC18K0851.

References

Benishek, V. (2018). "Lightcurve and Rotation Period Determinations for Seven Asteroids." *Minor Planet Bull.* **45**, 386-389.

Chang, C.; Ip, W.; Lin, H.; Cheng, Y.; Ngeow, C.; Yang, T.; Waszczak, A.; Kulkarni, S.; Levitan, D.; Sesar, B.; Laher, R.; Surace, J.; Prince, T.A. (2014). "313 New Asteroid Rotation Periods from Palomar Transient Factory Observations." *Astrophys. J.* **788**, A17.

Erasmus, N.; Navarro-Meza, S.; McNeill, A.; Trilling, D.E.; Sickafoose, A.A.; Denneau, L.; Flewelling, H.; Heinze, A.; Tonry, J.L. (2020). "Investigating Taxonomic Diversity within Asteroid Families through ATLAS Dual-band Photometry." *Astrophys. J. Suppl. Ser.* **247**, A13.

Howell, S.B. (1989). "Two-dimensional Aperture Photometry: Signal-to-noise Ratio of Point-source Observations and Optimal Data-extraction Techniques." *PASP* **101**, 616-622.

Slivan, S.M.; Binzel, R.P.; Boroumand, S.C.; Pan, M.W.; Simpson, C.M.; Tanabe, J.T.; Villastrigo, R.M.; Yen, L.L.; Ditteon, R.P.; Pray, D.P.; Stephens, R.D. (2008). "Rotation Rates in the Koronis Family, Complete to $H \approx 11.2$." *Icarus* **195**, 226-276.

Slivan, S.M. (2012). "Epoch Data in Sidereal Period Determination. I. Initial Constraint from Closest Epochs." *Minor Planet Bull.* **39**, 204-206.

Slivan, S.M. (2013). "Epoch Data in Sidereal Period Determination. II. Combining Epochs from Different Apparitions." *Minor Planet Bull.* **40**, 45-48.

Slivan, S.M.; Hosek Jr., M.; Kurzner, M.; Sokol, A.; Maynard, S.; Payne, A.V.; Radford, A.; Springmann, A.; Binzel, R.P.; Wilkin, F.P.; Mailhot, E.A.; Midkiff, A.H.; Russell, A.; Stephens, R.D.; Gardiner, V.; and 5 colleagues (2023). "Spin vectors in the Koronis family: IV. Completing the sample of its largest members after 35 years of study." *Icarus* **394**, A115397.

Slivan, S.M.; Barrera, K.; Colclasure, A.M.; Cusson, E.M.; Larsen, S.S.; McLellan-Cassivi, C.J.; Moulder, S.A.; Nair, P.R.; Namphy, P.D.; Neto, O.S.; Noto, M.I.; Redden, M.S.; Rhodes, S.J.; Youssef, S.A. (2024). "Lightcurves and Derived Results for Koronis Family Member (5139) Rumoi, Including a Discussion of Measurements for Epochs Analysis." *Minor Planet Bull.* **51**, 6-10.

Waszczak, A.; Chang, C.; Ofek, E.O.; Laher, R.; Masci, F.; Levitan, D.; Surace, J.; Cheng, Y.; Ip, W.; Kinoshita, D.; Helou, G.; Prince, T.A.; Kulkarni, S. (2015). "Asteroid Light Curves from the Palomar Transient Factory Survey: Rotation Periods and Phase Functions from Sparse Photometry." *Astron. J.* **150**, A75.

LIGHTCURVE AND ROTATION PERIOD ANALYSIS OF 1532 INARI

Wayne Hawley
Old Orchard Observatory (Z09)
Fiddington, UK
hawley.wayne@gmail.com

Brian Scott (247)
Launceston, UK

Patrick Wiggins
University of Utah (718)

Jennie McCormick
Farm Cove Observatory (E85)
24 Rapallo Place, Farm Cove
Auckland 2012, NEW ZEALAND

James D. Armstrong
University of Hawaii Institute for Astronomy
(L09, Q58, Q59, Z17, Z21)
34 Ohia Ku Street
Pukalani, HI 96768 USA

Emmanuel Kardasis
Pelagia-Eleni Observatory (247)
Glyfada-Athens, GREECE

Frederick Pilcher
Organ Mesa Observatory (G50)
4438 Organ Mesa Loop
Las Cruces, NM 88011 USA

Tim Haymes
Southside Observatory (Y98)
Steeple Aston
Oxfordshire, UK

Grant J. Privett
LMPR Observatory (Y82)
Broad Chalke, UK

Paul C. Leyland
Tacande Observatory (J22)
La Palma, SPAIN

Joan Genebriera
Astropriorat Observatory (M02)
Catalonia, SPAIN

(Received: 2024 July 12)

Photometric observations of asteroid 1532 Inari were obtained between 2024 Jan 17 and Jun 12. Analysis of the observations found a synodic rotation period of 266.6 ± 0.2 h and maximum lightcurve amplitude 1.23 ± 0.09 mag.

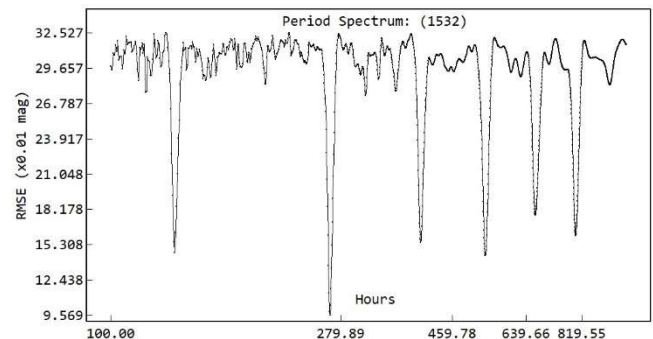
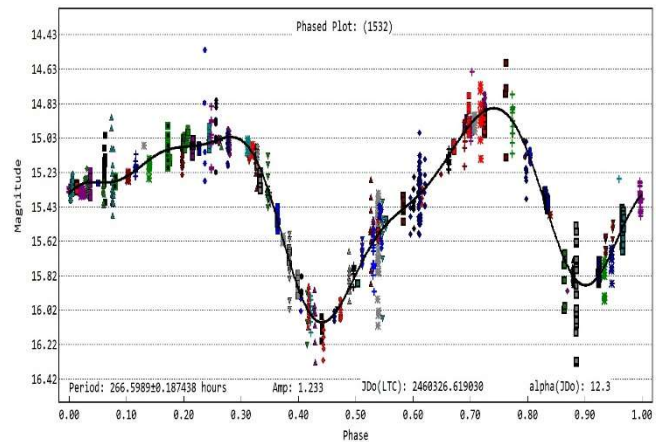
1532 Inari is a main-belt asteroid member of the Eos family that was discovered on 1938 Sep 16 by Y. Vaisala at Turku. It has an approximate diameter of 24.5 km (JPL, 2023). The Lightcurve Database (LCDB; Warner et al., 2009) lists a rotation period of 25 h (Behrend, 2008web) with a quality figure of 1+ and 0.09 maximum magnitude for its lightcurve, i.e., much smaller than the value reported here; however, this figure is based on fragmentary data.

Images were obtained from observatories around the globe. Several of the co-authors used their own equipment and some used the Las Cumbres Observatory facilities. Photometry and period determination were carried out with *TychoTracker Pro* Version 11.3. (TT).

The photometric analysis was performed using standard differential techniques on images with the comparison stars employed selected by TT to be within the colour range of $+0.50 < (B-V) < +0.90$. The Asteroid Terrestrial-impact Last Alert System (ATLAS) catalog (Tonry et al., 2015; Kostov and Bonev, 2017) was used as the source of reference stars.

TT's period determination operates by finding model light curves - comprising a user-defined number of Fourier components which best fit the asteroid photometric data. The program lists the candidate periods found within a user-defined period range and sampling frequency, based on minimizing Root Mean Square Errors (RMSE), between modelled and photometric magnitudes. The candidate periods are listed in increasing RMSE value and the entire suite of RMSE values is plotted as a "periodogram" for quality control. In these periodograms 1532 Inari yielded a clear 'best-fit' period solution having well defined 'stalactites' as shown in the following figures.

Periodograms often exhibit several possible candidate periods, in which case an examination of the rotational phase plot for each of these is then conducted looking for a credible lightcurve. Where the object shape is the dominant factor in producing the observed magnitude changes, typically when lightcurve amplitudes are >0.2 mag, the rotational phase plot often has two peaks and two troughs (bimodal) and this is usually chosen as the most likely for such asteroids.



Number	Name	yyyy mm/dd	Phase	L _{PAB}	B _{PAB}	Period (h)	P.E.	Amp	A.E.	Grp
1532	Inari	2024 01/17-06/12	*0.2, 20.1	151	0	266.6	0.2	1.23	0.09	606

Table I. Observing circumstances and results. The phase angle is given for the first and last date. If preceded by an asterisk, the phase angle reached a minimum during the period. L_{PAB} and B_{PAB} are the approximate phase angle bisector longitude/latitude at mid-date range (see Harris et al., 1984). Grp is the asteroid family/group (Warner et al., 2009).

Observatory	Telescope	CCD/CMOS	Filter	Sess
Old Orchard (Z09, Hawley)	0.35-m SCT <i>f</i> /6.7	SX694 Trius Pro (2×2)	SR	17
University of Utah, (718, Wiggins)	0.35-m SCT <i>f</i> /5.5	ST-10XME (3×3)	C	34
Farm Cove (E85, McCormick)	0.35-m SCT <i>f</i> /10	ST-8XME (2×2)	C	2
Brian Scott, Launceston, UK (247)	0.28-m SCT <i>f</i> /7	SX-H674 (2×2)	L	2
Siding Spring LCO-Clamshell #1 (Q58, Armstrong)	0.4-m <i>f</i> /8	SBIG STL6303 (1×1)	SR	4
Siding Spring LCO-Clamshell #2 (Q59, Armstrong)	0.4-m <i>f</i> /8	SBIG STL6303 (1×1)	SR	2
Sutherland LCO-Aqawan A (L09, Armstrong)	0.4-m <i>f</i> /8	SBIG STL6303 (1×1)	SR	5
Southside Observatory (Y98, Haymes)	0.28-m SCT <i>f</i> /5.8	QHY174mGPS (1×1)	C	1
LMPR Observatory Broad Chalke, UK (Y82, Privett)	0.3-m <i>f</i> /4	SX694 Trius Pro (2×2)	C	3
Pelagia-Eleni Observatory Glyfada-Athens Greece (247, Kardasis)	0.28-m SCT <i>f</i> /10	ASI183MM PRO (4×4)	V	10
Organ Mesa, Las Cruces (G50, Pilcher)	0.35-m SCT <i>f</i> /10	SBIG STL-1001E (1×1)	C	1
Tenerife Observatory - Aqawan A#2 (Z17, Armstrong)	0.4-m <i>f</i> /8	SBIG STL6303 (1×1)	SR/V	4
Tenerife Observatory - Aqawan A#1 (Z21, Armstrong)	0.4-m <i>f</i> /8	SBIG STL6303 (1×1)	SR/V	4
Tacande Observatory (J22, Leyland)	0.4-m Dillworth <i>f</i> /6.5	SX814 Trius Pro (2×2)	V	1
Astropriorat Observatory (M02, Genebriera)	0.46-m RC <i>f</i> /8.0	Moravian G4-16000/KAF-16803 (2×2)	V	10

Table II. List of observatories, observers, telescope, camera, filter(s), and number of sessions observed.

In this paper no attempt is made to find an absolute magnitude and a value of $G = 0.15$ has been used throughout the calculations. Time-series magnitude estimates from different nights and observing locations using a variety of imaging equipment were offset in magnitude to bring them into alignment when producing the raw and rotational-phase plots. The same offset was used for each instance of an individual imaging setup. All the observations will be loaded into the Asteroid Lightcurve Data Exchange Format (ALCDEF) database following publication. Some individual datapoints have been combined by stacking during period analysis to improve the signal-to-noise ratio.

Dips in the results from the period analysis have been checked to see if they are monomodal or bimodal and a bimodal period has been chosen for the best-fit result. Our analysis used more data points obtained during 103 observing sessions (a total of 1200 exposures) during 2024 January to June. We found a synodic rotation period of 266.6 ± 0.2 h and a lightcurve with a peak-to-peak amplitude of 1.23 ± 0.09 mag. The results and observing circumstances are summarized in Table I. Table II lists the observatories, observer, and equipment details.

Acknowledgements

Our thanks are extended to Daniel Parrott, author of *TychoTracker Pro*.

This work has made use of data from the Asteroid Terrestrial-impact Last Alert System (ATLAS) project. ATLAS is primarily funded to search for near earth asteroids through NASA grants NN12AR55G, 80NSSC18K0284, and 80NSSC18K1575; byproducts of the NEO search include images and catalogs from the survey area. The ATLAS science products have been made possible

through the contributions of the University of Hawaii Institute for Astronomy, the Queen's University Belfast, the Space Telescope Science Institute, and the South African Astronomical Observatory.

The ATLAS Catalog makes use of the formulae to convert Pan-STARRS *griz* to BVRI. (Kostov and Bonev, 2017)

This work makes use of observations from the Las Cumbres Observatory global telescope network.

References

- Behrend, R. (2008web). Observatoire de Geneve web site. http://obswww.unige.ch/~behrend/page_cou.html
- Harris, A.W.; Young, J.W.; Scaltriti, F.; Zappala, V. (1984). "Lightcurves and phase relations of the asteroids 82 Alkmene and 444 Gyptis." *Icarus* **57**, 251-258.
- JPL (2023). Small-Body Database Lookup. https://ssd.jpl.nasa.gov/tools/sbdb_lookup.html
- Kostov, A.; Bonev, T. (2017). "Transformation of Pan-STARRS1 gri to Stetson BVRI magnitudes. Photometry of small bodies observations." *Bulgarian Astron. J.* **28**, 3.
- Tonry, J.L.; Denneau, L.; Flewelling, H.; Heinze, A.N.; Onken, C.A.; Smartt, S.J.; Stadler, B.; Weiland, H.J.; Wolf, C. (2018). "The ATLAS All-Sky Stellar Reference Catalog." *Astrophys. J.* **867**, A105.
- Warner, B.D.; Harris, A.W.; Pravec, P. (2009). "The Asteroid Lightcurve Database." *Icarus* **202**, 134-146. Updated 2023 Oct. <https://www.minorplanet.info/php/lcdb.php>

**PHOTOMETRIC OBSERVATIONS OF
ASTEROID 1602 INDIANA**

Alessandro Marchini, Riccardo Papini,
Joao Pedro Savino, Sabina Schintu
Astronomical Observatory, University of Siena (K54)
Via Roma 56, 53100 - Siena, ITALY
marchini@unisi.it

Simone Scali
University of Dundee, Dundee, UK

Ahmad Atiyha, Michel Hanania
Bethlehem University, PALESTINE

(Received: 2024 July 15)

Photometric observations of the inner main-belt asteroid 1602 Indiana were conducted to verify its synodic rotation period. We found $P = 2.601 \pm 0.001$ h with $A = 0.14 \pm 0.02$ mag, in perfect agreement with the previously published results.

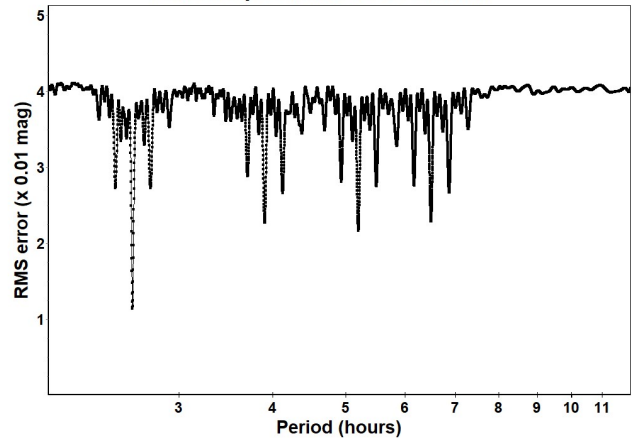
CCD photometric observations of the main-belt asteroid 1602 Indiana were carried out in April 2024 at the Astronomical Observatory of the University of Siena (K54). We used a 0.30-m $f/5.6$ Maksutov-Cassegrain telescope, SBIG STL-6303E NABG CCD camera; the pixel scale was 2.30 arcsec when binned at 2×2 pixels, a Clear filter and 180 seconds of exposure time.

Data processing and analysis were done with *MPO Canopus* (Warner, 2018). All images were calibrated with dark and flat-field frames and the instrumental magnitudes converted to R magnitudes using solar-colored field stars from a version of the CMC-15 catalogue distributed with *MPO Canopus*. Table I shows the observing circumstances and results.

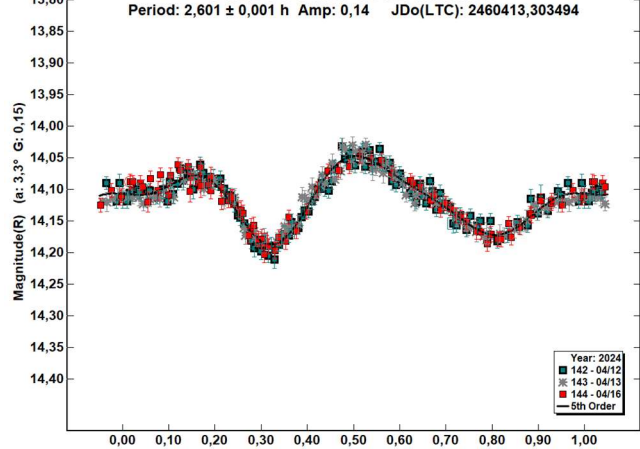
1602 Indiana (1950 GF) was discovered by Goethe Link Observatory at Brooklyn in 1950 March 14. It is an inner main-belt asteroid with a semi-major axis of 2.245 AU, eccentricity 0.104, inclination 4.162° , and an orbital period of 3.36 years. Its absolute magnitude is $H = 12.30$ (JPL, 2024). The NEOWISE satellite infrared radiometry survey (Mainzer et al., 2019) found a diameter $D = 7.970 \pm 0.810$ km using an absolute magnitude $H = 12.49$.

Observations were conducted over four nights and collected 299 data points. The period analysis shows a rotational period of $P = 2.601 \pm 0.001$ h with an amplitude $A = 0.14 \pm 0.02$ mag, in perfect agreement with the previously results published in the Asteroid Lightcurve Database (Franco et al., 2017; Klinglesmith et al., 2017; Warner et al., 2009).

Period Spectrum: 1602 Indiana



Phased Plot: 1602 Indiana



Acknowledgements

Joao Pedro Savino and Sabina Schintu are students of the course in Physics and Advanced Technologies who are attending their internship in our observatory; Simone Scali is a visiting student from the University of Dundee; Ahmad Atiyha and Michel Hanania are two colleagues from Bethlehem University involved in an Erasmus+ Staff Training Programme. All of them collaborated in images acquisition and further light curve analysis.

References

Franco, L.; Baj, G.; Tinella, V.; Bachini, M.; Succi, G.; Casalnuovo, G.B.; Bacci, P. (2017). "Rotation Periods for Three Main-belt Asteroids." *Minor Planet Bull.* **44**, 311-312.

Number	Name	2024/mm/dd	Phase	L _{PAB}	B _{PAB}	Period(h)	P.E.	Amp	A.E.	Grp
1602	Indiana	04/12-04/16	3.2, 4.2	201	5	2.601	0.001	0.14	0.02	MB-I

Table I. Observing circumstances and results. The phase angle is given for the first and last date. If preceded by an asterisk, the phase angle reached an extremum during the period. L_{PAB} and B_{PAB} are the approximate phase angle bisector longitude/latitude at mid-date range (see Harris et al., 1984). Grp is the asteroid family/group (Warner et al., 2009).

Harris, A.W.; Young, J.W.; Scaltriti, F.; Zappala, V. (1984). "Lightcurves and phase relations of the asteroids 82 Alkmene and 444 Gyptis." *Icarus* **57**, 251-258.

JPL (2024). Small Body Database Search Engine. <https://ssd.jpl.nasa.gov>

Klinglesmith, D.A. III; Hendrickx, S.; Kimber, C.; Madden, K. (2017). "CCD Asteroid Photometry from Etscom Observatory." *Minor Planet Bull.* **44**, 244-246.

Mainzer, A.K.; Bauer, J.M.; Cutri, R.M.; Grav, T.; Kramer, E.A.; Masiero, J.R.; Sonnett, S.; Wright, E.L. (2019). "NEOWISE Diameters and Albedos V2.0" *NASA Planetary Data System*, <https://doi.org/10.26033/18S3-2Z54>.

Warner, B.D.; Harris, A.W.; Pravec, P. (2009). "The Asteroid Lightcurve Database." *Icarus* **202**, 134-146. Updated 2023 Oct. <https://minplanobs.org/mpinfo/php/lcdb.php>

Warner, B.D. (2018). MPO Software, *MPO Canopus* v10.7.7.0. Bdw Publishing. <http://bdwpublishing.com/>

COLLABORATIVE ASTEROID PHOTOMETRY FROM UAI: 2024 APRIL-JUNE

Lorenzo Franco
Balzaretto Observatory (A81), Rome, ITALY
lor_franco@libero.it

Giulio Scarfi
Iota Scorpis Observatory (K78), La Spezia, ITALY

Alessandro Marchini
Astronomical Observatory, University of Siena (K54)
Via Roma 56, 53100 - Siena, ITALY

Marco Iozzi
HOB Astronomical Observatory (L63)
Capraia Fiorentina, ITALY

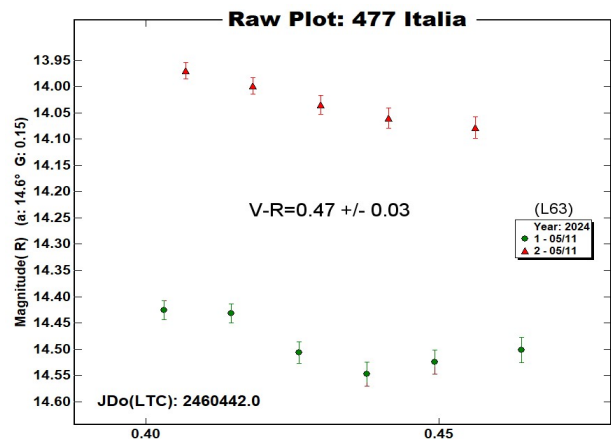
(Received: 2024 July 10)

Photometric observations of two asteroids were acquired for 477 Italia, and (21374) 1997 WS22.

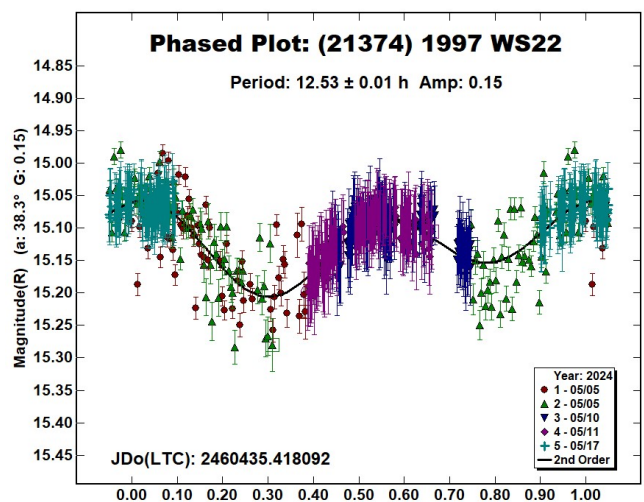
Collaborative asteroid photometry was done inside the Italian Amateur Astronomers Union (UAI; 2024) group. The targets were selected mainly in order to acquire lightcurves for shape/spin axis modeling. Table I shows the observing circumstances and results.

The CCD observations of two asteroids were made in 2024 April - June using the instrumentation described in the Table II. Unfortunately, the bad weather during the quarter did not allow for more observations. Lightcurve analysis was performed at the Balzaretto Observatory with *MPO Canopus* (Warner, 2023). All the images were calibrated with dark and flat frames and converted to standard magnitudes using solar-colored field stars from CMC15 and ATLAS catalogues, distributed with *MPO Canopus*.

477 Italia is an S-type (Bus and Binzel, 2002) inner main-belt asteroid. Multiband photometry was made by M. Iozzi (L63) on 2024 May 11. We found $V-R = 0.47 \pm 0.03$. This color index is close to the value found by Buchheim (2006; 0.48 ± 0.05) and consistent with an S-type asteroid (Shevchenko and Lupishko, 1998; 0.49 ± 0.05).



(21374) 1997 WS22 is an Amor Near-Earth asteroid. Collaborative observations were made over five nights by A. Marchini (K54) and G. Scarfi (K78), near its close approach to the Earth. The period spectrum shows a deeper minimum with a bimodal solution of $P = 12.53 \pm 0.01$ h and an amplitude $A = 0.15 \pm 0.06$ mag. This solution differs from the previous solutions found by Warner (2014; 3.405 ± 0.005), Carbognani (2014; 2.292 ± 0.004), Vaduvescu et al. (2017; 2.4 ± 0.1), Warner (2018; 1.96 ± 0.01).

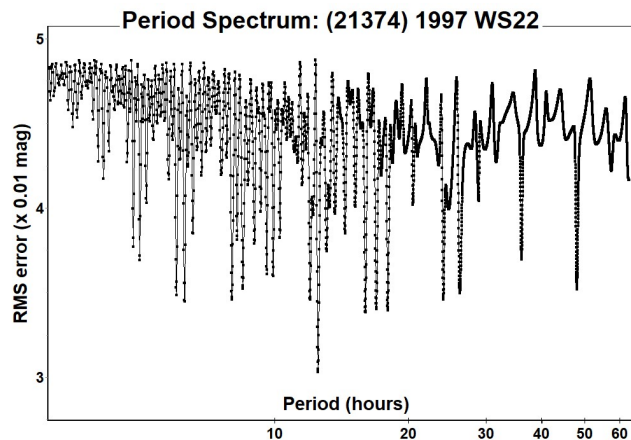


Number	Name	2024 mm/dd	Phase	L _{PAB}	B _{PAB}	Period(h)	P.E.	Amp	A.E.	Grp
477	Italia	05/11	14.5	198	-2					MB-I
21374	1997 WS22	05/04-05/17	38.4, 9.7	235	16	12.53	0.01	0.15	0.06	NEA

Table I. Observing circumstances and results. The first line gives the results for the primary of a binary system. The second line gives the orbital period of the satellite and the maximum attenuation. The phase angle is given for the first and last date. If preceded by an asterisk, the phase angle reached an extrema during the period. L_{PAB} and B_{PAB} are the approximate phase angle bisector longitude/latitude at mid-date range (see Harris et al., 1984). Grp is the asteroid family/group (Warner et al., 2009).

Observatory (MPC code)	Telescope	CCD	Filter	Observed Asteroids (#Sessions)
Iota Scorpii (K78)	0.40-m RCT f/6.1	CMOS QHY 268	C	21374 (3)
Astronomical Observatory, University of Siena (K54)	0.30-m MCT f/5.6	SBIG STL-6303e(bin 2×2)	C	21374 (2)
HOB Astronomical Observatory (L63)	0.20-m SCT f/6.0	ATIK 383L+	V, Rc	477 (1)

Table II. Observing Instrumentations. MCT: Maksutov-Cassegrain, RCT: Ritchey-Chretien, SCT: Schmidt-Cassegrain.



References

Buchheim, R.K. (2006). "Photometry of asteroids 133 Cyrene, 454 Mathesis, 477 Italia, and 2264 Sabrina." *Minor Planet Bulletin* **33**, 29-30.

Bus, S.J.; Binzel, R.P. (2002), "Phase II of the Small Main-Belt Asteroid Spectroscopic Survey - A Feature-Based Taxonomy." *Icarus* **158**, 146-177.

Carbognani, A. (2014). "Asteroids Lightcurves at OAVdA: 2013 December - 2014 June." *Minor Planet Bulletin* **41**, 265-270.

Harris, A.W.; Young, J.W.; Scaltriti, F.; Zappala, V. (1984). "Lightcurves and phase relations of the asteroids 82 Alkmene and 444 Gyptis." *Icarus* **57**, 251-258.

Shevchenko, V.G.; Lupishko, D.F. (1998). "Optical properties of Asteroids from Photometric Data." *Solar System Research* **32**, 220-232.

UAI (2024), "Unione Astrofili Italiani" web site. <https://www.uai.it>

Vaduvescu, O.; Macias, A.A.; Tudor, V.; Predatu, M.; Galád, A.; Gajdoš, Š.; Világi, J.; Stevance, H.F.; Errmann, R.; Unda-Sanzana, E.; Char, F.; Peixinho, N.; Popescu, M.; Sonka, A.; Cornea, R.; Suci, O.; Toma, R.; Santos-Sanz, P.; Sota, A.; Licandro, J.; Serracart, M.; Morate, D.; Mocnik, T.; Diaz Alfaro, M.; Lopez-Martinez, F.; McCormac, J.; Humphries, N. (2017). "The EURONEAR Lightcurve Survey of Near Earth Asteroids." *Earth Moon Planets* **120**, 41-100.

Warner, B.D.; Harris, A.W.; Pravec, P. (2009). "The Asteroid Lightcurve Database." *Icarus* **202**, 134-146.

Warner, B.D. (2014). "Near-Earth Asteroid Lightcurve Analysis at CS3-Palmer Divide Station: 2014 March-June." *Minor Planet Bulletin* **41**, 213-224.

Warner, B.D. (2018). "Near-Earth Asteroid Lightcurve Analysis at CS3-Palmer Divide Station: 2017 October-December." *Minor Planet Bulletin* **45**, 138-147.

Warner, B.D. (2023). MPO Software, MPO Canopus v10.8.6.20. Bdw Publishing. <http://minorplanetobserver.com>

LIGHTCURVE ANALYSIS AND PERIOD DETERMINATION FOR ASTEROID 16405 TESTUDO

Melissa Hayes-Gehrke, Blake Wallace, Daniel Luo,
Charles Parrott, Zoe Phillips, Jordan Bellevue, Alex Rzomp,
Ryan Henrikson, Jason Ator, Jonathan Herrera,
Anirudha Kumar, Luke Needham
Department of Astronomy
University of Maryland, College Park, Maryland, 20742 USA
mhayesge@umd.edu

(Received: 2024 June 3 Revised: 2024 July 1)

Photometric observations of the asteroid 16405 Testudo (1985 DA2) were conducted between 2024 April 3 - 16 using CCD telescopic images from Australia. Using lightcurve analysis, the rotation period for the asteroid was determined from the images in *MPO Canopus*. The rotation period found was 22.0 ± 0.1 h.

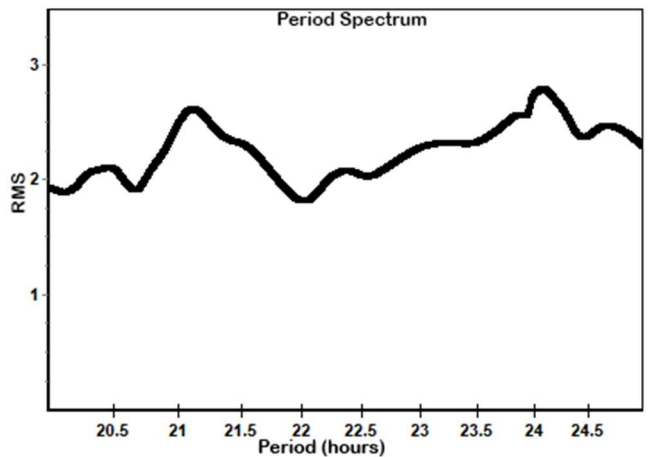
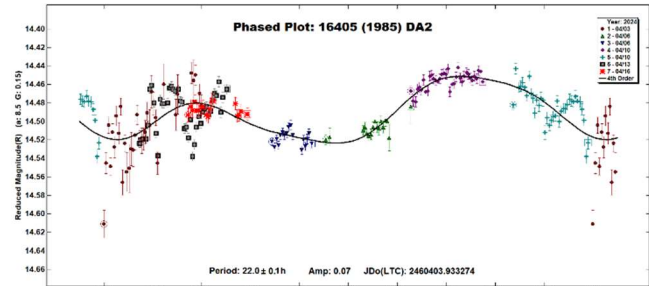
16405 Testudo is a main-belt asteroid discovered by H. Debehogne on 1985 February 20 at the La Silla Observatory in Coquimbo, Chile. The preliminary designation is 1985 DA2 and the name “Testudo” was recently approved and revised in this manuscript. The asteroid has an eccentricity of 0.237, a semi-major axis of 2.315 AU, inclination of 6.592° , and an orbital period of 3.522 years. Its diameter has been estimated at 4.199 km, with an absolute magnitude of 13.96 and a geometric albedo of 0.306 (JPL, 2016).

This research was conducted to determine the rotation period of the asteroid 16405 Testudo. Photometric data gathering occurred over five nights between 2024 April 3 - 16. There were 75, 36, 75, 81, and 33 images taken on 2024 April 3, 6, 10, 13, and 16, respectively. No previously reported period solutions were found in the LCDB for 1985 DA2 (LCDB; Warner et al., 2009).

Images were taken at Siding Spring Observatory (MPC Q62) in New South Wales, Australia, using a 0.50-m f/6.8 Corrected Dall-Kirkham telescope, FLI-PL6303E CCD camera with an array of 3072×2048 pixels, and AstroDon Tru-Balance Gen 2 E series Luminance filter. An exposure time of 300 seconds was used for each image, with 1×1 binning at a scale of 0.81 arcsec/pix (iTelescope Support Document). The data processing and period analysis were performed using *MPO Canopus*. Comparison star magnitudes were obtained from the ATLAS catalog within the *MPO Canopus* software. Using differential and aperture photometry, lightcurve analysis by *MPO Canopus* produced a period solution of 22.0 ± 0.1 h with an amplitude of 0.07 (Warner, 2012).

The lightcurve of asteroid 16405 Testudo exhibits a periodic variation in brightness, indicative of its rotation. With a well-defined rotation period of 22.0 ± 0.1 h, the asteroid demonstrates a stable rotation state. The amplitude measuring 0.07 magnitudes suggests relatively smooth surface features, resulting in subtle variations in brightness as it rotates.

While this period gave a bimodal phased lightcurve, the noise present in sessions 1 and 6, along with the lack of fit in session 5 necessitate further observations to confirm this result. The RMS value was 1.817, but the RMS plot reveals that there is not a clear minimum in the RMS values, suggesting that phased lightcurves of other periods would produce similarly good fits. The observational data for this extended period exhibits notable gaps, primarily stemming from the absence of daytime and some nighttime observations throughout the duration of the study. These significant gaps in data pose a considerable challenge in constructing a comprehensive phased lightcurve.



Acknowledgements

Funding for the photometric observations and access to the necessary software was provided by the Department of Astronomy at the University of Maryland - College Park. This research was made possible in part by the iTelescope team for providing assistance and access to their equipment.

References

Harris, A.W.; Young, J.W.; Scaltriti, F.; Zappala, V. (1984). “Light curves and phase relations of asteroids 82 Alkeme and 444 Gytis.” *Icarus* **57**, 251-258.

iTelescope Support Document.

<https://support.itelescope.net/support/solutions/articles/231917-telescope-30>.

Number	Name	yyyy mm/dd	Phase	L _{PAB}	B _{PAB}	Period(h)	P.E.	Amp	A.E.	Grp
16405	Testudo	2024 04/03-04/16	*8.70, 8.40	200.76	-10.17	22.0	0.1	0.07	0.05	MB-A

Table I. Observing circumstances and results. The phase angle is given for the first and last date. If preceded by an asterisk, the phase angle reached an extrema during the period. LPAB and BPAB are the approximate phase angle bisector longitude and latitude at mid-date range (see Harris et al., 1984). Grp is the asteroid family/group (Warner et al., 2009).

JPL (2016). Small Body Database Search Engine.
http://ssd.jpl.nasa.gov/sbdb_query.cgi

Warner, B.D.; Harris, A.W.; Pravec, P. (2009). "The Asteroid Light Curve Database." *Icarus* **202**, 134-146. Updated 2023 Oct. 1
<http://www.minorplanet.info/lightcurvedatabase.html>

Warner, B.D. (2012). MPO Software, MPO Canopus version 10.8.6.20. Bdw Publishing.
<https://minplanobs.org/BdwPub/php/mpocanopus.php>

LIGHTCURVE ANALYSIS OF (415029) 2011 UL21

Lorenzo Franco
 Balzaretto Observatory (A81), Rome, ITALY
 lor_franco@libero.it

Albino Carbognani
 Virgil Observatory (M60), Loiano, ITALY

Giulio Scarfi
 Iota Scorpis Observatory (K78), La Spezia, ITALY

Nico Montigiani, Massimiliano Mannucci
 Osservatorio Astronomico Margherita Hack (A57)
 Florence, ITALY

Marco Iozzi
 HOB Astronomical Observatory (L63)
 Capraia Fiorentina, ITALY

Giorgio Baj
 M57 Observatory (K38), Saltrio, ITALY

Alessandro Coffano, Wladimiro Marinello
 Osservatorio Serafino Zani (130), Lumezzane (BS), ITALY

(Received: 2024 July 15)

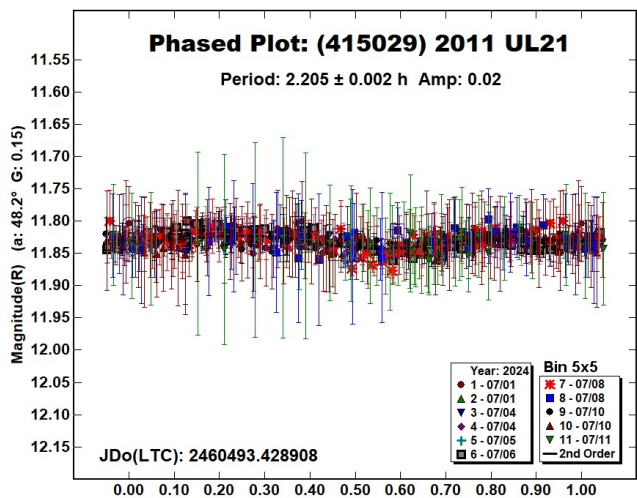
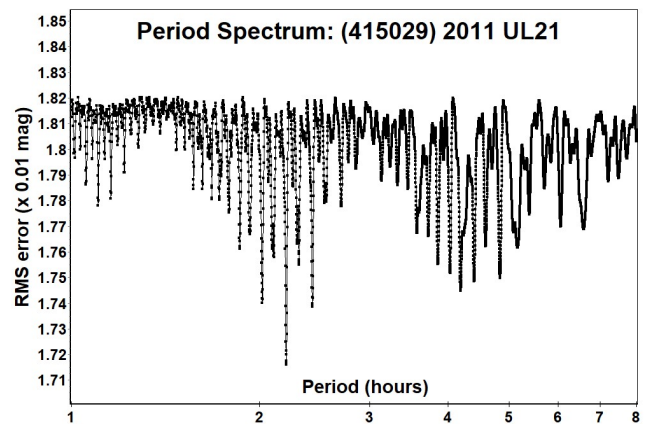
Collaborative photometric observations were carried out for the near-Earth asteroid (415029) 2011 UL21 by the Italian Amateur Astronomers Union group. We find a synodic rotation period of 2.205 ± 0.002 hours, amplitude 0.02 ± 0.02 magnitudes.

(415029) 2011 UL21 is an Apollo Near-Earth asteroid, classified as Potentially Hazardous Asteroid (PHA). Collaborative observations were made over seven nights, following its close approach to the Earth by the Italian Amateur Astronomers Union (UAI; 2024) group. Table I shows the observing circumstances and results, while Table II describe the used instrumentation.

Lightcurves analysis was done with *MPO Canopus* (Warner, 2023). All the images were calibrated with dark and flat frames and converted to standard magnitudes using solar colored field stars from CMC15 and ATLAS catalogues, distributed with *MPO Canopus*.

The low amplitude of the lightcurve in this apparition makes it difficult to determine the rotation period with certainty. The period spectrum shows a deeper solution with $P = 2.205 \pm 0.002$ h and an amplitude $A = 0.02 \pm 0.02$ mag. This solution differs from the previous periods found by Warner (2018a; 1.562 ± 0.001 , 2018b; 2.732 ± 0.002 , 2021; 3.31 ± 0.01).

Goldstone (2024) radar observations place an upper bound of 2.5 h on the primary rotation period, which is in good agreement with our result. Furthermore, Goldstone imaging on June 27, 2024, revealed that (415029) 2011 UL21 is a binary system. However, no mutual events were observed in the lightcurves during our observation campaign; probably, the illumination geometry was not favorable for their observation.



References

Goldstone (2024), Radar Observations.
<https://echo.jpl.nasa.gov/asteroids/june2024.goldstone.planning.html>

Harris, A.W.; Young, J.W.; Scaltriti, F.; Zappala, V. (1984). "Lightcurves and phase relations of the asteroids 82 Alkmene and 444 Gyptis." *Icarus* **57**, 251-258.

Number	Name	2024 mm/dd	Phase	L _{PAB}	B _{PAB}	Period(h)	P.E.	Amp	A.E.	Grp
415029	2011 UL21	07/01-07/10	48.1, 42.4	265	19	2.205	0.002	0.02	0.02	NEA

Table I. Observing circumstances and results. The first line gives the results for the primary of a binary system. The second line gives the orbital period of the satellite and the maximum attenuation. The phase angle is given for the first and last date. If preceded by an asterisk, the phase angle reached an extrema during the period. L_{PAB} and B_{PAB} are the approximate phase angle bisector longitude/latitude at mid-date range (see Harris et al., 1984). Grp is the asteroid family/group (Warner et al., 2009).

Observatory (MPC code)	Telescope	CCD	Filter	#Sessions
Virgil Observatory (M60)	0.30-m NRT f/4.0	ASI 533 MM	C	3
Iota Scorpii (K78)	0.40-m RCT f/6.1	CMOS QHY 268	Rc	2
Osservatorio Astronomico Margherita Hack (A57)	0.35-m SCT f/8.3	SBIG ST10XME (bin 2×2)	Rc	2
HOB Astronomical Observatory (L63)	0.20-m SCT f/6.0	ATIK 383L+ (bin 2×2)	C	1
M57 (K38)	0.35-m RCT f/5.3	SBIG STT1603ME	Rc	1
Osservatorio Serafino Zani (130)	0.40-m RCT f/6.5	Moravian C4-16000 (bin 2×2)	C	1

Table II. Observing Instrumentations. NRT: Newtonian Reflector, RCT: Ritchey-Chretien, SCT: Schmidt-Cassegrain.

UAI (2024), “Unione Astrofili Italiani” web site.
<https://www.uai.it>

Warner, B.D.; Harris, A.W.; Pravec, P. (2009) “The asteroid lightcurve database.” *Icarus* **202**, 134-146. Updated 2024 July.
<https://minplanobs.org/alcdef/index.php>

Warner, B.D. (2018a). “Near-Earth Asteroid Lightcurve Analysis at CS3-Palmer Divide Station: 2017 October-December.” *Minor Planet Bulletin* **45**, 138-147.

Warner, B.D. (2018b). “Near-Earth Asteroid Lightcurve Analysis at CS3-Palmer Divide Station: 2018 April-June.” *Minor Planet Bulletin* **45**, 366-379.

Warner, B.D. (2021). “Near-Earth Asteroid Lightcurve Analysis at the Center for Solar System Studies: 2021 January – March.” *Minor Planet Bulletin* **48**, 294-302.

Warner, B.D. (2023). MPO Software, MPO Canopus v10.8.6.20. Bdw Publishing. <http://minorplanetobserver.com>

LIGHTCURVE PHOTOMETRY AND ANALYSIS OF 5167 JOEHARMS

Melissa Hayes-Gehrke, Riley Gray, Samantha Linico, Paul Ng, Hita Thota, Oluwadamilola Akintoye, Michael Brown, Christine Egan, Andrew Xie, James Keenan, Richard Martinez, Ethan Tang, Daniel Yang
 Astronomy Department, 1113 PSC bldg 415
 College Park, MD 20742, USA
 mhayesge@umd.edu

Stephen Brincat
 Fl.5 George Tayar Street
 San Gwann SGN 3160, MALTA
 stephenbrincat@gmail.com

(Received: 2024 June 3)

Photometric observations were made of the main-belt asteroid 5167 Joeharms from 2024 April 3 to April 16, at an observatory in Beryl Junction, Utah, on iTelescope’s T21. Using MPO Canopus, the asteroid was determined to have a rotation period of 5.3204 ± 0.0025 h and an amplitude of 0.14.

5167 Joeharms is a main-belt asteroid that has been the subject of limited previous research. The importance of establishing its rotation period and understanding its physical characteristics contributes significantly to the broader database of known asteroids, aiding in the classification and study of main belt asteroids. 5167 Joeharms has an eccentricity of approximately 0.207, a semi-major axis of 2.666 AU, and a sidereal orbital period of 1590.27 days (JPL, 2023; Warner et al., 2009).

The observations were conducted from the U93: Skygems Dreamscope during the nights of April 3, 6, 10, 13, and 16 from 10pm to 6am UTC. The T21 telescope was utilized for the observations, equipped with a FLI-PL6303E CCD camera and Planewave 17" CDK OTA used with a luminance filter, set to a 300-second exposure duration (iTelescope, 2024). Configuration adjustments and quality control measures were strictly adhered to ensure accurate data capture.

Our collaborator, Stephen M. Brincat, observed from Flarestar Observatory in San Gwann, Malta using a Schmidt Cassegrain Telescope and Moravian G2-1600 Camera (aperture 0.25m, 0.99" pixel scale, 25°×17' FOV). Clear filters were used.

Data analysis was performed using MPO Canopus. Each session involved auto-matching the first image of the day to locate nearby stars, followed by MPO Canopus using 5 comparison stars. Special adjustments were made to account for days with meridian flips (Warner et al., 2019).

The determined rotation period of 5.3204 ± 0.0025 hours for 5167 Joeharms suggests a typical rotation speed for asteroids of its size and composition. The lightcurve’s amplitude variations indicate a high likelihood of an irregular shape with distinctly different maxima.

Acknowledgements

This research was made possible through the instructions and funding of Dr. Melissa Hayes-Gehrke of the Astronomy department at The University of Maryland, College Park.

Tools and setup necessary for observation were provided through use of iTelescope’s remote telescope service.

References

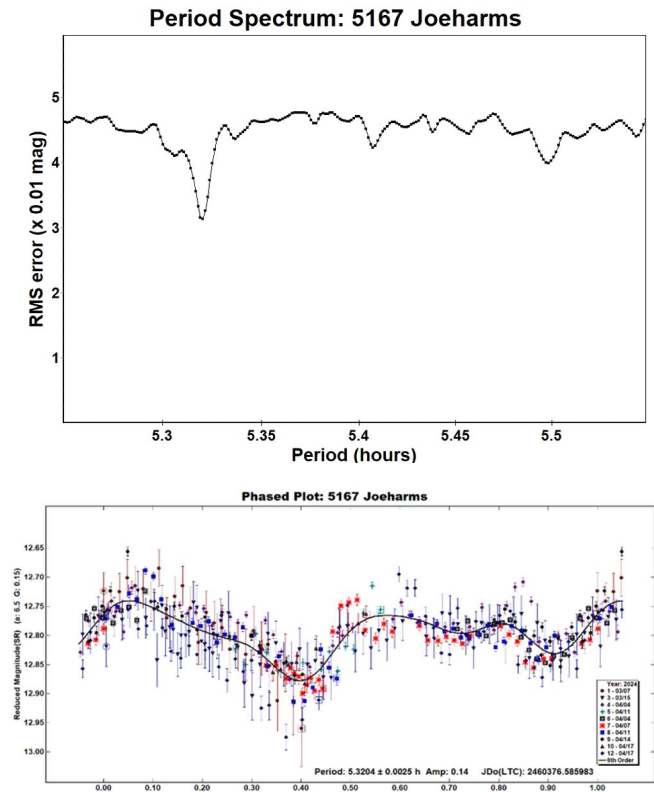
Harris, A.W.; Young, J.W.; Scaltriti, F.; Zappala, V. (1984). "Lightcurves and phase relations of the asteroids 82 Alkmene and 444 Gyptis." *Icarus* **57**, 251-258.

iTelescope (2024). <https://www.itelescope.net/>

JPL (2023). Small-Body Database Lookup. 5167 Joeharms. https://ssd.jpl.nasa.gov/tools/sbdb_lookup.html#/?sstr=5167

Warner, B.D.; Harris, A.W.; Pravec, P. (2009). "The Asteroid Lightcurve Database." *Icarus* **202**, 134-146. Updated 2023 Oct. <https://minplanobs.org/mpinfo/php/lcdb.php>

Warner, B.D. (2019). MPO Canopus Software Version 10.8.1.1. Bdw Publishing. <https://minplanobs.org/BdwPub/php/displayhome.php>



Number	Name	yyyy mm/dd	Phase	L _{PAB}	B _{PAB}	Period(h)	P.E.	Amp	A.E.	Grp
5167	Joeharms	2024 04/03-04/16	6.4, 11.5	180.5	4.9	5.3204	0.0025	0.14	0.067	LLA

Table I. Observing circumstances and results. The phase angle is given for the first and last date. If preceded by an asterisk, the phase angle reached an extrema during the period. LPAB and BPAB are the approximate phase angle bisector longitude/latitude at mid-date range (see Harris et al., 1984).

LIGHTCURVE ANALYSIS OF 7851 AZUMINO AND ESTIMATED ROTATION PERIOD

Melissa Hayes-Gehrke, John Brownfield, Samuel Cleary,
Ryan El Kochta, Desiree Gardner, Vishnu Kumar,
Vicky Mai, James Matheson, Thomas Mitchell,
Henri Riviera, Dominic Smith, Justin Tung,
Lucas Magnus Welinder
Department of Astronomy
University of Maryland, College Park, MD 20742 USA
mhayesge@umd.edu

(Received: 2024 June 3)

A lightcurve for the asteroid 7851 Azumino was created using *MPO Canopus* using data taken from T30 near Coonabarabran, Australia. From this analysis, a rotation period of 31.472 ± 0.329 h and a magnitude variation of 0.42 ± 0.04 mag was obtained.

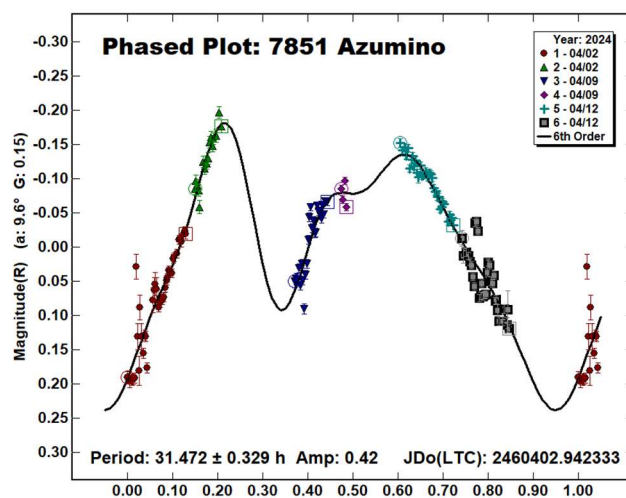
7851 Azumino (1996 YW2) was discovered by Naoto Satō at the Chichibu Observatory in December 1996. This main-belt asteroid was named to recognize a rice field also named Azumino near the Japanese Northern Alps. This asteroid has a semi-major axis of 2.204 AU and an eccentricity of 0.163. It also has a diameter of 4.966 km and an absolute magnitude of 13.59 (JPL, 2024).

University of Maryland observers used iTelescope T30, located at Siding Spring Observatory in Australia. Images were taken from 2024 Apr 2 to 2024 Apr 12. T30 is a corrected Dall-Kirkham telescope featuring a focal length of 2262 mm and an aperture of 508 mm. The FLI-PL6303E CCD camera taking the pictures has a pixel size of 9 square microns, a resolution of 0.81 arcsec per pixel, and an array of 3072 by 2048. All images were taken using the luminance filter with an exposure time of 300 s and with a binning of 1 (Telescope 30).

We used *MPO Canopus* (Warner, 2020) to analyze the data observed from each night, including photometric and lightcurve analysis. Our results, along with the dates on which the asteroid was observed are presented in Table I.

We believe that we are the first to find a rotation period for 7851 Azumino; we did not find any prior work in the Asteroid Lightcurve Database (LCDB; Warner et al., 2009). We determined a period of 31.472 ± 0.329 h, and a magnitude variation of 0.42 ± 0.04 mag.

Due to the limited amount of data used in our period analysis, the period we obtained is not the only possibility; we preferred it because it is bimodal, as we would expect of an asteroid. We note that this is a fairly long rotation period for an asteroid.



Acknowledgments

Use of the iTelescope remote observatory was made possible by funding from the University of Maryland Department of Astronomy. Images were filtered using the *DS9* software, and lightcurve analysis was performed using *MPO Canopus*.

References

- JPL. (2024). Small-Body Database Browser. <http://ssd.jpl.nasa.gov/sbdb.cgi>
- Harris, A.W.; Young, J.W.; Scaltriti, F.; Zappala, V. (1984). "Lightcurves and phase relations of the asteroids 82 Alkmene and 444 Gyptis." *Icarus* **57**, 251-258.
- "Telescope 30." iTelescope Support Document. <https://support.itelescope.net/support/solutions/articles/231917-telescope-30>.
- Warner, B.D.; Harris, A.W.; Pravec, P. (2009). "The Asteroid Light Curve Database." *Icarus* **202**, 134-146. Updated 2023 Oct. <http://www.minorplanet.info/lightcurvedatabase.html>
- Warner, B.D. (2020). MPO Software, *MPO Canopus* version 10.8.6.20. <https://minplanobs.org/BdwPub/php/mpocanopus.php>

Number	Name	20yy/mm/dd	Phase	L _{PAB}	B _{PAB}	Period(h)	P.E.	Amp	A.E.	Grp
7851	Azumino	24 4/2-4/12	9.8, 5.6	208	-7	31.472	0.329	0.46	0.04	MB-M

Table I. Observing circumstances and results. The phase angle is given for the first and last date. If preceded by an asterisk, the phase angle reached an extrema during the period. L_{PAB} and B_{PAB} are the approximate phase angle bisector longitude/latitude at mid-date range (see Harris et al., 1984). Grp is the asteroid family/group (Warner et al., 2009).

ASTEROID LIGHTCURVES FOR SIX ASTEROIDS

Milagros Colazo

Astronomical Observatory Institute, Faculty of Physics,
Adam Mickiewicz University,
ul. Słoneczna 36, 60-286 Poznań, POLAND.
Grupo de Observadores de Rotaciones de Asteroides (GORA),
ARGENTINA, <https://aoacm.com.ar/gora/index.php>
milirita.colazovinovo@gmail.com

Giuseppe Ciancia

CapoSudObservatory (GORA CS1 and CS2) -
Palizzi Marina (Reggio Calabria-ITALIA)

Nicola Montecchiari

Elijah Observatory (MPC M27) -
Lajatico (Pisa- ITALIA)

Raúl Melia

Observatorio de Raúl Melia Carlos Paz (GORA RMC) -
Carlos Paz (Córdoba-ARGENTINA)

Paolo Aldinucci

Osservatorio Astronomico di Orciatice (OAL and D41) -
Lajatico (Pisa- ITALIA)

Alberto García

]Observatorio Río Cofio (MPC Z03) -
Robledo de Chavela (Madrid-ESPAÑA)

B.Montealeone

Osservatorio Astronomico "La Macchina del Tempo" (MPC M24)
- Ardore Marina (Reggio Calabria- ITALIA)

Néstor Suárez

Observatorio Antares (MPC X39) -
Pilar (Buenos Aires-ARGENTINA)

Mario Morales

Observatorio de Sencelles (MPC K14) -
Sencelles (Mallorca-Islas Baleares-ESPAÑA)

Alejandro Moreschi

Observatorio Chopis (GORA OM3) -
Mercedes (Buenos Aires-ARGENTINA)

Francisco Santos

Observatorio Astronómico Giordano Bruno (MPC G05) -
Piconcillo (Córdoba-ESPAÑA)

Marcos Anzola

Observatorio Astronómico Vuelta por el Universo (GORA OMA)
- Córdoba (Córdoba-ARGENTINA)

Víctor Amelotti

Observatorio Astronómico Naos (GORA NAO) -
Alta Gracia (Córdoba-ARGENTINA)

Aldo Wilberger

Observatorio Los Cabezones (MPC X12) -
Santa Rosa (La Pampa-ARGENTINA)

Ariel Stechina

Observatorio de Ariel Stechina 1 (GORA OAS) -
Reconquista (Santa Fe-ARGENTINA)

Carlos Colazo

Observatorio Astronómico El Gato Gris (MPC I19) -
Tanti (Córdoba-ARGENTINA)

(Received: 2024 July 15 Revised: 2024 August 12)

Synodic rotation periods and amplitudes are reported for
minor planets: 57 Mnemosyne, 191 Kolga, 236 Honoria,
1428 Mombasa, 1532 Inari, and 1614 Goldschmidt.

The periods and amplitudes of asteroid lightcurves presented in this paper are the product of collaborative work by the GORA (Grupo de Observadores de Rotaciones de Asteroides) group. In all the studies, we have applied relative photometry assigning V magnitudes to the calibration stars.

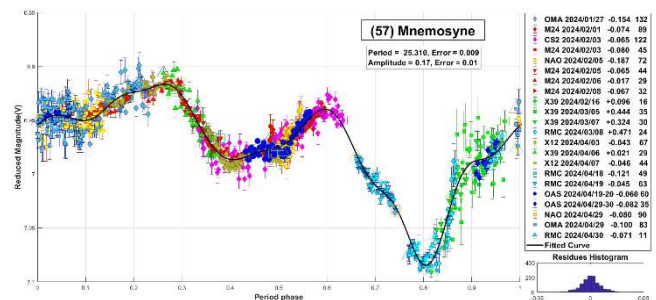
The image acquisition was performed without filters and with exposure times of a few minutes. All images used were corrected using dark frames and, in some cases, bias and flat-field corrections were also used. Photometry measurements were performed using *FotoDif* software and for the analysis, we employed *Periodos* software (Mazzone, 2012).

Below, we present the results for each asteroid studied. The lightcurve figures contain the following information: the estimated period and period error and the estimated amplitude and amplitude error. In the reference boxes, the columns represent, respectively, the marker, observatory MPC code, or - failing that - the GORA internal code, session date, session offset, and several data points.

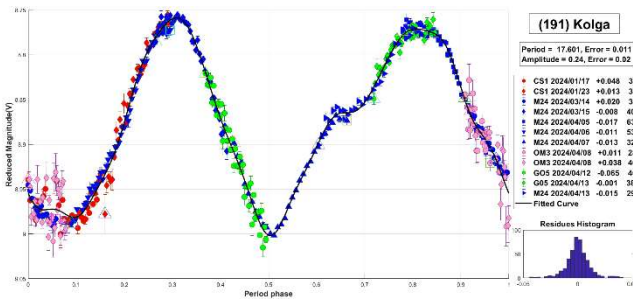
Targets were selected based on the following criteria: 1) those asteroids with magnitudes accessible to the equipment of all participants, 2) those with favorable observation conditions from Argentina or Spain or Italy, i.e. with negative or positive declinations δ , respectively, and 3) objects with few periods reported in the literature and/or with Lightcurve Database (LCDB) (Warner et al., 2009) quality codes (U) of less than 3.

In this work, we present measurements of periods corresponding to asteroids previously analyzed by our team. These lightcurves display improved results and are part of a new long-term project that we are initiating.

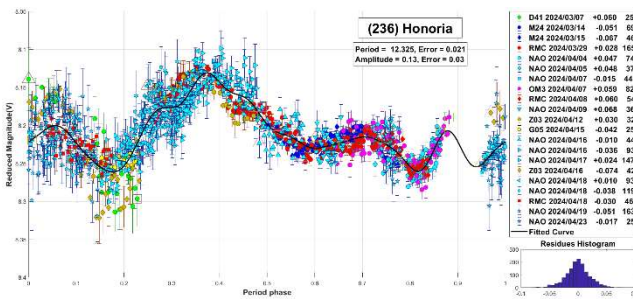
57 Mnemosyne. It is an S-type asteroid, discovered in 1859 by R. Luther. The initial measured periods reported were approximately 12 hours (Harris et al., 1992; Ditteon and Hawkins, 2007; Behrend, 2016web). Pilcher (2019) found a period $P = 25.310$ h. We previously measured the period of this asteroid, obtaining a result of $P = 26.12 \pm 0.01$ h (Colazo et al., 2021). In this work, we present the following result: $P = 25.310 \pm 0.009$ h with $\Delta m = 0.17 \pm 0.01$ mag, which is closer to the value measured by Pilcher. The Julian Date for zero phase, light-time corrected is $JDo(LTC) = 2460336.606489$.



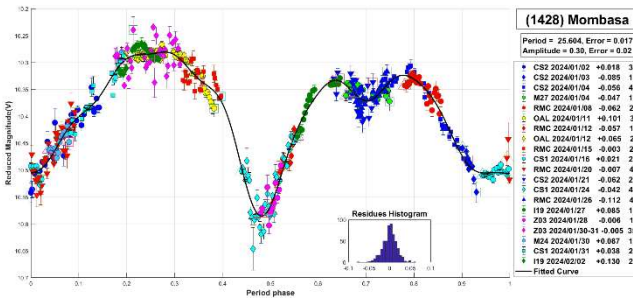
191 Kolga. It is an XC-type asteroid, discovered in 1878 by C.H.F. Peters. Behrend (2005web) found the period to be $P = 17.604$ h. We previously measured the period of this asteroid, obtaining a result of $P = 17.59 \pm 0.01$ h (Colazo et al., 2021). In this paper, we present a period of 17.601 ± 0.011 h with $\Delta m = 0.24 \pm 0.02$ mag. $JDo(LTC) = 2460326.5411912217$.



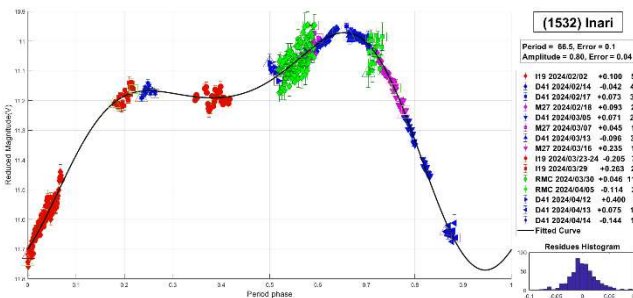
236 Honoria. It is an S-type asteroid, discovered in 1884 by J. Palisa. Lagerkvist et al. (1987) reported a period of $P = 12.338$ h. We previously measured the period of this asteroid, obtaining a result of $P = 12.338 \pm 0.008$ h (Colazo et al., 2021; 2022). In this work, we present the following result: $P = 12.325 \pm 0.021$ h with $\Delta m = 0.13 \pm 0.03$ mag, obtained under different viewing illumination and geometry. $JDo(LTC) = 2460377.3312493293$.



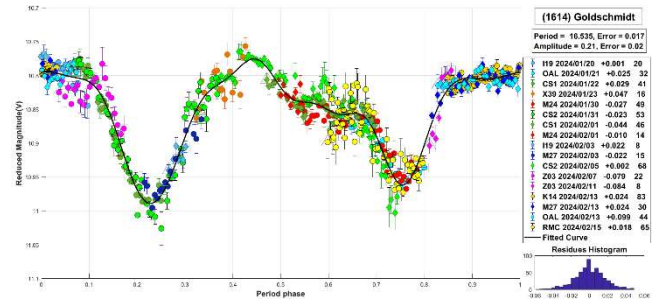
1428 Mombasa. It was discovered in 1937 by C. Jackson. The more recent period published in the literature corresponds to $P = 16.67$ h (Hawkins and Ditteon, 2008). In this work, we provide rather different results and propose a longer period of $P = 25.604 \pm 0.017$ h and $\Delta m = 0.30 \pm 0.02$ mag. $JDo(LTC) = 2460312.449777841$.



1532 Inari. It is an S-type asteroid, discovered in 1938 by Y. Vaisala. The more recent period published in the literature corresponds to $P = 25$ h (Behrend, 2008web). In this work, we propose a longer period of $P = 66.5 \pm 0.1$ h with $\Delta m = 0.08 \pm 0.04$ mag. $JDo(LTC) = 2460342.617510007$.



1614 Goldschmidt. It was discovered in 1952 by A. Schmitt. The more recent period published in the literature corresponds to $P = 16.54$ h (Polakis, 2019). However, the author did not present a light curve with full coverage. We measured a period of 16.535 ± 0.017 h with $\Delta m = 0.21 \pm 0.02$ mag, achieving good coverage. $JDo(LTC) = 2460329.5924063786$.



Acknowledgements

We would like to express our gratitude to Brian Warner for his invaluable suggestions and explanations, which have significantly contributed to the enhancement of our results. We want to thank Julio Castellano as we used his *FotoDif* program for preliminary analyses, Fernando Mazzone for his *Periods* program, which was used in final analyses, and Matías Martini for his *CalculadorMDE v0.2* used for generating ephemerides used in the planning stage of the observations. This research has made use of the Small Bodies Data Ferret (<http://sbn.psi.edu/ferret/>), supported by the NASA Planetary System. This research has made use of data and/or services provided by the International Astronomical Union's Minor Planet Center.

References

Behrend, R. (2005web, 2008web, 2016web). Observatoire de Geneve web site. http://obswww.unige.ch/~behrend/page_cou.html

Castellano, J. FotoDif software. <http://www.astrosurf.com/orodeno/fotodif/>

Colazo, M.; Stechina, A.; Fornari, C.; Santucho, M.; Mottino, A.; Pulver, E.; Melia, R.; Suárez, N.; Scotta, D.; Chapman, A.; Oey, J.; Meza, E.; Bellocchio, E.; Morales, M.; Speranza, T.; Romero, F.; Suligoy, M.; Passarino, P.T.; Borello, M.; Farfán, R.; Limón, F.; Delgado, J.; Naves, R.; Colazo, C. (2021). "Asteroid Photometry and Lightcurve Analysis at Gora Observatories." *Minor Planet Bulletin* **48**, 50-55.

Colazo, M.; Morales, M.; Fornari, C.; Chapman, A.; García, A.; Santos, F.; Melia, R.; Suárez, N.; Stechina, A.; Scotta, D.; Martini, M.; Santucho, M.; Moreschi, A.; Wilberger, A.; Mottino, A.; Bellocchio, E.; Quiñones, C.; Speranza, T.; Llanos, R.; Altuna, L.; Caballero, M.; Romero, F.; Galarza, C.; Colazo, C.R. (2022). "Photometry and Light Curve Analysis of Eight Asteroids by GORA'S Observatories." *Minor Planet Bulletin* **49**, 48-51.

Ditteon, R.; Hawkins, S. (2007). "Asteroid Lightcurve Analysis at the Oakley Observatory - October-November 2006." *Minor Planet Bulletin* **34**, 59-64.

Hawkins, S.; Ditteon, R. (2008). "Asteroid Lightcurve Analysis at the Oakley Observatory - May 2007." *Minor Planet Bulletin* **35**, 1-4.

Number	Name	yy/ mm/dd- yy/ mm/dd	Phase	L _{PAB}	B _{PAB}	Period(h)	P.E.	Amp	A.E.	Grp
57	Mnemosyne	24/01/27-24/04/30	*11.2, 16.8	156	-11	25.310	0.009	0.17	0.01	MB-O
191	Kolga	24/01/17-24/04/13	*18.3, 04.5	195	7	17.601	0.011	0.24	0.02	MB-O
236	Honorina	24/03/07-24/04/23	01.1, 14.2	165	-2	12.325	0.021	0.13	0.03	MB-O
1428	Mombasa	24/01/02-24/02/02	05.0, 15.0	93	-7	25.604	0.017	0.30	0.02	MB-O
1532	Inari	24/02/02-24/04/14	*06.9, 17.5	149	-1	66.526	0.026	0.80	0.04	Eos
1614	Goldschmidt	24/01/20-24/02/15	*09.5, 03.3	141	-7	16.535	0.017	0.21	0.02	MB-O

Table I. Observing circumstances and results. The phase angle is given for the first and last date. If preceded by an asterisk, the phase angle reached an extremum during the period. L_{PAB} and B_{PAB} are the approximate phase angle bisector longitude/latitude at mid-date range (see Harris et al., 1984). Grp is the asteroid family/group (Warner et al., 2009). MB-O: main-belt outer; Eos: 221 Eos.

Observatory	Telescope	Camera
D41 Osservatorio Astronomico di Orciatico	SCT (D=355mm; f=7.4)	CCD SBIG ST10XME
G05 Obs.Astr.Giordano Bruno	SCT (D=203mm; f=6.3)	CCD Atik 420 m
I19 Obs.Astr.El Gato Gris	SCT (D=355mm; f=10.6)	CCD SBIG STF-8300M
K14 Obs.Astr.de Sencelles	Newtonian (D=250mm; f=4.0)	CCD SBIG ST-7XME
M24 Oss.Astr.La Macchina del Tempo	RCT (D250mm; f=8.0)	CMOS ZWO ASI 1600MM
M27 Elijah Observatory	RCT (D250mm; f=6.0)	CCD QSI 683
X12 Obs.Astr.Los Cabezones	Newtonian (D=200mm; f=5.0)	CMOS QHY 174M
X39 Obs.Astr.Antares	Newtonian (D=250mm; f=4.72)	CCD QHY9 Mono
Z03 Obs.Astr.Río Cofio	SCT (D=254mm; f=6.3)	CCD SBIG ST-8XME
CS1 CapoSudObservatory	RCT (D=400mm; f=5.7)	CCD Atik 383L+Mono
CS2 CapoSudObservatory	Newtonian (D=254mm; f=4.7)	CCD Atik 420 Mono
NAO Obs.Astr.Naos	Newtonian (D=200mm; f=5.0)	CMOS ZWO 178
OAL Osservatorio Astronomico di Orciatico	SCT (D=355mm; f=7.4)	CCD SBIG ST10XME
OAS Obs.Astr.de Ariel Stechina 1	Newtonian (D=254mm; f=4.7)	CCD SBIG STF-402
OMA Obs.Astr.Vuelta por el Universo	Newtonian (D=150mm; f=5.0)	CMOS POA Neptune-M
OM3 Obs.Astr.Chopis	Newtonian (D=200mm; f=4.5)	CMOS ZWO ASI294MC-PRO
RMC Obs.Astr.de Raúl Melia Carlos Paz	Newtonian (D=254mm; f=4.7)	CMOS QHY 174M

Table II. List of observatories and equipment.

Harris, A.W.; Young, J.W.; Scaltriti, F.; Zappala, V. (1984). "Lightcurves and phase relations of the asteroids 82 Alkmene and 444 Gyptis." *Icarus* **57**, 251-258.

Harris, A.W.; Young, J.W.; Dockweiler, T.; Gibson, J.; Poutanen, Á.; Bowell, E. (1992). "Asteroid lightcurve observations from 1981." *Icarus* **95**, 115-147.

Lagerkvist, C.I.; Hahn, G.; Magnusson, P.; Rickman, H. (1987). "Physical studies of asteroids XVI-Photoelectric photometry of 17 asteroids." *Astronomy and Astrophysics Supplement Series* **70**, 21-32.

Mazzone, F.D. (2012). Periodos software, version 1.0. <http://www.astrosurf.com/salvador/Programas.htm>

Pilcher, F. (2019). "New Lightcurves of 50 Virginia, 57 Mnemosyne, 59 Elpis 194 Prokne, 444 Gyptis, and 997 Priska." *Minor Planet Bulletin*, **46**, 445-448.

Polakis, T. (2019). "Lightcurves of Twelve Main-Belt Minor Planets." *Minor Planet Bulletin* **46**, 287-292.

Warner, B.D.; Harris, A.W.; Pravec, P. (2009). "The Asteroid Lightcurve Database." *Icarus* **202**, 134-146. Updated 2023 June. <http://www.minorplanet.info/lightcurvedatabase.html>

LIGHTCURVE ANALYSIS FOR FIVE MAIN BELT ASTEROIDS

Gonzalo Fornas AVA - J57, CAAT
Centro Astronómico del Alto Turia, SPAIN
gon@iicv.es

Fernando Huet AVA - Z93
Rafael Barberá, AVA - J57, CAAT
Centro Astronómico del Alto Turia, SPAIN

Álvaro Fornas AVA - J57, CAAT
Centro Astronómico del Alto Turia, SPAIN

Gonzalo Fornas (Jr.),
Vicente Mas, AVA - J57, CAAT,
Centro Astronómico del Alto Turia, SPAIN

(Received: 2024 July 17)

Photometric observations of five main-belt asteroids were obtained from 2014-2023. We derived the following rotational synodic periods: 435 Ella, 4.62267 ± 0.0007 h; 1105 Fragaria, 5.426 ± 0.001 h; 1248 Jugurtha, 12.191 ± 0.002 h; 2343 Siding Spring, 2.10633 ± 0.00003 h; 7055 Fabiopagan, 4.1684 ± 0.016 h. Sideral periods were found for 435 Ella, $4.6228035 \pm 5 \times 10^{-7}$ h, 1105 Fragaria, $5.4314465 \pm 2 \times 10^{-6}$ h; 1248 Jugurtha, $12.190522 \pm 5 \times 10^{-5}$ h; 2343 Siding Spring, $2.106505 \pm 2 \times 10^{-6}$ h; 7055 Fabiopagan, $4.168785 \pm 5 \times 10^{-6}$ h.

We report on the photometric analysis result for five main-belt asteroids made by the Asociación Valenciana de Astronomía (AVA). This work was done from the Astronomical Center Alto Turia (CAAT, MPC J57) located in Aras de los Olmos, Valencia, Observatorio Zonalunar (MPC J08), and Vallbona Observatory with MPC code J67, operated by members of the Valencian Astronomy Association (AVA, <http://www.astroava.org>). This database shows graphic results of the data, mainly lightcurves with the plot phased to a given period.

Observatory	Telescope (meters)	CCD
C.A.A.T. (J57)	0.45 DK	SBIG STL-11002
Zonalunar (J08)	0.20 NW	QHY6
Vallbona (J67)	0.25 SCT	SBIG ST7-XME

Table 1. List of instruments used for the observations.

In this article, we focused on asteroids for which we had data from several appearances, both obtained by us and from data published in the Asteroid Data Exchange Format web site (ALCDEF; <https://alcdef.org>). The hope was to be able to calculate the rotation periods with greater accuracy.

Images were measured using *MPO Canopus* (Bdw Publishing) with a differential photometry technique. The comparison stars were restricted to near solar-color to minimize color dependencies, especially at larger air masses. The lightcurves show the synodic rotation period. The amplitude (peak-to-peak) that is shown is that for the Fourier model curve and not necessarily the true amplitude.

In a second step we used the method given by Slivan (2012; 2013, Eqs. 3-5, implemented on <http://www.koronisfamily.com>). With this method, from the maximum lux of different apparitions, we tried to limit the error intervals to know exact number of rotations of the asteroid, which univocally leads us to know its sideral

period. This is a valid method for data of the “dense” type, obtained continuously during an entire observation session.

In a third step we use the software *MPO LC Invert* (Bdw Publishing), which uses the inversion method described by Kaasalainen and Torppa (2001) and Kaasalainen et al. (2001). This software uses the code written by J. Durech based on the original FORTRAN code written by Kaasalainen to implement the period Scan. The advantage of this method is that it allows the use of “dense” data such as we obtained together with “sparse” data available in databases from Catalina, Usno, Atlas, Palomar, etc.

This is an iterative method that, based on an initial estimate of the period given by the lightcurve, finds the local minimum of χ^2 and gives the corresponding solution. The procedure starts with six initial poles for each trial period and selects the period that gives the lowest χ^2 . If there is a clear minimum in χ^2 when plotted as a function of the period, we can assume it as a correct solution, but is not always a clear one. We include only those asteroids that gave an unambiguous result.

The range of periods to be scanned is reduced, since we know the synodic period of the asteroid, having solved the lightcurves for several apparitions. This saves time in calculations. When making the calculation, weighted coefficients were used to take into account the density of the data. We assigned a value of 1 to “dense” data and a value of 0.3 for “sparse” data.

Error estimates in the inversion method are not obvious. The smallest separation, ΔP , of the local minima (Kaasalainen et al. 2001) in the period parameter space is roughly given by

$$\Delta P \approx 0.5 \times P^2 / \Delta t$$

where Δt is the full epoch range of the data set. This derives from the fact that the maxima and minima of a double sinusoidal lightcurve for periods P and $P \pm \Delta P$ are at the same epochs after Δt time.

As stated by Kaasalainen et al. (2001), “The period error is mostly governed by the epochs of the lightcurves. If the best local χ^2 minimum of the period spectrum is clearly lower than the others, one can obtain an error estimate of, say, a hundredth part of the smallest minimum width ΔP since the edge of a local minimum ravine always lies much higher than its bottom”.

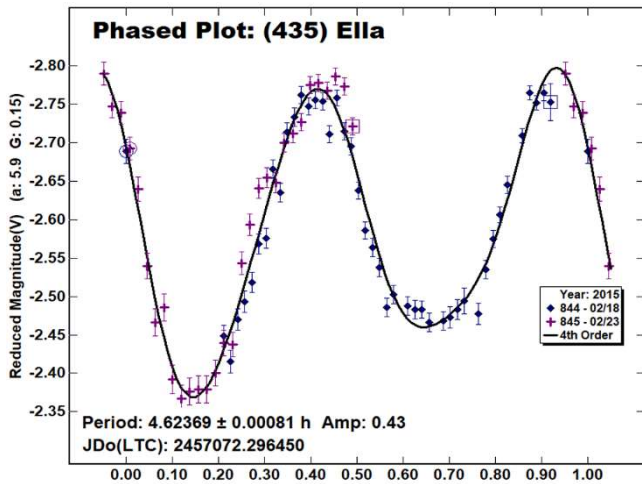
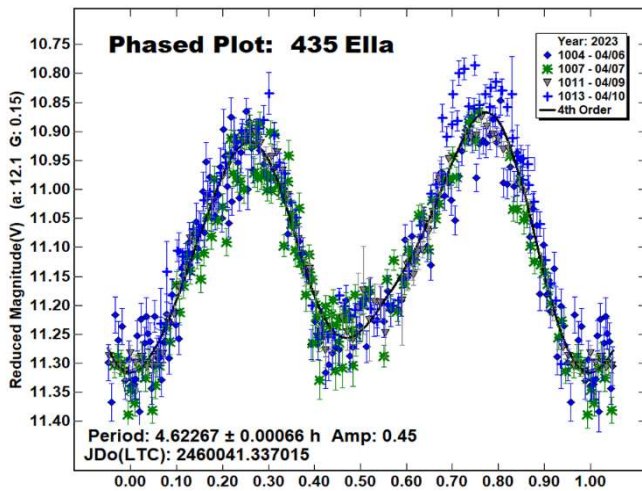
Durech et al. (2016) proposes an estimate of error of

$$\Delta P \approx (1/10 \times 0.5) \times P^2 / \Delta t$$

1/10 means that the period accuracy is 1/10 of the difference between local minima in the periodogram.

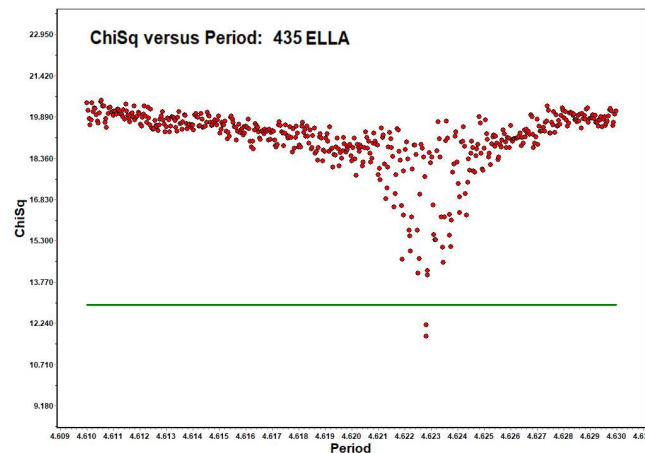
Once the period and period error were determined, we made a final adjustment with the Slivan method in order to find the best period approach.

435 Ella. This inner main-belt asteroid was discovered on 1898 Sep 11 by M.F. Wolf and A. Schwassmann, at Heidelberg. We made observations on 2023 Apr 6-10. From our data, we derived a synodic rotation period of 4.62267 ± 0.0007 h and an amplitude of 0.45 mag. Observations from 2015 Feb 8-23 led to a period of 4.624 ± 0.008 h with an amplitude of 0.44 mag, Dose (2020), whose data are available on the ALCDEF site, found a 4.622 h period. Marciniak et al. (2012) found 4.622802 looking for the spin axis.



We tried the method given by Slivan for data from 2020-2023, which were the closest-in-time apparitions in the data set. Unfortunately, the errors were too large to reach a unique solution.

We used *MPO LCInvert* with data from surveys Catalina (536 points, 2003/11/21 - 2023/3/28), Palomar (117 points, 2015/1/50 - 2022/5/13), USNO (200 points, 1998/9/14 - 2013/8/10), and Atlas (962 points, 2017/7/29 - 2023/3/25) with a weight of 0.3 and all the dense data referred were given a weight of 1.0. The result is a sidereal period of 4.622853 h.



A generic estimate of period error is given by

$$P_{err} = 10/360 \times P^2/T$$

where P is the period and T is the total time range of the data. The based on the 2020-2023 is 4×10^{-5} h. We again used the Slivan method with maximum lightcurve times of

- 2015 Feb 23: JD 2457077.38572020
- 2020 May 19: JD 2458988.7799
- 2023 Apr 10: JD 2460045.3379

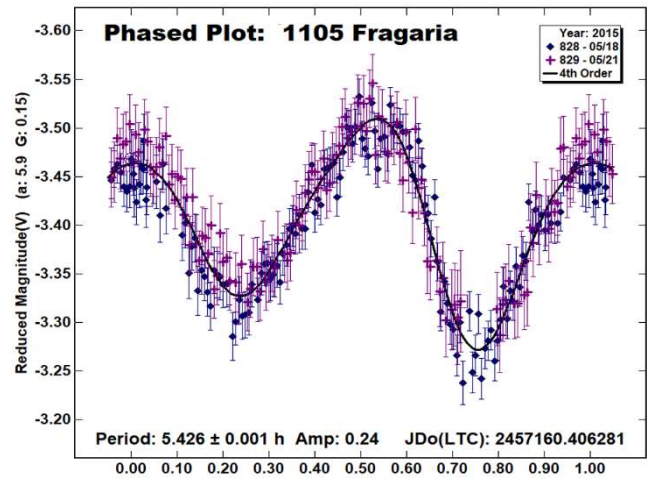
The new error of 0.00004 h gives an unambiguous solution of 4.6228035 ± 0.0000007 h with an amplitude of 0.24 mag. Marciniak et al. (2012) found a period of 4.622802 h.

1105 Fragaria. This outer main-belt asteroid was discovered on 1929 Jan 1 by K. Reinmuth at Heidelberg observatory. We made observations from 2015 May 18-21. From our original data, we derived a synodic rotation period of 5.426 ± 0.001 h and an amplitude of 0.24 mag. On the ALCDEF site, we found data from T. A. Polakis obtained 2017 Dec 18-23 (Polakis, 2018) with a period of 5.4312 ± 0.0008 h.

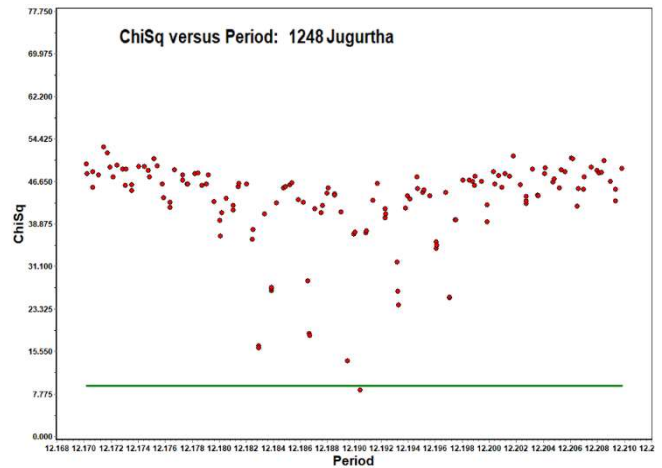
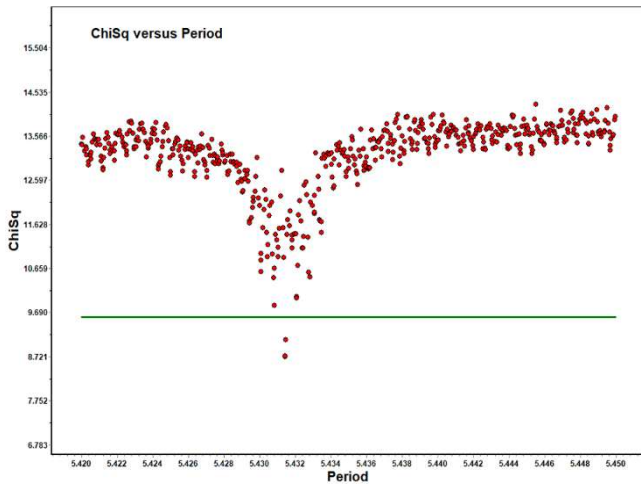
The times of the maximum lightcurve values applied in the Slivan method were:

- 2015 May 21: JD 2457164.4780
- 2017 Dic 21: JD 2458108.6573

Unfortunately, the result was ambiguous because our error interval was too wide to get a unique solution.



The “period scan” feature in *MPO LCInvert* used data weighted 0.3 from several all-sky surveys: Catalina (347 points, 2003/5/5 - 2023/4/2), Palomar (40 points, 2014/3/5 - 2021/11/22), USNO (187 points, 1998/4/4 - 2013/1/13), and ATLAS (1,173 points, 2017/11/23 - 2023/4/1). Dense data from our own observations and Polakis were given 1.0. We found a sidereal period of $5.431447 \text{ h} \pm 0.00005 \text{ h}$.



Using this more accurate solution the Slivan method gave an unambiguous sidereal period of 5.4314465 ± 0.000002 h with an amplitude of 0.24 mag. Durech et al. (2018) found a period of 5.431437 h and Martikainen et al. (2021) found 5.431440 h.

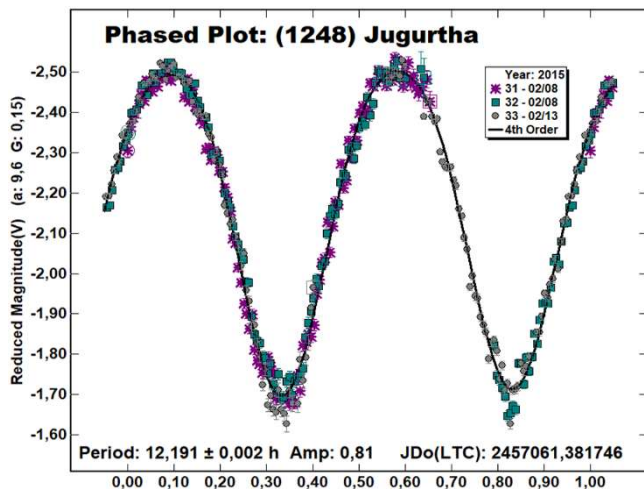
1248 Jugurtha. This middle main-belt asteroid was discovered on 1932 Sep 1 by C. Jackson at Johannesburg. We made observations from 2015 Feb 8-13. From our data, we derived a rotation period of 12.191 ± 0.002 h and an amplitude of 0.81 mag. Durech et al. (2016) found 12.19047 h looking for the spin axis. Worman and Olson (2004) found 12.190 h and Koff (2002) found 12.1897 h.

The period scan used sparse data (all weighted 0.3) from Catalina (450 points, 2005/10/2 - 2023/1/22), Palomar (123 points, 2014/12/22 - 2021/1/18), USNO (214 points, 1998/3/3 - 2012/6/2), and ATLAS (896 points, 2017/6/18 - 2023/1/24) and dense data (weight = 1.0) from our own observations and Koff. The result was a sidereal period of 12.19047 ± 0.00005 h, which agrees with Durech et al. (2016).

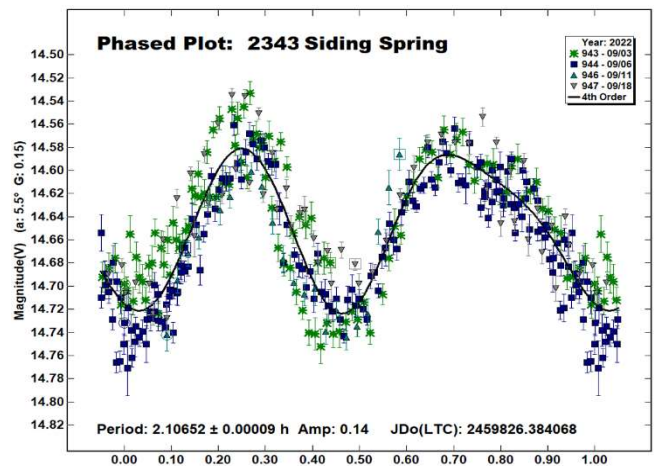
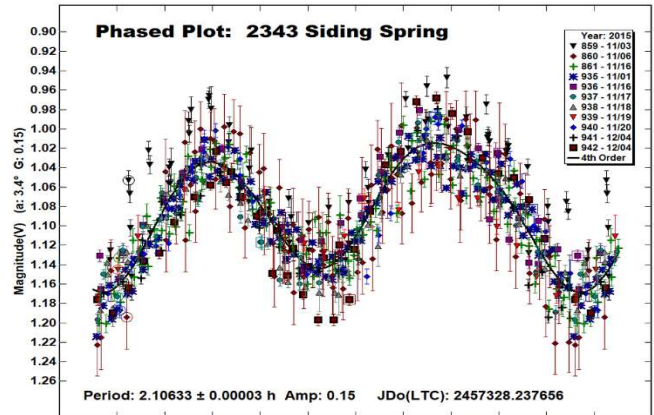
The times for the maximum lightcurve values were

- 2001 Jan 03: JD 2451912.5341
- 2015 Feb 13: JD 2457067.2710

This gave a new error of 0.00005 h and an unambiguous solution with Slivan method of 12.190522 h with an amplitude of 0.24 mag.



(2343) Siding Spring. This inner main-belt asteroid was discovered on 1979 Jun 25 by E.F. Helin and S.J. Bus at Siding Spring, Australia. We made observations from 2015 Nov 03-16. On the ALCDEF site, we found data from Julian Oey (2015/11/16-12/19) and Vladimir Benishek (2015/11/01-12/04).



Since these data were from the same apparition, we joined them to ours to improve the quality of the result. The result was a rotation synodic period of 2.10633 ± 0.00003 h and an amplitude of 0.15 mag. In ALCDEF we also found data from 2022 by R.G. Farfan (2022/9/3), F. García (2022/9/3-18), E.F. Mananes (2022/9/6-10), and E. Fernández (2022/9/6-10). Including these data found a synodic period of 2.10652 ± 0.00009 h and an amplitude of 0.15 mag.

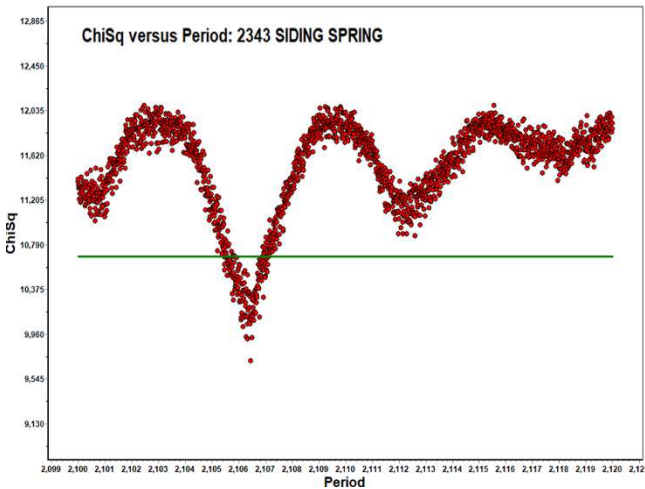
We use again the calculation method given by Slivan. The times of the maximum values in the lightcurves were:

2015 Nov 1: JD 2457328.4305

2022 Sep 6: JD 2459828.5125

The resulting error 0.00003 h was too large to reach a unique solution.

Sparse data from Catalina (465 points, 2003/4/22 - 2023/3/5), Palomar (43 points, 2019/8/28 - 2022/6/29), and ATLAS (566 points, 2017/6/15 - 2023/3/18) in the period scan found a sidereal period of 2.106498 ± 0.000002 h.



With this new error restriction, we applied the Slivan method, arriving at a unique sidereal period solution of 2.106505 h. Pollock et al. (2015) and Oey et al. (2017) found synodic periods of 2.10637 and 2.10639 h, respectively and Behrend (2015web) got 2.10659 h, all of which are consistent with our results. We could not confirm their discovery of a satellite for the asteroid.

(7055) Fabiopagan. This inner main-belt asteroid was discovered on 1989 May31 by H.E. Holt at Palomar. We made observations from 2014 May 03-05 and found a synodic rotation period of 4.1684 ± 0.016 h and an amplitude of 0.56 mag. Pravec (2007web) and Stephens (2007) found a period of 4.16845 h. We merged the two groups of data from 2007 available in ALCDEF and obtained a synodic period of 4.16847 ± 0.00005 h and an amplitude of 0.6 mag.

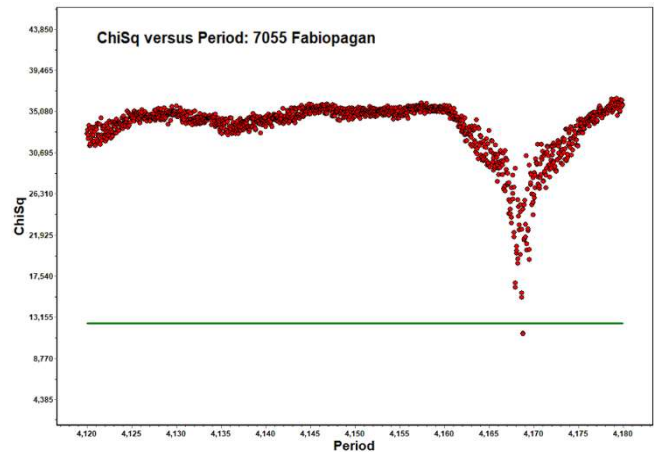
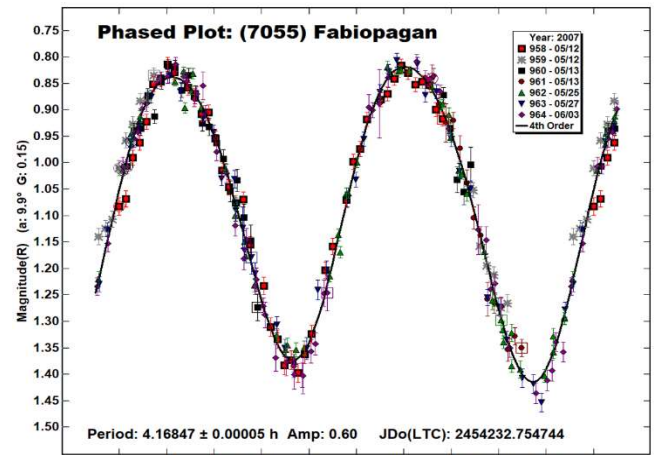
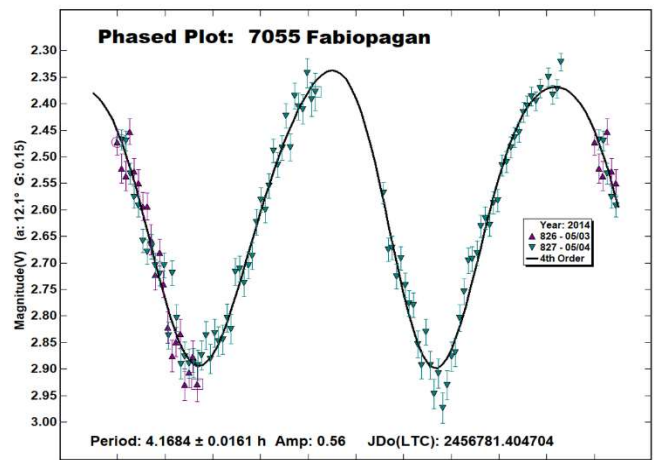
We used the period scan with sparse data ($w = 0.3$) from Catalina (562 points, 2005/11/4 - 2023/3/28), Palomar (180 points, 2014/12/22 - 2021/1/18), USNO (214 points, 2014/4/24 - 2021/6/12), and ATLAS (650 points, 2017/6/20 - 2023/3/18) and dense data from our own observations (2014), Pravec et al. (2007web), and Stephens (2007) with a weight of 1.0. These led to a sidereal period of 4.168782 ± 0.000005 h, which agrees with Hanus et al. (2013), who found 4.168782 h.

We used Slivan's method with maximum lightcurves values at

2014 May 03: JD 2456781.5647

2007 May 12: JD 2454232.77407

From this, we got an unambiguous sidereal period of 4.168785 h. This matches Hanus et al. (2013), who found 4.16878 h.



Acknowledgements

We would like to express our gratitude to Brian Warner for supporting the CALL web site and his suggestions and to Dr. Stephen Slivan for his advice.

Number	Name	yyyy mm/dd	Phase	L _{PAB}	B _{PAB}	Period(h)	P.E.	Amp	A.E	Grp
435	Ella	2015 02/18-02/23	5.8,7.9	135	2	4.62267	0.0007	0.45	0.02	MB-I
	E.V. Dose	2020 05/18-05/27	*3.2,1.4	243	-2					
1105	Fragaria	2015 05/18-05/21	5.1,5.8	247	11	5.426	0.001	0.24	0.02	MB-O
	T.A. Polakis	2017 12/18-12/23	2.6,2.9	87	-7					
248	Jugurtha	2015 02/08-02/13	9.9,11.7	117	8	12.191	0.002	0.81	0.02	MB-M
	R.A. Koff	²¹ 2000 11/29-01/11	22.7,20.5	160	-4					
2343	Siding Spring	2015 11/03-03/16	3.4,11.6	36	0	2.10633	0.00003	0.15	0.02	MB-I
	Julian Oey	2015 11/16-12/19	11.7,25.6	41	-1					
	V. Benishek	2015 11/01-12/04	2.1,21.0	41	0					
	R.G Farfan	2022 09/03	6.1	348	2					
	F. García	2022 09/03	6.1	348	2					
	E.F. Mananes	2022/09/06-09/10	4.2,2.2	348	2					
	E. Fernández	2022 09/06-09/10	4.2,2.2	348	2					
7055	Fabiopagan	2014/05/03-05/04	12.1-12.2	213	22	4.1684	0.016	0.56	0.02	MB-I

Table I. Synodic Periods. Observing circumstances and results. The phase angle values are for the first and last date. L_{PAB} and B_{PAB} are the approximate phase angle bisector longitude and latitude at mid-date range (see Harris et al., 1984). Grp is the asteroid family/group (Warner et al., 2009). MB-I/M/O: Main-belt inner/middle/outer.

Number	Name	yyyy mm/dd	Phase	L _{PAB}	B _{PAB}	Period(h)	P.E.	Grp
435	Ella	2015 02/18-02/23	5.8,7.9	135	2	4.6228035	0.0000005	MB-I
	E.V. Dose	2020 05/18-05/27	*3.2,1.4	243	-2			
1105	Fragaria	2015 05/18-05/21	5.1,5.8	247	11	5.4314465	0.000002	MB-O
	T.A. Polakis	2017 12/18-12/23	2.6,2.9	87	-7			
1248	Jugurtha	2015 02/08-02/13	9.9,11.7	117	8	12.190522	0.00005	MB-M
	R.A. Koff	²¹ 2000 11/29-01/11	22.7,20.5	160	-4			
2343	Siding Spring	2015 11/03-11/16	3.4,11.6	36	0	2.106505	0.00000	MB-I
	Julian Oey	2015 11/16-12/19	11.7,25.6	41	-1			
	V. Benishek	2015 11/01-12/04	2.1,21.0	41	0			
	R.G Farfan	2022 09/03	6.1	348	2			
	F. García	2022 09/03	6.1	348	2			
	E.F. Mananes	2022 09/06-09/10	4.2,2.2	348	2			
	E. Fernández	2022 09/06-09/10	4.2,2.2	348	2			
7055	Fabiopagan	2014 05/03-05/04	12.1-12.2	213	22	4.168785	0.000005	MB-I

Table II. Sidereal Periods. Observing circumstances and results. The phase angle values are for the first and last date. L_{PAB} and B_{PAB} are the approximate phase angle bisector longitude and latitude at mid-date range (see Harris et al., 1984). Grp is the asteroid family/group (Warner et al., 2009). MB-I/M/O: Main-belt inner/middle/outer.

References

Behrend, R. (2015web). Observatoire de Geneve web site.
http://obswww.unige.ch/~behrend/page_cou.html

Dose, E.V. (2020). "A New Photometric Workflow and Lightcurves of Fifteen Asteroids." *Minor Planet Bull.* **47**, 324-330.

Durech, J.; Hanus, J.; Oszkiewicz, D.; Vanco, R. (2016). "Asteroid models from the Lowell photometric database." *Astron. Astrophys.* **587**, A48.

Durech, J.; Hanus, J.; Ali-Lagoa, V. (2018). "Asteroid models reconstructed from the Lowell Photometric Database and WISE data." *Astron. Astrophys.* **617**, A57.

Hanus, J.; Marchis, F.; Durech, J. (2013). "Sizes of main-belt asteroids by combining shape models and Keck adaptive optics observations." *Icarus* **226**, 1045-1057.

Harris, A.W.; Young, J.W.; Scaltriti, F.; Zappala, V. (1984). "Lightcurves and phase relations of the asteroids 82 Alkmene and 444 Gyptis." *Icarus* **57**, 251-258.

Kaasalainen, M; Torppa, J. (2001). "Optimization Methods for Asteroid Lightcurve Inversion. I Shape Determination." *Icarus* **143**, 24-36.

Kaasalainen, M; Torppa, J.; Muinonen, K. (2001). "Optimization Methods for Asteroid Lightcurve Inversion. II The complete Inversion Problem." *Icarus* **153**, 37-51.

Koff, R.A. (2002). "Lightcurve Photometry of Asteroid (1248) Jugurtha." *Minor Planet Bull.* **29**, 75-76.

Marciniak, A.; Bartczak, P.; Santana-Ros, T.; Michalowski, T.; Antonini, P. and 33 colleagues (2012). "Photometry and models of selected main belt asteroids. IX. Introducing interactive service for asteroid models." *Astron. Astrophys.* **545**, A131.

Martikainen, J.; Muinonen, K.; Penttila, A.; Cellino, A.; Wang, X.-B. (2021). "Asteroid absolute magnitudes and phase curve parameters from Gaia photometry." *Astron. Astrophys.* **649**, A98.

Oey, J.; Williams, H.; Groom, R.; Pray, D.; Benishek, V. (2017). "Lightcurve Analysis of Binary and Potential Binary Asteroids in 2015." *Minor Planet Bull.* **44**, 193-199.

Polakis, T. (2018). "Lightcurve Analysis for Eleven Main-belt Asteroids." *Minor Planet Bull.* **45**, 199-203.

Pollock, J.; Caton, D.; Hawkins, R.; Pravec, P.; et al. (2015). *CBET* **4206**.

Pravec, P.; Wolf, M.; Sarounova, L. (2007web). <http://www.asu.cas.cz/~ppracvec/neo.htm>

Slivan, S.M. (2012). "Epoch Data in Sidereal Period Determination. I. Initial Constraint from Closest Epochs." *Minor Planet Bull.* **39**, 204-206.

Slivan, S.M. (2013). "Epoch Data in Sidereal Period Determination II. combining Epochs from Different Apparitions." *Minor Planet Bull.* **40**, 45-48

Stephens, R.D. (2007). "Photometry from GMARS and Santana Observatories - April to June 2007." *Minor Planet Bull.* **34**, 102-103.

Warner, B.D.; Harris, A.W.; Pravec, P. (2009). "The Asteroid Lightcurve Database." *Icarus* **202**, 134-146. <https://minplanobs.org/alcddef/index.php>

Worman, W.E.; Olson, M.P. (2004). "CCD photometry of 1248 Jugurtha". *Minor Planet Bull.* **31**, 42.

LIGHTCURVES OF ELEVEN ASTEROIDS

Eric V. Dose
3167 San Mateo Blvd NE #329
Albuquerque, NM 87110
mp@ericdose.com

(Received: 2024 July 13)

We present lightcurves and synodic rotation periods for eleven asteroids including the family parent asteroids 1911 Schubart and 2085 Henan.

We present asteroid lightcurves obtained via the workflow process described by Dose (2020) and later improved (Dose, 2021). This workflow applies to each image, which includes an ensemble of typically 25-80 nearby comparison ("comp") stars selected from the ATLAS refcat2 catalog (Tonry et al., 2018). This abundance of comp stars and our custom diagnostic plots allow for rapid identification and removal of outlier, variable, and poorly measured comp stars.

The product of this custom workflow is one night's time series of absolute Sloan r' (SR) magnitudes for one target asteroid. These absolute magnitudes are corrected for instrument transforms, sky extinction, and image-to-image ("cirrus") fluctuations, and thus they represent absolute magnitudes at the top of earth's atmosphere. These magnitudes are imported directly into *MPO Canopus* software (Warner, 2021) where they are adjusted for distance and phase-angle dependence, then fit by Fourier analysis including identifying any aliases, and plotted.

Phase-angle corrections are made by applying an *H-G* model and finding the *G* value that minimizes best-fit RMS error across all nights' data for that apparition. When we cannot estimate such a *G* value, usually due to a narrow range of phase angles, we apply the Minor Planet Center's default value of 0.15. No nightly zero-point adjustments (Delta Comps in *MPO Canopus*) were made to any session, other than by estimating *G*.

Lightcurve Results

Eleven asteroids were observed from New Mexico Skies observatory at 2310 meters elevation in southern New Mexico. Images were acquired with: a 0.50-m PlaneWave OTA on a PlaneWave L-500 mount and equatorial wedge, and a SBIG AC4040M CMOS camera cooled to -22°C (or to -15°C after April 22) and fitted with a Schott GG495 yellow filter.

This equipment was operated remotely via *ACP* software (DC-3 Dreams), running one-night plan files generated by python scripts (Dose, 2020). Exposure times targeted 2.5-5 millimagitudes uncertainty in asteroid instrumental magnitude, subject to a minimum exposure of 90 seconds to ensure suitable comp-star photometry, and to a maximum of 480 seconds.

FITS images were calibrated using temperature-matched, exposure-matched, median-averaged dark images and recent flat images of a flux-adjustable light panel. Calibrated images were plate-solved by *TheSkyX* (Software Bisque) and target asteroids were identified in *Astrometrica* (Herbert Raab). All photometric images were visually inspected; the author excluded images with inadequate tracking or seeing quality, excessive interference by cloud or moon, or having stars, satellite tracks, cosmic ray artifacts, residual image artifacts, or other apparent light sources within 12 arcseconds of the target asteroid's signal centroid. Images passing these screens were submitted to the workflow.

Number	Name	yyyy mm/dd	Phase	L _{PAB}	B _{PAB}	Period(h)	P.E.	Amp	A.E.	Grp
858	El Djezair	2024 03/22-05/27	*13.9, 14.4	214	6	29.660	0.002	0.22	0.02	MB-O
1285	Julietta	2024 02/05-05/28	*10.3, 18.9	164	-4	15.230	0.001	0.10	0.04	MB-O
1556	Wingolfia	2023-4 12/24-02/13	*6.7, 9.8	112	7	18.402	0.002	0.19	0.03	MB-O
1911	Schubart	2024 02/24-07/07	*12.1, 14.4	204	-2	11.921	0.001	0.26	0.05	SHU
1965	van de Kamp	2024 03/20-06/06	*2.0, 21.4	183	3	62.468	0.005	0.52	0.04	MB-I
2085	Henan	2024 02/13-05/06	1.4, 21.5	142	2	221.490	0.090	0.81	0.08	HEN
2410	Morrison	2024 02/19-05/25	*16.8, 26.9	182	3	274.950	0.060	0.44	0.04	MB-I
3089	Oujianquan	2024 04/23-05/27	*15.1, 4.8	244	10	14.618	0.001	0.39	0.03	MB-O
4297	Eichhorn	2024 05/02-05/18	*9.4, 5.0	236	8	4.138	0.001	0.11	0.03	MB-I
6663	Tatebayashi	2024 04/11-05/04	14.9, 10.3	225	19	17.939	0.002	0.23	0.03	EUN
7309	Shinkawakami	2024 05/06-05/25	22.0, 27.1	188	2	4.982	0.001	0.78	0.08	MB-I

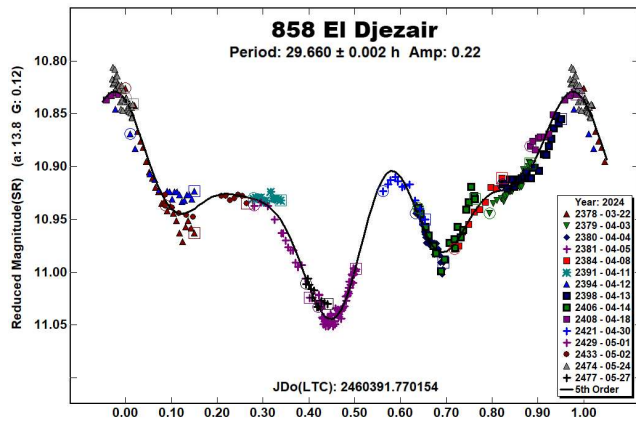
Table I. Observing circumstances and results. The phase angle is given for the first and last date. If preceded by an asterisk, the phase angle reached an extrema during the period. L_{PAB} and B_{PAB} are the approximate phase angle bisector longitude/latitude at mid-date range (see Harris et al., 1984). Grp is the asteroid family/group (Warner et al., 2009).

The GG495 light-yellow filter used here requires only modest first-order transforms to yield magnitudes in the standard Sloan r' (SR) passband. In our hands, using this (rather than a clear filter or no filter) improves night-to-night reproducibility to a degree outweighing loss of signal-to-noise ratio caused by ~15% loss of measured flux.

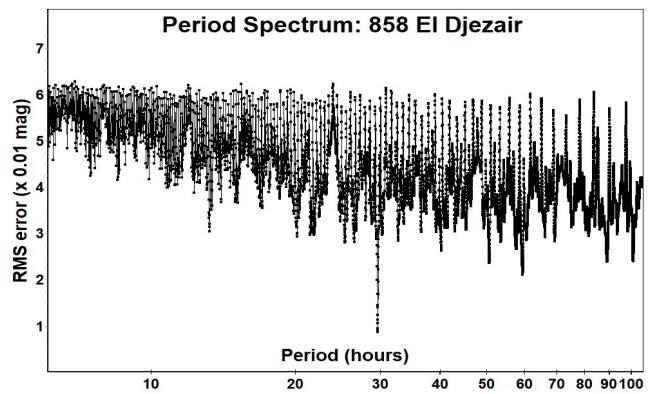
Our workflow employs as comp stars all ATLAS refcat2 entries with: distance of at least 15 arcseconds from image boundaries and from other catalogued flux sources, no catalog VARIABLE flag, SR magnitude within [-2, +1] of the target asteroid's SR magnitude on that night (except that very faint asteroids used comp stars with magnitudes in the range 14 to 16), Sloan r'-i' color value within [0.10, 0.34], and absence of variability as seen in session plots of each comp star's instrumental magnitude vs time.

In this report, "period" denotes an asteroid's synodic rotation period, and "mmag" denotes millimagitudes (0.001 magnitude). In the lightcurves below, *MPO Canopus* v10 shows "SR" for both Pan-STARRS and Sloan r' values.

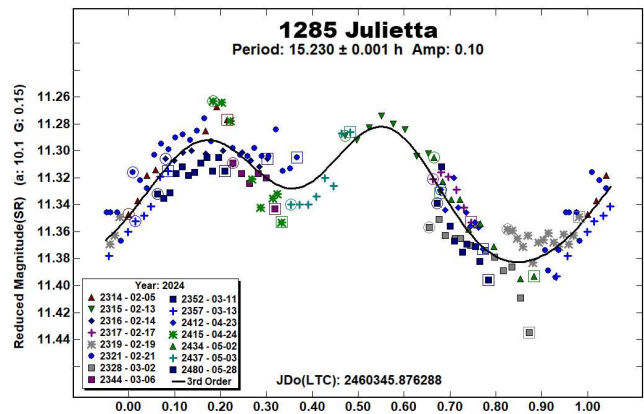
858 El Djezair. There has been no clear consensus on the rotation period of this outer main-belt asteroid (22.31 h, Warner, 2005; 19.0 h, Behrend, 2007web; 14.830 h, Polakis, 2019; 33.525 h, Colazo et al., 2021; 29.639 h, Dose, 2022; 31.16 h, Polakis, 2023). Our new data from the 2024 apparition indicate a complex lightcurve shape and a rotation period of 29.660 ± 0.002 h, both findings agreeing with our 2022 report. A *G* value of 0.12 slightly improved the Fourier fit relative to the MPC default value of 0.15; RMS error is 9 mmag.

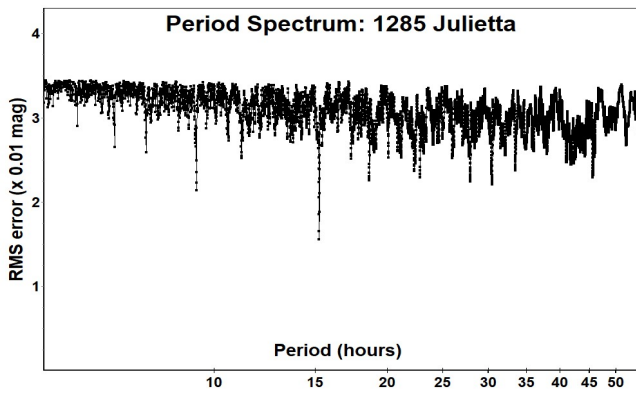


Fifteen nights of data resulted in a period spectrum dominated by one signal at our new period estimate.

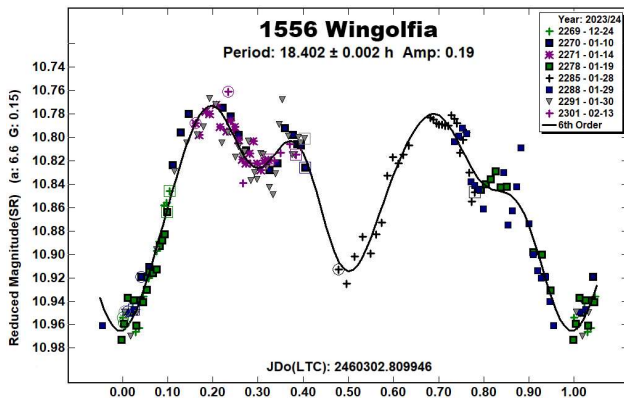


1285 Julietta. For this outer main-belt asteroid, the two previous reports of rotational period differ (6.69 h, Behrend, 2003web; 20.3 h, Behrend, 2006web). From 15 nights' observations, we report an estimate of 15.230 ± 0.001 h and a bimodal lightcurve shape. The previous 6.69 h estimate is an alias of ours by 2 periods per 24 hours. Our data are consistent with a phase-angle *G* value of 0.15, and our RMS error is 16 mmag.

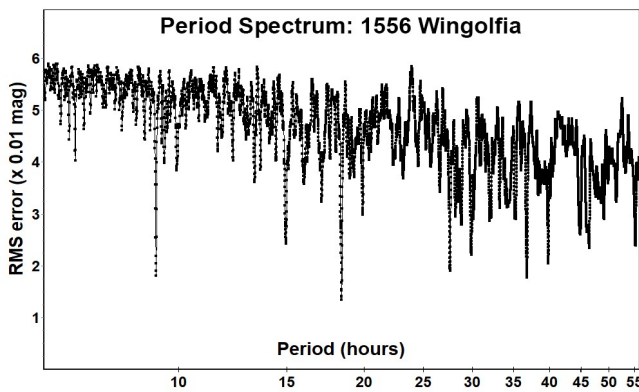




1556 Wingolfia. We report a period estimate of 18.402 ± 0.002 h for this outer main-belt asteroid, which is consistent with the sole previous known report of $P > 7$ h (Dotto et al., 1992). Our data are consistent with the MPC default G value of 0.15, and our Fourier fit RMS error is 13 mmag.

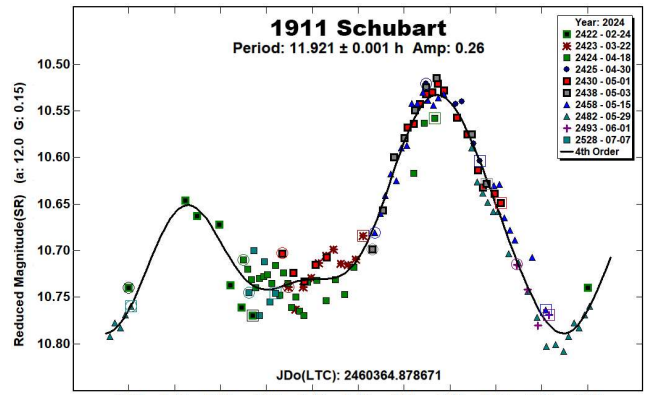


The period spectrum's primary signal is at the proposed bimodal period, with a secondary signal at half that duration.

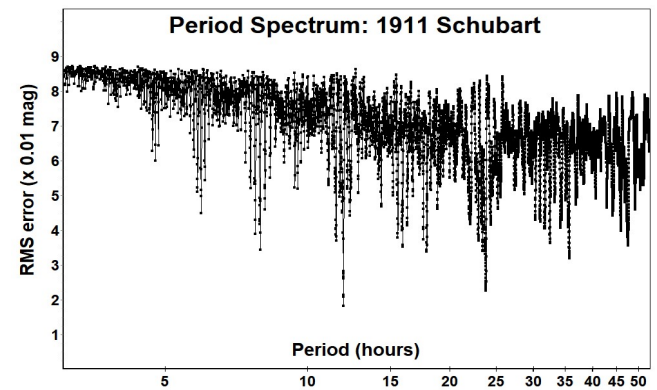


1911 Schubart. This is the parent body of the Schubart asteroid family (SHU, Family Identification Number 002; Nesvorný et al., 2015; Nesvorný et al., 2015). We estimate the rotation period to be 11.921 ± 0.001 h, in agreement with 2 of the 3 known published reports (11.915 h, Stephens, 2016; 7.9121 h, Warell, 2017; 11.930 h, Polakis, 2022). The 7.9121 h result is an alias of our result by 1 period per 24 h. Our best G estimate is 0.15, the MPC default value, and our Fourier fit RMS error is 18 mmag.

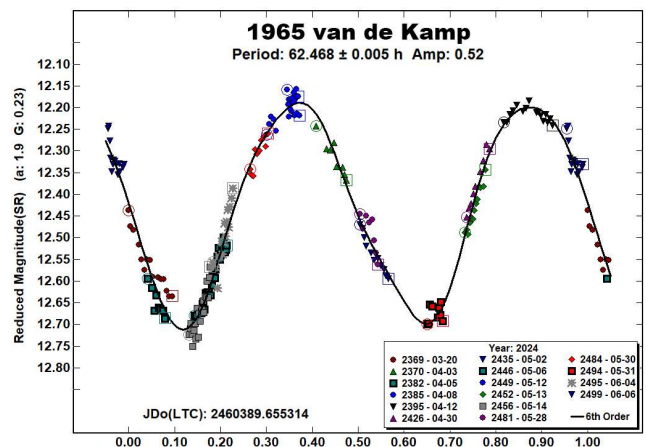
Our phase coverage suffers a gap of about 10% of the period, as do all three previously published lightcurves. This is surely due to the period's nearness to 12 hours. We urge future observers of 1911 Schubart to begin their observations early in its apparition, since it should be possible to gain full coverage within about 75 calendar days ($11.92\text{-hour period} / 0.16\text{ hours' phase advancement per day}$).



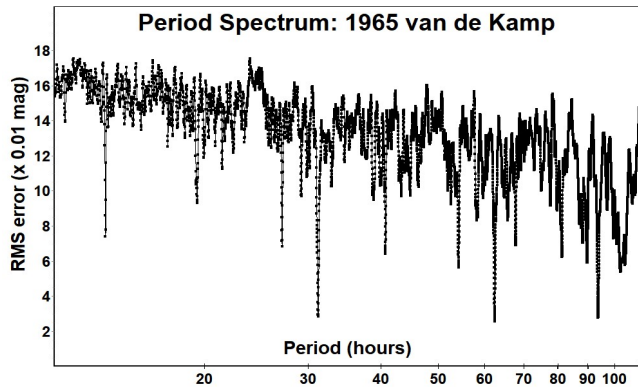
Our period spectrum is dominated by signals at the proposed period, with a secondary signal at twice that duration.



1965 van de Kamp. For this inner main-belt asteroid, we offer the first known central estimate of the rotation period as 62.468 ± 0.005 h, consistent with a previously reported lower limit of 24 hours (Hayes-Gehrke et al., 2011). Our best G estimate is 0.23, and our Fourier fit RMS error is 25 mmag.

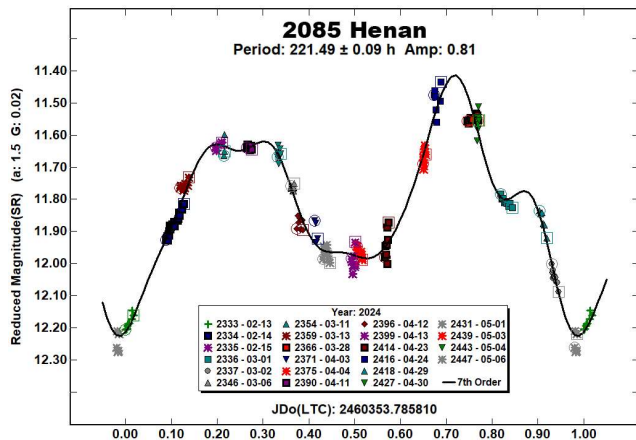


The period spectrum is dominated by our estimate of 62.468 h, and by a signal at half that duration, both signals being expected for a bimodal lightcurve of which the two halves are very similar.

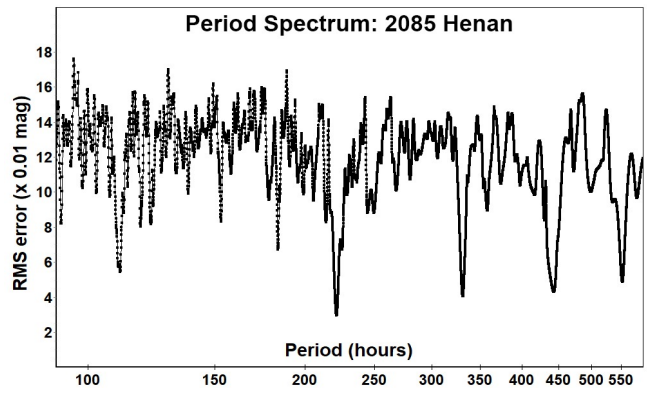


2085 Henan. This is the parent body of the Henan asteroid family (HEN, Family Identification Number 532; Nesvorný, 2015; Nesvorný et al., 2015). Estimates of its rotation period have most recently been near 220 h (>24 h, Behrend, 2004web; 110 h, Devogèle et al., 2017; 221.71 h, Āurech et al., 2020; 221.70955 h, Martikainen et al., 2021; 216.89 h, Dose, 2023).

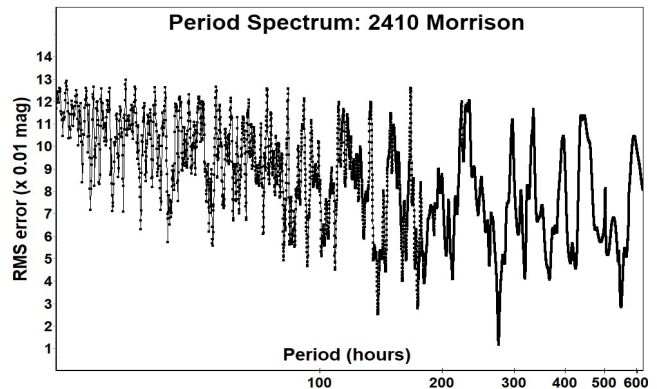
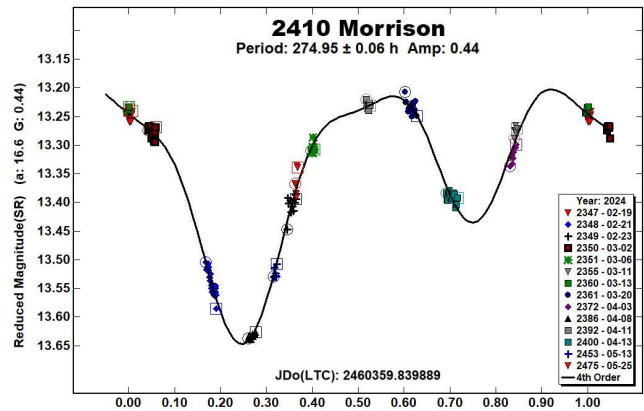
During its 2024 apparition, we observed 2085 Henan on 22 nights over 9 rotation periods, yielding practically complete coverage of the lightcurve, and from which we report a new period estimate of 221.49 ± 0.09 h. We detect no significant precession (“tumbling”) effect that was suggested in our 2023 report. Our G estimate is 0.02 — indeed it was difficult to get a stable Fourier solution with the MPC default value of 0.15. Our RMS error of fit is 30 mmag.



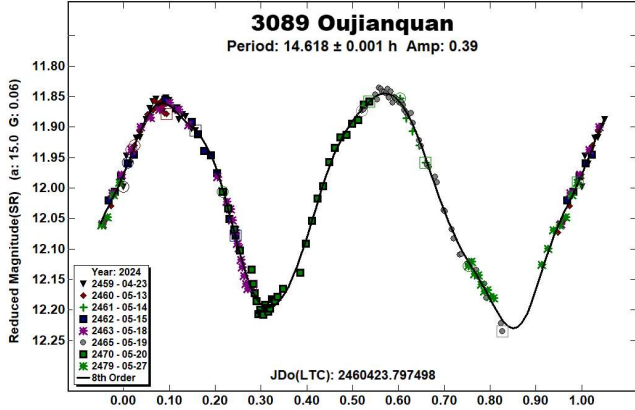
The period spectrum’s primary signal is at our 221.49 h estimate, with secondary signals at multiples of one-half period, as expected for a clearly bimodal lightcurve.



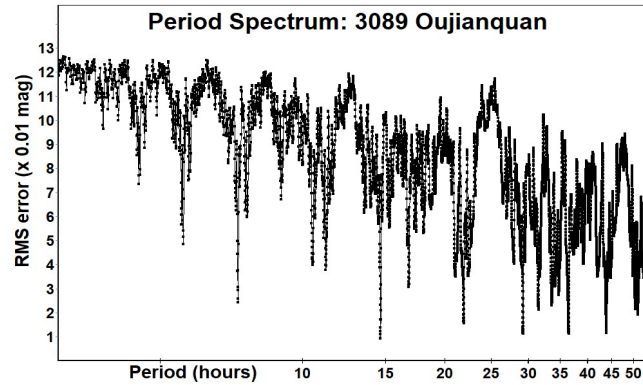
2410 Morrison. For this inner main-belt asteroid, we report a period of 274.95 ± 0.06 h. We have found no previously published period reports. The lightcurve is bimodal with differing brightness minima, and we found no evidence of precession (“tumbling”) effect. Our best G value was 0.44; we could not obtain a stable Fourier fit with the MPC default value of 0.15. Our RMS error is 12 mmag.



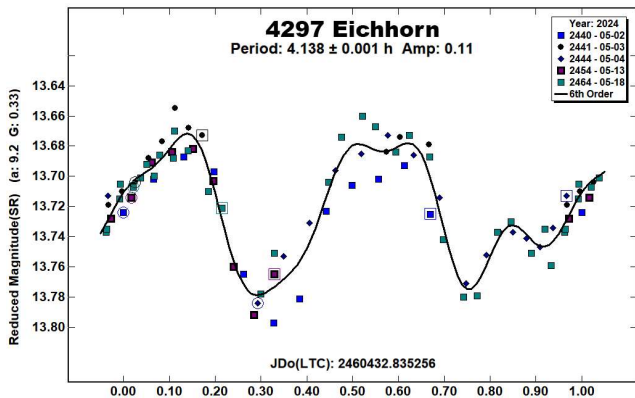
3089 Oujianquan. We report a rotation period of 14.618 ± 0.001 h for this outer main-belt asteroid, in agreement with Clark’s later estimate (14.328 h, 2015) and with the survey result of Āurech et al. (14.6194 h, 2020). Clark’s earlier estimate (2007) of 11.198 h is an alias of our estimate by 0.5 period per 24 h. Our lightcurve is clearly bimodal with nearly equal halves that differ mainly in each shape’s approximating the time-reverse of the other. Our best G value was 0.06, and the RMS error of fit is 9 mmag.



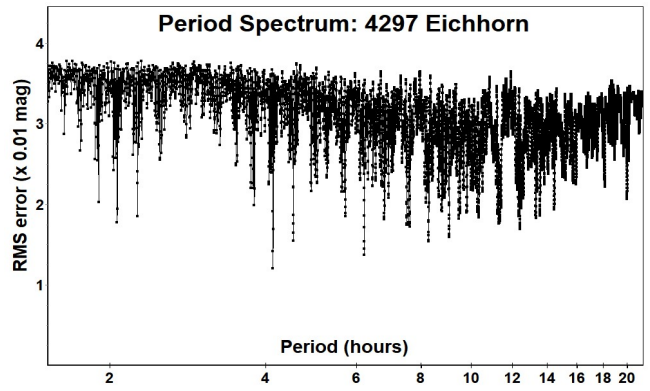
The period spectrum’s primary signal is at our proposed period, with secondary signals at multiples of one-half period, as is characteristic of bimodal lightcurves with nearly equal halves.



4297 Eichhorn. We report a rotation period of 4.138 ± 0.001 h for this inner main-belt asteroid, in fair agreement with the sole known previous report (4.105 h, Salvaggio et al., 2018). Our best G value is 0.33, and our Fourier fit RMS error is 12 mmag.

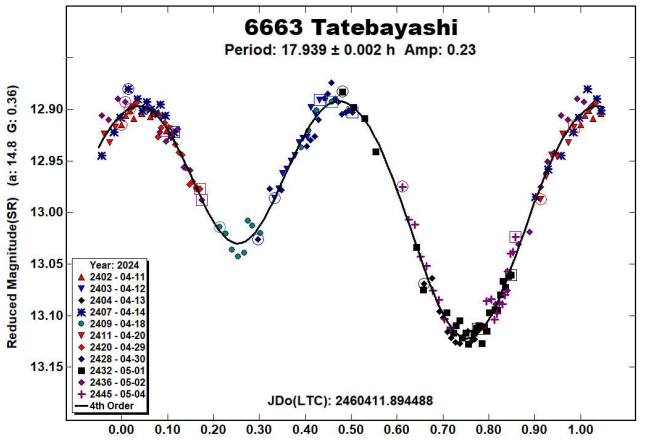


Our period spectrum’s strongest signal is at our proposed period, but with many secondary signals.

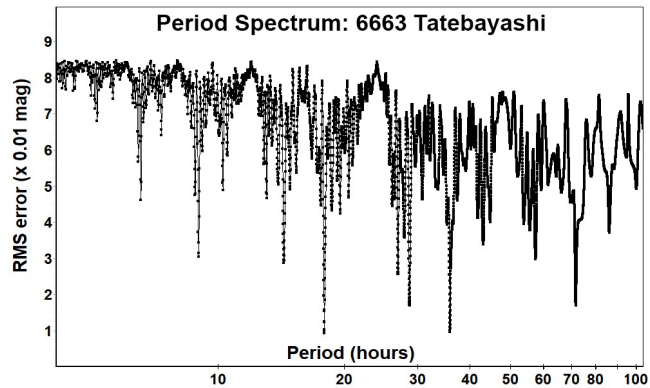


In retrospect, we took too few nights of data for this relatively faint, low-amplitude asteroid. We encourage follow-up observations of (4297) Eichhorn. Its next favorable opposition will be in 2028, with negative declinations benefitting the Southern Hemisphere, but with most of both hemispheres able to cover the full period within a given night.

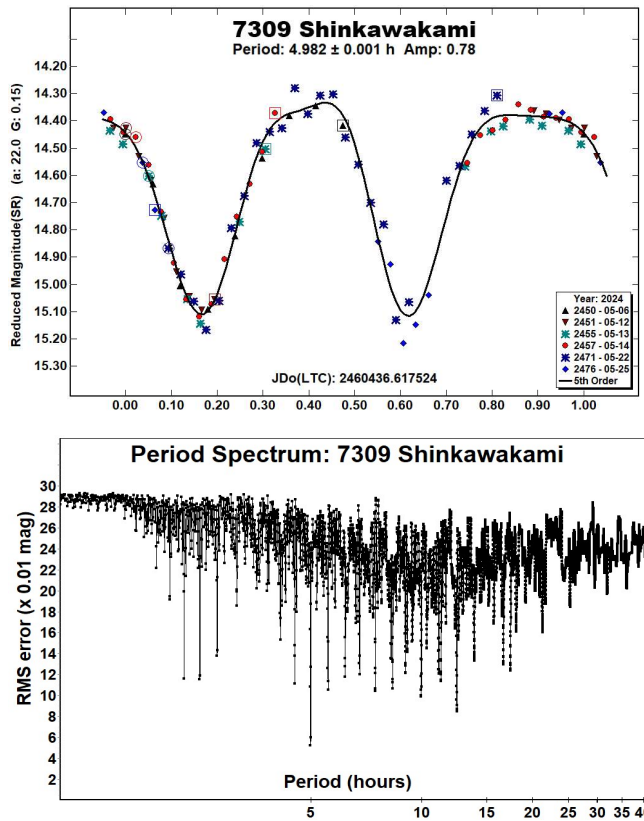
6663 Tatebayashi. For this Eunomia-family asteroid, we report a rotation period of 17.939 ± 0.002 h, at variance from the sole known previous report (4.8 h, Aznar, 2011 web). Our best G value is 0.36, and our Fourier fit RMS error is 9 mmag.



Our period spectrum shows primary signals at our proposed period and at twice that duration. The previously reported 4.8 h period does not appear in our period spectrum, and we cannot account for it either by aliasing or by multiples or fractions of our proposed period.



7309 Shinkawakami. We found this inner main-belt asteroid in images of 1965 van de Kamp and estimate its rotation period to be 4.982 ± 0.001 h, with a bimodal lightcurve of very high amplitude. We know of no previous reports of its lightcurve or period. Our best G estimate equals the MPC default value of 0.15, and our RMS error is 43 mmag.



Acknowledgements

The author thanks all contributors to the ATLAS paper (Tonry et al., 2018) for providing openly and without cost the ATLAS refcat2 catalog. Our work also makes extensive use of the python language interpreter and of several supporting packages (notably: astropy, ccdproc, ephemeris, matplotlib, pandas, photutils, requests, skyfield, and statsmodels), all made available openly and without cost.

References

- Aznar, A. (2011web). Retrieved from LCDB July 9 2024.
- Behrend, R. (2003web, 2004web, 2006web, 2007web). Observatoire de Genève web site. http://obswww.unige.ch/~behrend/page_cou.html
- Clark, M. (2007). "Lightcurve Results for 1318 Nerina, 2222 Lermontov, 3015 Candy, 2089 Oujianquan, 3155 Lee, 6410 Fujiwara, 6500 Kodaira, (8290) 1992 NP, 9566 Rykhlova, (42923) 1999 SR18, and 2001 FY." *Minor Planet Bull.* **34**, 19-22.
- Clark, M. (2015). "Asteroid Photometry from the Preston Gott Observatory." *Minor Planet Bull.* **42**, 15-20.

Colazo, M.; Stechina, A.; Fornari, C.; Suárez, N.; Melia, R.; Morales, M.; Bellocchio, E.; Pulver, E.; Speranza, T.; Scotta, D.; Wilberger, A.; Mottino, A.; Meza, E.; Romero, F.; Tourne Passarino, P.; Suligoy, M.; Llanos, R.; Chapman, A.; Martini, M.; Colazo, C. (2021). "Asteroid Photometry and Lightcurve Analysis at GORA's Observatories, Part IV." *Minor Planet Bull.* **48**, 140-143.

Devogèle, M. and 53 colleagues (2017). "Shape and spin determination of Barbarian asteroids." *Astron. Astrophys.* **607**, A119.

Dose, E.V. (2020). "A New Photometric Workflow and Lightcurves of Fifteen Asteroids." *Minor Planet Bull.* **47**, 324-330.

Dose, E.V. (2021). "Lightcurves of Nineteen Asteroids." *Minor Planet Bull.* **48**, 69-76.

Dose, E.V. (2022). "Lightcurves of Seventeen Asteroids." *Minor Planet Bull.* **49**, 141-148.

Dose, E.V. (2023). "Lightcurves of Twelve Asteroids." *Minor Planet Bull.* **50**, 151-157.

Dotto, E.; Barucci, M.A.; Fulchignoni, M.; Di Martino, M.; Rotundi, A.; Burchi, R.; Di Paolantonio, A. (1992). "M-type asteroids: rotational properties of 16 objects." *Astrophys. J. Suppl. Series* **95**, 195-211.

Đurech, J.; Tonry, J.; Erasmus, N.; Denneau, L.; Heinze, A.N.; Flewelling, H.; Vančo, R. (2020). "Asteroid models reconstructed from ATLAS photometry." *Astron. Astrophys.* **643**, A59.

Harris, A.W.; Young, J.W.; Scaltriti, F.; Zappala, V. (1984). "Lightcurves and phase relations of the asteroids 82 Alkmene and 444 Gyptis." *Icarus* **57**, 251-258.

Hayes-Gehrke, M.N.; Fromm, T.; Junghans, P.; Lochan, I.; Murphy, S. (2011). "Lightcurves for 1965 van de Kamp and 4971 Hoshinohiroba." *Minor Planet Bull.* **38**, 204-205.

Martikainen, J.; Muinonen, K.; Penttilä, A.; Cellino, A.; Wang, X.-B. (2021). "Asteroid absolute magnitudes and phase curve parameters from *Gaia* photometry." *Astron. Astrophys.* **649**, A98.

Nesvorný, D. (2015). "Nesvorný HCM Asteroids Families V3.0." NASA Planetary Data Systems, id. EAR-A-VARGBET-5-NESVORNYFAM-V3.0.

Nesvorný, D.; Broz, M.; Carruba, V. (2015). "Identification and Dynamical Properties of Asteroid Families." In *Asteroids IV* (P. Michel, F. DeMeo, W.F. Bottke, R. Binzel, Eds.). Univ. of Arizona Press, Tucson, also available on astro-ph.

Polakis, T. (2019). "Lightcurves of Twelve Main-belt Minor Planets." *Minor Planet Bull.* **46**, 287-292.

Polakis, T. (2022). "Lightcurves for Thirteen Minor Planets." *Minor Planet Bull.* **49**, 131-135.

Polakis, T. (2023). "Lightcurves for Ten Minor Planets." *Minor Planet Bull.* **50**, 211-214.

Salvaggio, F.; Banfi, M.; Marchini, A.; Papini, R. (2018). "Lightcurve and Rotation Period Determination for 2578 Saint-Exupery, 4297 Eichhorn, 10132 Lummelunda and (21766) 1999 RW208." *Minor Planet Bull.* **45**, 171-173.

Stephens, R.D. (2016). "Asteroids observed from CS3: 2016 April-June." *Minor Planet Bull.* **43**, 336-338.

Tonry, J.L.; Denneau, L.; Flewelling, H.; Heinze, A.N.; Onken, C.A.; Smartt, S.J.; Stalder, B.; Weiland, H.J.; Wolf, C. (2018). "The ATLAS All-Sky Stellar Reference Catalog." *Astrophys. J.* **867**, A105.

Warell, J. (2017). "Lightcurve Observations of Nine Main-belt Asteroids." *Minor Planet Bull.* **44**, 304-305.

Warner, B.D. (2005). "Asteroid Lightcurve Analysis at the Palmer Divide Observatory - Spring 2005." *Minor Planet Bull.* **32**, 90-92.

Warner, B.D. (2021). *MPO Canopus* Software, version 10.8.4.11. BDW Publishing. <http://www.bdwpublishing.com>

Warner, B.D.; Harris, A.W.; Pravec, P. (2009). "The asteroid lightcurve database." *Icarus* **202**, 134-146. <https://minplanobs.org/MPInfo/php/lcdb.php>

ROTATIONAL PERIOD AND LIGHTCURVE DETERMINATION FOR SEVEN MINOR PLANETS

Mike Wiles
Chiricahua Skies Observatory
4126 N. Twilight Cir.
Mesa, AZ 85207
mikewilesaz@gmail.com

(Received: 2024 July 11)

Photometric measurements of CCD observations on five main-belt asteroids were made from 2023 December through 2024 June. Phased lightcurves were created for each one. Three of the asteroids have no prior published period solutions. All the data have been submitted to the ALCDEF database.

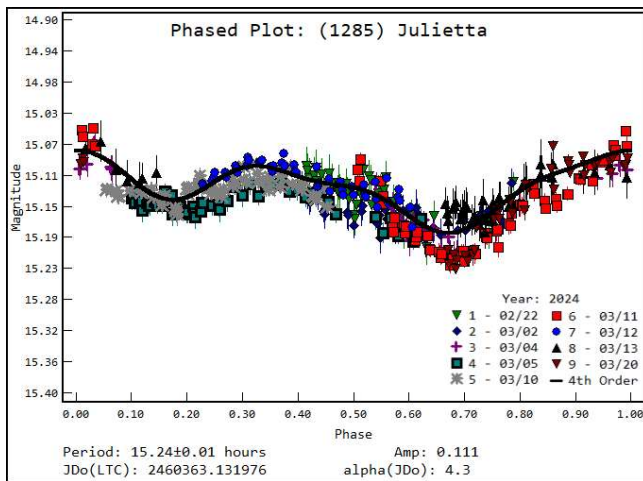
Photometric CCD observations of five main-belt asteroids were performed at Chiricahua Skies Observatory (MPC V43) near Sunizona, AZ. Images were taken using a 0.35m *f*/7.2 Corrected Dall-Kirkham telescope and Teledyne CCD47-10 sensor yielding an image scale of 1.05 arcsec/pixel. Table I shows observing circumstances and results. All images for these observations were obtained between 2023 December and 2024 June.

Data reduction and period analysis were done using *Tycho* (Parrott, 2024). The asteroid and five or more comparison stars were measured. Comparison stars were selected with colors within the range of $0.5 < B-V < 0.95$ to correspond with color ranges of asteroids.

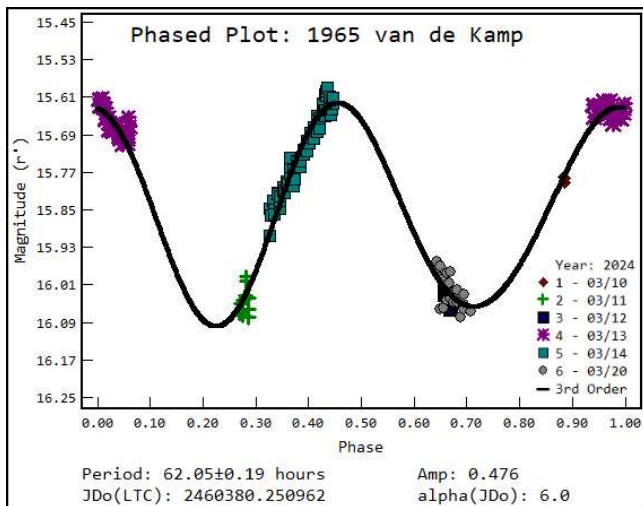
Comparison star magnitudes were obtained from the ATLAS catalog (Tonry et al., 2018), which is incorporated directly into *Tycho*. A measuring aperture equal to $4 \times$ FWHM of the target was used for asteroids and comp stars. This was typically a radius of 6 pixels on the measuring aperture. Interference from field stars resulted in the exclusion of affected observations. Period determination was done using *Tycho*.

Asteroids were selected from the CALL website (Warner, 2011), either for having uncertain periods or no reported period at all. In this set of observations, three of the seven asteroids had no previous period analysis. The Asteroid Lightcurve Database (LCDB) Warner et al. (2009) was consulted to locate previously published results. All new data for these asteroids has been submitted to the ALCDEF database.

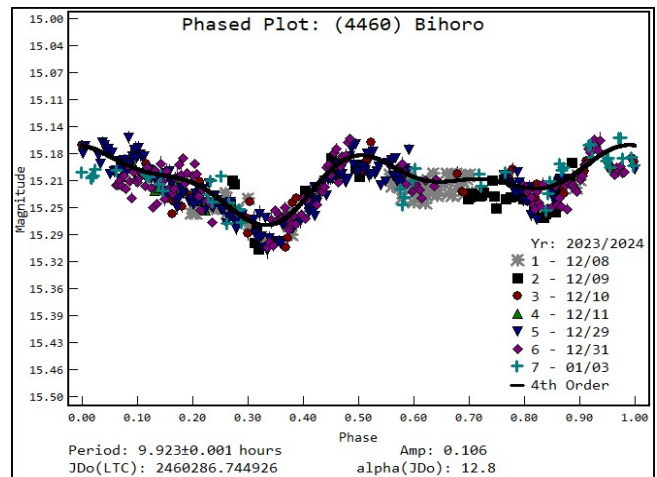
1285 Julietta has several varying periods published in the LCDB between 2003 and 2008 including Behrend (2003web, 6.69 ± 0.05 h), Behrend (2006web, 20.3 ± 0.1 h), and Behrend (2008web, > 12 h). During the 2024 apparition, 432 observations were obtained over nine nights to calculate a period solution of 15.24 ± 0.01 hours and an amplitude of 0.11 ± 0.02 magnitude. This period does not agree with previously published solutions.



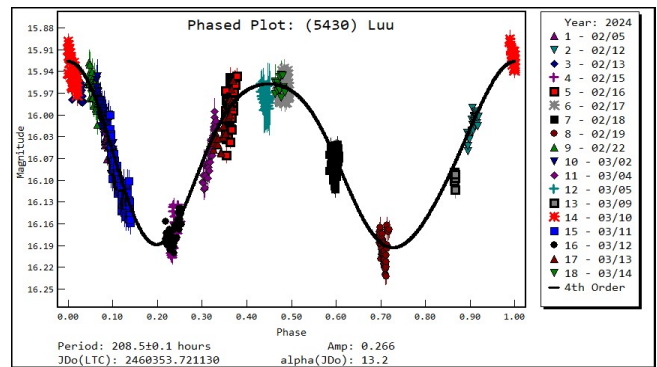
1965 van de Kamp is an inner main-belt asteroid discovered on Palomar Schmidt plates in 1960 by van Houten and van Houten. Hayes-Gehrke et al. (2011) reported that their data was inconclusive, but that the solution was probably > 36 hours. The author was able to determine a period solution of 62.05 ± 0.19 hours from data collected in 2024 March. CCD images were collected over six nights resulting in 170 observations. Because of the incomplete coverage of the entire phase, this solution should be considered one of low confidence. This asteroid is worthy of additional study on its next apparition. Amplitude of the lightcurve is 0.48 ± 0.02 magnitude.



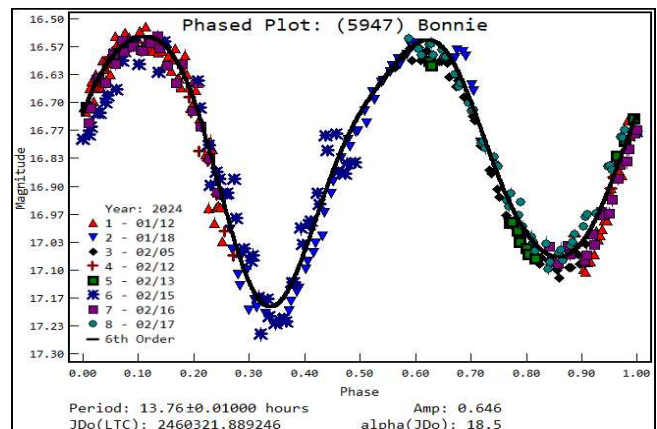
4460 Bihoro was discovered in 1990 February by Endate and Watanabe at Kitami Observatory in eastern Hokkaido, Japan. No previous period solutions have been reported in the LCDB. In 2023 December and 2024 January, observations were conducted over a period of seven nights, resulting in 542 photometric observations. The lightcurve constructed from the data yields a period solution of 9.923 ± 0.001 h. The amplitude of the lightcurve is 0.11 ± 0.02 mag.



5430 Luu is a Phocaea family asteroid discovered by Carolyn Shoemaker at Palomar in 1988. When consulting the LCDB, multiple period solutions were found. Warner (2006) published a period of 13.55 ± 0.02 h. Behrend (2010web; 2021web) reported periods of 4.44 ± 0.05 h and 36.2 ± 1.0 h, respectively. In 2024, observations were made on 18 days of a relatively long 37-day window. During that time, a total of 739 images were captured and used to calculate a period of 208.5 ± 0.1 h, disagreeing with the previously published periods. The amplitude is 0.27 ± 0.02 mag.



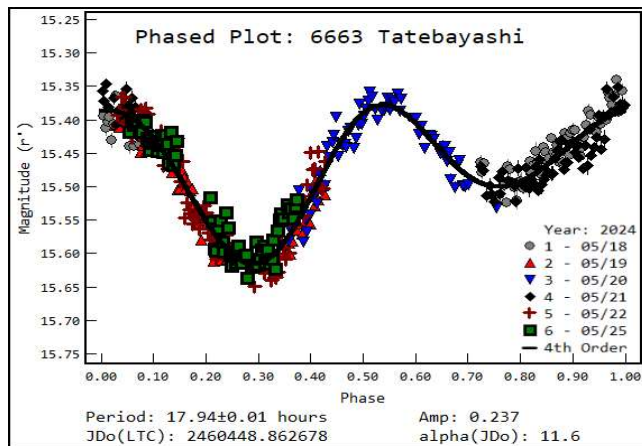
5947 Bonnie is a main-belt asteroid discovered by Carolyn Shoemaker at Palomar in 1985. Bonamico (2020) published a period of 13.414 ± 0.003 h. During an eight-night interval, 355 images were obtained. Constructing a lightcurve with these measurements yielded a period of 13.76 ± 0.01 h, in close agreement with Bonamico's previously published result. The amplitude is 0.65 ± 0.04 mag.



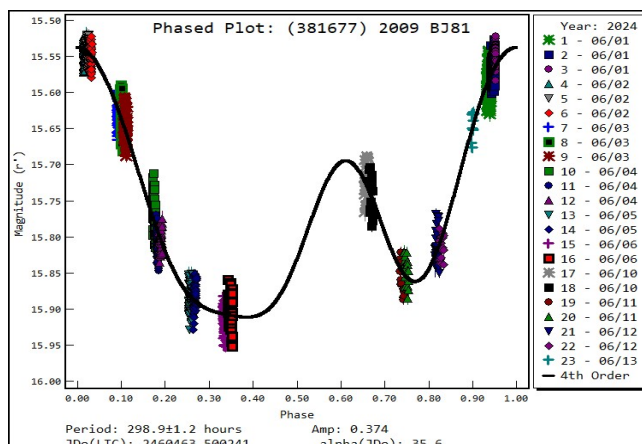
Number	Name	yyyy mm/dd	Phase	L _{PAB}	B _{PAB}	Period(h)	P.E.	Amp	A.E.	Grp
1285	Julietta	24/02/22-03/20	*4.4, 6.1	164	-3	15.24	0.01	0.11	0.02	MB-I
1965	van de Kamp	24/03/10-03/20	1.9, 6.0	183	3	62.05	0.19	0.48	0.02	MB-I
4460	Bihoro	23/12/08-01/03	11.4, 12.8	90	29	9.923	0.001	0.11	0.16	MB-I
5430	Luu	24/02/05-03/14	*15.26, 14.94	160	21	208.5	0.1	0.27	0.01	PHO
5947	Bonnie	24/01/12-02/17	9.8, 18.6	159	16	13.76	0.01	0.65	0.04	MB-M
6663	Tatebayashi	24/05/18-05/25	11.6, 13.4	227	19	17.94	0.01	0.24	0.02	MB-I
381677	2009 BJ81	24/06/01-06/13	25.9, 36.9	239	16	298.9	1.2	0.37	0.02	NEA

Table I. Observing circumstances and results. The phase angle is given for the first and last date. If preceded by an asterisk, the phase angle reached an extrema during the period. L_{PAB} and B_{PAB} are the approximate phase angle bisector longitude/latitude at mid-date range (see Harris et al., 1984). Grp is the asteroid family/group (Warner et al., 2009). PHO: Phocaea group/family.

6663 Tatebayashi was discovered in 1993 by T. Kobayashi at Oizumi. In the LCDB, the only reported period solution is 4.8 ± 0.1 hours by Aznar (2011web). The citation in the LCDB does not provide further reference information, and the author was unable to locate corroborating reference material for that published solution. CCD images were collected over six nights during 2024 May, resulting in 461 observations. The calculated period is 17.94 ± 0.01 hours with an amplitude of 0.24 ± 0.02 magnitude. This disagrees with the published period by Aznar.



(381677) 2009 BJ81 is a near-Earth asteroid discovered in 2008 October by Spacewatch at Kitt Peak. Warner and Stephens (2019) published a period of 325 ± 0.1 hours. In 2024 May, the asteroid passed within 0.12 AU of Earth. During that time, it was observed on ten nights. The calculated period from these observations is 298.9 ± 1.2 hours with an amplitude of 0.37 ± 0.02 magnitude. This is in agreement with the period by Warner and Stephens.



Acknowledgements

The author would like to thank Tom Polakis for his many years of encouragement and mentorship. Thanks also go out to Daniel Parrott for his responsive support of questions regarding the *Tycho* software package.

References

- Aznar, A. (2011web). Web reference, as cited in LCDB. Inaccessible directly on 2024-07-01.
- Behrend, R. (2003web; 2006web; 2008web; 2010web; 2021web). Observatoire de Geneve web site. <http://obswww.unige.ch/~behrend/page4cou.html>
- Bonamico, R. (2020). "Determining the Rotational Periods and Lightcurves of Three Main-Belt Asteroids." *Minor Planet Bulletin* **47**, 347.
- Harris, A.W.; Young, J.W.; Scaltriti, F.; Zappala, V. (1984). "Lightcurves and phase relations of the asteroids 82 Alkeme and 444 Gyptis." *Icarus* **57**, 251-258.
- Hayes-Gehrke, M.; Fromm, T.; Junghans, P.; Lochan, I.; Murphy, S.: (2011). "Lightcurves for 1965 van de Kamp and 4971 Hoshinohiroba." *Minor Planet Bulletin* **38**, 204-205.
- Parrot, D. (2024). Tycho software. <https://www.tycho-tracker.com>
- Tonry, J.L.; Denneau, L.; Flewelling, H.; Heinze, A.N.; Onken, C.A.; Smartt, S.J.; Stalder, B.; Weiland, H.J.; Wolf, C. (2018). "The ATLAS All-Sky Stellar Reference Catalog." *Astrophys. J.* **867**, A105.
- Warner, B.D. (2006). "Asteroid lightcurve analysis at the Palmer Divide Observatory - March - June 2006." *Minor Planet Bulletin* **33**, 85.
- Warner, B.D. (2011). Collaborative Asteroid Lightcurve Link website. <http://www.minorplanet.info/call.html>
- Warner, B.D.; Harris, A.W.; Pravec, P. (2009). "The Asteroid Lightcurve Database." *Icarus* **202**, 134-146. Updated 2023 Oct. <http://www.minorplanet.info/lightcurvedatabase.html>
- Warner, B.D.; Stephens, R.: (2019). "Near-Earth Asteroid Lightcurve Analysis at the Center for Solar System Studies: 2019 January-April." *Minor Planet Bulletin* **46**, 304-314.

PHOTOMETRIC INVESTIGATION AND ROTATIONAL CHARACTERIZATION OF SEVEN MAIN-BELT ASTEROIDS

Stephen M. Brincat
Flarestar Observatory (MPC: 171)
Fl.5 George Tayar Street
San Gwann SGN 3160, MALTA
stephenbrincat@gmail.com

Marek Bucek
Luckystar Observatory (MPC: M55)
Dr. Lučanského 547
Važec, 032 61 SLOVAKIA

Charles Galdies
Znith Observatory
Armonie, E. Bradford Street
Naxxar NXR 2217, MALTA

Martin Mifsud
Manikata Observatory
51, Penthouse 7, Sky Blue Court
Dun Manwel Grima Street
Manikata MLH 5013, MALTA

Normand Rivard
À la belle étoile Observatory
796, rang des Écossais
Sainte-Brigide-d'Iberville (Québec)
J0J 1X0 CANADA

Winston Grech
Antares Observatory
76/3, Kent Street
Fgura FGR 1555, MALTA

Vincent Zammit
Stellar Horizon Observatory
No.8, Maranatha, Triq Tal-Fieres
Kirkop KKP 1502, MALTA

Michael Richmond, Drew Demers, Mimi Harrison,
Sebastian Montes, Jason Sergio, Veran Stanek
RIT Observatory (MPC: 920)
Rochester Institute of Technology (RIT)
1 Lomb Memorial Dr.
Rochester, NY 14623, USA

(Received: 2024 July 8 Revised: 2024 July 22)

This study presents photometric measurements and lightcurve analysis for seven main-belt asteroids using observatories in Malta, Slovakia, Canada, and the United States. Synodic rotation periods and amplitudes were determined for 612 Veronika, 1532 Inari, 2240 Tsai, 4288 Tokyotech, 9333 Hiraimasa, (13042) 1990 QE, and (26187) 1996 XA27. These results enhance the understanding of the asteroids' rotational properties and highlight the importance of multi-site observations.

Photometric observations of seven main-belt asteroids were carried out from six observatories located on the Maltese mainland, Slovakia, Canada and the United States. Observations of asteroids for 612 Veronika, 1532 Inari, 2240 Tsai, 4288 Tokyotech, 9333 Hiraimasa, (13042) 1990 QE, and (26187) 1996 XA27 were

obtained from the observatories shown in Table I. All of our images were taken through a clear filter (or unfiltered) with Rc zero-point and calibrated through dark and flat-field subtraction.

Our equipment was either controlled remotely over the Internet or from a location near each telescope. Image acquisition was conducted via *Sequence Generator Pro* (Binary Star Software) by all Maltese Observatories. The Slovakian and Canadian observatories employed the *NINA* telescope control software (Berg, 2023) to acquire their images and for telescope automation. RIT Observatory employed *Maxim DL* (Ver. 6.16) for their observatory operations and image acquisition. For our image analysis, we used version 10 of *MPO Canopus* software (Warner, 2017), to gather differential aperture photometry and for lightcurve construction. Table I shows details of the instrumentation used and observation runs for each respective target. We used the Comparison Star Selector (CSS) feature developed by *MPO Canopus* to choose near-solar color comparison stars. All brightness measurements were based on the Asteroid Terrestrial-impact Last Alert System (ATLAS) catalogue (Tonry et al., 2018).

Observatory	Tel and Type	Camera	Observed Asteroids (#Runs)
Antares Obs.	0.28-m SCT	SBIG ST-11	9333 (6)
Flarestar Obs. (MPC: 171)	0.25-m SCT	Moravian G2-1600	612 (5) 1532 (9) 4288 (3)
Luckystar Obs. (MPC: M55)	0.25-m SCT	Atik 460EX	13042 (2) 26187 (4)
Stellar Horizon Obs.	0.30-m SCT	ASI 6200MM	1532 (1)
RIT Obs. (MPC: 920)	0.30-m SCT	ASI 6200MM	1532 (2)
A la belle étoile Obs.	0.2-m MK	Moravian G2-1600	1532 (3)
Znith Obs.	0.2-m SCT	Moravian G2-1600	1532 (1) 2240 (3)

Table I. Instrumentation and Observation Runs. SCT: Schmidt-Cassegrain; MK: Maksutov-Cassegrain

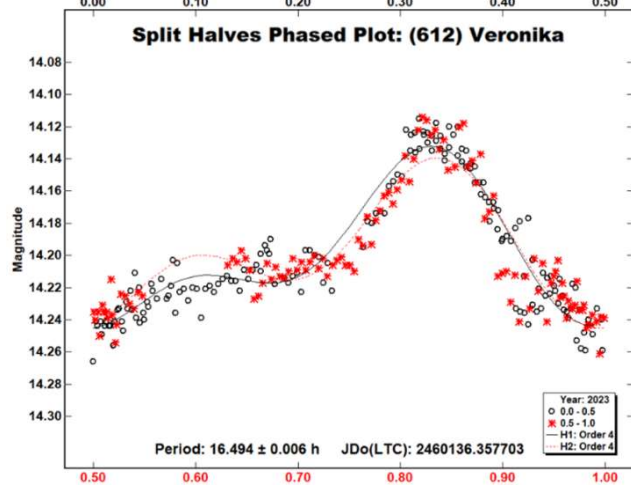
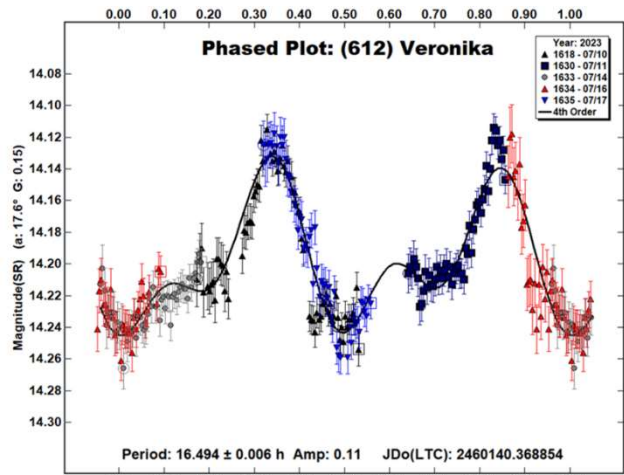
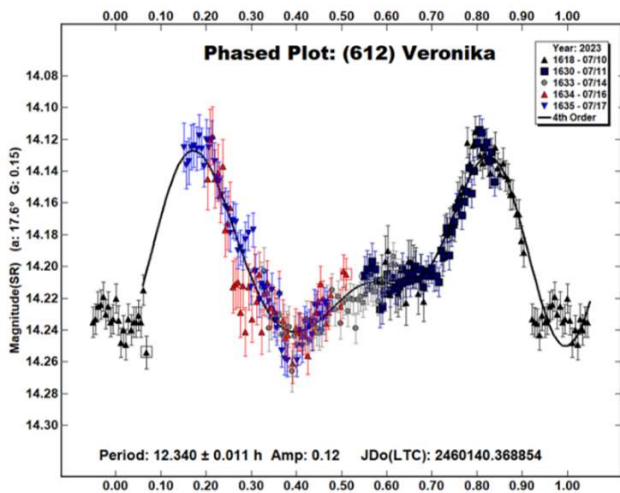
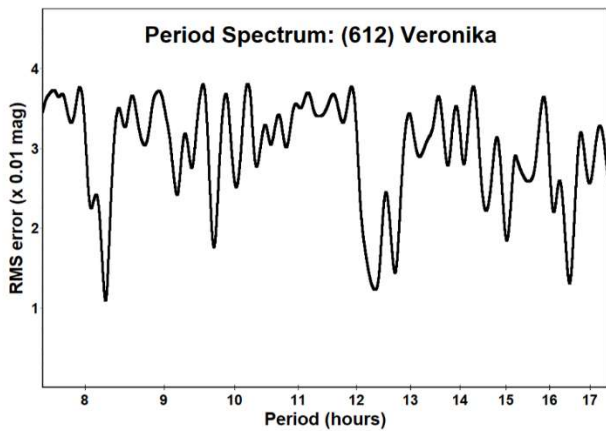
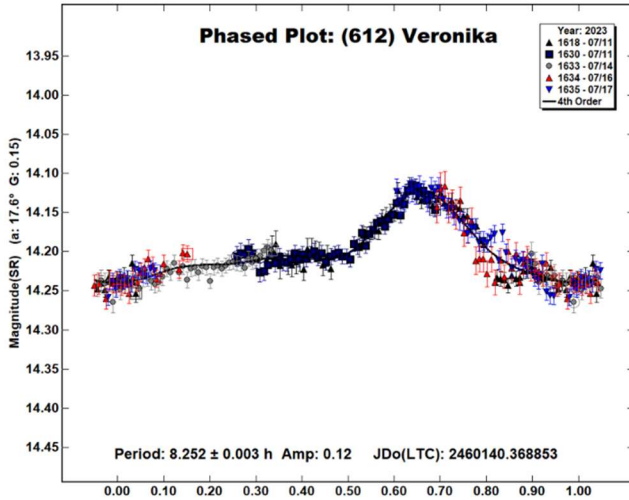
612 *Veronika* is a main-belt asteroid that was discovered on 1906 October 8 by A. Kopff at Heidelberg. Although this asteroid was named after “Veronika,” Schmadel (2012) states that the reference to this name to a person or occurrence is unknown.

According to the Small-Body Database at JPL, asteroid Veronika has an estimated diameter of 138.767 ± 0.519 km based on an absolute magnitude (H) of 10.93. It orbits the sun with a semi-major axis of 3.153 AU with an eccentricity of 0.259 and period of 5.559 years (JPL, 2024). The Asteroid Lightcurve Database (LCDB; Warner et al., 2009) lists asteroid 612 Veronika as having a rotation period of 8.243 h with an amplitude that ranges from 0.09 to 0.14 mag.

(612) Veronika was observed from Flarestar Observatory over five nights from 2023 July 11-17. Data analysis derived its synodic rotation period as 8.252 ± 0.003 h with an amplitude of 0.12 ± 0.03 mag. This solution is in line with the results published in the LCDB database. The resultant period spectrum reveals two other possible periods of 12.340 ± 0.011 h with an amplitude of 0.12 mag and

another at double the period of the 8.252 h solution at 16.494 ± 0.006 h with an amplitude of 0.11 mag.

The split-halves plot of the 16.494 h period shows that the two halves of the double period are morphologically quite similar, thus allowing for the published period of 8.252 h. Hence, we believe that the 8.252 h is the correct period. The period spectrum distinctly shows a possible solution of 12.340 h, but this likely a half-rotation period alias since it is half-way between 8.25 h and 16.50 h.



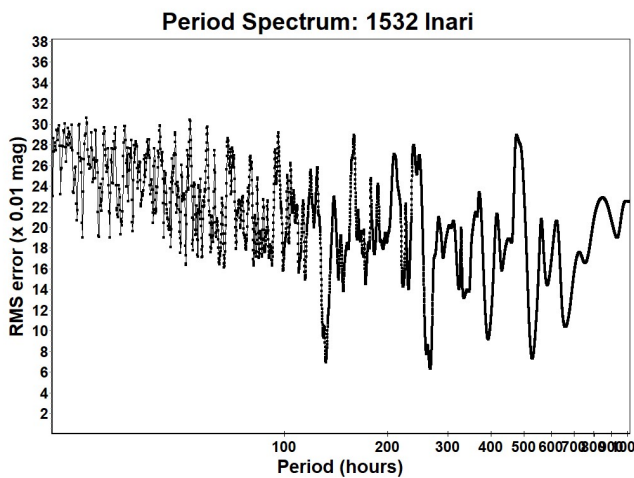
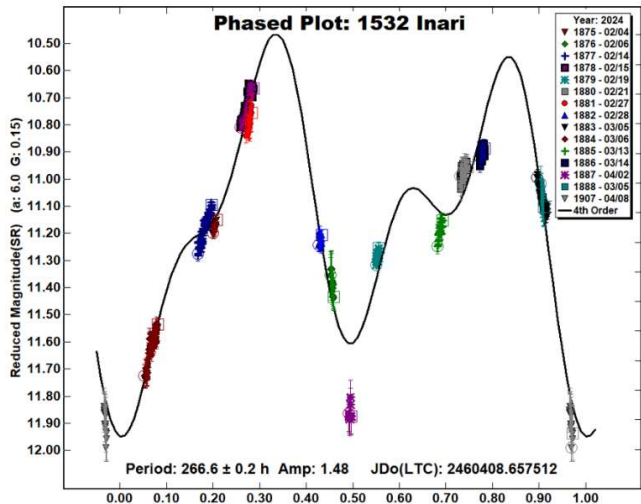
1532 Inari is a stony main-belt asteroid that belongs to the 606 Eos Family and was discovered on 1938 September 16 by Y. Vaisala at Turku. This asteroid was named after one of the principal lakes of Finland (Schmadel, 2012).

The LCBD (Warner et al., 2009) lists Inari as having an average estimated diameter of 28.42 km with an absolute magnitude of $H = 10.75$. The asteroid orbits the sun at a semi-major axis of 3.004 AU. Its orbit has an eccentricity of 0.047 and a period of 5.207 years (JPL, 2024).

Prior to this observation campaign, the LCBD database listed the rotation period of this asteroid as around 25 hours with a maximum amplitude of 0.09 with a U quality value of 1+ (Behrend, 2008web). The year 2024 was marked by presenting an opportunity to observe this asteroid during an apparition that exhibits one of five brighter observation opportunities from 1995-2050. As the 25-hour period is nearly commensurate with Earth's rotation period, we sent a call for observations to international observatories away from our usual central European locations.

In addition to the data supplied by the European Observatories (Flarestar Observatory: Stellar Horizon Observatory and Znith Observatory), we received data from *Observatoire à la belle étoile* in Canada and from the Rochester Institute of Technology University (RIT Observatory) in the US.

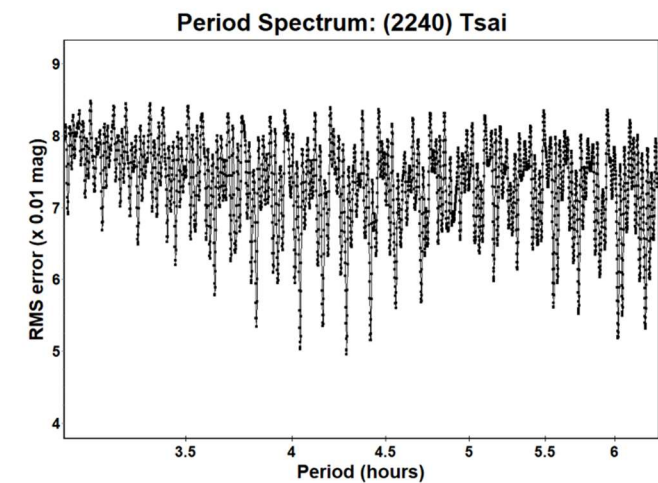
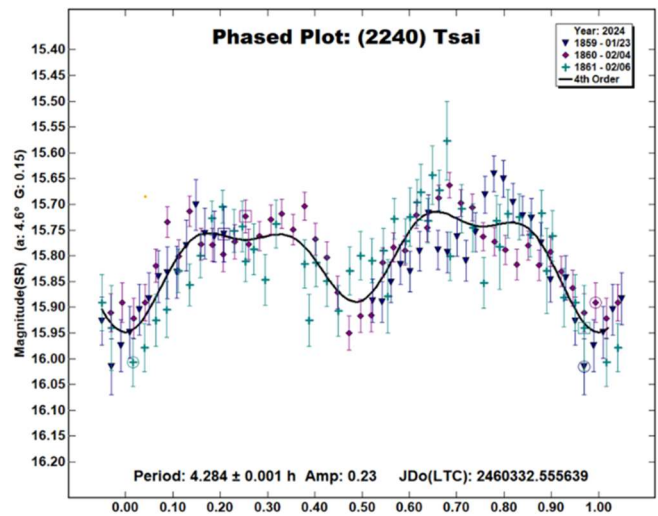
(1532) Inari was observed by our group during 15 runs, commencing on 2024 February 4 and terminating on 2024 April 8. Our results based on 572 data points yielded a synodic period of 266.6 ± 0.2 h with an amplitude of 1.48 ± 0.06 mag. Our derived period is near the period published by Polakis (2024) of 271.8 ± 0.7 hours.



2240 Tsai is a carbonaceous main-belt asteroid that was discovered on 1978 December 30. This celestial body was discovered at the Agassiz Station of the Harvard College Observatory.

The asteroid is named in recognition of Tsai Chang-Hsien, who has served as the director of the Taipei Observatory since the conclusion of World War II. An avid observer of planetary bodies and variable stars, Tsai Chang-Hsien has also been a prolific advocate for the field of astronomy. For more than three decades, he has played a pivotal role in educating the public and fostering amateur interest in astronomy.

The estimated diameter of the asteroid Tsai was derived to be 24.395 ± 0.469 km. Its absolute magnitude (H) is listed as 12.01 on JPL (2024). This minor planet orbits the sun with a semi-major axis of 3.156 AU with an orbital eccentricity of 0.146 and a period of 5.61 years (JPL, 2024).



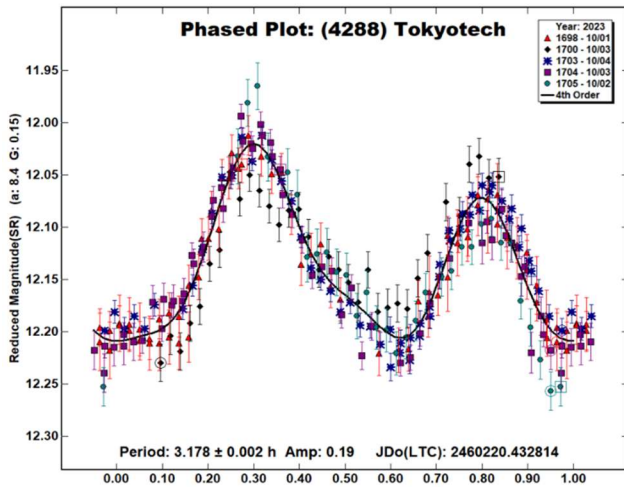
Observations were conducted from Znith Observatory over three nights from 2024 January 23 to February 6. Due to weather constraints, we could not gather additional data; however, our results indicate a synodic period of 4.284 ± 0.001 h with an amplitude of 0.23 ± 0.06 mag. The same period was derived even when we discarded the run with the noisiest data (observation run: 1861 acquired on 2024 Feb 6). This is slightly different from the published $U = 2$ quality period of 4.41563 ± 0.00002 h by Āurech et al. (2020) that utilized data from the Asteroid Terrestrial-impact Last Alert System (ATLAS) all-sky survey to derive its spin axis and shape.

4288 Tokyotech is a main-belt asteroid belonging to the 502 Eunomia family, discovered on 1989 October 8 by T. Kojima at Chiyoda. This asteroid is named after the Tokyo Vocational School that was established in 1881, The institution is now known as the Tokyo Institute of Technology and was granted university status in 1929. Today, it stands as Japan's largest national university focused exclusively on science and technology.

This minor planet orbits the sun with a semi-major axis of 2.63 AU, eccentricity 0.178, and orbital period of 4.26 years (JPL, 2024). The JPL Small-Bodies Database Browser lists the diameter of 4288 Tokyotech as 12.296 ± 0.087 km. It has an absolute magnitude $H = 11.70$.

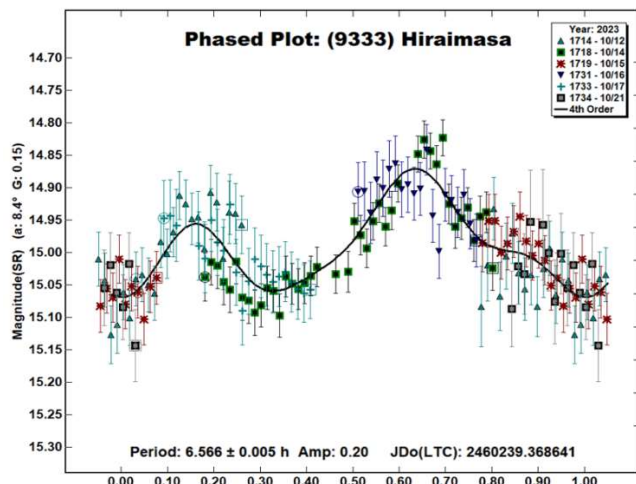
4288 Tokyotech has been reported to be a binary system (Augustin et al., 2019). As observed during 2019, 2.6-hr-long mutual phenomena were detected by the authors. Their results show that the body rotates at a period of 3.18 ± 0.00024 h and has an amplitude of 0.18 magnitude. Attenuations up to 0.15 mag were observed with a period of 30.276 h that were the result of the satellite making mutual phenomena.

The asteroid was observed over three nights from 2023 October 1-4. Our results yielded a composite rotation period of 3.178 ± 0.002 h and amplitude of 0.19 ± 0.03 mag. Our derived period is consistent with that of Augustin et al. (2019) published as 3.1800 ± 0.0003 h in the LCDB.



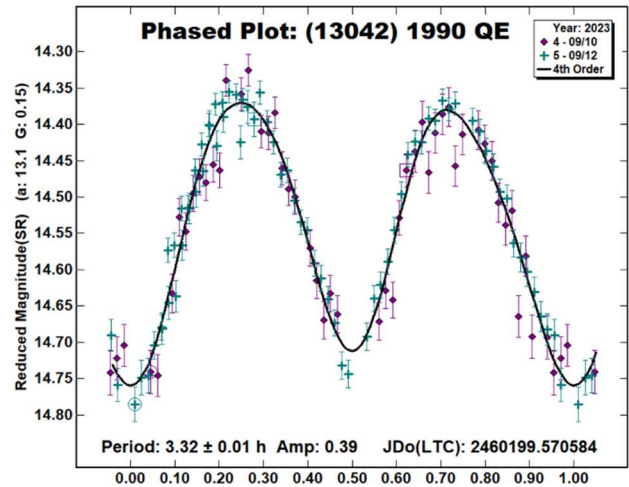
(9333) Hiraimasa is an inner main-belt asteroid that was discovered on 1990 Oct 15 by K. Endate and K. Watanabe at Kitami, Japan. This asteroid has been named in honor of Professor Masanori Hirai (b. 1943) who has specialized in stellar spectroscopic studies of cool stars with a focus on carbon stars. The estimated diameter was derived to be 9.651 ± 0.161 km based on an absolute magnitude $H = 12.93$; it orbits the sun with a semi-major axis of 2.581 AU. The orbit has an eccentricity of 0.176 and period of 4.15 years (JPL, 2024).

9333 Hiraimasa was observed from Antares Observatory on six nights between 2023 October 12 and October 21. We determined the period of asteroid Hiraimasa to be 6.566 ± 0.005 h with an amplitude of 0.20 ± 0.04 mag. Our period is near the published period of 6.911 h that was based on a $U = 2+$ value (Polakis, 2020).

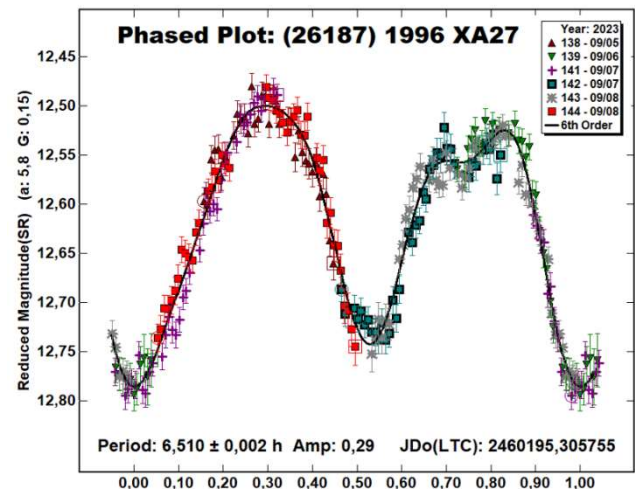


(13042) 1990 QE is a middle main-belt asteroid that belongs to the 2007 Prokne Family. This asteroid was discovered on 1990 August 18 by E.F. Helin at Palomar. The LCDB lists the diameter of this asteroid as 5.69 km with an absolute magnitude of $H = 13.94$. The asteroid orbits at a semi-major axis of 2.568 AU with an eccentricity of 0.240. The orbital period of this asteroid is 4.12 years (JPL, 2024).

1990 QE was observed on two nights from Luckystar Observatory. The derived synodic period was found to be 3.32 ± 0.01 h with an amplitude of 0.39 ± 0.03 mag. No published period could be found for (13042) 1990 QE in the LCDB.



(26187) 1996 XA27 is a main inner-belt asteroid that belongs to the 2011 Klumpkea family. This asteroid was discovered on 1996 December 12 by the Beijing Schmidt CCD Asteroid Program at Xinglong. The LCDB lists an estimated diameter of 9.6 ± 0.2 km based on an absolute magnitude $H = 12.29$. This asteroid orbits the Sun at a semi-major axis of 3.109 AU with an eccentricity of 0.247. The orbital period is 4.48 years (JPL, 2024).



(26187) 1996 XA27 was observed from Luckystar Observatory on four nights from 2023 September 5-8, from which we derived the synodic period to be 6.510 ± 0.002 h with an amplitude of 0.29 ± 0.02 mag. No published period could be found the LCDB for this asteroid.

Number	Name	yyyy mm/dd	Phase	L _{PAB}	B _{PAB}	Period(h)	P.E.	Amp	A.E.	Grp
612	Veronika	2023 07/11-07/17	24.8, 24.7	333	14	8.252	0.003	0.12	0.03	MB
1532	Inari	2024 02/04-04/08	5.8, 16.4	150	0	266.6	0.2	1.48	0.06	Eos
2240	Tsai	2024 01/23-02/06	4.9, 10.4	112	1	4.284	0.001	0.23	0.06	Themis
4288	Tokyotech	2023 10/01-10/04	8.4, 9.0	2	-13	3.178	0.002	0.19	0.03	Eunomia
9333	Hiraimasa	2023 10/12-10/21	8.4, 11.7	8	9	6.566	0.005	0.20	0.04	MB
13042	1990 QE	2023 09/10-09/12	13.1, 12.9	355	18	3.32	0.01	0.39	0.03	Prokne
26187	1996 XA27	2023 09/05-09/08	5.7, 6.4	340	11	6.510	0.002	0.29	0.02	Klumpkea

Table II. Observing circumstances and results. The phase angle is given for the first and last date. L_{PAB} and B_{PAB} are the approximate phase angle bisector longitude and latitude at mid-date range (see Harris et al., 1984). Grp is the asteroid family/group (Warner et al., 2009).

Acknowledgements

We express our gratitude to Dr. Richard Binzel and Brian Warner for their invaluable guidance. We also acknowledge Brian Warner for his contributions to the development of *MPO Canopus* and his dedication to maintaining the CALL website (Warner, 2016). Additionally, this research has made use of the JPL's Small-Body Database (JPL, 2024).

References

- Augustin, D.; Behrend, R.; Deldem, M.; Starkey, D.; Bosch, J.M.; Soldan, F.; et al. (2019). "(4288) Tokyotech." Central Bureau Electronic Telegrams **4705**.
- Behrend, R. (2008web). Observatoire de Geneve web site. http://obswww.unige.ch/~behrend/page_cou.html
- Berg, S. (2023). "Nighttime Imaging 'N' Astronomy (NINA)" web site. <https://nighttime-imaging.eu/>. Last accessed 2023 June 29.
- Ďurech, J.; Tonry, J.; Erasmus, N.; Denneau, L.; Heinze, A.N.; Flewelling, H.; Vančo, R. (2020). "Asteroid models reconstructed from ATLAS photometry." *Astronomy & Astrophysics* **643**, A59.
- Harris, A.W.; Young, J.W.; Scaltriti, F.; Zappala, V. (1984). "Lightcurves and phase relations of the asteroids 82 Alkmene and 444 Gyptis." *Icarus* **57**, 251-258.
- JPL (2024). Small-Body Database Browser - JPL Solar System Dynamics web site. <http://ssd.jpl.nasa.gov/sbdb.cgi>. Last accessed 2023 July 11.
- Polakis, T. (2020). "Photometric Observations of Twenty-Three Minor Planets." *Minor Planet Bulletin* **47**, 94-101.
- Polakis, T. (2024). "Photometric Observations of Thirteen Minor Planets." *Minor Planet Bulletin* **51**, 264-268.
- Schmadel, L.D. (2012). "Catalogue of Minor Planet Names and Discovery Circumstances." In *Dictionary of Minor Planet Names*. Springer, Berlin, Heidelberg.
- Tonry, J.L.; Denneau, L.; Flewelling, H.; Heinze, A.N.; Onken, C.A.; Smartt, S.J.; Stalder, B.; Weiland, H.J.; Wolf, C. (2018). "The ATLAS All-Sky Stellar Reference Catalog." *Astrophys. J.* **867**, A105.
- Warner, B.D.; Harris, A.W.; Pravec, P. (2009). "The Asteroid Lightcurve Database." *Icarus* **202**, 134-146. Updated 2024 April. <https://minplanobs.org/MPInfo/php/lcdbsummaryquery.php>
- Warner, B.D. (2016). Collaborative Asteroid Lightcurve Link website. <http://www.minorplanet.info/call.html>. Last accessed: 26 September 2018.
- Warner, B.D. (2017). MPO Software. *MPO Canopus* version 10.7.10.0. Bdw Publishing. <https://bdwpublishing.com/>

LIGHTCURVES AND ROTATION PERIODS OF 49 PALES, 62 ERATO, 901 BRUNSLIA, 995 STERNBERGA, AND 1114 LORRAINE

Frederick Pilcher
Organ Mesa Observatory (G50)
4438 Organ Mesa Loop
Las Cruces, NM 88011 USA
fpilcher35@gmail.com

(Received: 2024 July 9 Revised: 2024 July 26)

Synodic rotation periods and amplitudes are found for 49 Pales, 20.704 ± 0.001 hours, 0.15 ± 0.02 magnitudes with 4 unequal maxima and minima per cycle; 62 Erato 9.217 ± 0.001 hours, 0.11 ± 0.01 magnitudes with an irregular lightcurve; 901 Brunslia 3.1359 ± 0.0001 hours, 0.12 ± 0.01 magnitudes; 1114 Lorraine 20.703 ± 0.003 hours, 0.15 ± 0.02 magnitudes with an irregular lightcurve. For 995 Sternberga years of opposition, celestial longitudes, synodic rotation periods, and amplitudes are, respectively: 2013, 86° , 11.191 ± 0.002 hours, 0.10 ± 0.02 magnitudes; 2024, 213° , 11.202 ± 0.002 hours, 0.05 ± 0.01 magnitudes with one maximum and minimum per rotational cycle.

Observations to obtain the data used in this paper were made at the Organ Mesa Observatory with a 0.35-meter Meade LX200 GPS Schmidt-Cassegrain (SCT) and SBIG STL-1001E CCD. Exposures were 60 seconds, unguided, with a clear filter. Photometric measurement and lightcurve construction are with *MPO Canopus* software. To reduce the number of points on the lightcurves and make them easier to read, data points have been binned in sets of 3 with a maximum time difference of 5 minutes.

49 Pales. Two early published rotation periods were by Schober et al. (1979), 10.42 hours; and by Tedesco (1979), 10.3 hours. For many years the period was believed to be near 10.4 hours. Behrend (2013web) published a very sparse lightcurve which suggested a period <10 hours. Pilcher et al. (2016) made a much more comprehensive investigation that found a period 20.704 hours with an unsymmetric quadrimodal lightcurve. Behrend (2016web) complemented this study with a period 20.7057 hours. Five subsequent studies confirm both the longer period and the unsymmetric quadrimodal lightcurve: Pilcher (2017), 20.705 hours; Pilcher (2018), 20.709 hours; Pilcher (2021), 20.702 hours; Pilcher (2022), 20.702 hours, and Behrend (2020web), 20.7102 hours. New observations on 9 nights 2024 May 7 - June 3 provide a fit to a period 20.704 ± 0.001 hours, again with an unsymmetric quadrimodal lightcurve, and amplitude 0.15 ± 0.02 magnitudes (Fig. 1). It is noteworthy that all the lightcurves published from 2016 onward have very nearly the same amplitudes and shapes despite being from diverse celestial longitudes. This indicates that the orbital plane and equatorial rotational plane are nearly parallel. Whether the rotation is prograde or retrograde is undetermined.

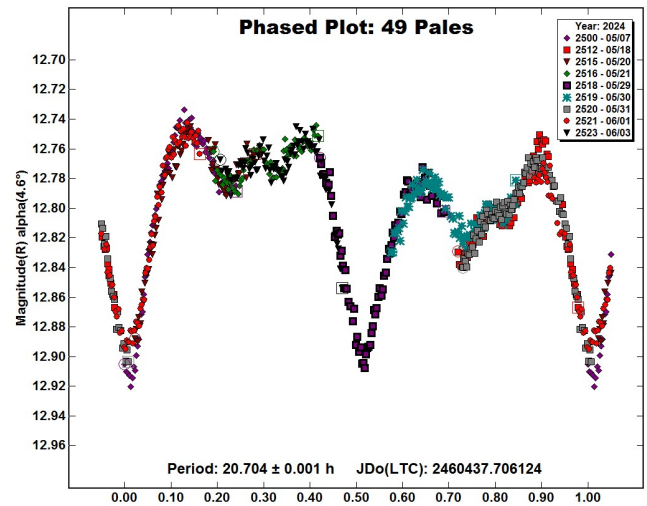


Figure 1. Lightcurve of 49 Pales phased to a rotation period of 20.704 hours.

62 Erato. The Lightcurve Database, Warner et al. (2009), lists eight published rotation periods of 62 Erato in the range from 9.2 to 9.23 hours, amplitudes 0.12 to 0.28 magnitudes, and scattered along the ecliptic. New observations on five nights 2024 May 5 - June 4 provide a good fit to an irregular lightcurve with period 9.217 ± 0.001 hours, amplitude 0.11 ± 0.01 magnitudes (Fig. 2). This new finding is in the mid-range of many previously published periods and has the smallest amplitude yet observed.

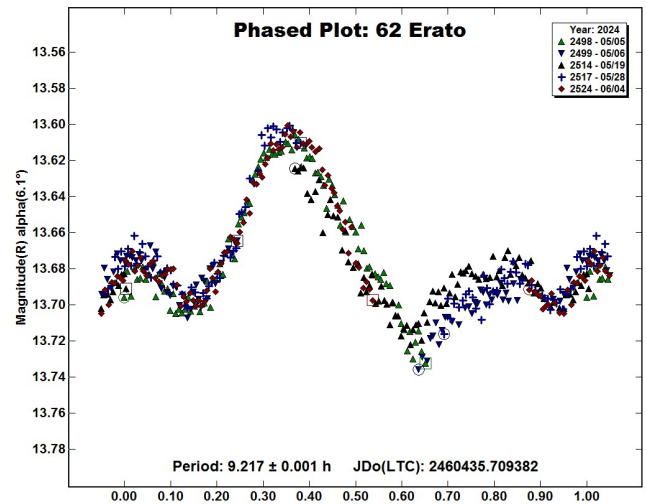


Figure 2. Lightcurve of 62 Erato phased to a rotation period of 9.217 hours.

901 Brunslia. Eight published periods listed in the Asteroid lightcurve database, Warner et al. (2009), all in the range between 3.1335 and 3.1363 hours. A single discordant period of 4.872 hours has been published by Wisniewski et al. (1997). New observations on four nights 2024 June 18 - July 26 provide an excellent fit to a slightly asymmetric bimodal lightcurve with period 3.1359 ± 0.0001 hours, amplitude 0.12 ± 0.01 magnitudes (Fig. 3). This new result is consistent with all previously published periods except for 4.872 hours (Wisniewski et al., 1997), which is now definitively ruled out.

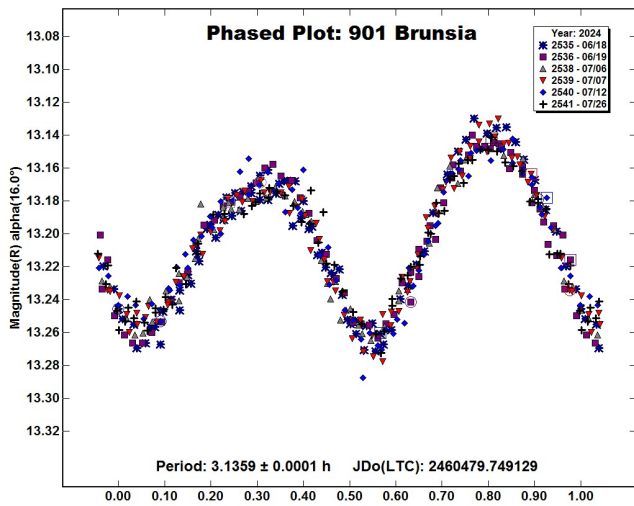


Figure 3. Lightcurve of 901 Brunisia phased to a rotation period of 3.1359 hours.

995 Sternberga. Early observations showed many discordant rotation periods: Barucci et al. (1992), 16.406 hours; Behrend (2004web), >12 hours; Stephens (2005), 15.26 hours; Stephens (2013), 14.62 hours. More recent rotation period determinations have been near either 11.2 hours or 22.4 hours: Marciniak et al. (2014), 22.404 hours; Marciniak et al. (2018), 11.192 hours; Colazo et al. (2022), 22.392 hours. This author presents here observations from two separate oppositions at two widely different celestial longitudes to resolve the ambiguity between 11.2 hours and 22.4 hours.

995 Sternberga. December, 2013. Observations not previously published on 5 nights 2013 Dec. 6-15, near celestial longitude 86°, provide a good fit to an asymmetric bimodal lightcurve with period 11.191 ± 0.002 hours, amplitude 0.10 ± 0.02 magnitudes (Fig. 4). A split halves diagram of the double period 22.38 hours (Fig. 5) shows that the two halves are identical and rules out the double period.

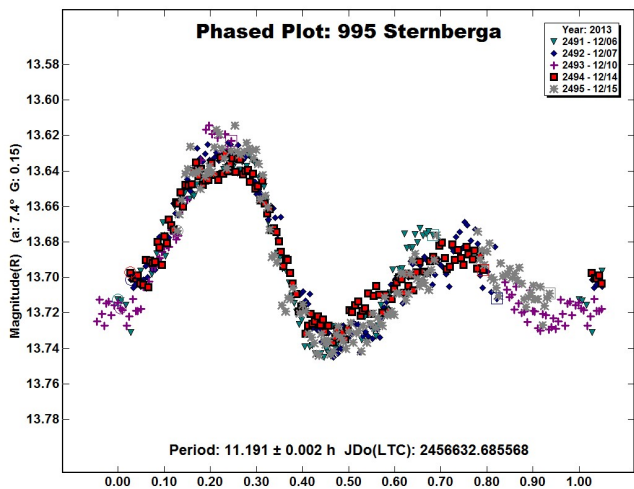


Figure 4. Lightcurve of 995 Sternberga for the year 2013 phased to a rotation period of 11.191 hours.

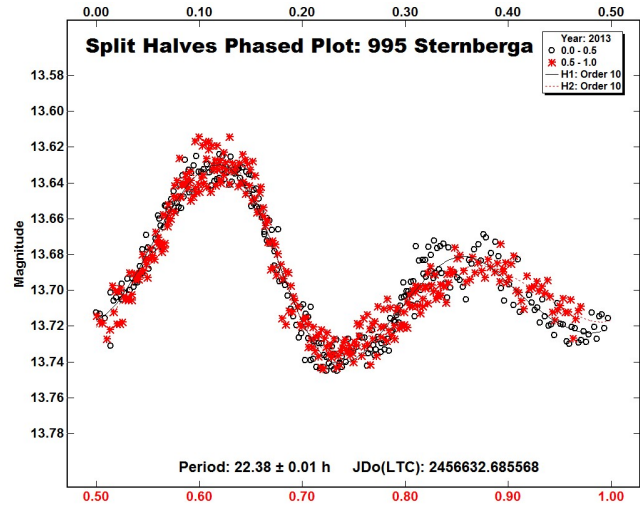


Figure 5. Split halves lightcurve of 995 Sternberga for the year 2013 phased to the double period of 22.38 hours.

995 Sternberga. April-May, 2024. Observations on 9 nights 2024 April 2 - May 1, near celestial longitude 213°, provide a good fit to a lightcurve with period 11.202 ± 0.002 hours, amplitude 0.05 ± 0.01 magnitudes with one maximum and minimum per rotational cycle (Fig. 6). The data cover both halves of a split halves diagram of the double period 22.405 hours (Fig. 7) and are identical within errors of measurement. Again, the double period can be rejected.

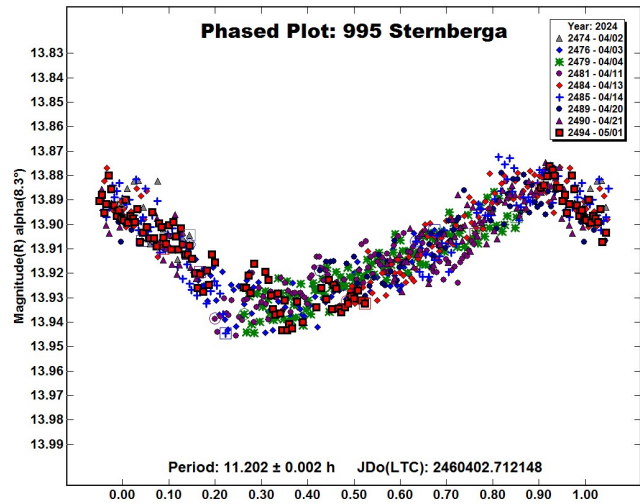


Figure 6. Lightcurve of 995 Sternberga for the year 2024 phased to a rotation period of 11.202 hours.

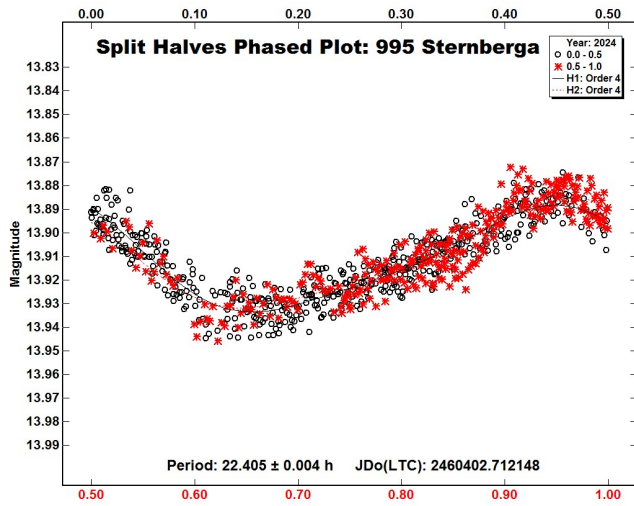


Figure 7. Split halves lightcurve of 995 Sternberga for the year 2024 phased to the double period of 22.405 hours.

1114 Lorraine. Previously published rotation periods are by Behrend (2005web), 32 hours based on a fragmentary lightcurve; Ditteon et al. (2018), 20.71 hours; and Dose, (2021) 20.68 hours. New observations on 10 nights 2024 June 2 - July 5 provide a fit to an irregular lightcurve with period 20.703 ± 0.003 hours, amplitude 0.15 ± 0.02 magnitudes (Fig. 8). This new result is consistent with Ditteon et al. (2018) and with Dose (2021). The 32-hour period reported by Behrend (2005web) is now ruled out.

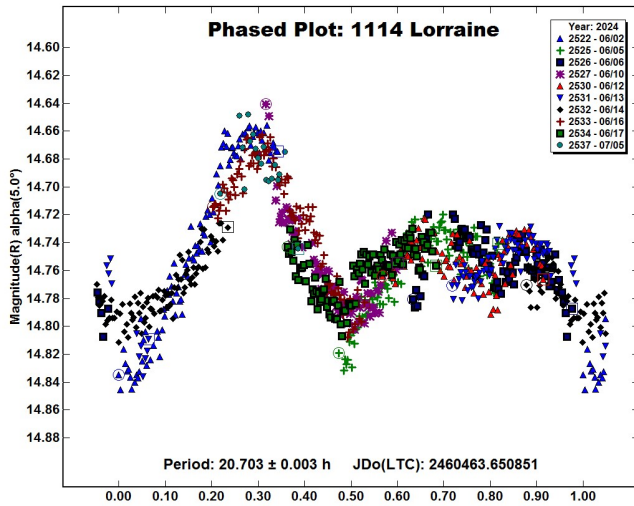


Figure 8. Lightcurve of 1114 Lorraine phased to a rotation period of 20.703 hours.

References

Barucci, M.A.; DiMartino, M.; Fulchignoni, M.A. (1992). "Properties of small asteroids: photoelectric observations." *Astron. J.* **103**, 1679-1686.

Behrend, R. (2004web, 2005web, 2013web, 2016web, 2020web). Observatoire de Geneve web site. http://obswww.unige.ch/~behrend/page_cou.html

Colazo, M.; Monteleone, B.; Santos, F.; Morales, M.; García, A.; Suárez, N.; Altuna, L.; Caballero, M.; Romero, F.; Speranza, T.; Bellocchio, E.; Santucho, M.; Fornari, C.; Melia, R.; Stechina, A.; Scotta, D.; Arias, N.; Chapman, A.; Ciancia, G.; Wilberger, A.; Anzola, M.; Mottino, A.; Colazo, C. (2022). "Asteroid Photometry and Lightcurve Results for Seven Asteroids" *Minor Planet Bull.* **49**, 189-192.

Ditteon, R.; Adam, A.; Doyel, M.; Gibson, J.; Lee, S.; Lynville, D.; Michalik, D.; Turner, R.; Washburn, K. (2018). "Lightcurve analysis of minor planets observed at the Oakley Southern Sky Observatory, 2016 October - 2017 March." *Minor Planet Bull.* **45**, 13-16.

Dose, E.V. (2021). "Lightcurves of eighteen asteroids." *Minor Planet Bull.* **48**, 125-132.

Harris, A.W.; Young, J.W.; Scaltriti, F.; Zappala, V. (1984). "Lightcurves and phase relations of the asteroids 82 Alkmene and 444 Gyptis." *Icarus* **57**, 251-258.

Marciniak, A.; Pilcher, F.; Santana-Ros, T.; Oszkiewicz, D.; Kankiewicz, P. (2014). "Against the biases in physics of asteroids: Photometric survey of long-period and low-amplitude asteroids." *Proceedings of Asteroids, Comets, Meteors*. p 333.

Marciniak, A.; Bartczak, P.; Müller, T., and 40 co-authors (2018). "Photometric survey, modelling, and scaling of long-period and low-amplitude asteroids." *Astron. Astrophys.* **610**, A7.

Pilcher, F.; Benishek, V.; Klinglesmith, D.A. (2016). "Rotation Period, Color Indices, and H-G Parameters for 49 Pales." *Minor Planet Bull.* **43**, 182-183.

Pilcher, F. (2017), "Rotation Period Determinations for 49 Pales, 96 Aegle, 106 Dione, 375 Ursula, and 576 Emanuela." *Minor Planet Bull.* **44**, 249-251.

Pilcher, F. (2018). "New lightcurves of 33 Polyhymnia, 49 Pales, 289 Nenetta, 504 Cora, and 821 Fanny." *Minor Planet Bull.* **45**, 356-359.

Pilcher, F. (2021). "Lightcurves and rotation periods of 49 Pales, 383 Janina, and 764 Gedania." *Minor Planet Bull.* **48**, 5-6.

Number	Name	yyyy/mm/dd	Phase	L _{PAB}	B _{PAB}	Period(h)	P.E	Amp	A.E.
49	Pales	2024/05/07-2024/06/03	*4.6, 3.9	241	-3	20.704	0.001	0.15	0.02
62	Erato	2024/05/05-2024/06/04	*6.1, 3.5	244	2	9.217	0.001	0.11	0.01
901	Brunsia	2024/06/18-2024/07/26	*16.0, 7.5	292	2	3.1359	0.0001	0.12	0.01
995	Sternberga	2013/12/06-2013/12/15	7.4, 5.4	86	-11	11.191	0.002	0.10	0.01
995	Sternberga	2024/04/02-2024/05/01	*8.4, 3.4	213	-3	11.202	0.002	0.05	0.01
1114	Lorraine	2024/06/02-2024/07/05	*5.0, 9.4	259	12	20.703	0.003	0.15	0.02

Table I. Observing circumstances and results. The phase angle is given for the first and last date, unless a minimum (second value) was reached. L_{PAB} and B_{PAB} are the approximate phase angle bisector longitude and latitude at mid-date range (see Harris et al., 1984).

Pilcher, F. (2022). "Lightcurves and rotation periods of 49 Pales, 424 Gratia, 705 Erminia, 736 Harvard, 1261 Legia, 1541 Estonia, and 6371 Heinlein." *Minor Planet Bull.* **49**, 185-188.

Schober, H.-J.; Scaltriti, F.; Zappala, V. (1979). "Photoelectric photometry and rotation periods of three large and dark asteroids - 49 Pales, 88 Thisbe, and 92 Undina." *Astron. Astrophys. Suppl. Ser.* **36**, 1-8.

Stephens, R.D. (2005). "Rotational periods of 743 Eugenis, 995 Sternberga, 1185 Nikko, 2892 Filipenko, 3144 Brosche, and 3220 Murayama." *Minor Planet Bull.* **32**, 27-28.

Stephens, R.D. (2013). "Asteroids observed from Santana and CS3 Observatories 2012 July-September." *Minor Planet Bull.* **40**, 34-35.

Tedesco, E.F. (1979). PhD Dissertation, New Mexico State University.

Warner, B.D.; Harris, A.W.; Pravec, P. (2009). "The Asteroid Lightcurve Database." *Icarus* **202**, 134-146. Updated 2023 Sept. 16. <http://www.MinorPlanet.info/php/lcdb.php>

Wisniewski, W.Z.; Michalowski, T.M.; Harris, A.W.; McMillan, R.S. (1997). "Photometric observations of 125 asteroids." *Icarus* **126**, 395-449.

PHOTOMETRIC OBSERVATIONS OF TEN MINOR PLANETS

Tom Polakis
Command Module Observatory
121 W. Alameda Dr.
Tempe, AZ 85282
tpolakis@cox.net

(Received: 2024 June 11)

Photometric measurements were made for ten main-belt asteroids, based on CCD observations made from 2024 March through 2024 May. Phased lightcurves were created for all 10 asteroids. All the data have been submitted to the ALCDEF database.

CCD photometric observations of ten main-belt asteroids were performed at Command Module Observatory (MPC V02) in Tempe, AZ. Images were taken at V02 using a 0.32-m f/6.7 Modified Dall-Kirkham telescope, SBIG STXL-6303 CCD camera, and a 'clear' glass filter. Exposure time for the images was 2 minutes. The image scale after 2x2 binning was 1.76 arcsec/pixel. Table I shows the observing circumstances and results. All of the images for these asteroids were obtained between 2024 March and 2024 May. Images taken at V02 were calibrated using a dozen bias, dark, and flat frames. Flat-field images were made using an electroluminescent panel. Image calibration and alignment was performed using *MaxIm DL* (Diffraction Limited, 2017) software.

The data reduction and period analysis were done using *Tycho* (Parrott, 2024). In these fields, the asteroid and three to five comparison stars were measured. Comparison stars were selected with colors within the range of $0.5 < B-V < 0.95$ to correspond with color ranges of asteroids. In order to reduce the internal scatter in the data, the brightest stars of appropriate color that had peak ADU counts below the range where chip response becomes nonlinear were selected. *Tycho* plots instrumental vs. catalog magnitudes for solar-colored stars, which is useful for selecting comp stars of suitable color and brightness.

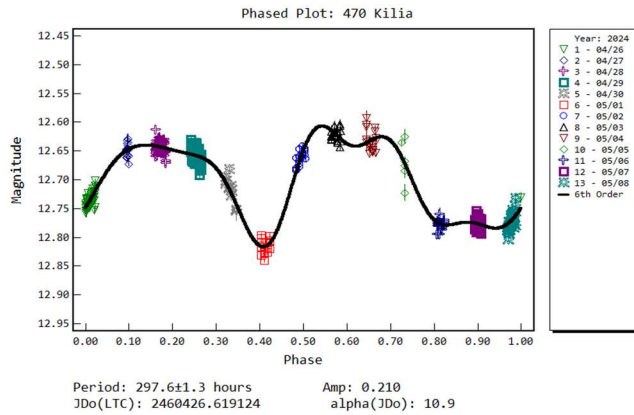
The clear-filtered images were reduced to Sloan r' to minimize error with respect to a color term. Comparison star magnitudes were obtained from the ATLAS catalog (Tonry et al., 2018), which is incorporated directly into *Tycho*. The ATLAS catalog derives Sloan $griz$ magnitudes using a number of available catalogs. The consistency of the ATLAS comp star magnitudes and color-indices allowed the separate nightly runs to be linked often with no zero-point offset required or shifts of only a few hundredths of a magnitude in a series.

Data reduction for V02 images used a 9-pixel (16 arcsec) diameter measuring aperture for asteroids and comp stars. It was typically necessary to employ star subtraction to remove contamination by field stars.

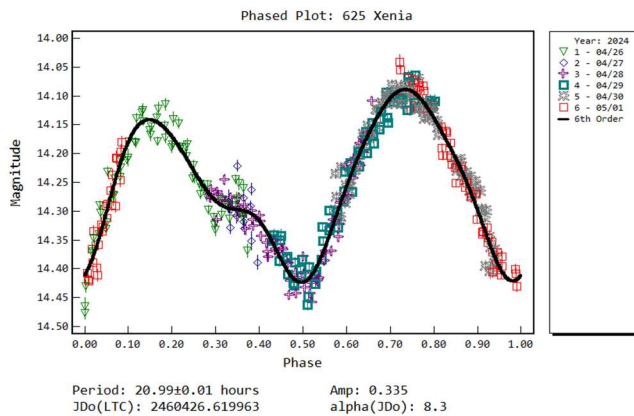
For the asteroids described here, the RMS scatter on the phased lightcurves is noted, which gives an indication of the overall data quality including errors from the calibration of the frames, measurement of the comp stars, the asteroid itself, and the period-fit. Period determination was done using the *Tycho* Fourier-type FALC fitting method (Harris et al., 1989). Phased lightcurves show the maximum at phase zero. Magnitudes in these plots are apparent and scaled by *Tycho* to the first night.

Asteroids were selected from the CALL website (Warner, 2011), either for having uncertain periods or for needing more lightcurves for shape modeling. In this set of observations, five of the ten asteroids had $U = 2$, and five were rated as $U=3$. The Asteroid Lightcurve Database (LCDB; Warner et al., 2009) was consulted to locate previously published results. All the new data for these asteroids can be found in the ALCDEF database.

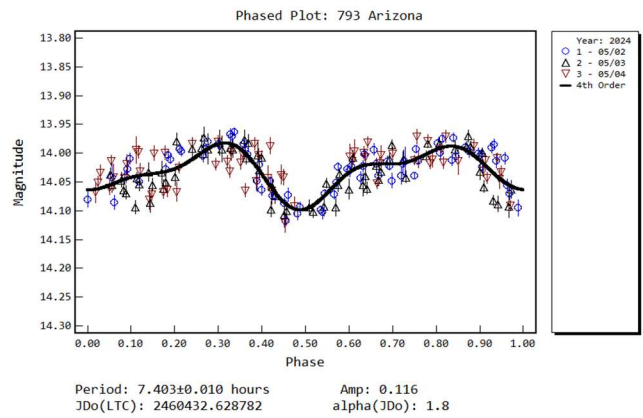
470 Kilia was discovered by Luigi Carnera in 1901 at Heidelberg. Recent period calculations include Pál et al. (2020), 294.537 ± 0.005 h; Pilcher and Polakis (2020), $296.0 + 2.0$ h; and Colazo et al. (2022), 297.655 ± 0.012 h. During 13 nights, 387 images were used to determine a synodic period of 297.6 ± 1.3 h. The lightcurve has an amplitude of 0.210 mag, and an RMS error on the fit of 0.012 mag.



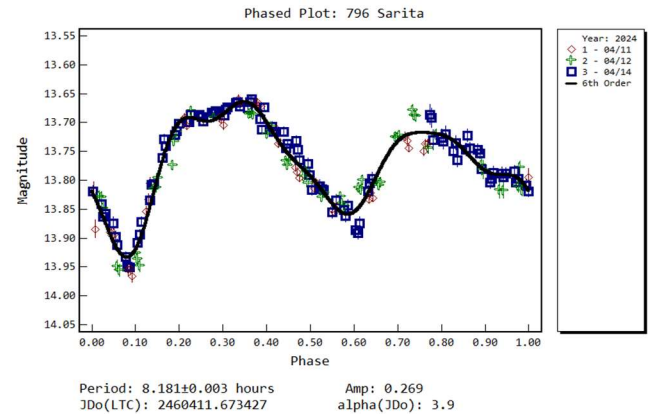
625 Xenia. This main-belt asteroid lies in a highly eccentric orbit. It was discovered in 1907 at Heidelberg by August Kopff. Hanus et al. (2016) determined a rotation period of 21.0122 ± 0.0005 h, and Martikainen et al. (2021) computed 21.012150 ± 0.000035 h. In six nights, 410 data points were acquired, yielding a period solution of 20.99 ± 0.01 h. The amplitude is 0.335 ± 0.031 mag.



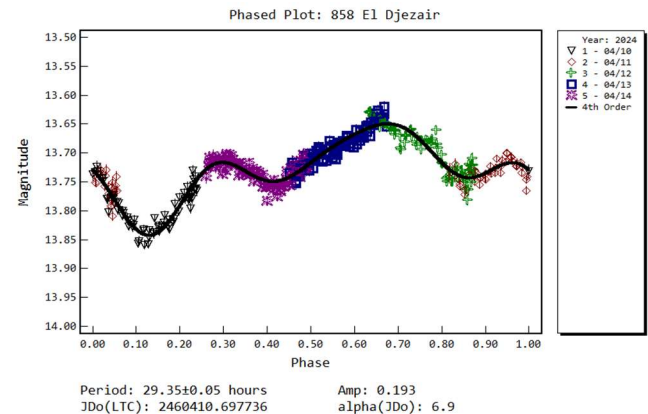
793 Arizona was discovered at Flagstaff in 1907 by Percival Lowell. Among the many agreeing period solutions is one by Ďurech et al. (2020), who computed 7.39849 ± 0.00004 h. A total of 210 images were gathered on three nights. The resulting period is 7.403 ± 0.010 h, with an amplitude of 0.116 ± 0.023 mag.



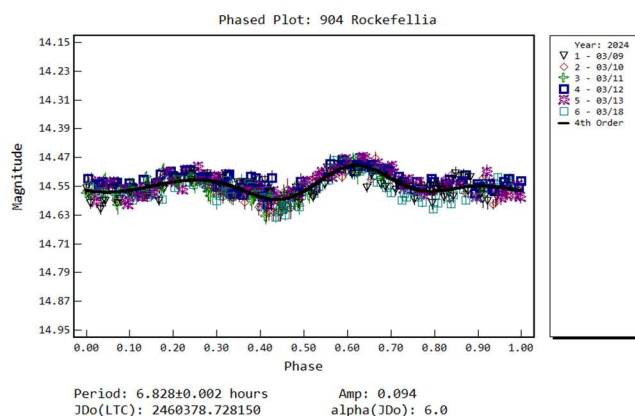
796 Sarita lies in a highly inclined and eccentric orbit, and came to an unfavorable opposition in 2024. It was discovered by Karl Reinmuth at Heidelberg in 1914. Skiff et al. (2019) computed a period of 8.1756 ± 0.0005 h, and Franco et al. (2022) obtained a solution of 8.176 ± 0.002 h. During three nights, 192 data points were acquired. The result is a period of 8.181 ± 0.003 h, with an amplitude of 0.269 ± 0.024 mag.



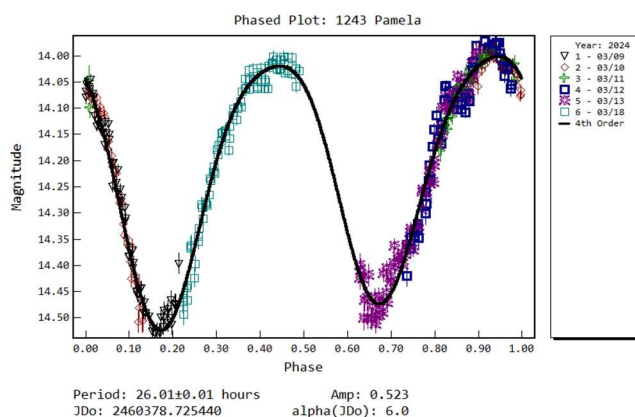
858 El Djézair. This outer main-belt asteroid was discovered in 1916 at Algiers by Frédéric Sy. The LCDB shows several discordant period solutions. Colazo et al. (2021) obtained 33.525 ± 0.013 h, Dose (2023) computed 29.639 ± 0.003 h, and Polakis (2023) published 31.16 ± 0.25 h. During this opposition, 296 images were taken on five nights. The resulting period is 29.35 ± 0.05 h, agreeing best with Dose. The amplitude of the lightcurve is 0.193 mag, with an RMS error on the fit of 0.014 mag.



904 Rockefelleria was discovered in 1918 by Max Wolf at Heidelberg. There are many agreeing period solutions, the most recent of which is Huet et al. (2023), who published 6.834 ± 0.006 h. During six nights, 544 data points were obtained. The computed rotation period is 6.828 ± 0.002 h, with an amplitude of 0.094 ± 0.021 mag.

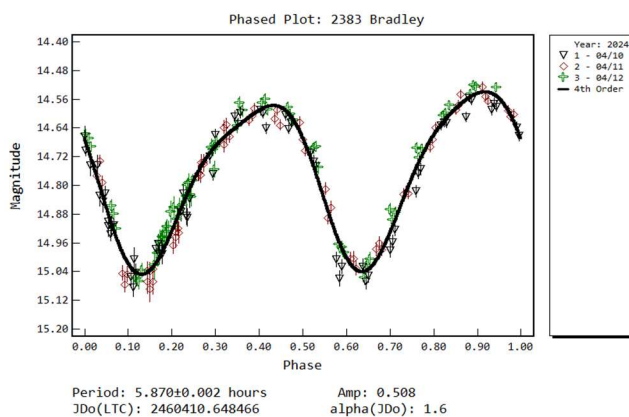


1243 Pamela was discovered by Cyril Jackson at Johannesburg in 1932. Its rotation period is well established. Polakis (2023) published a value of 25.96 ± 0.02 h. A total of 442 data points were obtained during six nights, producing a computed rotation period of 26.01 ± 0.01 h. The amplitude is 0.523 ± 0.024 mag.

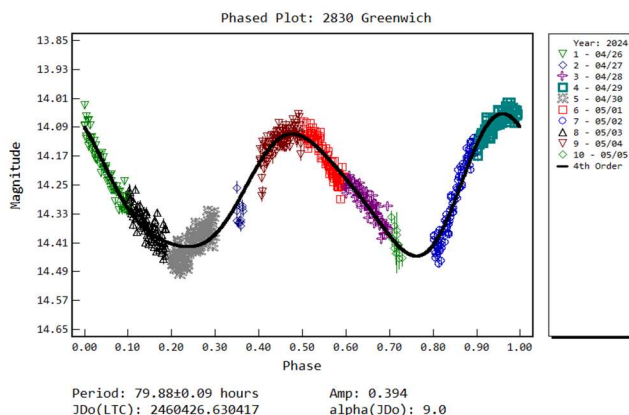


2383 Bradley was discovered by Ted Bowell at Flagstaff in 1981. The single entry in the LCDB is that of Warell (2017), who published a value of 5.823 ± 0.003 h. After three nights, 190 data points were used to compute a synodic period of 5.870 ± 0.002 h,

in agreement with Warell. The amplitude of the lightcurve is 0.508 ± 0.031 mag.



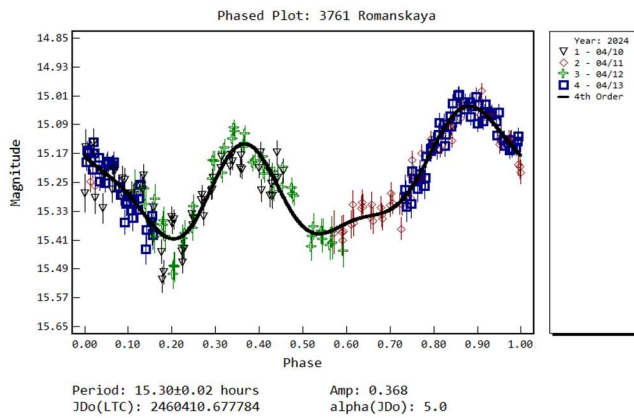
2830 Greenwich. This Phocaea-family asteroid was discovered in 1980 at Flagstaff by Ted Bowell. Martikainen et al. (2021) calculated a rotation period of 80.57506 ± 0.00041 h. The slow rotator required 10 nights of observation, during which 670 images were gathered. A period of 79.88 ± 0.09 h was computed, agreeing with previous assessments. The lightcurve amplitude is 0.394 ± 0.029 mag.



3761 Romanskaya was discovered by Grigory Neujmin in 1936 at Simeis. Durech et al. (2019) obtained a period of 15.27461 ± 0.00002 h, and Clark (2020) computed 9.587 ± 0.003 h. Four nights and 255 images were used to calculate a rotation period of 15.30 ± 0.02 h, with an amplitude of 0.368 ± 0.039 mag.

Number	Name	yy/mm/dd	Phase	L _{PAB}	B _{PAB}	Period(h)	P.E.	Amp	A.E.	Grp
470	Kilia	24/04/26-05/08	11.0/16.4	198	5	297.6	1.3	0.21	0.01	MB-I
625	Xenia	24/04/26-05/01	8.3, 9.7	202	15	20.99	0.01	0.34	0.03	MB-M
793	Arizona	24/05/02-05/04	1.9, 2.7	217	-1	7.403	0.010	0.12	0.02	MB-O
796	Sarita	24/04/11-01/14	3.9, 2.8	212	1	8.181	0.003	0.27	0.02	MB-M
858	El Djézair	24/04/10-04/14	6.9, 5.4	213	7	29.35	0.05	0.19	0.01	MB-O
904	Rockefelleria	24/03/09-03/18	6.0, 2.9	183	-6	6.828	0.002	0.09	0.02	MB-O
1243	Pamela	24/03/09-04/18	*6.0, 5.7	175	-15	26.01	0.01	0.52	0.02	MB-O
2383	Bradley	24/04/10-04/12	1.5, 0.6	203	-1	5.870	0.002	0.51	0.03	MB-I
2830	Greenwich	24/04/26-05/05	9.9, 11.4	211	10	79.88	0.09	0.39	0.03	PHO
3761	Romanskaya	24/04/10-04/13	5.0, 3.7	212	1	15.30	0.02	0.37	0.04	MB-O

Table I. Observing circumstances and results. The phase angle is given for the first and last date. If preceded by an asterisk, the phase angle reached an extrema during the period. L_{PAB} and B_{PAB} are the approximate phase angle bisector longitude/latitude at mid-date range (see Harris et al., 1984). Grp is the asteroid family/group (Warner et al., 2009).



Acknowledgments

The author would like to express his gratitude to Brian Skiff for his indispensable mentoring in data acquisition and reduction. Thanks also go out to Daniel Parrott for support of his *Tycho* software package.

References

- Clark, M. (2020). "Asteroid Photometry from the Preston Gott Observatory." *Minor Planet Bull.* **47**, 163-165.
- Colazo, M.; Stechina, A.; Fornari, C.; Suárez, N.; Melia, R.; Morales, M.; Bellocchio, E.; Pulver, E.; Speranza, T.; Scotta, D.; Wilberger, A.; Mottino, A.; Meza, E.; Romero, F.; Tourne Passarino, P.; Suligoy, M.; Llanos, R.; Chapman, A.; Martini, M.; Colazo, C. (2021). "Asteroid Photometry and Lightcurve Analysis at GORA's Observatories, Part IV." *Minor Planet Bull.* **48**, 140-143.
- Colazo, M.; Mottino, A.; Scotta, D.; Speranza, T.; Fornari, C.; Stechina, A.; Morales, M.; García, A.; Santos, F.; Santucho, M.; Suárez, N.; Wilberger, A.; Arias, N.; Melia, R.; Bellocchio, E.; Martini, M.; Borello, M.; Galarza, C.; Chapman, A.; Colazo, C. (2022). "Photometry and Light Curve Analysis of Six Asteroids by GORA's Observatories." *Minor Planet Bull.* **49**, 125-127.
- Dose, E. (2023). "Lightcurves of Seventeen Asteroids." *Minor Planet Bull.* **49**, 141-148.
- Diffraction Limited (2017). *MaxIm DL* software. <https://diffractionlimited.com/product/maxim-dl/>
- Ďurech, J.; Hanuš, J.; Vančo, R. (2019). "Inversion of asteroid photometry from Gaia DR2 and the Lowell Observatory photometric database." *Astron. Astrophys.* **631**, 2-7.
- Ďurech, J.; Tonry, J.; Erasmus, N.; Heinze, A.N.; Flewelling, H.; Vančo, R. (2020). "Asteroid models reconstructed from ATLAS photometry." *Astron. Astrophys.* **643**, 59-63.
- Franco, L.; Marchini, A.; Papini, R.; Iozzi, M.; Bacci, P.; Maestripieri, M.; Baj, G.; Galli, G.; Mortari, F.; Gabellini, D.; Ruocco, N.; Tinelli, L.; Montigiani, N.; Mannucci, M.; Scarfi, G.; Salvaggio, F. (2022). "Collaborative Asteroid Photometry from UAI: 2021 October - December." *Minor Planet Bull.* **49**, 128-130.
- Hanus, J.; Ďurech, J.; Oszkiewicz, D.A. and 155 co-authors (2016). "New and updated convex shape models of asteroids based on optical data from a large collaboration network." *Astron. Astrophys.* **586**, 108-131.
- Harris, A.W.; Young, J.W.; Scaltriti, F.; Zappala, V. (1984). "Lightcurves and phase relations of the asteroids 82 Alkmene and 444 Gypsis." *Icarus* **57**, 251-258.
- Harris, A.W.; Young, J.W.; Bowell, E.; Martin, L.J.; Millis, R.L.; Poutanen, M.; Scaltriti, F.; Zappala, V.; Schober, H.J.; Debehogne, H.; Zeigler, K.W. (1989). "Photoelectric Observations of Asteroids 3, 24, 60, 261, and 863." *Icarus* **77**, 171-186.
- Huet, F.; Fornas, G.; Fornas, A. (2023). "Lightcurve Analysis for Six Main-belt Asteroids." *Minor Planet Bull.* **50**, 170-172.
- Martikainen, J.; Muinonen, K.; Penttilä, A.; Cellino, A.; Wang, X.-B. (2021). "Asteroid absolute magnitudes and phase curve parameters from Gaia photometry." *Astron. Astrophys.* **649**, 98-106.
- Pál, A.; Szakáts, R.; Kiss, C.; Bódi, A.; Bognár, Z.; Kalup, C.; Kiss, L.L.; Marton, G.; Molnár, L.; Plachy, E.; Sárneczky, K.; Szabó, G.M.; Szabó, R. (2020). "Solar System Objects Observed with TESS - First Data Release: Bright Main-belt and Trojan Asteroids from the Southern Survey." *Ap. J. Suppl. Ser.* **247**, id. 26-34.
- Parrott, D. (2024). *Tycho* software. <https://www.tycho-tracker.com/>
- Pilcher, F.; Polakis, T. (2020). "A Photometric Study of 470 Kilia." *Minor Planet Bull.* **47**, 247-248.
- Polakis, T. (2023). "Lightcurves for Ten Minor Planets." *Minor Planet Bull.* **50**, 211-214.
- Skiff, B.; McLelland, K.; Sanborn, J.; Pravec, P.; Koehn, B. (2019). "Lowell Observatory Near-Earth Asteroid Photometric Survey (NEAPS): Paper 3." *Minor Planet Bull.* **46**, 238-265.
- Tonry, J.L.; Denneau, L.; Flewelling, H.; Heinze, A.N.; Onken, C.A.; Smartt, S.J.; Stalder, B.; Weiland, H.J.; Wolf, C. (2018). "The ATLAS All-Sky Stellar Reference Catalog." *Astrophys. J.* **867**, A105.
- Warell, J. (2017). "Lightcurve Observations of Nine Main-belt Asteroids." *Minor Planet Bull.* **44**, 304-305.
- Warner, B.D., (2011). Collaborative Asteroid Lightcurve Link website. <http://www.minorplanet.info/call.html>
- Warner, B.D.; Harris, A.W.; Pravec, P. (2009). "The Asteroid Lightcurve Database." *Icarus* **202**, 134-146. Updated 2020 Aug. <http://www.minorplanet.info/lightcurvedatabase.html>

**ASTEROID LIGHTCURVE ANALYSIS
AT THE CENTER FOR SOLAR SYSTEM STUDIES
PALMER DIVIDE STATION:
2024 APRIL - JUNE**

Brian D. Warner
Center for Solar System Studies (CS3)
446 Sycamore Ave.
Eaton, CO 80615 USA
brian@MinPlanObs.org

(Received: 2024 July 15)

CCD photometric observations of seventeen Hungarias and one Hilda asteroid were made at the Center for Solar System Studies Palmer Divide Station in between 2024 April and June. Among the Hungarias, 1727 Mette, 2150 Nyctimene, (18890) 2000 EV25, 20936 Nemrut Dagi, and 52316 Daveslater were known binary asteroids or are potential new binary discoveries. The Hungaria asteroid 4764 Joneberhart appears to be in a tumbling state. In 2024, the data for 5967 Edithlevy also appear to indicate tumbling, yet a revisit to data from 2010 show it to be a possible binary. The rotation period for the only Hilda asteroid, 4446 Carolyn, based on the 2024 data and a revisit to those from 2016 was revised from about 40 hours to 30 hours.

CCD photometric observations of seventeen Hungarias and one Hilda asteroid were made at the Center for Solar System Studies Palmer Divide Station in between 2024 April and June as part of an ongoing general study of asteroid rotation periods with a concentration on near-Earth, Hungaria, and Hilda group/family asteroids.

Telescope	Camera
0.30-m f/6.3 SCT	SBIG STL-1001E
0.35-m f/9.1 SCT (×3)	FLI Microline 1001E

Table I. List of available telescopes and CCD cameras at CS3-PDS. The exact combination for each telescope/camera pair can vary due to maintenance or specific needs.

Table I lists the five telescope/CCD camera pairs available at CS3-PDS. All the cameras use CCD chips from the KAF 1001 blue-enhanced family and so have essentially the same response. The pixel scales ranged from 1.24-1.60 arcsec/pixel. All lightcurve observations were made with no or a clear filter. The exposures varied depending on the asteroid's brightness.

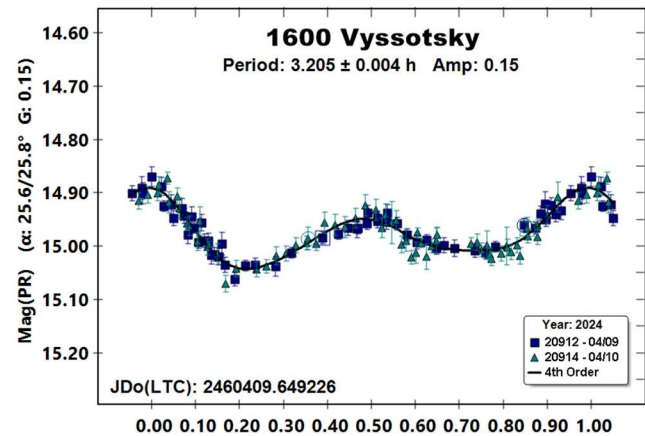
To reduce the number of times and amounts of adjusting nightly zero-points, the ATLAS catalog r' magnitudes on the Pan-STARRS photometric system (PR; Tonry et al., 2018) are used. Those adjustments are usually $\leq \pm 0.03$ mag. The rare larger corrections may have been related in part to using unfiltered observations, poor centroiding of the reference stars, and not correcting for second-order extinction. Another cause may be selecting what appears to be a single star but is actually an unresolved pair.

The Y-axis values are ATLAS SR “sky” (catalog) magnitudes. The values in the parentheses give the phase angle(s), a , along with the value of G used to normalize the data to the comparison stars and asteroid phase angle used in the earliest session. This, in effect, adjusts all the observations so that they seem to have been made at a single fixed date/time and phase angle. Presumably, any remaining variations are due only to the asteroid's rotation and/or albedo changes.

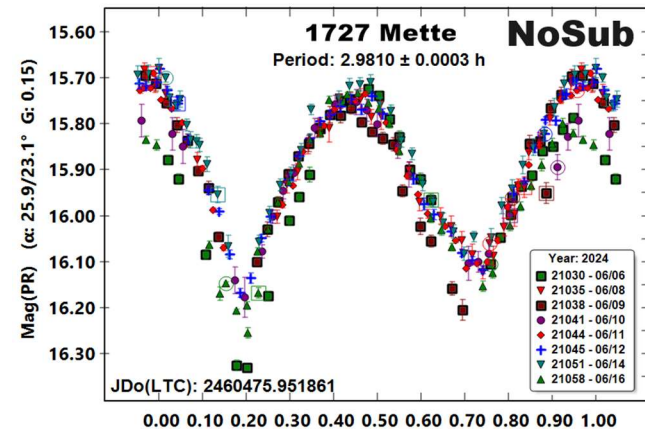
There can be up to three phase angles. If two, the values are for the first and last night of observations. If three, the middle value is the extrema (maximum or minimum) reached between the first and last observing runs. The X-axis shows rotational phase from -0.05 to 1.05. If the plot includes the amplitude, e.g., “Amp: 0.65,” this is the amplitude of the Fourier model curve and *not necessarily the adopted amplitude for the lightcurve*.

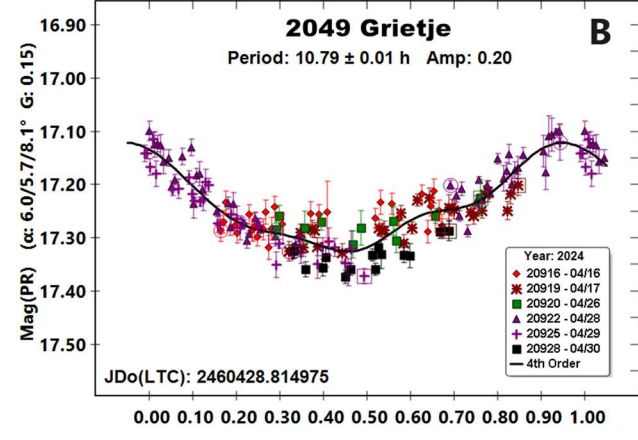
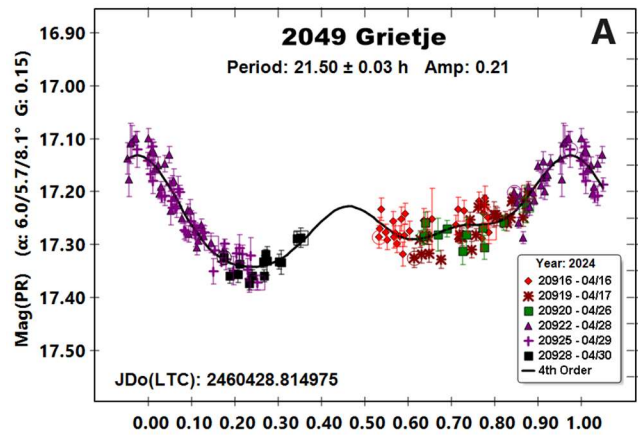
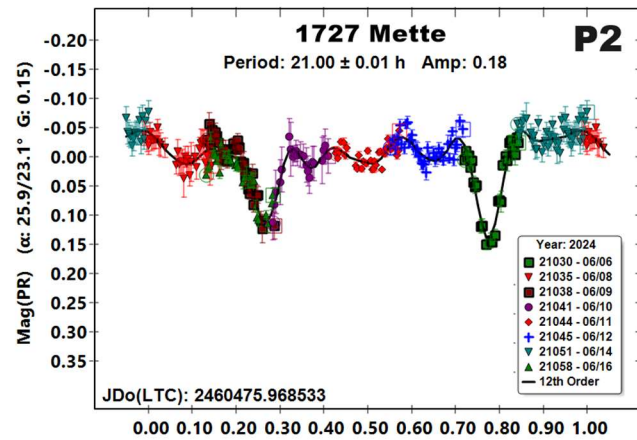
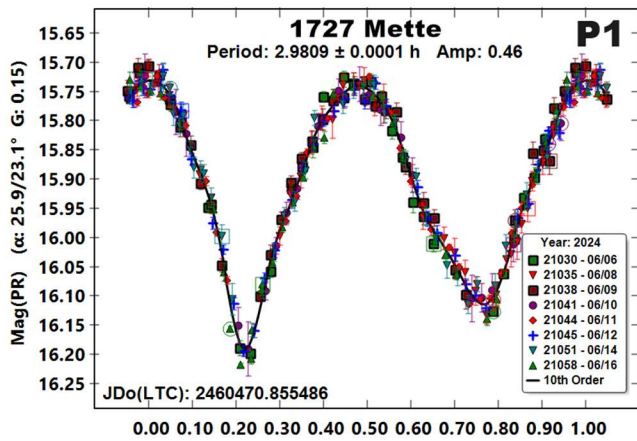
For brevity, only some of the previous results are referenced. A more complete listing is in the asteroid lightcurve database (Warner et al, 2009; “LCDB” from here on).

1600 Vyssotsky. The 2024 apparition was the eighth one observed at the Palmer Divide Observatory (PDO, Colorado) or CS3-PDS. Past results were revised several times as new data and analysis became available. See Stephens and Warner (2019a; and references therein). The final results were all near 3.20 h, as was the one based on 2024 observations. Pole solutions by Warner et al. (2008) and Wang and Xu (2021) both favored $(\lambda, \beta)_{J2000} = (356^\circ, 7^\circ)$. The new data will be used to further refine the solution.

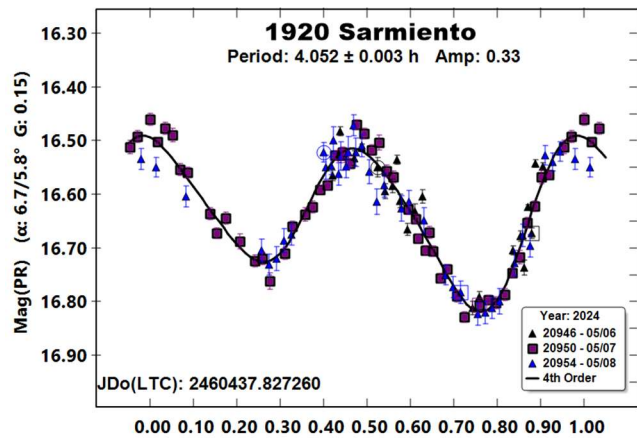


1727 Mette. This Hungaria was found to be a binary by Warner et al. (2013) and Warner and Stephens (2013) and has been observed several times since at CS3. The “NoSub” plot shows the result of a single-period search near 2.98 h for the primary. The remaining two plots show the results of a dual-period search using *MPO Canopus*. While the periods are close to those in 2013, the estimated effective secondary/primary diameter ratio is not: $D_s/D_p \geq 0.38$ vs. 0.22 in 2013, when the L_{PAB} was 184° from that in 2024.





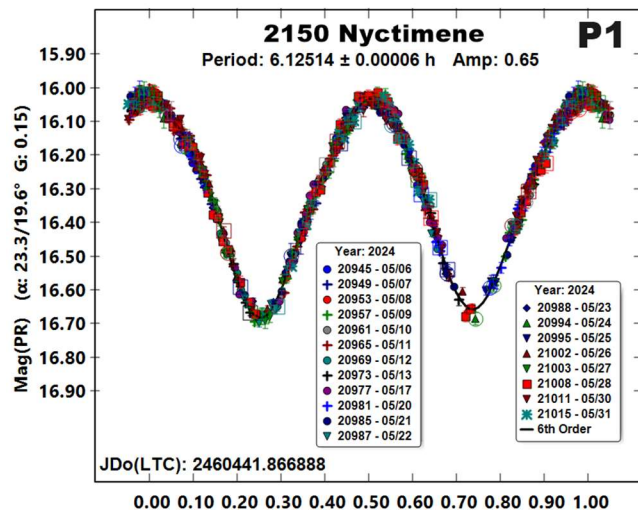
1920 Sarmiento. Observations 2024 May (the fifth apparition observed at CS3) found a period that is essentially the same as previous results, e.g., Stephens et al. (2021). The amplitude of 0.33 mag ($L_{PAB} = 233^\circ$) is near the maximum reported, 0.35 mag ($L_{PAB} = 45^\circ$), the two being nearly diametrically opposed. The minimum amplitude (0.23 mag) was at $L_{PAB} = 183^\circ$, or at 50° from the line joining those at maximum amplitude.

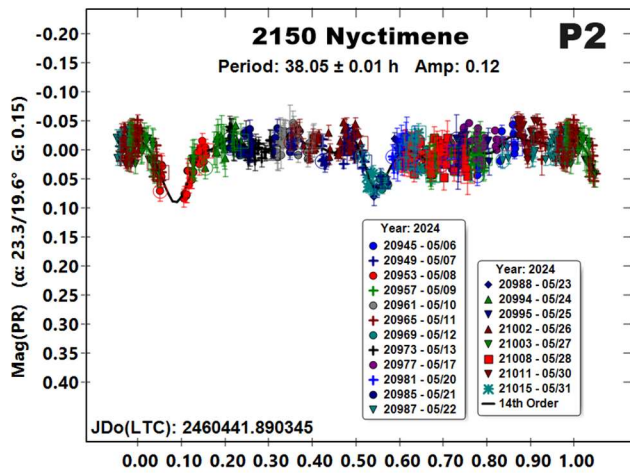


2049 Grietje. Previously reported periods for this Hungaria group member have ranged from 8.910 h (Warner, 2016) to 9.56 h (Warner, 2023), the second being a revision after re-analysis of 2016 data. The 2024 data led to an ambiguous solution, while the preferred period of 21.50 h (“A”) has a gap in coverage, the split-halves plot shows two different halves. The amplitude of only 0.21 mag allows for other solutions, including the alternate of 10.79 h (“B”), somewhat similar to those in Warner (2023).

2150 Nyctimene. None of the analysis of data from numerous previous apparitions at PDO or CS3 from 2006 to 2019 gave an indication of this Hungaria member being binary. However, there is close agreement among the previously reported dominant periods, e.g., Warner (2017; 6.133 h). In support of this being a new binary discovery, the *Asteroids with Satellites* web site (Johnston, 2024) does not list Nyctimene.

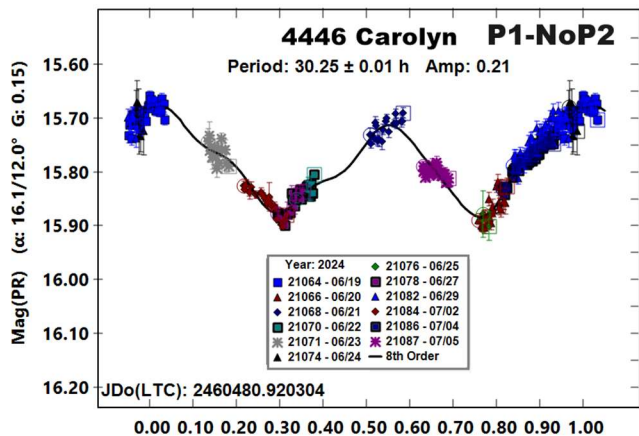
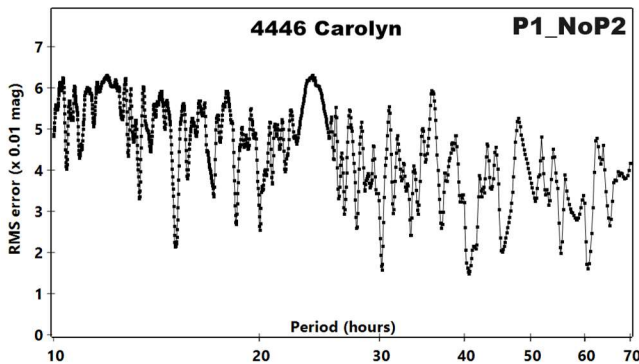
The two mutual events (occultations/eclipses) seem well-established, although one is not completely covered by the data. Using the shallower event of 0.05 mag, the estimated ratio of effective diameters is $D_s/D_p \geq 0.22 \pm 0.02$.





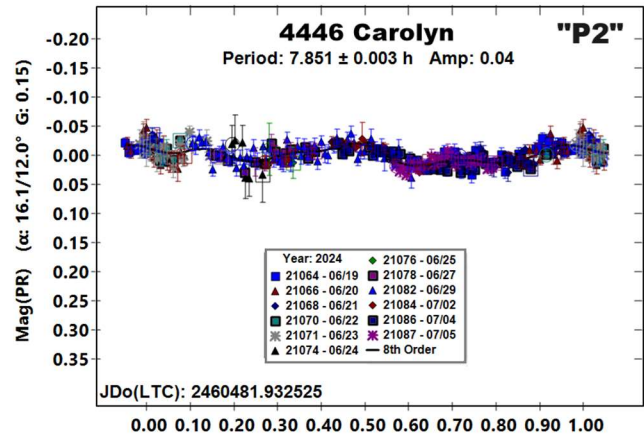
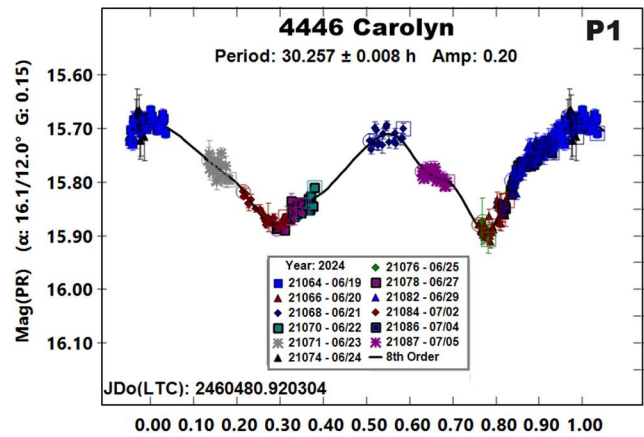
4446 Carolyn. This was a case not of refining a previous result, but changing it entirely. Warner et al. (2017) found what seemed to be a very secure period of 40.92 h, $A = 0.22$ mag, based on data obtained at CS3 in 2016. They used either the CMC-15 (Muinos, 2017) or APASS (Henden et al., 2009) star catalogs for comp star V magnitudes. The original CMC-15 does not have native V magnitudes, but the version supplied with *MPO Canopus* did have BVRI mags derived from conversion formulae. Favoring the converted CMC-15, with V errors $\leq \pm 0.05$ mag, and the low amplitude may have played a part in the story to come.

Single-period analysis of the 2024 observations (“P1_NoP2”) did show a solution near 40 hours but only a weak one at half-period. Not shown is the double period since the period spectrum showed common signs of unlikely rotational aliases. On the other hand, there are also strong solutions near 30 h and its double of 60 h. Attempts to force the 2024 data to near 40 h were unsatisfactory.



Given all this, period searches were made near 30 h, which produced $P = 30.257 \pm 0.008$ h and $A = 0.20$ mag. Since the L_{PAB} values were identical in 2017 and 2024, the similarity in amplitudes is expected. Admittedly, the 2024 data set is sparser than in 2017, still it seemed sufficient to compare the disparate periods, which are not quite at a 4:3 ratio (2.96:1). The difference in the data set densities may explain why not an exact integral ratio.

To get as good a fit as possible, the dual-period feature of *MPO Canopus* was used to find a secondary period of 7.851 h and $A = 0.04$ mag. This seems to be more a noise/smoothing filter since without the subtraction, there is only a marginal difference in the dominant lightcurve.



The data from 2016 were downloaded from the ALCDEF web site (<https://alcdef.org>). These data contain only the computed magnitude of the object and so it is not possible to recreate the ensemble differential photometry using the instrumental magnitudes of the object and comp stars. The advantage there would be to change the catalog magnitudes of the comparison stars from V to PR (Pan-STAARS r’) from the ATLAS refcat2 (Tonry et al., 2018), which has very low systematic errors and so nightly zero-point adjustments virtually disappear.

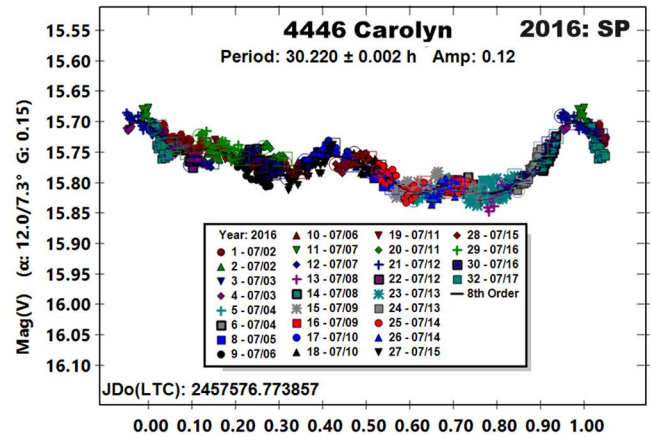
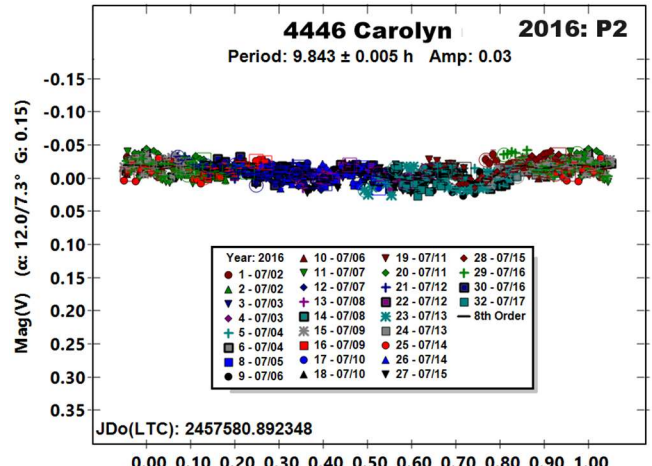
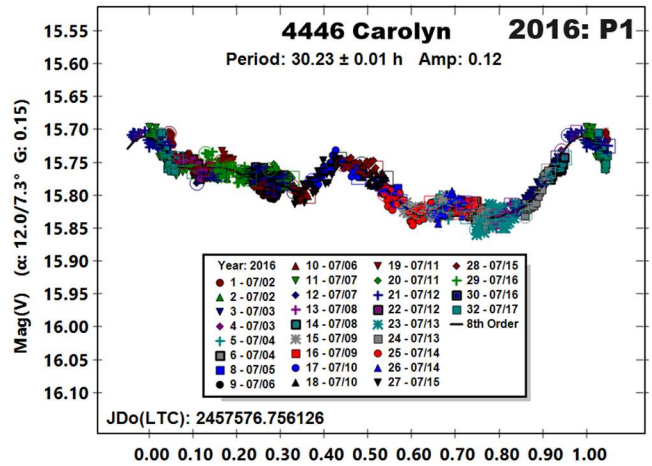
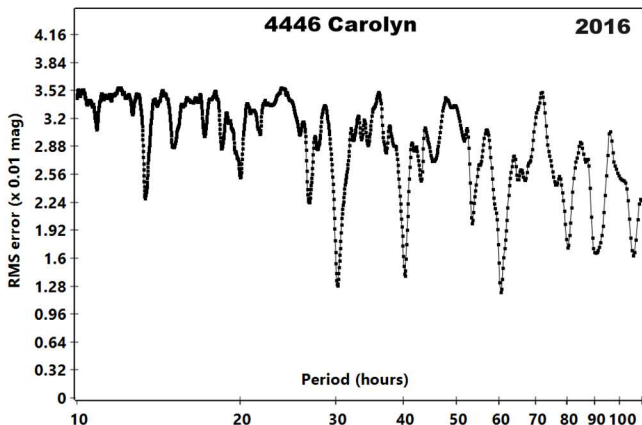
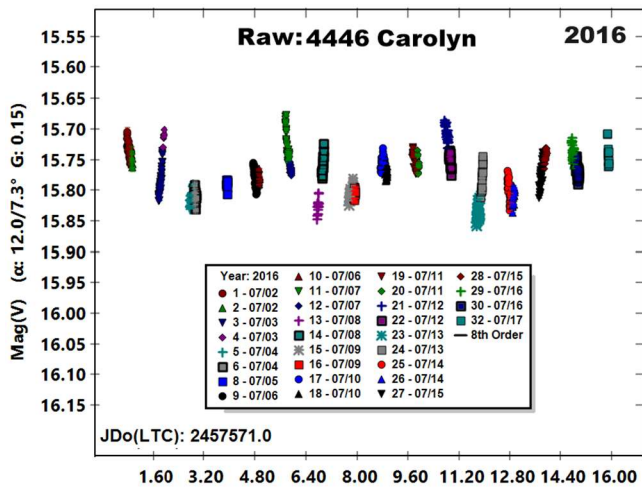
When the ALCDEF data were imported, each night was a “session” with common comp stars. For each session, the phase angle and estimated magnitude based on the known H and adopted G , 0.15 in this case, had to be computed along with differentials in the estimated magnitude ± 6 hours of the mid-date of the observations in the session. Also computed were the Earth and Sun distances. All this allowed applying phase and distance corrections to the ALCDEF magnitudes, which were raw sky values.

The plot of the raw data (with zero-points = 0.0), corrected for phase and distance, follows a mostly symmetrical curve, but this only after excluding data from four nights. Those four nights were not symmetrically spaced, which might have indicated a secondary period worth exploring. The subsequent analysis searched for periods from 10 to 100 hours. The period spectrum closely resembles the one from 2024 in that the 30 h and 60 h periods dominate over 40 h.

Tumbling was excluded from the analysis for both apparitions. The odds of this particular asteroid being in a tumbling state are extremely remote (see Pravec et al., 2005; 2014) due very small or no YORP (Yarkovsky-O'Keefe-Radzievskii-Paddack) effect (Rubincam, 2000) at the solar distances of the Hildas, as are those from a recent-enough collision with another object.

Once a solution was found, $P = 30.23$ h (combined with a P_2 noise filter of 9.843 h, $A = 0.03$ mag; "P2"), the period was fixed and the excluded sessions were reintroduced one night at a time. All but one short session on the second-half of a night fit nicely into place after making zero-point offsets of up to 0.13 mag. These might be explained because of using the V magnitudes from one catalog for most nights but from the other catalog on the four nights. The fact that the slopes of the data fit almost perfectly to the lightcurve from the pre-determined period and then after allowing a new period search helps support this possibility.

As in 2024, the secondary period was essentially a noise/smoothing filter and so the lightcurve using a single-period search ("SP") differed very little from the two-period solution. It's unlikely that the secondary periods have a true physical cause.

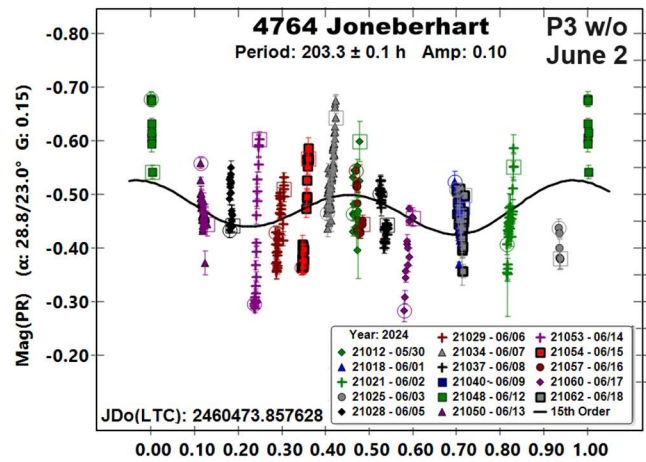
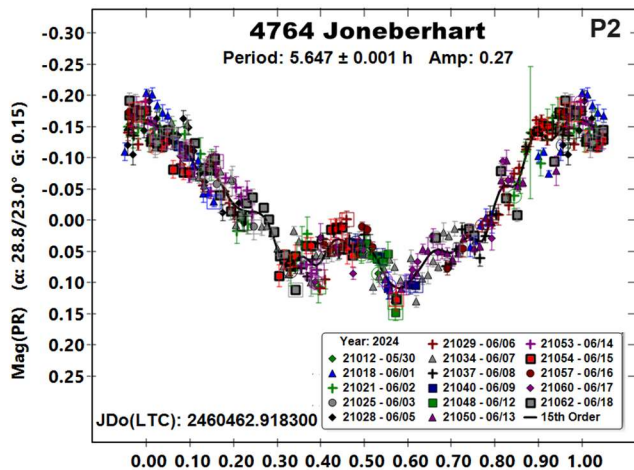
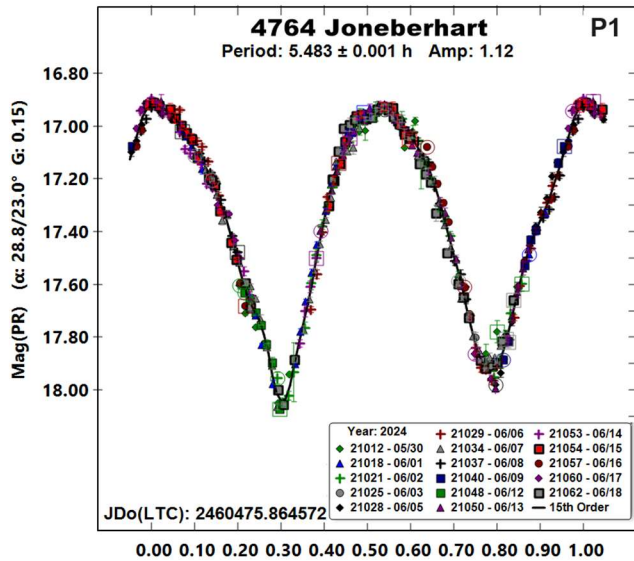
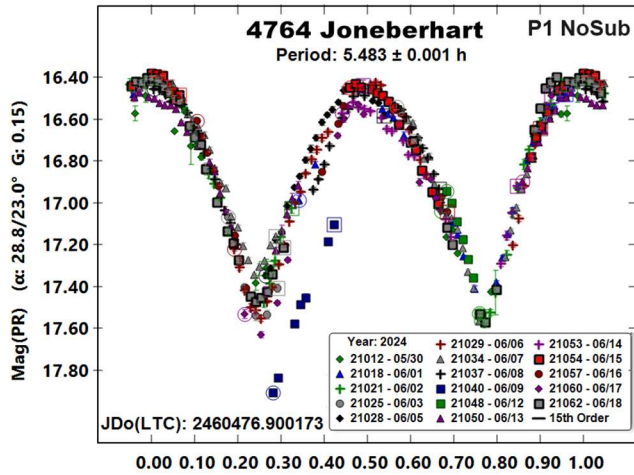


4764 Joneberhart. As in previous years, e.g., (Warner, 2007; Stephens, 2016), the data from the observations showed a strong, dominant period close to 5.48 h. The amplitude has ranged from 0.91 to 1.17 mag over the years. However, in 2024, there were undeniable deviations from the single-period solution that could not be removed by changing the period, increasing the precision, or using unusually large zero-point offsets.

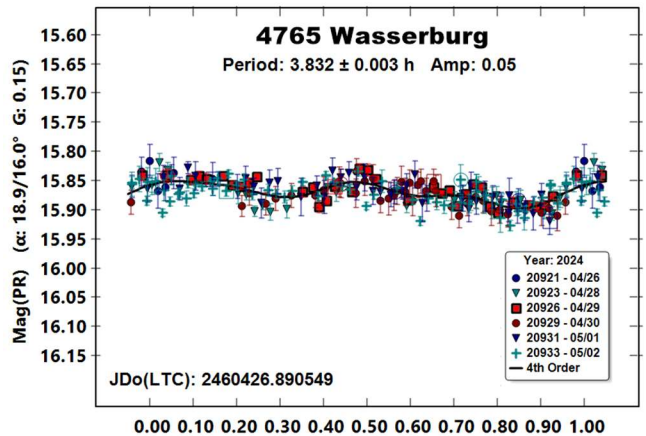
The dual-period search of *MPO Canopus* was used to find a strong secondary period of 5.647 h, $A = 0.27$ mag. It takes going out to 35:34 to get close to an integral ratio (35:33.984). This seems too extreme for the periods to be harmonics of one another, but it cannot be ruled out entirely.

A third period of 203.3 ± 0.1 h (“P3”) produced “P1,” but only after excluding one wayward session. The period was found using a second-order fit since higher orders led to strange lightcurves with amplitudes in the hundreds of magnitudes. A higher-order was used to get the best fit for the two shorter periods with all zero-point adjustments ≤ 0.03 mag and most at 0.0 or ± 0.01 mag.

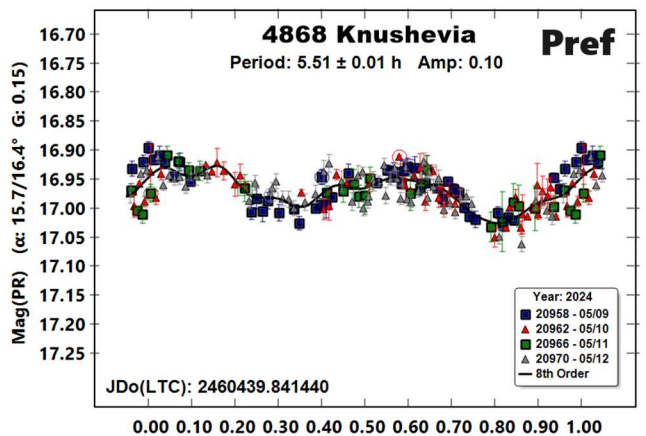
Petr Pravec (private communications, 2024) reviewed the data and found 5.483 h, 5.635 h, and 203.27 but made clear that these were not necessarily the true periods of rotation and precession.

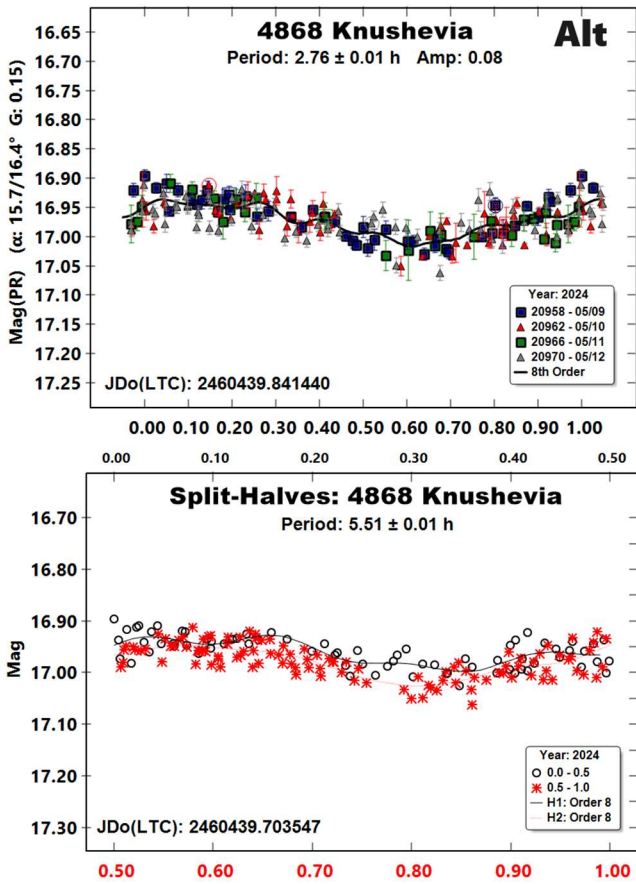


4765 Wasserburg. Pravec et al. (2019) used an extensive set of observations obtained over several years to find a pole of $(\lambda, \beta)_{J2000} = (235^\circ, 8.0^\circ)$ for this Hungaria family member. All previously reported periods were very close to 3.62 h. However, no amount of coaxing could get the 2024 data to fit that period, at least not without excluding a number of sessions and/or applying unacceptably large zero-point offsets. There’s an expression: “A man with one watch knows the time. A man with two watches can’t be sure.”



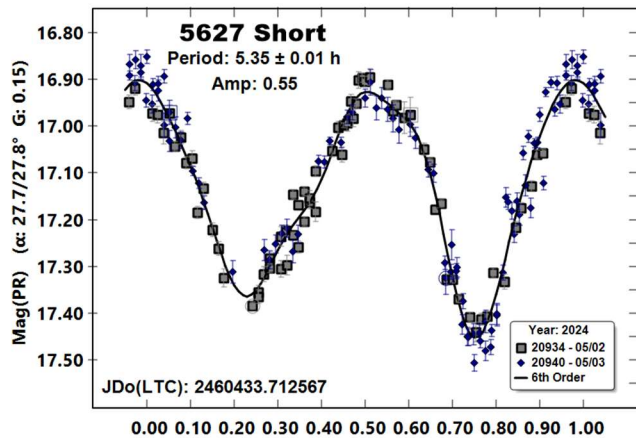
4868 Knushevia. The periods reported previously for this true Hungaria member have ranged from 2.783 h (Stephens and Warner, 2020), to 3.1422 h (Warner and Stephens, 2015) to several near 4.5 h, e.g., Warner (2010b). Enter the data from 2024 and an entirely new set of possibilities.





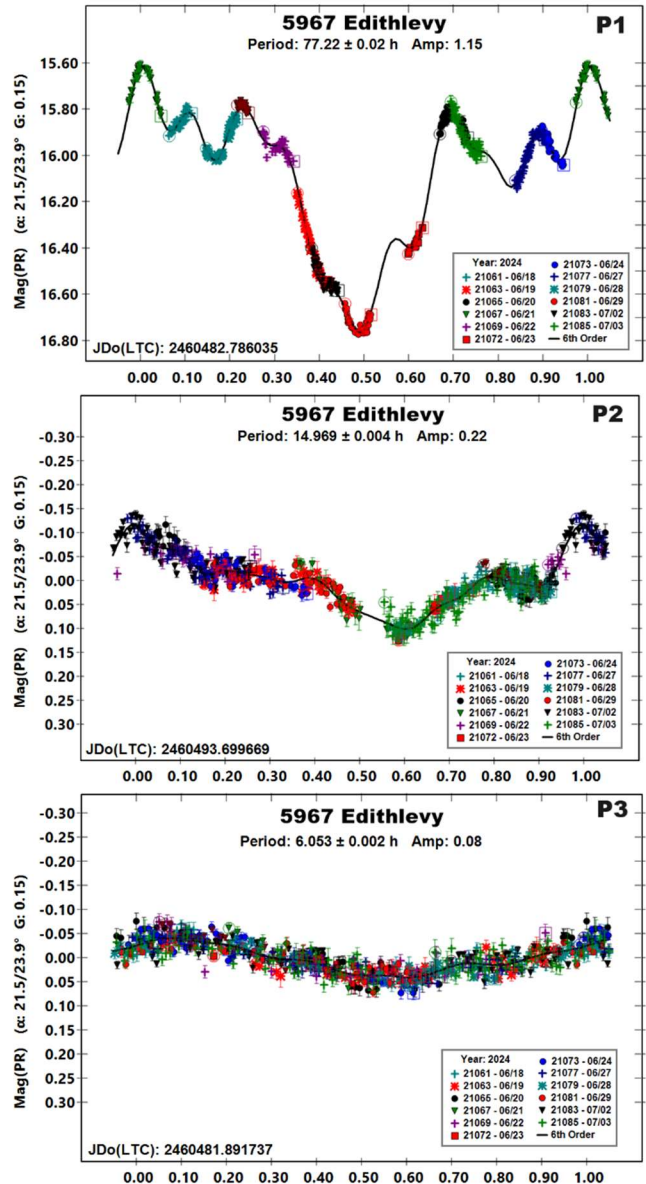
Two solutions were more probable than others, one being a monomodal lightcurve and the other bimodal. The preferred solution is 5.51 h, which is bimodal. This is supported by the split-halves plot, which shows that the two halves might be just enough asymmetrical to favor the 2.76-h, monomodal lightcurve. The alternate solution is not too far removed from the one found by Stephens and Warner (2020).

5627 Short. Stephens and Warner (2019b) found a period of 5.365 h for this member of Hungaria orbital space. The L_{PAB} was 189° in 2024, or about 30° from the 2019 position, when the amplitude was smaller. Observations at L_{PAB} near 230° or 310° would give an approximate pole longitude for the asteroid.



5967 Edithlevy. Given the dominant period of 77 h based on the 2024 data, there is a good chance the Hungaria family member is tumbling (Pravec et al., 2005; 2014), as did the previous result of 66 h (Warner, 2010b).

MPO Canopus cannot properly analyze tumbling asteroids. It can find a dominant period, if there is one to be found, in this case, 77.22 h. Subtracting the Fourier curve from the data found a secondary period of 14.969 h. Subtracting those two results found a third period of 6.053 h. Possibly, but not necessarily, there might be a linear combination of $n/6.053 + m/14.969 = x/77.2$, where n , m , and x are integers.

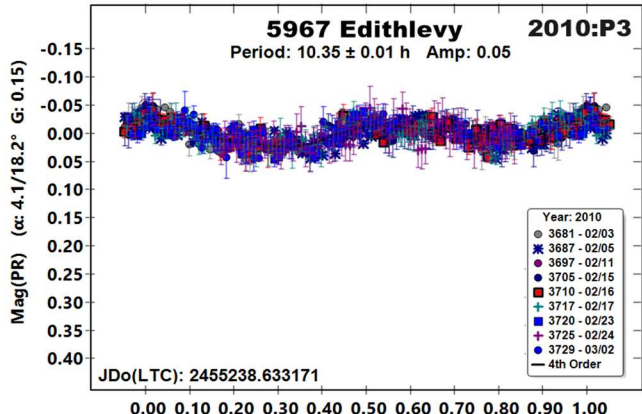
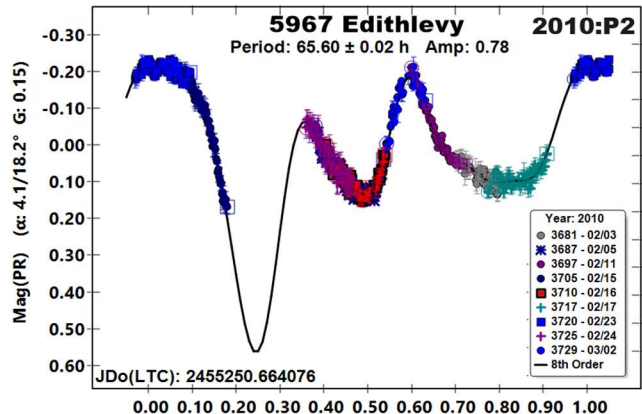
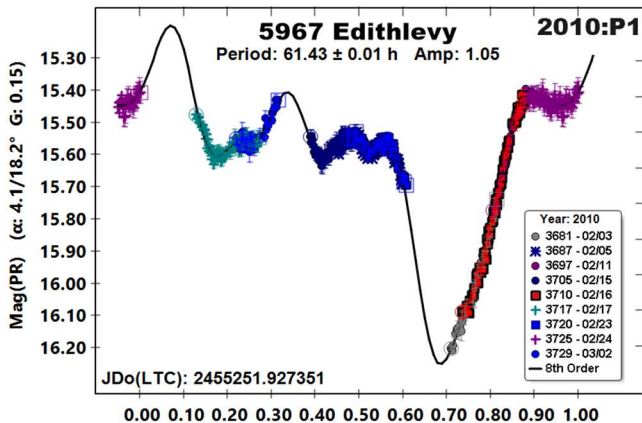


The 2010 data were revisited to test if something similar could be found. At that time, only a single period 66 h was reported (Warner, 2010b), because of the limited capabilities of *MPO Canopus*. Those data used Rc magnitudes for the comp stars. Since the instrumental magnitudes were available, all the calculations were done anew after switching to ATLAS refcat2 PR magnitudes for the comp stars.

Alan Harris (*private communications*, 2010) gives this rule of thumb for tumbling asteroids:

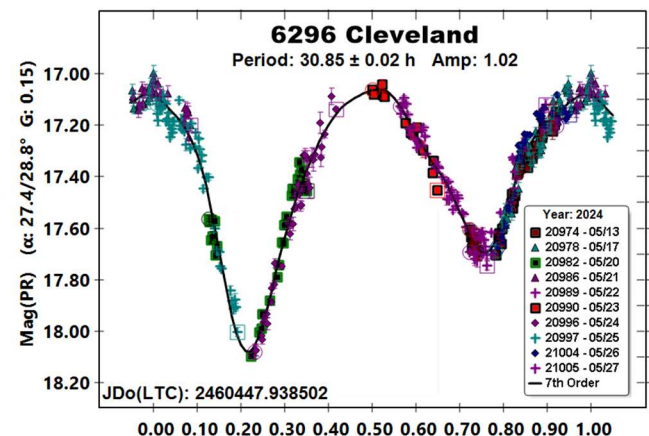
“...the rotation and wobble [precession] frequencies cannot be separated by more than a factor of about the inverse amplitude of variation. Thus, for something varying by 1 magnitude, the two periods must be of the same order; for 0.1 magnitude, they might be as much as a factor of [ten] different...”

The two, true amplitudes (not the Fourier curves amplitudes) from the 2010 data are approximately 0.8 mag, meaning a factor of about 1.25 between the two periods. The dominant periods that were found were 61.43 h and 65.60 h, thus making them compatible with Harris’ constraints as well as consistent with the original result. As is often the case, a small amplitude third period can be found by *MPO Canopus* after subtracting the two dominant periods of a tumbler: 10.35 h that is acting as smoothing filter and unlikely real.

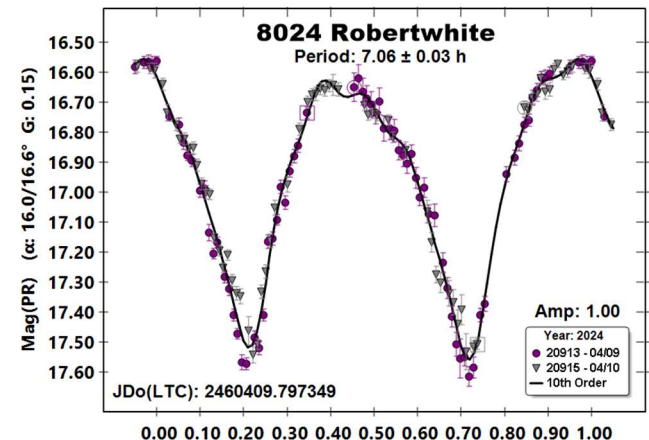


The different solutions are not surprising given the software and data set limitations. However, the new analysis from both years confirms the suspected tumbling and that the dominant period is on the order of 60-80 h, and more likely 64-68 h. Remember that even with proper software, the data sets do not allow finding a unique solution for the periods of rotation and precession (Pravec et al., 2005; 2014).

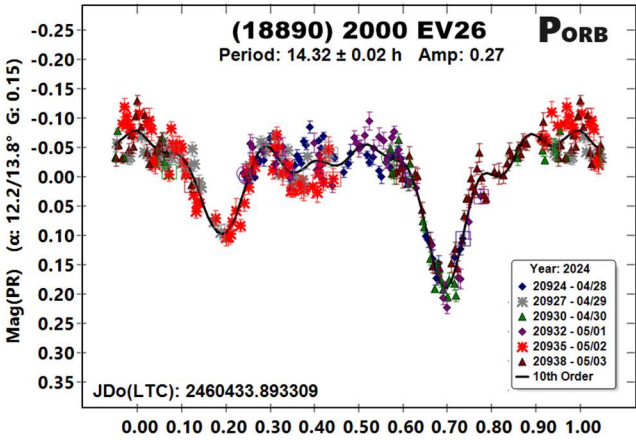
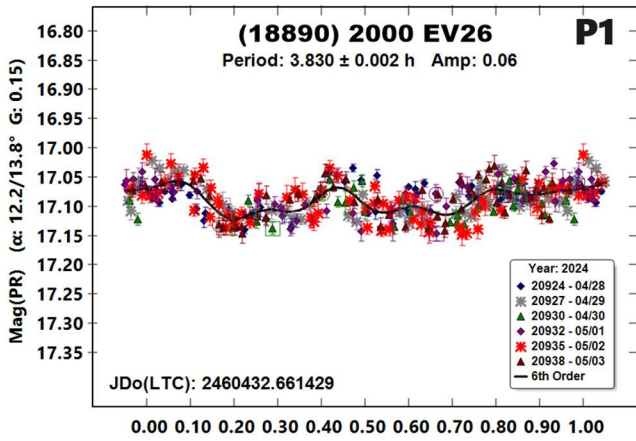
6296 Cleveland. Originally reported to have a period of 15.38 h (Warner, 2006) or 15.65 h (Warner, 2008), observations at PDO in 2011 found a unique solution of 30.84 h (Warner, 2011), aided by the large amplitude of 0.70 mag, whereas the previous results were based on amplitudes of 0.20 and 0.11 mag, respectively. Modeling by Durech et al. (2020) confirmed the 30.8-hour solution as did analysis of the 2024 observations made at CS-3. The images from 2006 and 2008 have yet to be recovered after a hard drive failure. They will have to be remeasured since the coordinates of the comp stars were not stored at the time.



8024 Robertwhite. The two previous results from CS3 were 7.063 h (Warner, 2013b; 2015a). The result of the analysis of the 2024 data is in good agreement. Of the three apparitions, 2024 had the largest amplitude, but only by 0.1 mag above the smallest.

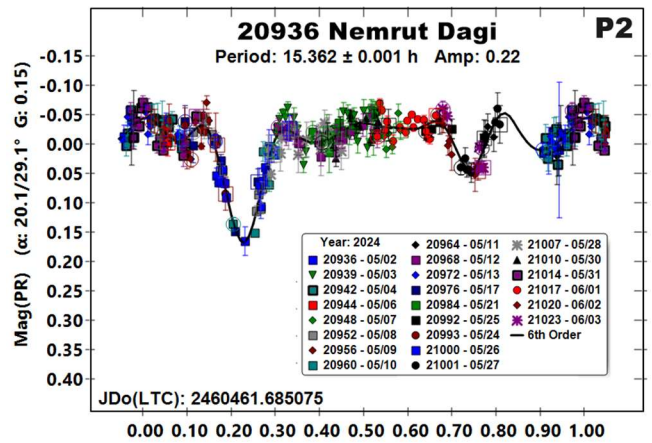
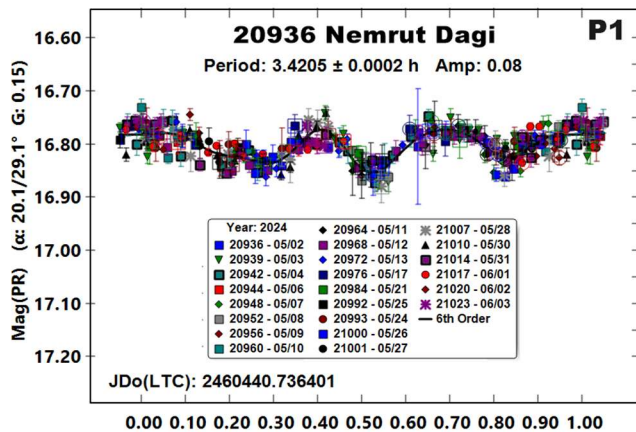


(18890) 2000 EV26. Warner (2015b) reported the binary discovery, finding a primary rotation period of 3.8216 h and satellite orbital period of 14.29 h. The estimated effective diameters ratio was $D_s/D_p \geq 0.27$. The 2024 results were $P = 3.830$ h, $P_{ORB} = 14.32$ h, and $D_s/D_p \geq 0.38$. The L_{PAB} at the two apparitions were about 120° apart, which may account for at least some of the difference in ratio estimates.

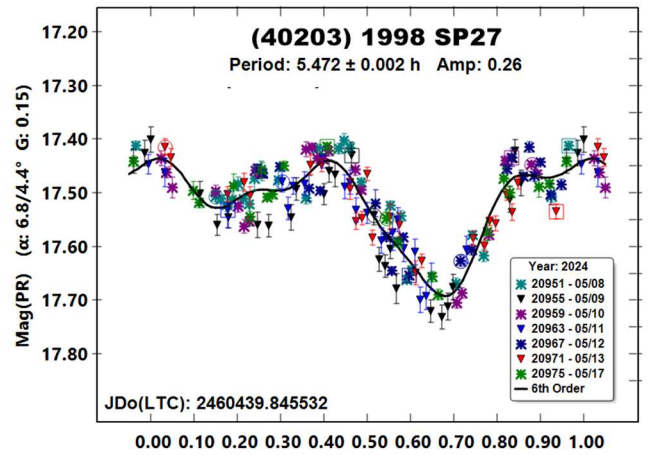


20936 Nemrut Dagi. Neither the *Asteroids with Satellites* web site (Johnston, 2024) or the LCDB report this as a binary asteroid. The observations made at CS3 in 2024 May and June appear to indicate otherwise. Despite having to remove a substantial number of observations due to interfering field stars, analysis of the data set led to a primary rotation period $P1 = 3.4205$ h and a satellite orbital $P2 = 15.362$ h. The mutual events, occultations or eclipses, had depths of about 0.08-0.19 mag. The shallower event leads to an estimated diameters ratio of $Ds/Dp \geq 0.28$.

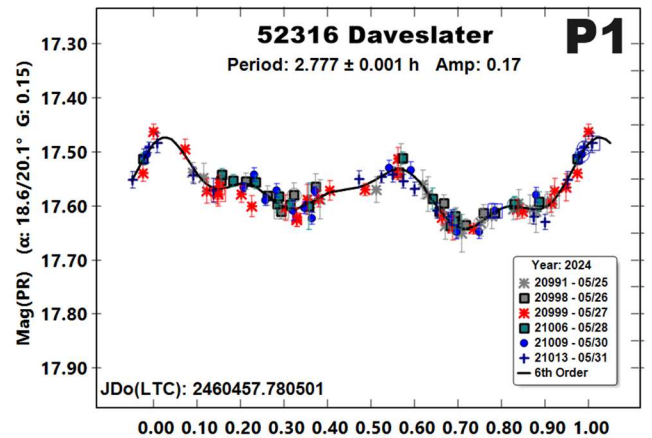
Given the low amplitude of the primary lightcurve and the relatively large phase angles, its trimodal shape is not particularly unusual. The large phase angles may also be responsible for what appears to be a “double mutual event” between 0.75-0.95 on the $P2$ plot. The cause could be shadowing effects on the two bodies, a shadow transit, or – less exotically – artifacts in the dual-period analysis.



(40203) 1998 SP27. Previous rotation period results from PDO/CS3 (Warner, 2010a; 2013b) were both close to 5.44 h. The data from 2024 produced a slightly longer period of 5.472 h; the lightcurve shape and somewhat noisy data set may help account for the difference.



52316 Daveslater. Warner (2013a) reported this to be a binary based on data from 2012 December with $P1 = 2.7629$ h, $P2 = 13.435$ h, and $Ds/Dp \geq 0.1$. The 2024 data analysis found $P1 = 2.77$ h, close to the earlier result. $P2$, however, was shorter, 13.192 h. The paucity of data in 2024 makes the confirmation of the 2013 values less than ideal. The Ds/Dp for 2024 was ≥ 0.26 . The difference in viewing aspects, as well as the sparse 2024 data set, are likely behind the different primary lightcurve amplitudes and orbital period.



Acknowledgements

This work includes data from the Asteroid Terrestrial-impact Last Alert System (ATLAS) project. ATLAS is primarily funded to search for near earth asteroids through NASA grants NN12AR55G, 80NSSC18K0284, and 80NSSC18K1575; byproducts of the NEO search include images and catalogs from the survey area. The ATLAS science products have been made possible through the contributions of the University of Hawaii Institute for Astronomy, the Queen's University Belfast, the Space Telescope Science Institute, and the South African Astronomical Observatory.

The author gratefully acknowledges a Shoemaker NEO Grants from the Planetary Society (2007). This was used to purchase some of the equipment used in this research.

References

Durech, J.; Tonry, J.; Erasmus, N.; Denneau, L.; Heinze, A.N.; Flewelling, H.; Vanco, R. (2020). "Asteroid models reconstructed from ATLAS photometry." *Astron. Astrophys.* **643**, A59.

Harris, A.W.; Young, J.W.; Scaltriti, F.; Zappala, V. (1984). "Lightcurves and phase relations of the asteroids 82 Alkmene and 444 Gyptis." *Icarus* **57**, 251-258.

Henden, A.A.; Terrell, D.; Levine, S.E.; Templeton, M.; Smith, T.C.; Welch, D.L. (2009). <http://www.aavso.org/apass>

Johnston, W.R. (2024). *Asteroids with Satellites* web site. Updated 2024 July 10. <https://www.johnstonsarchive.net/astro/asteroidmoons.html>

Muinos, J.L. (2017). *Carlsberg Meridian Catalog* web site. <http://svo2.cab.inta-csic.es/vocats/cmc15/>

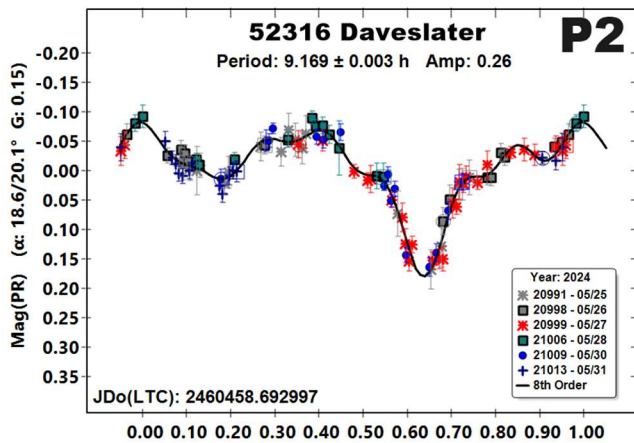
Nesvorny, D. (2015). "Nesvorny HCM Asteroids Families V3.0." NASA Planetary Data Systems, id. EAR-A-VARGBET-5-NESVORNYFAM-V3.0.

Nesvorny, D.; Broz, M.; Carruba, V. (2015). "Identification and Dynamical Properties of Asteroid Families." In *Asteroids IV* (P. Michel, F. DeMeo, W.F. Bottke, R. Binzel, Eds.). Univ. of Arizona Press, Tucson, also available on astro-ph.

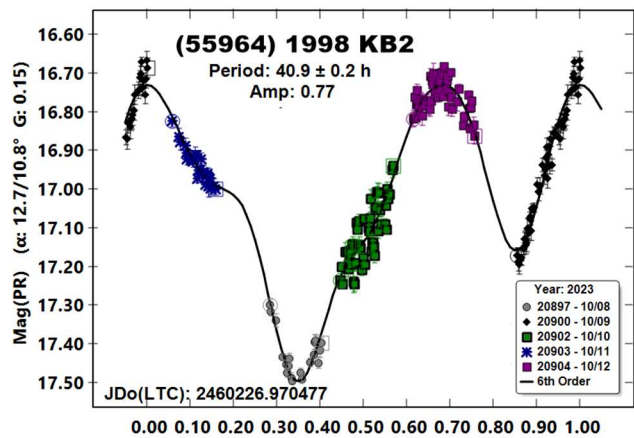
Pravec, P.; Harris, A.W.; Scheirich, P.; Kušnirák, P.; Šarounová, L.; Hergenrother, C.W.; Mottola, S.; Hicks, M.D.; Masi, G.; Krugly, Yu.N.; Shevchenko, V.G.; Nolan, M.C.; Howell, E.S.; Kaasalainen, M.; Galád, A.; Brown, P.; Degraff, D.R.; Lambert, J.V.; Cooney, W.R.; Foglia, S. (2005). "Tumbling asteroids." *Icarus* **173**, 108-131.

Pravec, P.; Scheirich, P.; Durech, J.; Pollock, J.; Kusnirak, P.; Hornoch, K.; Galad, A.; Vokrouhlicky, D.; Harris, A.W.; Jehin, E.; Manfroid, J.; Opitom, C.; Gillon, M.; Colas, F.; Oey, J.; Vrástil, J.; Reichart, D.; Ivarsen, K.; Haislip, J.; LaCluyze, A. (2014). "The tumbling state of (99942) Apophis." *Icarus* **233**, 48-60.

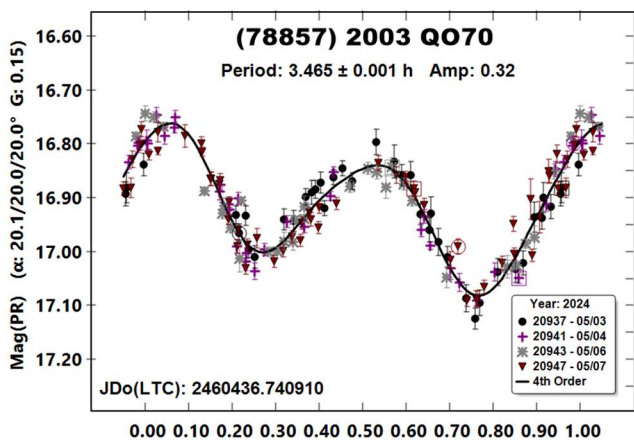
Pravec, P.; Fatka, P.; Vokrouhlicky, D.; Scherich, P.; Durech, J.; Scheeres, D.J.; Kusnirak, P.; Hornoch, K.; Galad, A.; and 41 colleagues (2019). "Asteroid Pairs: A Complex Picture." *Icarus* **333**, 429-463.



(55964) 1998 KB₂. This appears to be the first reported period for this collisional family member of the Hungarias. The period makes it a good candidate for tumbling (Pravec et al, 2005; 2014).



(78857) 2003 QO70. A previous result of 3.380 h was reported by Warner (2016). The higher-quality data set in 2024 allowed refining both the period (3.465 h, 0.32 mag) and quality of the result ($U = 2+$ to 3).



- Rubincam, D.P. (2000). "Radiative Spin-up and Spin-down of Small Asteroids." *Icarus* **148**, 2-11.
- Stephens, R.D. (2016). "Asteroids Observed from CS3: 2016 April - June." *Minor Planet Bull.* **43**, 336-339.
- Stephens, R.D.; Warner, B.D. (2019a). "Main-belt Asteroids Observed from CS3: 2018 October - December." *Minor Planet Bull.* **46**, 180-187.
- Stephens, R.D.; Warner, B.D. (2019b). "Main-belt Asteroids Observed from CS3: 2019 April to June." *Minor Planet Bull.* **46**, 449-456.
- Stephens, R.D.; Warner, B.D. (2020). "Main-belt Asteroids Observed from CS3: 2019 July to September." *Minor Planet Bull.* **47**, 50-60.
- Stephens, R.D.; Coley, D.R.; Warner, B.D. (2021). "Main-belt Asteroids Observed from CS3: 2021 January to March." *Minor Planet Bull.* **48**, 246-267.
- Tonry, J.L.; Denneau, L.; Flewelling, H.; Heinze, A.N.; Onken, C.A.; Smartt, S.J.; Stalder, B.; Weiland, H.J.; Wolf, C. (2018). "The ATLAS All-Sky Stellar Reference Catalog." *Astrophys. J.* **867**, A105.
- Wang, Y.-B.; Xu, Y. (2021). "Study on the asteroidal spin rates in the Hungaria region." *Astron. Nach.* **342**, 914-925.
- Warner, B.D. (2006). "Asteroid lightcurve analysis at the Palmer Divide Observatory - March - June 2006." *Minor Planet Bull.* **33**, 85-88.
- Warner, B.D. (2007). "Asteroid Lightcurve Analysis at the Palmer Divide Observatory - December 2006 - March 2007." *Minor Planet Bull.* **34**, 72-77.
- Warner, B.D. (2008). "Asteroid Lightcurve Analysis at the Palmer Divide Observatory: December 2007 - March 2008." *Minor Planet Bull.* **35**, 95-98.
- Warner, B.D. (2010a). "Asteroid Lightcurve Analysis at the Palmer Divide Observatory: 2009 September-December." *Minor Planet Bull.* **37**, 57-64.
- Warner, B.D. (2010b). "Asteroid Lightcurve Analysis at the Palmer Divide Observatory: 2009 December - 2010 March." *Minor Planet Bull.* **37**, 112-118.
- Warner, B.D. (2011). "Asteroid Lightcurve Analysis at the Palmer Divide Observatory: 2011 March - July." *Minor Planet Bull.* **38**, 190-195.
- Warner, B.D. (2013a). "Seeing Double Old and New: Observations and Lightcurve Analysis at the Palmer Divide Observatory of Six Binary Asteroids." *Minor Planet Bull.* **40**, 94-98.
- Warner, B.D. (2013b). "Asteroid Lightcurve Analysis at the Palmer Divide Observatory: 2013 February-March. The Final Report." *Minor Planet Bull.* **40**, 217-220.
- Warner, B.D. (2015a). "Asteroid Lightcurve Analysis at CS3-Palmer Divide Station: 2014 June-October." *Minor Planet Bull.* **42**, 54-60.
- Warner, B.D. (2015b). "A Sextet of Main-belt Binary Asteroid Candidates." *Minor Planet Bull.* **42**, 60-66.
- Warner, B.D. (2016). "Asteroid Lightcurve Analysis at CS3-Palmer Divide Station: 2016 April-July." *Minor Planet Bull.* **43**, 300-304.
- Warner, B.D. (2017). "Asteroid Lightcurve Analysis at CS3-Palmer Divide Station: 2016 July-September." *Minor Planet Bull.* **44**, 12-19.
- Warner, B.D. (2023). "Asteroid Lightcurve Analysis at the Center for Solar System Studies: Palmer Divide Station 2022 September-November." *Minor Planet Bull.* **50**, 164-170.
- Warner, B.D.; Higgins, D.; Pray, D.P.; Dyvig, R.; Vishnu, R.; Durech, J. (2008). "A Shape and Spin Model for 1600 Vysotsky." *Minor Planet Bull.* **35**, 13-14.
- Warner, B.D.; Harris, A.W.; Pravec, P. (2009). "The Asteroid Lightcurve Database." *Icarus* **202**, 134-146. Updated 2023 August. <https://www.minorplanet.info/php/lcdb.php>
- Warner, B.D.; Stephens, R.D.; Harris, A.W. (2013). *CBET 3402*.
- Warner, B.D.; Stephens, R.D. (2013). "1727 Mette: A New Hungaria Binary." *Minor Planet Bull.* **40**, 129-130.
- Warner, B.D.; Stephens, R.D. (2015). "The Hungaria Asteroid 4868 Knushevia: A Possible Binary." *Minor Planet Bull.* **42**, 188-189.
- Warner, B.D.; Stephens, R.D.; Coley, D.R. (2017). "Lightcurve Analysis of Hilda Asteroids at the Center for Solar System Studies: 2016 June-September." *Minor Planet Bull.* **44**, 36-41.

Number	Name	2024/mm/dd*	Phase	L _{PAB}	B _{PAB}	Period(h)	P.E.	Amp	A.E.	Grp/DR
1600	Vyssotsky	04/09-04/10	25.6, 25.8	170	27	3.205	0.004	0.15	0.01	9102
1727	Mette	06/06-06/16	25.8, 23.2	303	12	^B 2.9809 21.00	0.0001 0.01	0.46 0.17	0.02 0.02	9102 0.38
1920	Sarmiento	05/06-05/08	6.7, 5.8	233	8	4.052	0.003	0.33	0.02	003
2049	Grietje	04/16-04/30	*5.9, 8.1	212	9	^A 21.5 10.79	0.03 0.01	0.21 0.20	0.02 0.03	9102
2150	Nyctimene	05/07-05/31	23.1, 19.6	260	29	^F 6.12514 38.08	0.00006 0.02	0.65 0.11	0.02 0.01	9102 0.22
4446	Carolyn	06/19-07/05 16/07/02-07/17	16.1, 12.0 12.10, 7.50	312 310	8 8	^B 30.257 7.851 ^B 30.23 9.843	0.008 0.003 0.01 0.005	0.20 0.04 0.12 0.03	0.02 0.01 0.01 0.01	9107
4764	Joneberhart	05/30-06/18	28.8, 23.0	295	19	^T 5.483 5.647 203.3	0.001 0.001 0.1	1.12 0.27 0.7	0.02 0.03 0.1	003
4765	Wasserburg	04/16-05/02	23.1, 15.9	238	16	3.832	0.003	0.05	0.01	003
4868	Knushevia	05/09-05/12	15.7, 16.4	224	22	5.52	0.01	0.09	0.02	003
5627	Short	05/02-05/03	27.7, 27.8	189	32	5.35	0.01	0.55	0.03	9102
5967	Edithlevy	06/18-07/03 10/02/03-03/02	21.6, 24.0 4.0, 18.5	254 135	26 9	^F 77.22 14.969 6.053 ^F 61.43 65.60 10.35	0.02 0.004 0.002 0.01 0.02 0.01	1.15 0.22 0.08 0.9 0.8 0.05	0.05 0.03 0.01 0.1 0.1 0.01	003
6296	Cleveland	05/13-05/27	27.4, 28.8	211	36	30.85	0.02	1.02	0.05	9102
8024	Robertwhite	04/09-04/10	16.0, 16.6	177	2	7.06	0.03	1	0.03	003
18890	2000 EV26	04/28-05/02	12.2, 13.5	212	18	^B 3.830 14.32	0.002 0.02	0.06 0.20	0.01 0.02	9102 0.38
20936	Nemrut Dagi	05/02-05/31	20.1, 28.6	191	2	^B 3.4204 15.362	0.0002 0.001	0.09 0.15	0.01 0.02	9102 0.22
40203	1998 SP27	05/08-05/13	6.7, 4.7	234	7	5.478	0.002	0.42	0.03	003
52316	Daveslater	05/18-06/05	17.4, 21.5	224	21	^B 2.7199 13.192	0.0002 0.004	0.14 0.02	0.01 0.01	9102 0.26
55964	1998 KB2	23/10/08-10/12	12.6, 10.8	24	13	40.9	0.2	0.76	0.05	003
78857	2003 QO70	05/03-05/07	19.9, 19.9	233	25	3.465	0.001	0.32	0.02	9102

Table II. Observing circumstances and results. *All dates are from 2024, except when preceded by the last two digits of a year, 23 = 2023. The phase angle is given for the first and last date. If preceded by an asterisk, the phase angle reached an extremum during the period. L_{PAB} and B_{PAB} are the approximate phase angle bisector longitude/latitude at mid-date range (see Harris et al., 1984). The Grp column gives the asteroid family or group (Nesvorny 2015; Nesvorny et al. 2015). 003: collisional family member; 9102: Hungaria orbital space; 9107: Hilda asteroid (from orbital elements). ^AAmbiguous. ^BPrimary of binary asteroid. ^DDominant period of dual-period lightcurve. ^TDominant period of likely tumbler. For suspected binaries, the Grp/DR column on the second line gives the estimated dimeters ratio, D_s/D_p. second line All ratios are minimum values since no total events were seen. The multiple periods for a suspected tumbler are unlikely the periods of rotation and precession.

HUNGARIA ASTEROID 6859 DATEMASAMUNE: A SPLIT DECISION

Brian D. Warner
Center for Solar System Studies (CS3)
446 Sycamore Ave.
Eaton, CO 80615 USA
brian@MinPlanObs.org

(Received: 2024 July 15)

A review of data from 2006 through 2024 for the Hungaria orbital group member 6859 Datasamune was made in an attempt to consolidate numerous previously reported, and then revised multiple times, synodic rotation periods into a single, well-determined value. Instead, while a monomodal lightcurve with a period of 2.65 h was adopted, the double period, bimodal lightcurve cannot be formally excluded and more so, a secondary period of about 43 h was found in the data for all six apparitions.

CCS photometry observations of the Hungaria group member 6859 Datasamune (Nesvorný; Nesvorný et al., 2015) were made from 2024 June 3-17 at CS3-Palmer Divide Station. A 0.35-m Schmidt-Cassegrain telescope was combined with an FLI Micro-Line 1001E and clear filter. Exposures were 240 seconds and guided. The raw images were processed with master flat and dark frames using *MPO Canopus* (Warner, 2024).

To reduce the number of times and amounts of adjusting nightly zero-points, the ATLAS (Tonry et al., 2018) catalog PR magnitudes (r' on the Pan-STARRS photometric system) are used. Those adjustments are usually $\leq \pm 0.02$ mag. In very rare cases, larger corrections are used and may be related in part to using unfiltered observations, poor centroiding of the reference stars, and not correcting for second-order extinction. Another cause may be selecting what appears to be a single star but is actually an unresolved pair. For the analysis reported here, zero-point adjustments > 0.02 mag were not allowed.

The Y-axis values are ATLAS SR “sky” (catalog) magnitudes. The values in the parentheses give the phase angle(s), a , along with the value of G used to normalize the data to the comparison stars and asteroid phase angle used in the earliest session. This, in effect, adjusts all the observations so that they seem to have been made at a single fixed date/time and phase angle. Presumably, any remaining variations are due only to the asteroid’s rotation and/or albedo changes.

There can be up to three phase angles. If two, the values are for the first and last night of observations. If three, the middle value is the extrema (maximum or minimum) reached between the first and last observing runs. The X-axis shows rotational phase from -0.05 to 1.05. If the plot includes the amplitude, e.g., “Amp: 0.65,” this is the amplitude of the Fourier model curve and *not necessarily the adopted amplitude for the lightcurve*.

Background

A period of 12.95 h (Warner, 2006) was the first reported period based on observations at the Palmer Divide Observatory (PD; Colorado) or at CS3 (California). Observations in 2009 led to 22.1 h (Warner, 2010) and analysis of data obtained in 2011 (Warner, 2011) found 86.1 h. All of these have since been rated $U = 0$ (wrong) in the asteroid lightcurve database (LCDB; Warner

et al., 2009). Another try was made in 2016 (Warner, 2016); this led to 5.2879 h and the declaration, “The mystery may be (almost) finally solved.” The gods were laughing since it was admitted that the solution was not unique and that one of 2.644 h was still possible, depending on whether a bimodal lightcurve was accepted for the longer period and a monomodal lightcurve for the shorter period.

Harris et al. (2014) pointed out that lightcurves of low amplitude, $A \leq 0.10$ mag, and low phase angles could not be assumed to be just monomodal or bimodal, but could be trimodal and higher. The uncertainty diminishes with increasing amplitude, but it’s not until $A \geq 0.30$ mag that a bimodal lightcurve is virtually assured. These rules don’t apply at high phase angles, where shadowing effects have led to cases of a monomodal lightcurve with $A > 0.5$ mag.

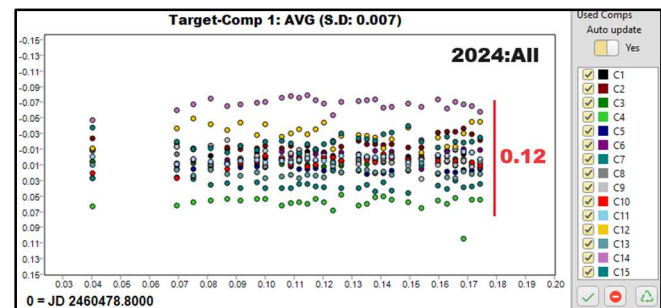
The 2024 data led to unexpected results, not only disputing the previously adopted period of 5.944 h, but discovering the possibility that the asteroid is a binary or, at the very least, there is a second period to be found. This started a detailed review of all data obtained at the 2006, 2009, 2011, 2016, and 2019 apparitions.

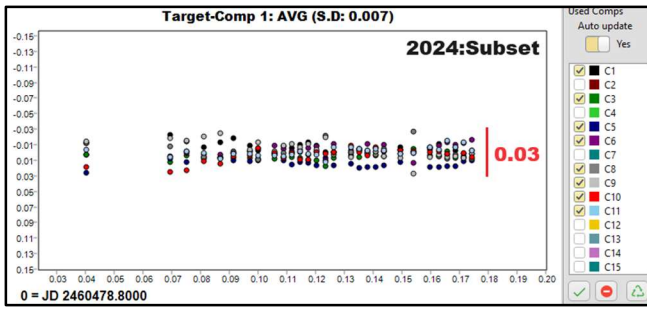
Data Revision and Analysis Methodology

The original measurements for all apparitions were available, meaning the instrumental magnitudes for the asteroid and the comp stars, and so the magnitudes for the target could be placed on a near common zero-point by changing the catalog magnitudes of the comp stars. This was required since various catalogs were used over time and so it would hard to determine the full effect of zero-point adjustments during each apparition. Since the amplitude was always low, even the small adjustment could change the period, even to the point where the solution jumped from a monomodal to bimodal lightcurve or vice versa.

To accomplish this first, critical step, it was necessary to use the Vizier (2024) web pages to access the ATLAS refcat2 catalog, which was easier in this case than using the Mikulski Archive for Space Telescopes (MAST, 2024) site. Fortunately, the RA and Declination for each comp star was available and so the tedious task of doing lookups for five comp stars for each night of observations began. A search radius of 1 arcsecond was used to eliminate close companions as much as possible. If no stars were found, the radius was expanded to 2 arcseconds. Beyond that, it was assumed that the star was not in the catalog. In the case where multiple stars were returned, even when going down to 0.5 arcsecond, the magnitude corresponded the closest to the original magnitude was adopted.

Then, for each session, it was necessary to check the fit the derived magnitude of the asteroid using ensemble photometry. The screen shots from *MPO Canopus* show the differential of the derived magnitudes of the asteroid minus the average of all the comp stars.

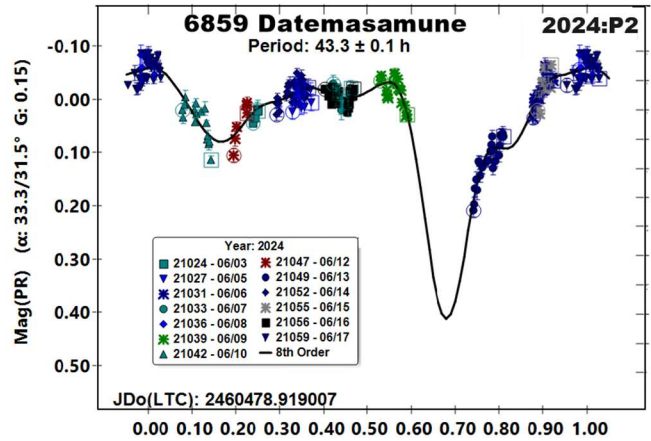
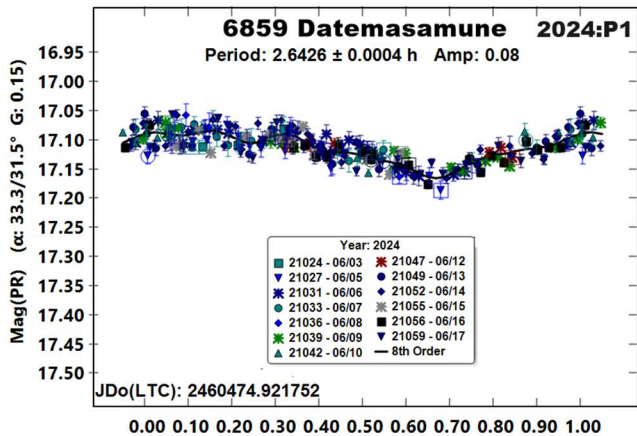
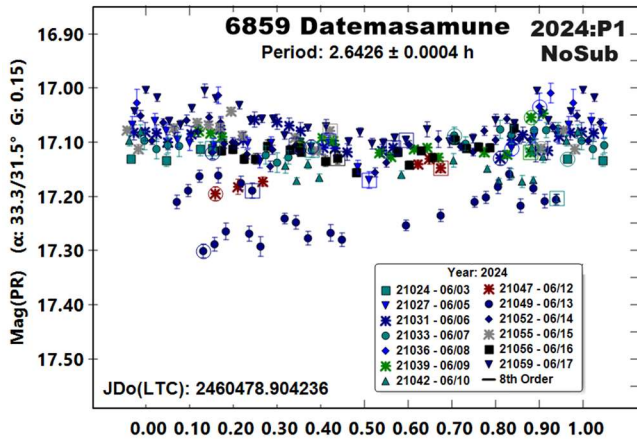




When using all comps, the standard deviation was about ± 0.12 mag, which would be approximately the errors bars for each data point on the lightcurve. After excluding the worst outliers, the standard deviation was reduced to ± 0.03 mag.

The original data allowed only five comp stars through the 2019 apparition; if at all possible, at least two were used. *MPO Canopus*, can subtract among three additive periods (tumblers are not additive; see Pravec et al., 2005; 2014). The period analysis is based on the FALC algorithm developed by Alan Harris (Harris et al., 1989).

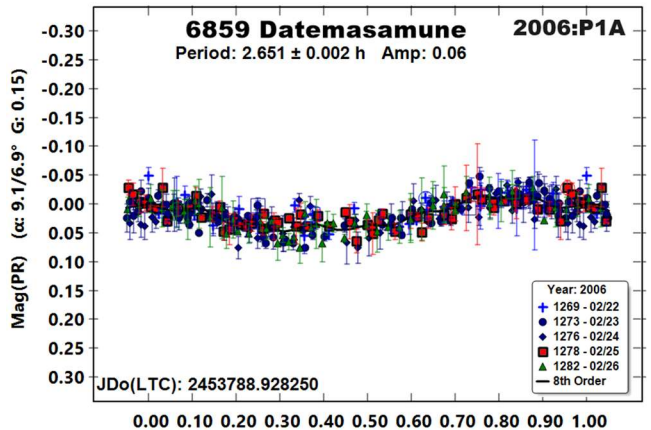
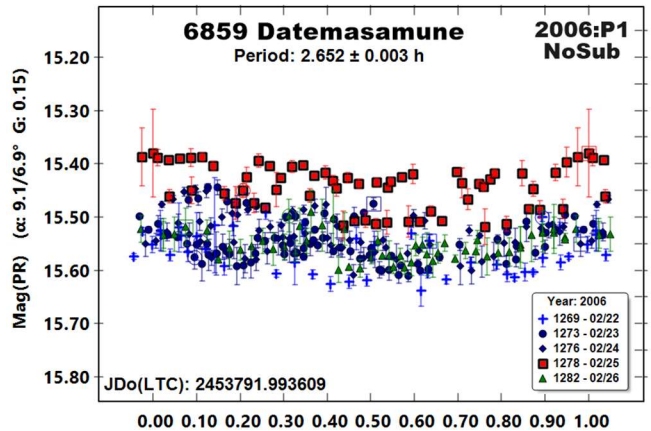
2024 Apparition. What started it all were the data obtained in 2024 June at CS3. The initial period search showed significant deviations, often attributed to a secondary period. A dual-period search found a primary period, $P_1 = 2.6426$ h, which doubled to $P_{2x} = 5.285$ h, is significantly different from the 5.944 h reported by Stephens and Warner (2019).

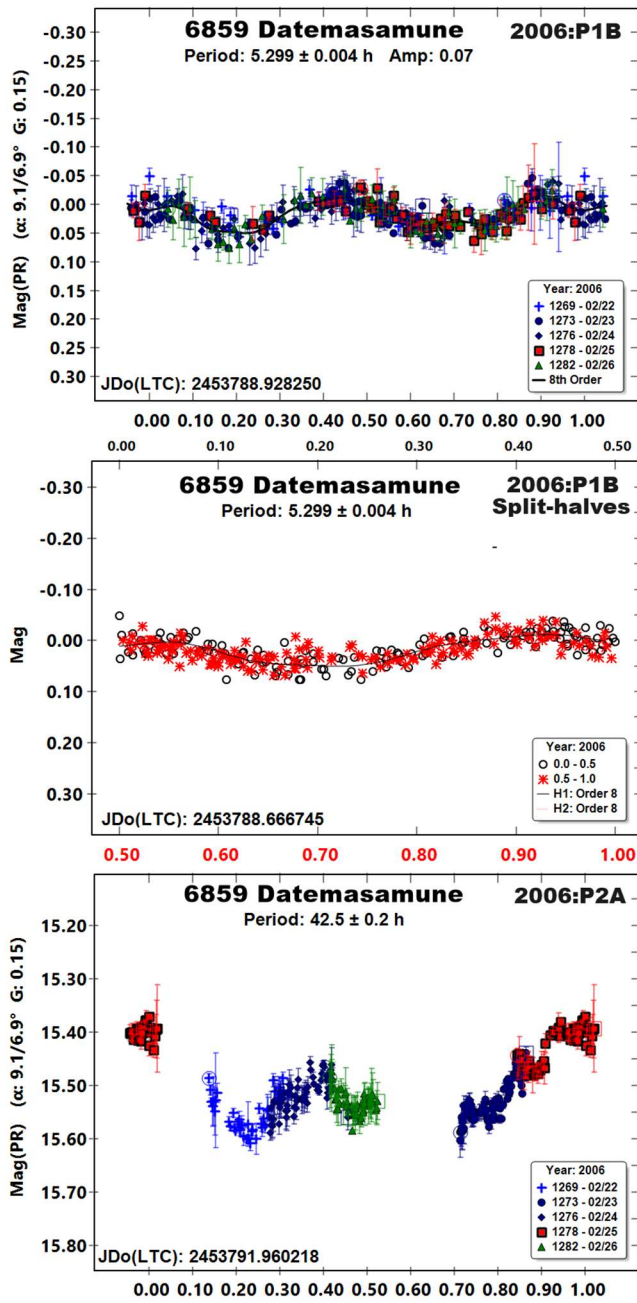


In that paper, they also re-analyzed data from the previous apparitions and adopted a bimodal lightcurve because of asymmetry of the halves. However, it's worth considering that the phase angle was near 31° at the time, which starts to introduce concerns about shadowing effects. Also, the lightcurve lacked full coverage, being sparse near 0.3 rotation phase.

The case for a secondary period in 2024 is based mostly on the apparent drops from the average curve that are separated in phase by 0.5, or too symmetrical to reject out-of-hand. This raised the questions about the earlier analysis.

2006 Apparition. The revised data from 2006 also show significant deviations from a single period solution. The search result for the dominant period was ambiguous, finding $P_A = 2.651$ h and $P_B = 5.299$ h. Again, neither one in line with the previous results.



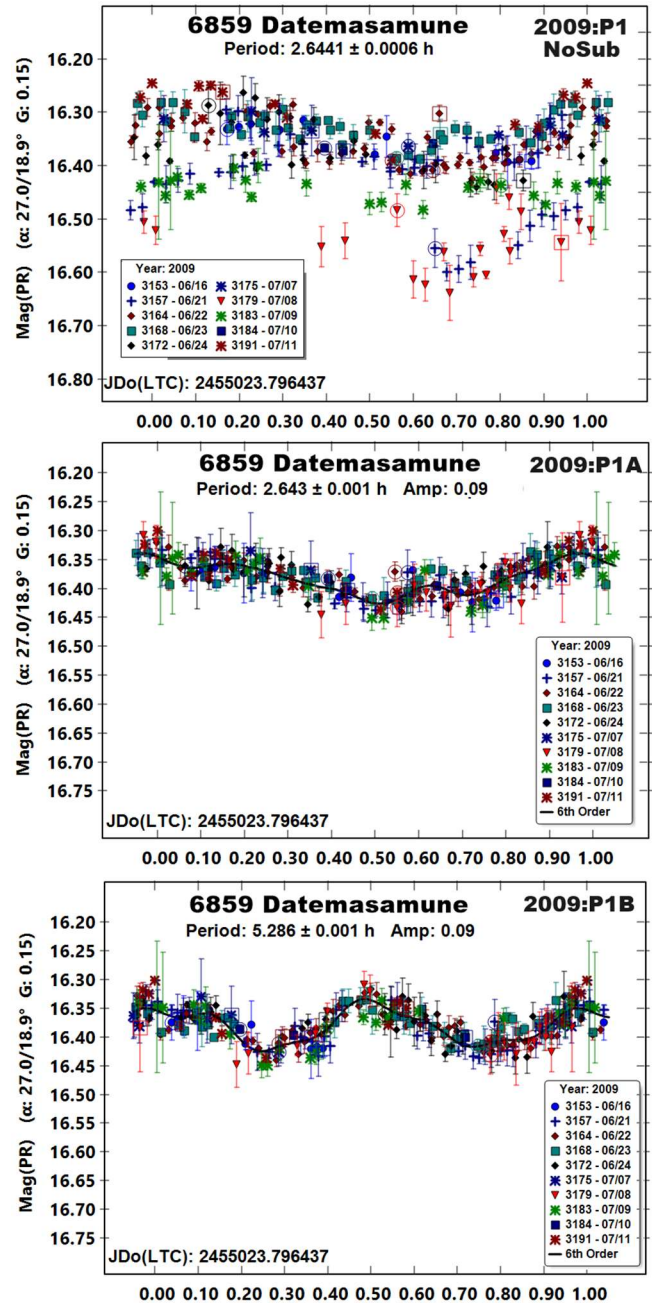


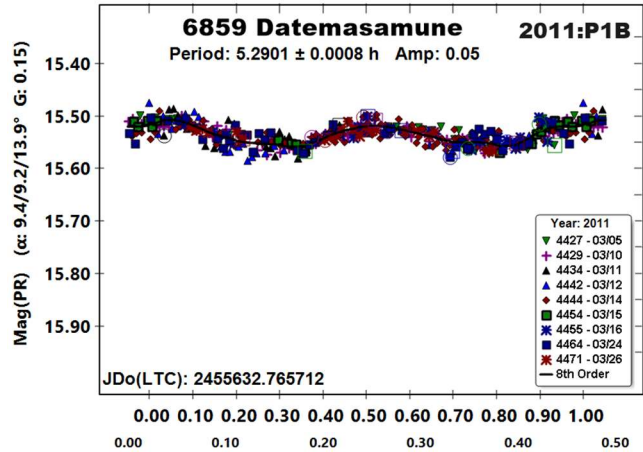
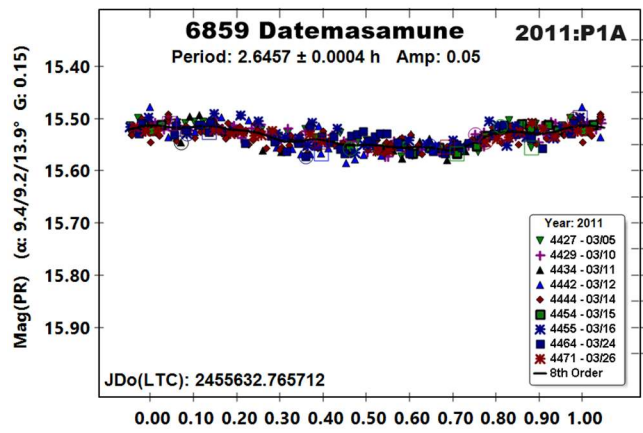
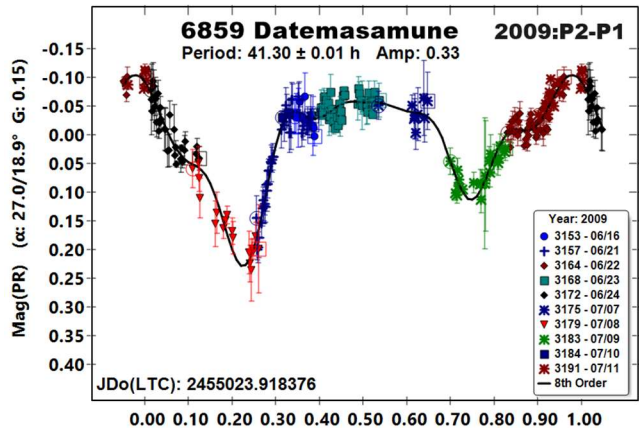
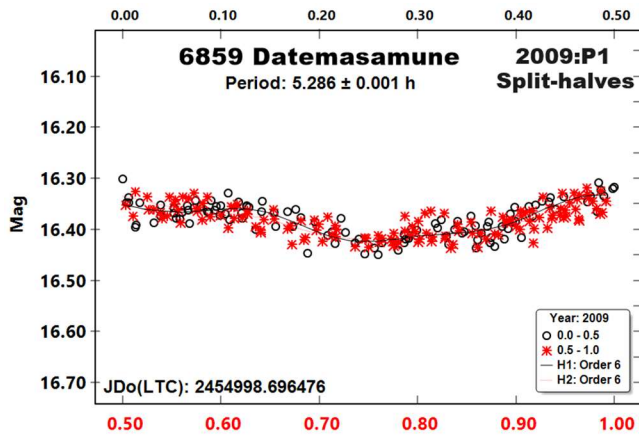
The shorter period, monomodal lightcurve was adopted based on the split-halves plot for the longer period. Here, the second-half of the lightcurve is superimposed on top of the first-half. If the two halves are highly symmetrical, this allows, but does not guarantee, that the half-period, 2.651 h in this case, is valid (Harris et al., 2014).

Subtracting the Fourier curve for 2.651 h did find a secondary period with an incomplete but nearly-symmetric bimodal lightcurve at a period of 42.5 h, which – given the density of the data sets in number of points and total time span – makes this compatible with $P_{2(2024)} = 43.3$ h.

2009 Apparition. A second period was not in doubt looking at the initial single-period search. The period spectrum showed strong solutions near 2.6 and 5.3 h. A review of the split-halves plot for the longer period again showed that the shorter period of $P_{1(2009)} = 2.643$ h was possible and favored.

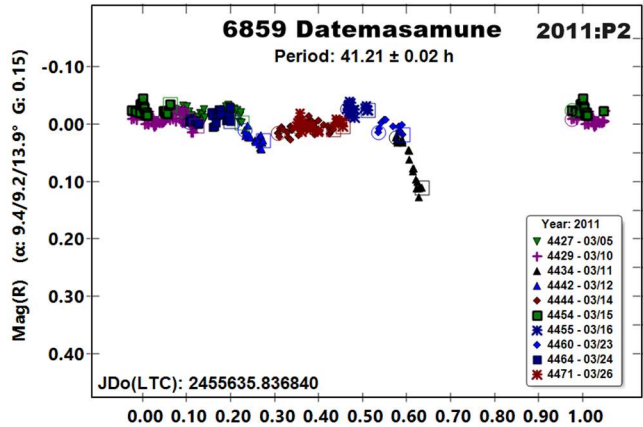
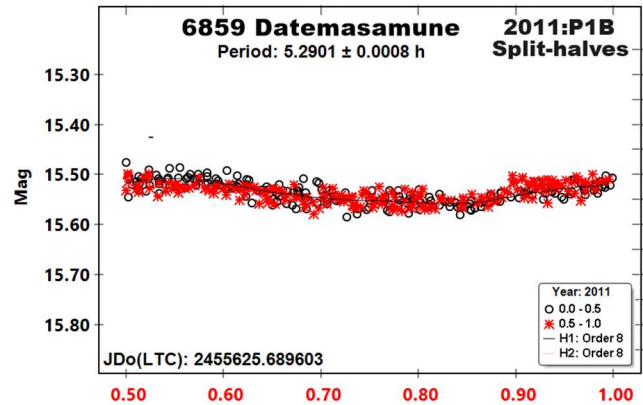
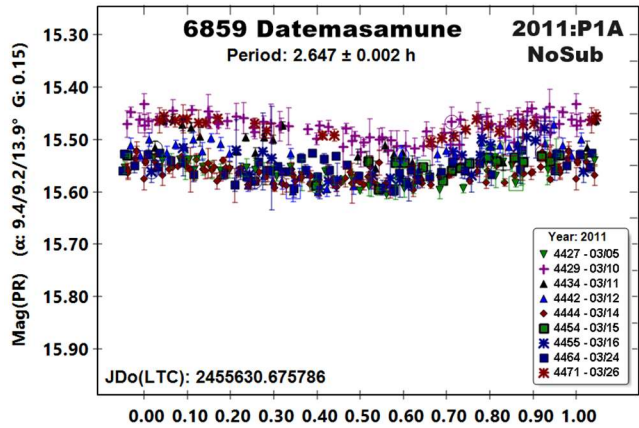
The 2009 data provided the strongest case for a second period. If assumed to be valid and due to a satellite, the amplitude of $P_{2(2009)} = 41.30$ h and “bowed” maximum indicate it is somewhat elongated. The mutual events (occultations/eclipses) are about 0.12 and 0.20 mag. Using the shallower one, the estimated effective diameters ratio is $D_s/D_p \geq 0.34 \pm 0.03$.

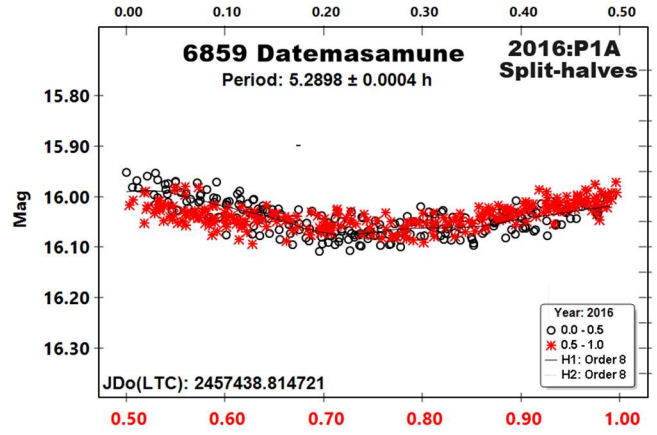
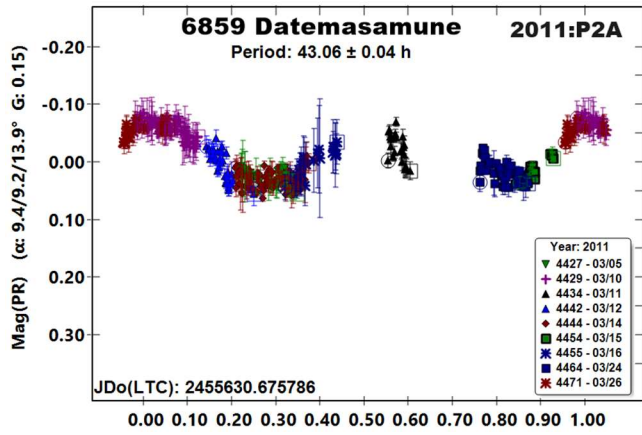




2011 Apparition. The presence of a second period was strongly suspected. As before, the primary period after the dual-period search was ambiguous at $P_{1A(2011)} = 2.6457$ h and $P_{1B(2011)} = 5.2901$ h and again the split-halves showed that the shorter period was just as possible. It was adopted for this paper.

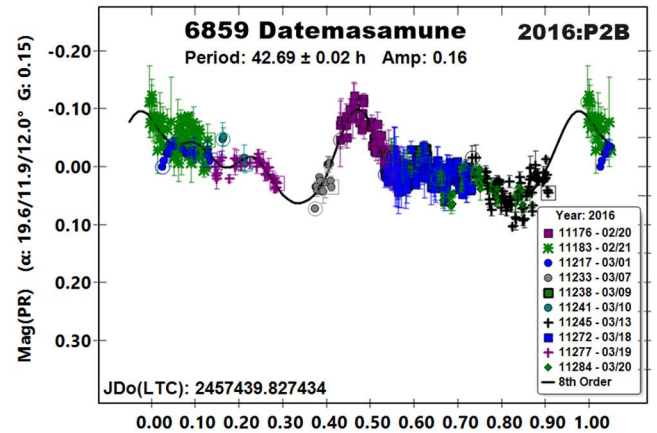
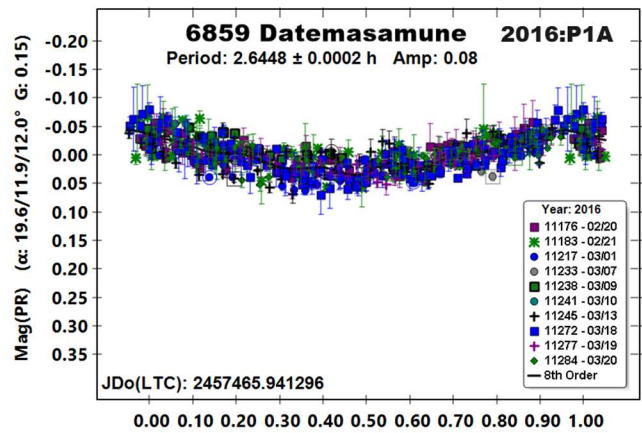
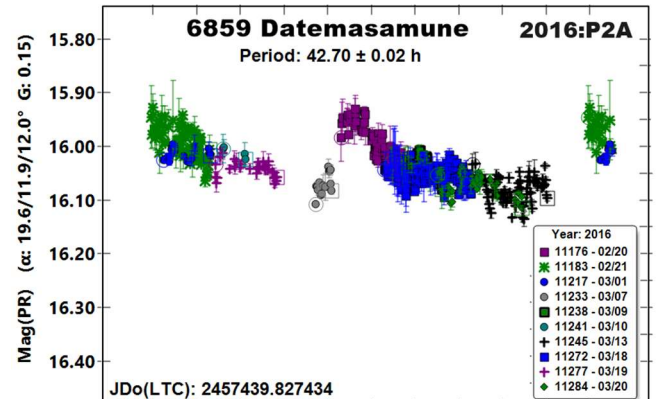
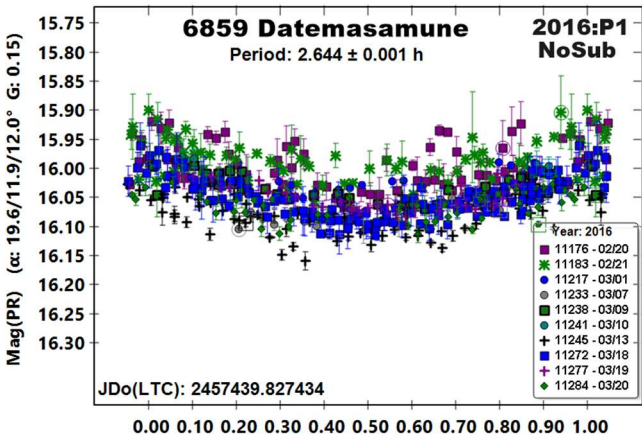
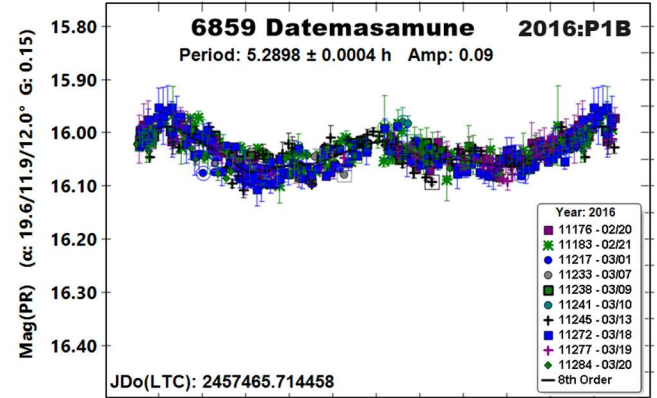
The search for the second period was intriguing. First the solution was forced to one near from 2009 (“2011:P2”). That was not encouraging. The search range was extended to 40-50 h, finding a period of 43.06 h ($P_{1A} = 2.6457$ h) and 43.09 ($P_{1B} = 5.2901$ h).





2016 Apparition. Analysis of the 2016 data was similar to before. There were obvious deviations from a single-period solution and the ambiguous solution was found the primary period led to the same conclusion as above, the lightcurve is monomodal, with $P_1 = 2.6448$ h. The split-halves plot was not the sole decider; the bimodal lightcurve was suspiciously too symmetric with sharp maximums at 0.0 and 0.5 rotation phase.

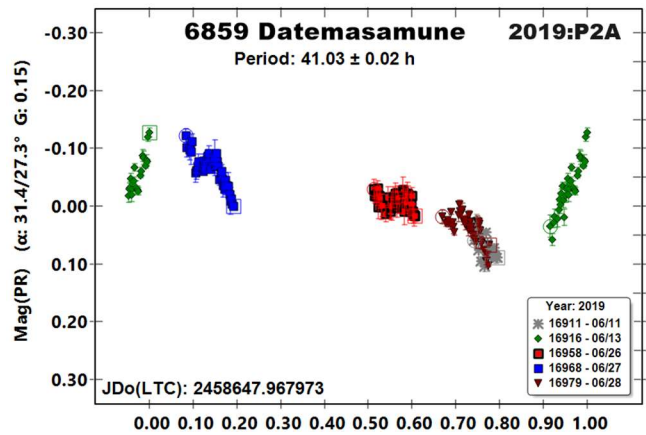
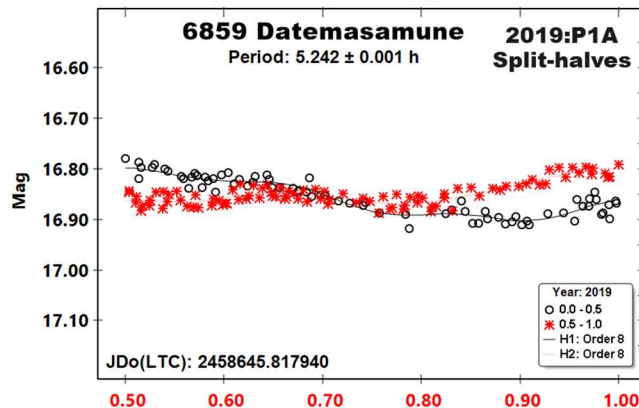
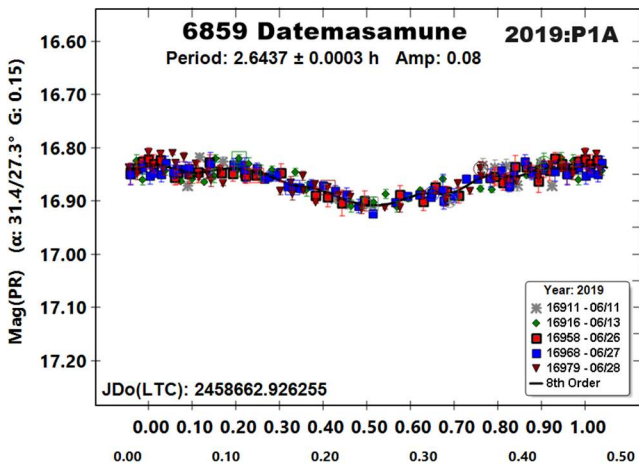
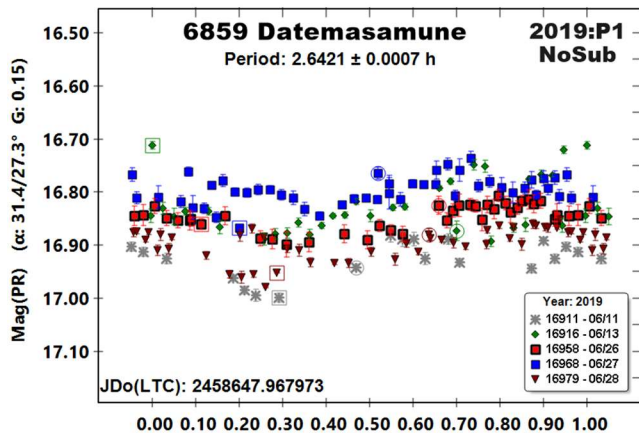
The case for a secondary period was the second weakest in 2016. Plots “2016:P2A” and “2016:P2B”, based on the short and long primary period solutions, respectively, are barely conclusive. Still, no other solution presented itself and it is in-line with earlier results.



2019 Apparition. The data set from 2019 was the sparsest of them all, but it made probably the most convincing case for the primary period lightcurve being monomodal with $P_{1(2019)} = 2.6437$ h based on the split-halves plot.

The solution for the second period, $P_{2(2019)} = 41.03$ h, is the most optimistic result in the entire analysis. The lightcurve presented an even worse fit when trying to force a period near 43 h, but that's to be expected given the very sparse coverage.

There were only five sessions over a span of seventeen days and only three that were consecutive. Such a large span with limited data that are unevenly spaced makes for the strong possibility of rotation alias, where the Fourier finds a period that doesn't correspond to the true number of rotations over the time range of the data.



Conclusions

It would be a display of hubris to claim that the final solution has been reached for this asteroid. The case for a synodic period near 2.65 h seems stronger than from previous analysis. Contributing to this is an apparent secondary period that may have been unintentionally nulled out by adjusting zero-points or the simple lack of a good data set.

It seems possible that the asteroid is binary, but there is only one apparition (2009) that supports this with some confidence.

The recommendations that stand out most are:

1. MoreData! If nothing else, a strong data set could help confirm or refute the possibility of a satellite. This means high-quality data (low noise) from a wide-range of longitudes. Longer sessions are preferred. Don't assume a few data points spaced over several hours are always sufficient to find a good solution for a long period.
2. Use a star catalog for comp star magnitudes that has low systematic errors and "popular" native magnitudes, i.e., not converted from one system to another. Right now, the ATLAS refcat2 is the best all-around source, at least for asteroid photometry.
3. Record and save the instrumental magnitudes of the target and comp stars. This allows re-creating differential photometry using different magnitudes of a different band for the comp stars. This doesn't apply only to unfiltered observations. Technically, although maybe not recommended, data taken through an Rc filter using PR (Pan-STAARS r') magnitudes would still report PR magnitudes. Combining data from multiple years and/or observers not all using the same filter can present some interesting challenges.
4. If there's a chance (assume that there is) that magnitudes from a different band and/or catalog might be used on the data later on, make sure it's possible to locate the original comp stars such that their new magnitudes can be obtained from the new source. The RA/Dec position is a good choice. The X/Y values on a particular image is not a good choice.

Number	Name	yyyy/mm/dd	Phase	L _{PAB}	B _{PAB}	Period(h)	P.E.	Amp	A.E.
6859	Datemasamune	2006/06/23-06/25	26.9, 26.2	306	23	2.651	0.002	0.06	0.01
						5.299	0.004	0.07	0.01
						42.5	0.2	0.20	0.05
		2009/06/16-07/11	*33.8, 33.4	200	24	2.6432	0.0003	0.09	0.01
						5.2860	0.0005	0.09	0.01
						41.30	0.01	0.25	0.02
		2011/03/05-03/26	9.5, 13.8	172	12	2.6457	0.0004	0.05	0.01
						5.2901	0.0008	0.05	0.01
						43.06	0.04		
		2016/02/20-03/20	*19.7, 12.0	179	13	2.6448	0.0002	0.08	0.02
						5.2898	0.0004	0.09	0.02
						42.70	0.02		
		2019/06/11-06/28	31.4, 27.4	312	20	2.6437	0.0003	0.08	0.01
						5.242	0.001	0.10	0.01
						41.03	0.02		
		2024/06/03-06/17	33.3, 31.7	315	18	2.6426	0.0004	0.08	0.01
						5.285	0.001	0.08	0.01
						43.3	0.1	0.27	0.05

Table II. Observing circumstances and results. The phase angle is given for the first and last date. If preceded by an asterisk, the phase angle reached an extremum during the period. L_{PAB} and B_{PAB} are the approximate phase angle bisector longitude/latitude at mid-date range (see Harris et al., 1984). For each year, the first line gives the adopted period. The second line is the alternative period. The third line is the secondary period, possibly due to a satellite.

Acknowledgements

This work includes data from the Asteroid Terrestrial-impact Last Alert System (ATLAS) project. ATLAS is primarily funded to search for near earth asteroids through NASA grants NN12AR55G, 80NSSC18K0284, and 80NSSC18K1575; byproducts of the NEO search include images and catalogs from the survey area. The ATLAS science products have been made possible through the contributions of the University of Hawaii Institute for Astronomy, the Queen's University Belfast, the Space Telescope Science Institute, and the South African Astronomical Observatory.

The author gratefully acknowledges a Shoemaker NEO Grants from the Planetary Society (2007). This was used to purchase some of the equipment used in this research.

References

Harris, A.W.; Young, J.W.; Scaltriti, F.; Zappala, V. (1984). "Lightcurves and phase relations of the asteroids 82 Alkmene and 444 Gypsis." *Icarus* **57**, 251-258.

Harris, A.W.; Young, J.W.; Bowell, E.; Martin, L.J.; Millis, R.L.; Poutanen, M.; Scaltriti, F.; Zappala, V.; Schober, H.J.; Debehogne, H.; Zeigler, K.W. (1989). "Photoelectric Observations of Asteroids 3, 24, 60, 261, and 863." *Icarus* **77**, 171-186.

Harris, A.W.; Pravec, P.; Galad, A.; Skiff, B.A.; Warner, B.D.; Vilagi, J.; Gajdos, S.; Carbognani, A.; Hornoch, K.; Kusnirak, P.; Cooney, W.R.; Gross, J.; Terrell, D.; Higgins, D.; Bowell, E.; Koehn, B.W. (2014). "On the maximum amplitude of harmonics on an asteroid lightcurve." *Icarus* **235**, 55-59.

MAST. (2024). Mikulski Archive for Space Telescopes web site. ATLAS refcat2 access: <https://archive.stsci.edu/hlsp/atlas-refcat2>

Nesvorny, D. (2015). "Nesvorny HCM Asteroids Families V3.0." NASA Planetary Data Systems, id. EAR-A-VARGBET-5-NESVORNYFAM-V3.0.

Nesvorny, D.; Broz, M.; Carruba, V. (2015). "Identification and Dynamical Properties of Asteroid Families." In *Asteroids IV* (P. Michel, F. DeMeo, W.F. Bottke, R. Binzel, Eds.). Univ. of Arizona Press, Tucson, also available on astro-ph.

Pravec, P.; Harris, A.W.; Scheirich, P.; Kušnirák, P.; Šarounová, L.; Hergenrother, C.W.; Mottola, S.; Hicks, M.D.; Masi, G.; Krugly, Yu.N.; Shevchenko, V.G.; Nolan, M.C.; Howell, E.S.; Kaasalainen, M.; Galád, A.; Brown, P.; Degraff, D.R.; Lambert, J.V.; Cooney, W.R.; Foglia, S. (2005). "Tumbling asteroids." *Icarus* **173**, 108-131.

Pravec, P.; Scheirich, P.; Durech, J.; Pollock, J.; Kusnirak, P.; Hornoch, K.; Galad, A.; Vokrouhlicky, D.; Harris, A.W.; Jehin, E.; Manfroid, J.; Opatom, C.; Gillon, M.; Colas, F.; Oey, J.; Vrstil, J.; Reichart, D.; Ivarsen, K.; Haislip, J.; LaCluyze, A. (2014). "The tumbling state of (99942) Apophis." *Icarus* **233**, 48-60.

Stephens, R.D.; Warner, B.D. (2019). "Main-belt Asteroids Observed from CS3: 2019 April to June." *Minor Planet Bull.* **46**, 449-456.

Tony, J.L.; Denneau, L.; Flewelling, H.; Heinze, A.N.; Onken, C.A.; Smartt, S.J.; Stalder, B.; Weiland, H.J.; Wolf, C. (2018). "The ATLAS All-Sky Stellar Reference Catalog." *Astrophys. J.* **867**, A105.

VizieR (2024). *Strasbourg Astronomical Data Center web site*. ATLAS refcat2 catalog lookup: <https://vizier.cds.unistra.fr/viz-bin/VizieR?-source=J/ApJ/867/105&-to=3>.

Warner, B.D. (2006). "Asteroid lightcurve analysis at the Palmer Divide Observatory - February-March 2006." *Minor Planet Bull.* **33**, 82-84.

Warner, B.D. (2010). "Asteroid Lightcurve Analysis at the Palmer Divide Observatory: 2009 June-September." *Minor Planet Bull.* **37**, 24-27.

Warner, B.D. (2011). “Asteroid Lightcurve Analysis at the Palmer Divide Observatory: 2011 March-July.” *Minor Planet Bull.* **38**, 190-195.

Warner, B.D. (2016). “Asteroid Lightcurve Analysis at CS3-Palmer Divide Station: 2015 December - 2016 April.” *Minor Planet Bull.* **43**, 227-233.

Warner, B.D. (2024). *MPO Canopus* v12.0.5.0 software. <https://bdwpublishing.com>

Warner, B.D.; Harris, A.W.; Pravec, P. (2009). “The Asteroid Lightcurve Database.” *Icarus* **202**, 134-146. Updated 2023 August. <https://www.minorplanet.info/php/lcdb.php>

LIGHTCURVE ANALYSIS FOR 6 NEAR-EARTH ASTEROIDS OBSERVED BETWEEN 2010 AND 2024

Peter Birtwhistle
Great Shefford Observatory
Phlox Cottage, Wantage Road
Great Shefford, Berkshire, RG17 7DA
United Kingdom
peter@birtwhistle.org.uk

(Received: 2024 July 12)

Lightcurves and amplitudes for six near-Earth asteroids observed from Great Shefford Observatory during close approaches between 2010-2018 and 2024 April-June are reported. All have rotation periods at or below the 2.2 h spin barrier and two are identified as having tumbling rotation.

Photometric observations of near-Earth asteroids during close approaches to Earth in 2010-2018 and 2024 April-June were made at Great Shefford Observatory using a 0.40-m Schmidt-Cassegrain and Apogee Alta U47+ CCD camera. All observations were made unfiltered and with the telescope operating with a focal reducer at $f/6$. The $1K \times 1K$, 13-micron CCD was binned 2×2 resulting in an image scale of 2.16 arc seconds/pixel. All the images were calibrated with dark and flat frames. *Astrometrica* (Raab, 2024) was used to measure photometry using APASS Johnson V band data from the UCAC4 catalogue (Zacharias et al., 2013). *MPO Canopus* (Warner, 2023), incorporating the Fourier algorithm developed by Harris (Harris et al., 1989) was used for lightcurve analysis.

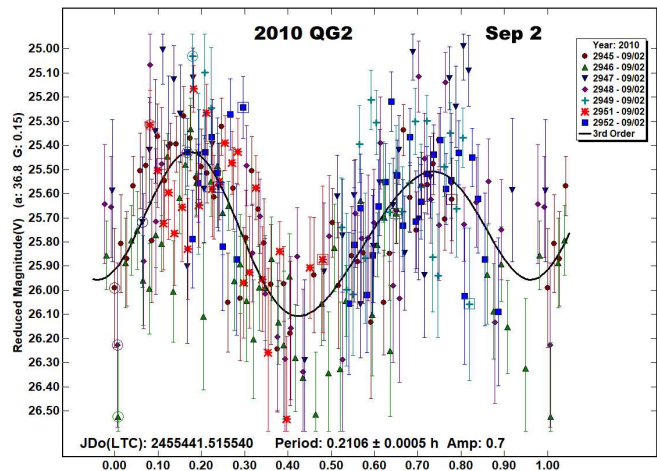
No previously reported results have been found in the Asteroid Lightcurve Database (LCDB; Warner et al., 2009), from searches via the Astrophysics Data System (ADS, 2024) or from wider searches unless otherwise noted. All size estimates are calculated using H values from the Small-Body Database Lookup (JPL, 2024b), using an assumed albedo for NEAs of 0.2 (LCDB readme.pdf file) and are therefore uncertain and offered for relative comparison only.

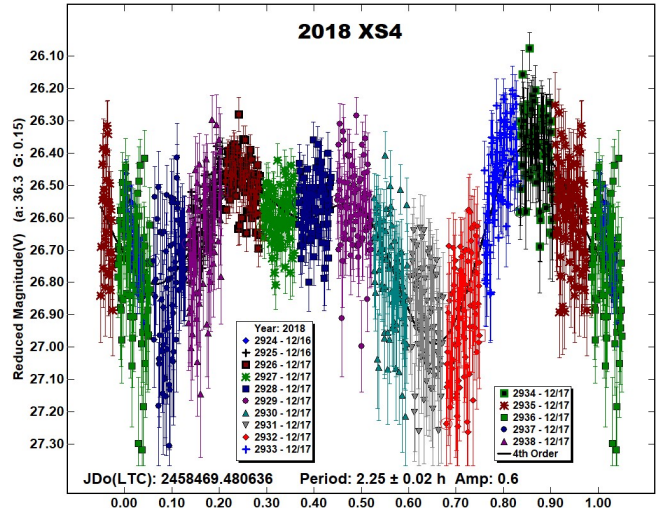
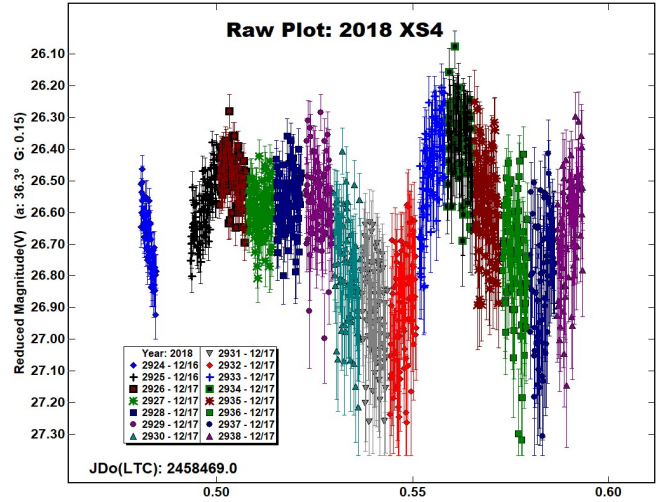
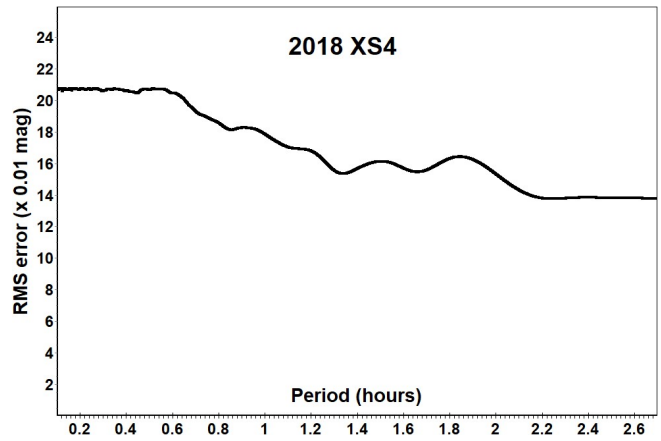
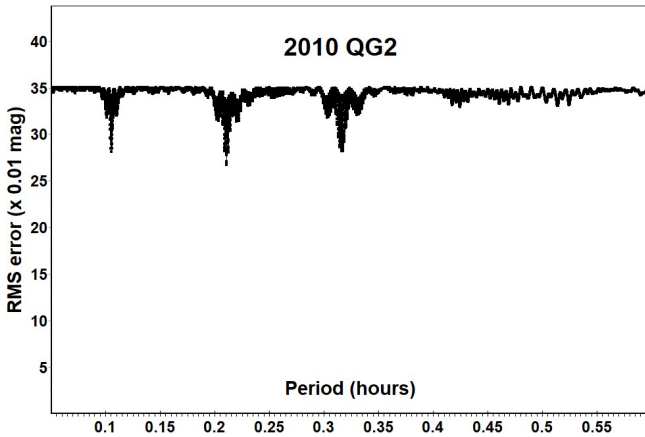
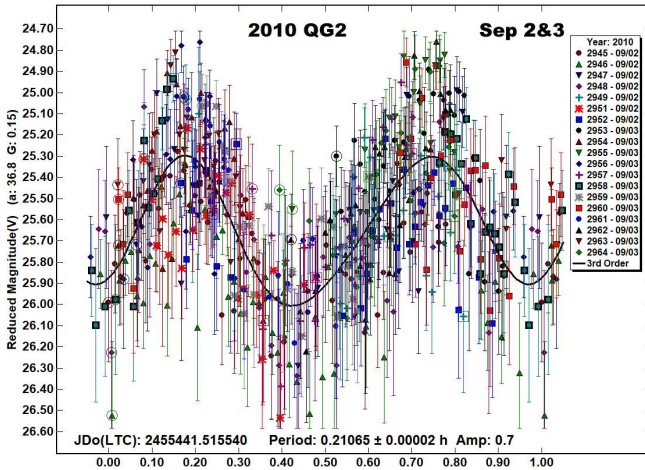
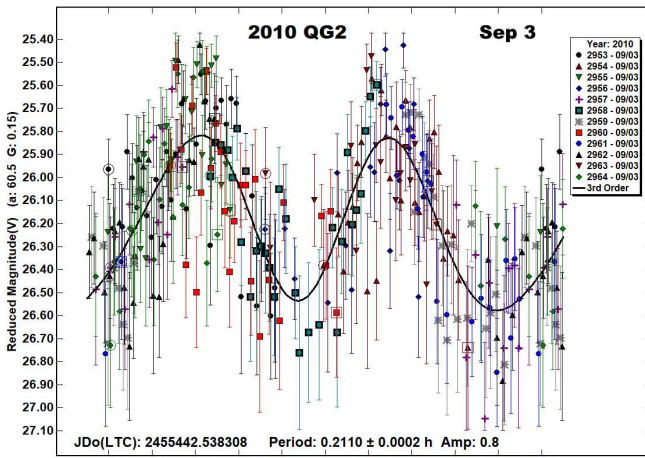
2010 QG2. This is an Apollo discovered by LINEAR on 2010 Aug 31 from their site in Socorro, New Mexico (Manca et al., 2010) and is listed by Sentry (JPL, 2024a) and NEODYs (NEODYs, 2024) as a virtual impactor with a number of low probability potential impacts starting in 2051. It was also observed by WISE on 2010 Sep 3.3 UTC, allowing a diameter of 38 ± 6 m and albedo p_v of 0.228 ± 0.064 to be determined (Mainzer et al., 2014). It approached Earth to within 4.6 Lunar Distances (LD) on 2010 Sep 3.6 UTC and was observed for 1.75 h starting on 2010 Sep 2.02 UTC and again over a span of 2.8 h starting on 2010 Sep 3.04 UTC.

Independent lightcurve analyses of the two nights are given, labelled Sep 2 and Sep 3 and show similar rotation periods of 0.2106 ± 0.0005 h and 0.2110 ± 0.0002 h, respectively, with the amplitude increasing from 0.7 to 0.8 magnitudes as the phase angle increased from 37° to 61° . Using the better-defined period from the Sep 3 solution to propagate errors back to Sep 2, the likely error in number of rotations ΔN between the two dates for an assumed bimodal lightcurve was derived from eq. (3) in Kwiatkowski et al. (2010):

$$\Delta N \approx \Delta t * \Delta P / P^2$$

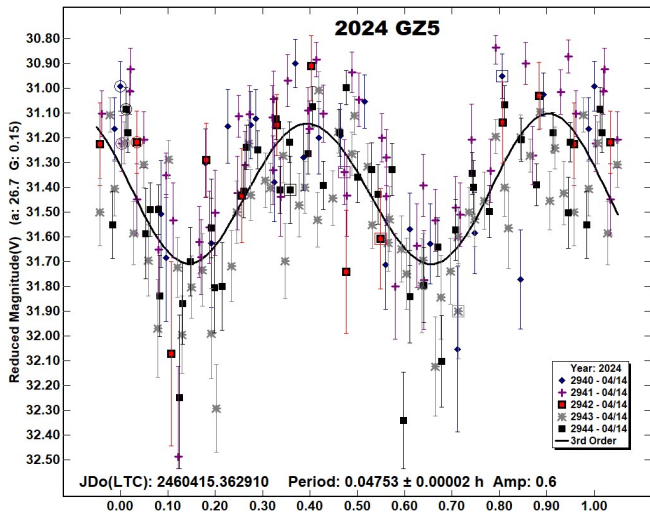
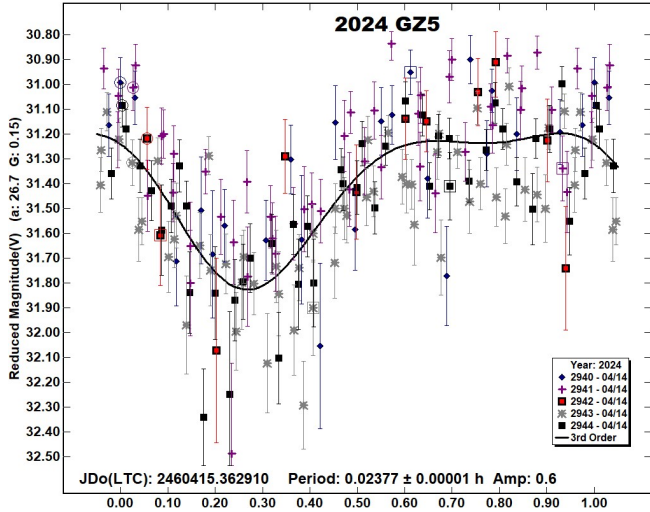
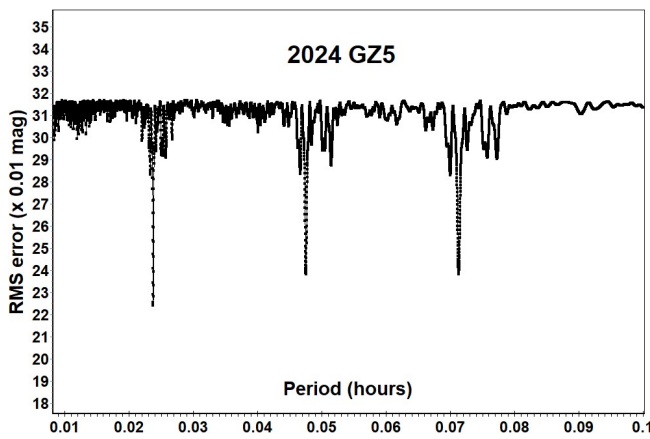
where Δt is the time interval separating the two lightcurves, P is the period from one of the individual solutions, and ΔP is the maximum period uncertainty, with Δt , ΔP , and P expressed in the same units. This gives $\Delta N \approx 0.1$, indicating that the two sets of observations can be matched to a tenth of a rotation and that the two data sets can be unambiguously combined, this producing the phased lightcurve labelled Sep 2&3 with a period of 0.21065 ± 0.00002 h. The period spectrum is from data from both nights and covers periods from 3-36 min.





2018 XS4. This Apollo ($H = 25.2$, $D \sim 27$ m) was discovered from the ATLAS-MLO site on 2018 Dec 14.3 UTC, 48 hours before passing Earth at 2.8 LD (Bacci et al., 2018). It was also detected by radar from Arecibo on 2018 Dec 18.3 UTC (JPL, 2024c). Photometry was obtained over a span of 2.7 h starting on 2018 Dec 16.98 UTC, when it was at a distance of 3.0 LD. The period spectrum and raw lightcurve indicate that the span of observations is not long enough to unambiguously determine the rotation period, or indeed whether or not it is tumbling. A phased lightcurve is given under the assumption that the minima at JD 2458469.49, near the start of the measurements, matches the minima at JD 2458469.58. However, the derived period of 2.25 ± 0.02 h is necessarily uncertain with so little overlap and defines only a likely lower limit to the rotation period.

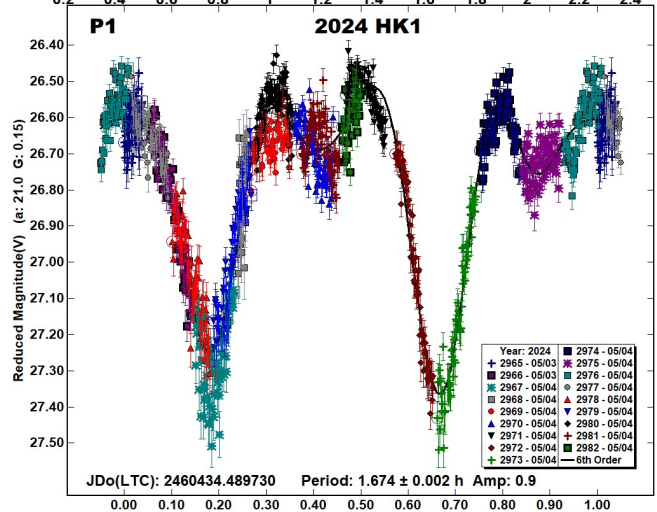
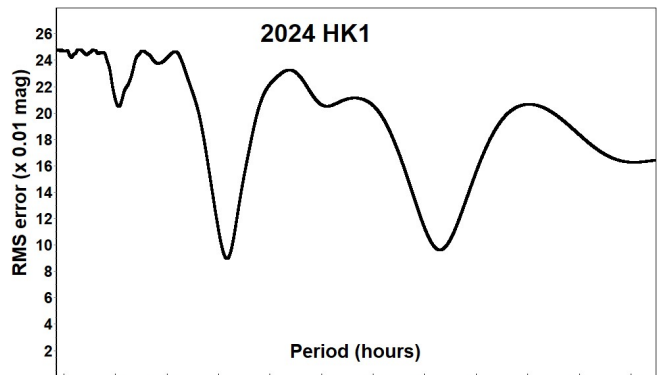
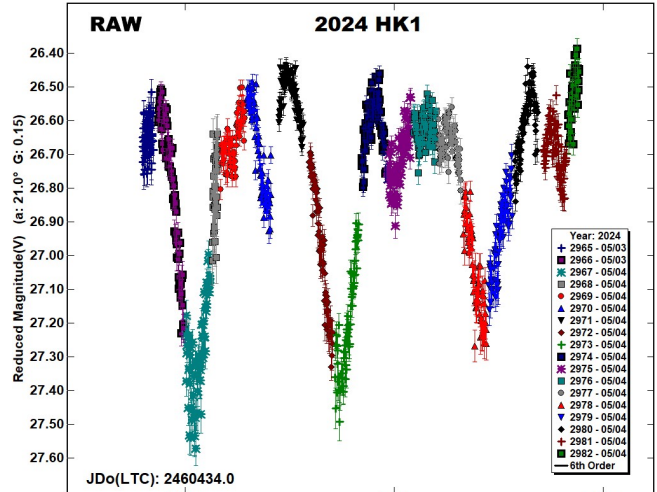
2024 GZ5. This is another very small Apollo ($H = 30.3$, $D \sim 2.6$ m) discovered by the Catalina Sky Survey on 2024 Apr 14.3 UTC and passed Earth at 0.2 LD on 2024 Apr 15.7 UTC (Bacci et al., 2024a). It is listed by Sentry (JPL, 2024a) and NEODyS (NEODyS, 2024) as a virtual impactor with a cumulative probability of 1 in 2,600 of it impacting with Earth starting in 2112. Images were obtained for 1.2 h over a 2.9 h span starting at 2024 Apr 14.86 UTC when 2024 GZ5 was at 0.8 LD. The best fit solution in the period spectrum is at 0.02377 ± 0.00001 h with only slightly inferior solutions at $\times 2$ and $\times 3$ this value.

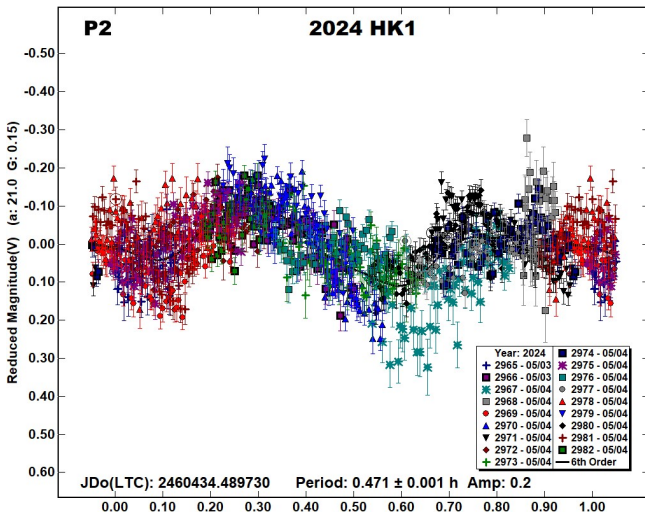


Lightcurves for rotation periods of 0.02377 h and 0.04753 h are given, but with only a 6% difference in the RMS error between those solutions and the large amount of noise in the measurements, it is unclear which of the solutions is correct. Considering the amplitude of 0.6, the bimodal lightcurve for the longer period is selected as the most likely.

2024 HK1. Pan-STARRS 2 discovered this Apollo ($H = 25.5$, $D \sim 24$ m) on 2024 Apr 21.5 UTC, nearly two weeks before it passed Earth at 1.8 LD on 2024 May 4.8 UTC (Buzzi et al., 2024). It was

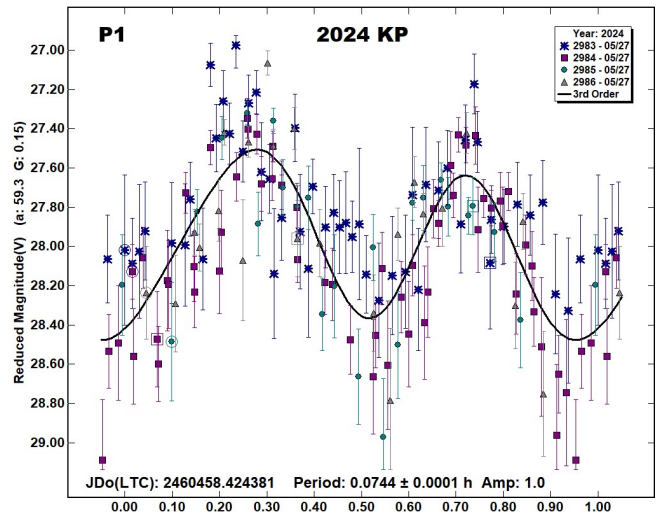
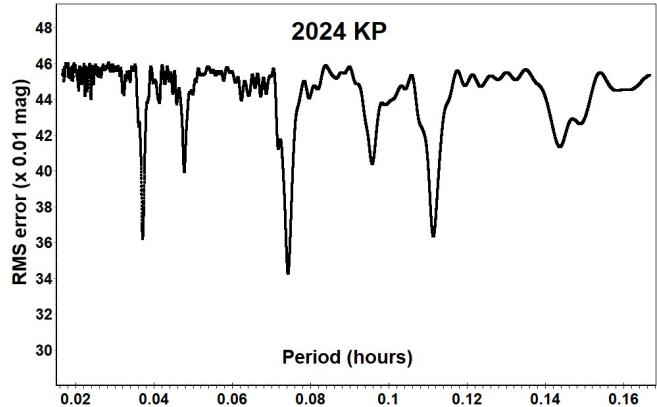
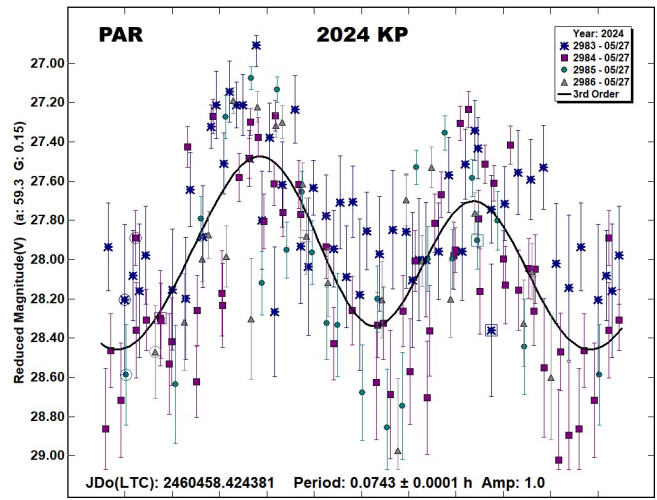
observed for 2.6 h starting at 2024 May 3.99 UTC when it was at 2.4 LD and moving at 88 - 97 arcsec/min. Exposures were limited to 6 s to keep trailing within the measurement aperture used in *Astrometrica*. A raw plot shows three deep minima of differing depths, each separated by several smaller amplitude irregular maxima, all suggesting that non-principal axis (NPAR) rotation, or tumbling may be present. The period spectrum shows potential solutions near 0.8 and 1.7 h and the *MPO Canopus* Dual-Period Search function finds the best fit to be an NPAR solution using the longer of those periods as the dominant period, resulting lightcurves are labelled P1 and P2. An NPAR solution initially seeded using 0.8 h as the dominant period is only slightly inferior, resulting in periods of 0.836 ± 0.001 h and 0.467 ± 0.002 h.

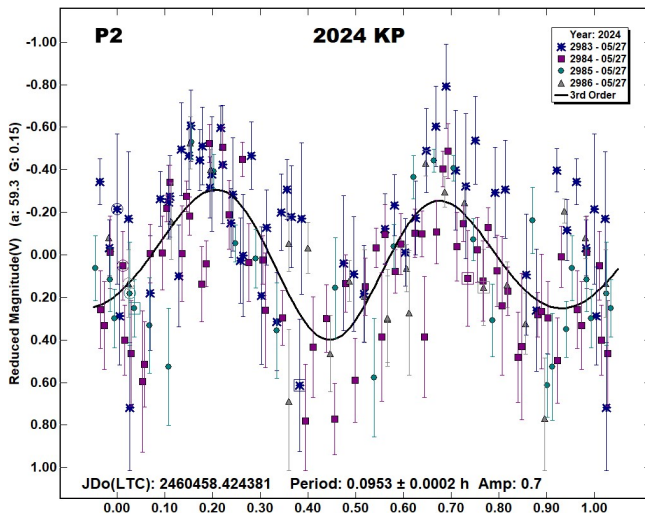




However, with the span of observations being not much longer than the derived periods, neither of the NPAR solutions can be regarded as secure and therefore it is expected that 2024 HK1 may be rated as PAR = -2 on the scale defined in Pravec et al. (2005) where NPA rotation is detected based on deviations from a single period but the second period is not resolved (Petr Pravec, personal communication).

2024 KP. This Apollo was a discovery ($H = 25.8$, $D \sim 20$ m) made by the ZTF collaboration at Palomar on 2024 May 27.3 UTC which approached Earth to 2.1 LD on 2024 May 29.4 UTC (Bacci et al., 2024b). It was observed for 48 min over a period of 78 min starting at 2024 May 27.92 UTC when 158 measurable images were obtained. Large magnitude variations were immediately evident over time scales of ~ 1 minute. If assuming a bimodal lightcurve, this implied a period of ~ 4 minutes and an optimal exposure length to limit the effects of lightcurve smoothing (Pravec et al., 2000) would be $\sim 0.185 \times 240 = 44$ seconds. However, with its apparent motion of 40 arcsec/min the practical exposure length to limit image trailing was shorter, at 13 s. An initial analysis of the lightcurve (labelled PAR) determined the period to be 4.5 min, but with a large amount of scatter in the curve. The period spectrum identifies this best-fit period, as well as monomodal and trimodal solutions at 1/2 and 3/2 that value. Also visible are slightly shallower, regularly spaced minima at 0.048, 0.096 and 0.144 h, indicating that non-principal axis rotation (NPAR) may be present. The Dual-Period Search function of *MPO Canopus* was used and extracted a well-defined pair of NPAR periods (labelled P1 and P2) despite the scatter and relatively short time span of observation. On the scale defined in Pravec et al. (2005) it is expected to be rated as PAR = -3 with NPA rotation reliably detected with the two periods resolved. (Petr Pravec, personal communication). The NPAR solution indicates the full amplitude of the tumbling rotation is 1.7 magnitudes.

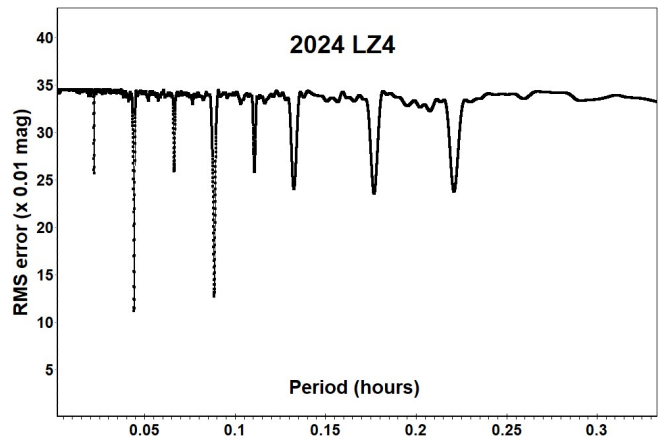




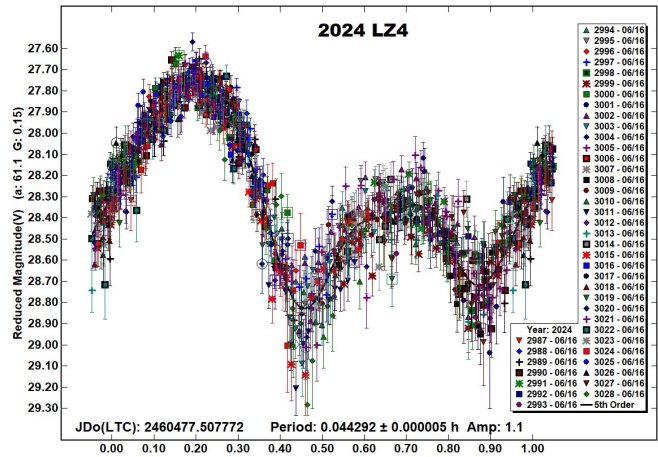
2024 LZ4. This Apollo ($H = 26.0$, $D \sim 18$ m) was discovered from Pleasant Groves Observatory on 2024 Jun 14.2 UTC and passed Earth at 0.7 LD on 2024 Jun 16.2 UTC (Bacci et al., 2024c). It was observed for 1.7 h starting at 2024 Jun 16.0 when its distance from Earth decreased from 1.0 to 0.8 LD and was $V \sim 15$ throughout. With the apparent speed increasing from 475 to 735 arcsec/min, exposures were reduced from 1.3 to 0.8 s to keep the length of trailing of 2024 LZ4 within the measurement aperture used in *Astrometrica*.

Number	Name	Integration times	Max intg/Pd	Min a/b	Pts	Flds
2010	QG2	2, 4	0.005	1.3 ¹	553	19
2018	XS4	4, 5	0.001 ²	1.3	1178	15
2024	GZ5	10–15	0.088	1.4	182	5
2024	HK1	2–5.9	0.003 ³	1.7	1113	18
2024	KP	6–13	0.049	1.7*	158	4
2024	LZ4	0.8–1.3	0.008	1.4*	921	42

Table I. Ancillary information, listing the integration times used (seconds), the fraction of the period represented by the longest integration time (Pravec et al., 2000), the calculated minimum elongation of the asteroid (Zappala et al., 1990), the number of data points used in the analysis and the number of times the telescope was repositioned to different fields. Notes: 1 = calculated using information from 2010 Sep 2.0 when phase angle was smallest, 2 = assumed minimum period of 2.25 h, 3 = assumed minimum period of 0.47 h, * = Value uncertain, based on phase angle > 40°.



The period spectrum indicates the best-fit solution has a period of 2.7 minutes, resulting in a well-defined asymmetric bimodal lightcurve. All the significant minima in the period spectrum are integer multiples of half of the best-fit period, with no evidence of tumbling being present. During the time it was under observation, 2024 LZ4 completed 37 rotations.



Acknowledgements

The author thanks Dr. Petr Pravec for his help reviewing the analyses of tumbling asteroids reported in this paper. The author also gratefully acknowledges a Gene Shoemaker NEO Grant from the Planetary Society (2005) and a Ridley Grant from the British Astronomical Association (2005), both of which facilitated upgrades to observatory equipment used in this study.

Number	Name	yyyy mm/dd	Phase	L _{PAB}	B _{PAB}	Period(h)	P.E.	Amp	A.E	PAR	H
2010	QG2	2010 09/02–09/03	36.8–64.1	4	-8	0.21065	0.00002	0.7	0.3		24.7
2018	XS4	2018 12/16–12/17	36.5–37.6	102	8	2.25	0.02	0.6	0.2		25.2
2024	GZ5	2024 04/14–04/14	25.7–23.7	193	4	0.04753	0.00002	0.6	0.3		30.3
2024	HK1	2024 05/03–05/04	20.8–19.4	214	4	1.674	0.002	0.9	0.1	-2	25.5
						0.471	0.001	0.2	0.1		
2024	KP	2024 05/27–05/27	59.2–60.0	240	30	0.0744	0.0001	1.0	0.4	-3	25.8
						0.0953	0.0002	0.7	0.4		
2024	LZ4	2024 06/16–06/16	61.1–75.6	248	30	0.044292	0.000005	1.07	0.16		26.1

Table II. Observing circumstances and results. The phase angle is given for the first and last date. If preceded by an asterisk, the phase angle reached an extrema during the period. L_{PAB} and B_{PAB} are the approximate phase angle bisector longitude/latitude at mid-date range (see Harris et al., 1984). Amplitude error (A.E.) is calculated as $\sqrt{2} \times$ (lightcurve RMS residual). PAR is the expected Principal Axis Rotation quality detection code (Pravec et al., 2005) and H is the absolute magnitude at 1 au from Sun and Earth taken from the Small-Body Database Lookup (JPL, 2024b).

References

- ADS (2024). Astrophysics Data System.
<https://ui.adsabs.harvard.edu/>
- Bacci, P.; Maestriperieri, M.; Tesi, L.; Fagioli, G.; Buzzi, L.; Fumagalli, A.; Sicoli, P.; Testa, A.; Jahn, J.; Elenin, L.; Birtwhistle, P.; Korlevic, K.; Okumura, S.; Nimura, T.; Denneau, L. and 4 colleagues (2018). “2018 XS4.” *MPEC* **2018-X133**.
<https://minorplanetcenter.net/mpec/K18/K18XD3.html>
- Bacci, P.; Maestriperieri, M.; Tesi, L.; Fagioli, G.; Pettarin, E.; Bressi, T.H.; Kowalski, R.A.; Beuden, T.; Carvajal, V.F.; Fay, D.; Fazekas, J.B.; Fuls, D.C.; Gibbs, A.R.; Grauer, A.D.; Groeller, H.; and 36 colleagues (2024a). “2024 GZ5.” *MPEC* **2024-G207**.
<https://minorplanetcenter.net/mpec/K24/K24GK7.html>
- Bacci, P.; Maestriperieri, M.; Pettarin, E.; Dupouy, P.; de Vanssay, J.B.; Losse, F.; Bacci, R.; Herman, J.; Lowe, T.; Minguez, P.; Schultz, A.; Smith, I.; Chambers, K.; de Boer, T.; Fairlamb, J.; and 47 colleagues (2024b). “2024 KP.” *MPEC* **2024-K113**.
<https://www.minorplanetcenter.net/mpec/K24/K24KB3.html>
- Bacci, P.; Maestriperieri, M.; Tesi, L.; Fagioli, G.; Pettarin, E.; Ruocco, N.; Holmes, R.; Linder, T.; Horn, L.; Fornas, A.; Fornas, G.; Arce, E.; Mas, V.; Tombelli, M.; Mazzanti, A.; and 15 colleagues (2024c). “2024 LZ4.” *MPEC* **2024-L145**.
<https://www.minorplanetcenter.net/mpec/K24/K24LE5.html>
- Buzzi, L.; Herman, J.; Lowe, T.; Minguez, P.; Schultz, A.; Smith, I.; Chambers, K.; de Boer, T.; Fairlamb, J.; Gao, H.; Huber, M.; Lin, C.-C.; Magnier, E.; Ramanjooloo, Y.; Wainscoat, R.; and 20 colleagues (2024). “2024 HK1.” *MPEC* **2024-H71**.
<https://minorplanetcenter.net/mpec/K24/K24H71.html>
- Harris, A.W.; Young, J.W.; Scaltriti, F.; Zappala, V. (1984). “Lightcurves and phase relations of the asteroids 82 Alkmene and 444 Gygis.” *Icarus* **57**, 251-258.
- Harris, A.W.; Young, J.W.; Bowell, E.; Martin, L.J.; Millis, R.L.; Poutanen, M.; Scaltriti, F.; Zappala, V.; Schober, H.J.; Debehogne, H.; Zeigler, K. (1989). “Photoelectric Observations of Asteroids 3, 24, 60, 261, and 863.” *Icarus* **77**, 171-186.
- JPL (2024a). Sentry: Earth Impact Monitoring.
<https://cneos.jpl.nasa.gov/sentry/>
- JPL (2024b). Small-Body Database Lookup.
https://ssd.jpl.nasa.gov/tools/sbdb_lookup.html
- JPL (2024c). Small-Body Radar Astrometry.
<https://ssd.jpl.nasa.gov/sb/radar.html>
- Kwiatkowski, T.; Buckley, D.A.H.; O'Donoghue, D.; Crause, L.; Crawford, S.; Hashimoto, Y.; Kniazev, A.; Loring, N.; Romero Colmenero, E.; Sefako, R.; Still, M.; Vaisanen, P. (2010). “Photometric survey of the very small near-Earth asteroids with the SALT telescope - I. Lightcurves and periods for 14 objects.” *Astronomy & Astrophysics* **509**, A94.
- Mainzer, A.; Bauer, J.; Grav, T.; Masiero, J.; Cutri, R. M.; Wright, E.; Nugent, C.R.; Stevenson, R.; Clyne, E.; Cukrov, G.; Masci, F. (2014). “The Population of Tiny Near-Earth Objects Observed by NEOWISE.” *Ap. J.* **784**, A110.
- Manca, F.; Testa, A.; Blythe, M.; Spitz, G.; Brungard, R.; Paige, J.; Festler, P. (2010). “2010 QG2.” *MPEC* **2010-R03**.
<https://minorplanetcenter.net/mpec/K10/K10R03.html>
- NEODyS (2024). Near Earth Objects Dynamic Site.
<https://newton.spacedys.com/neodys>
- Pravec, P.; Hergenrother, C.; Whiteley, R.; Sarounova, L.; Kusnirak, P.; Wolf, M. (2000). “Fast Rotating Asteroids 1999 TY2, 1999 SF10, and 1998 WB2” *Icarus* **147**, 477-486.
- Pravec, P.; Harris, A.W.; Scheirich, P.; Kušnirák, P.; Šarounová, L.; Hergenrother, C.W.; Mottola, S.; Hicks, M.D.; Masi, G.; Krugly, Yu.N.; Shevchenko, V.G.; Nolan, M.C.; Howell, E.S.; Kaasalainen, M.; Galád, A. and 5 colleagues. (2005). “Tumbling Asteroids.” *Icarus* **173**, 108-131.
- Raab, H. (2024). *Astrometrica* software, version 4.15.0.455.
<http://www.astrometrica.at/>
- Warner, B.D. (2023). *MPO Canopus* version 10.8.6.20, Bdw Publishing, Eaton, CO.
- Warner, B.D.; Harris, A.W.; Pravec, P. (2009). “The Asteroid Lightcurve Database.” *Icarus* **202**, 134-146. Updated 2023 Oct.
<https://www.minorplanet.info/php/lcdb.php>
- Zacharias, N.; Finch, C.T.; Girard, T.M.; Henden, A.; Bartlett, J.L.; Monet, D.G.; Zacharias, M.I. (2013). “The Fourth US Naval Observatory CCD Astroglyph Catalog (UCAC4).” *The Astronomical Journal* **145**, 44-57.
- Zappala, V.; Cellini, A.; Barucci, A.M.; Fulchignoni, M.; Lupishko, D.E. (1990). “An analysis of the amplitude-phase relationship among asteroids.” *Astron. Astrophys.* **231**, 548-560.

AN INVESTIGATION OF CLOSE PASSES OF DISTANT MINOR PLANETS THROUGHOUT THE SOLAR SYSTEM

H. Arda Güler
Dumlupınar B., 6800-16, Ankara, Türkiye
ardaguler09@gmail.com

(Received: 2024 June 18 Revised: 2024 July 2)

Perturbed orbits of distant minor planets are simulated and examined until the year 2100 and a list of close passes with the planets are presented.

Close passes of minor planets with the Earth are of great interest to astronomers due to their hazardous potential and observational opportunities; therefore, detailed listings of such close passes are available in a number of sources, such as the MPC website (MPC, 2024). This study mainly focuses on distant minor planets, objects that reside beyond the orbit of Jupiter for a significant part of their orbital periods ($a > 5.4$ AU), most of which are not expected to interact with the Earth. This excludes most of the known minor planets: main-belt asteroids, near-Earth objects (NEOs), Jupiter trojans and Atiras. It includes trans-Neptunian objects (TNOs; including Scattered Disc objects, SDOs), Centaurs and minor planets on highly eccentric orbits some of which may have perihelia closer to the Sun than that of Jupiter. This means that some minor planets classified as “distant” by the MPC may still make close passes to Inner Solar System planets. Earth approaches, in particular, can provide favorable conditions for minor planet observations. For the benefit of promoting physical studies of distant minor planets, Earth approaches are also presented within the results.

An orbit propagation study is performed on distant minor planets provided on Minor Planet Center data webpage (MPC, 2024). All simulations used for this study are started on 2024 January 1 to end on 2100 January 1.

Although making up a rather small portion of all known minor planets, due to the vast number of known distant minor planets, the workload is split into 554 parts, each containing 10 minor planets, with the last batch containing 9; simulating a total of 5539 minor planets. The primary assumption that allows such an arrangement is that the gravitational accelerations caused by distant minor planets themselves are negligible compared to the gravitational accelerations caused by the Sun and the planets. This results in a quicker completion of each orbit propagator run, and allows for saving simulation results in between runs for further examination.

A custom n-body orbit propagator is used for this study, using an 8th order symplectic integrator based on Haruo Yoshida’s method of constructing symplectic integration algorithms. (Yoshida, 1990) The mathematical and algorithmic examination of the orbit propagator is considered to be beyond the scope of the research being presented, as the results obtained are also validated using JPL Horizons System.

The initial cartesian state vectors - only including positions and velocities relative to the Solar System barycenter - for minor planets and planets are obtained via the JPL Horizons System API. A fixed time step of nearly 10 days (exactly 864000 seconds) has been used. At each time step, distances between each minor planet and planets are checked. Time points, the bodies involved in the close passes, and the exact distances between them are recorded whenever the distance between a minor planet and a planet drops below 0.5 AU.

The strength of the orbital perturbations are directly related to the gravitational accelerations acting on the minor planets. To classify the close passes according to the magnitudes of the perturbative gravitational accelerations, an arbitrary value of 1×10^{-7} km/s is selected, which corresponds to a distance of about 0.23 AU for Jupiter and 0.13 AU for Saturn, using a standard gravitational parameter (GM) of 126.687×10^6 km³/s² for Jupiter and 37.931×10^6 km³/s² for Saturn. (NASA GSFC, 2024).

The resulting list of close passes given in Table I are validated using the position data from JPL Horizons System at the obtained dates of close-passes. Presented distances are those obtained using the data from Horizons System (JPL, 2024). Jupiter passes with a distance closer than 0.23 AU are highlighted in bold. No Saturn passes with a distance closer than 0.13 AU were found.

Acknowledgements

This research has made use of data provided by the International Astronomical Union’s Minor Planet Center.

References

- JPL Solar System Dynamics (2024). Horizons System. <https://ssd.jpl.nasa.gov/horizons/>
- Minor Planet Center (2024). Minor Planet Center Data. <https://www.minorplanetcenter.net/data>
- NASA Goddard Space Flight Center Space Science Data Coordinated Archive (2024). Planetary Fact Sheets. <https://nssdc.gsfc.nasa.gov/planetary/planetfact.html>
- Yoshida, H. (1990). “Construction of higher order symplectic integrators.” *Physics Letters A* **150**, 262-268.

Minor Planet Designation	Planet Name	Date of Encounter (yyyy-mm-dd)	Distance (AU)	a (AU)	e	i (°)	q (AU)	Q (AU)	H
2024 JW	Earth	2024-04-20	0.4121	9.842	0.861	8.194	1.364	18.32	22.16
2023 RB	Saturn	2024-09-17	0.2621	28.679	0.717	4.676	8.120	49.237	10.43
2014 EU131	Jupiter	2025-04-25	0.3892	5.862	0.191	6.554	4.740	6.984	14.87
2011 SZ3	Mars	2027-12-21	0.1285	6.492	0.793	3.278	1.346	11.638	19.06
2014 FP59	Jupiter	2028-08-07	0.1555	5.967	0.361	4.569	3.812	8.122	16.3
2012 TN149	Jupiter	2029-09-11	0.4761	7.102	0.719	3.169	1.994	12.21	18.11
2019 QX115	Jupiter	2032-06-27	0.3800	5.689	0.212	4.366	4.486	6.893	16.05
2011 YU75	Mars	2032-09-05	0.4256	7.514	0.766	16.695	1.759	13.27	17.0
2019 QR115	Jupiter	2032-09-25	0.4430	5.624	0.237	6.522	4.289	6.96	16.36
2015 GB46	Mars	2033-01-03	0.1748	6.805	0.775	5.307	1.528	12.082	19.23
2012 TJ261	Saturn	2033-06-02	0.3227	6.340	0.447	6.358	3.506	9.174	15.55
2015 RC41	Mars	2033-12-19	0.2563	6.906	0.813	6.339	1.293	12.519	19.16

Minor Planet Designation	Planet Name	Date of Encounter (yyyy-mm-dd)	Distance (AU)	a (AU)	e	i (°)	q (AU)	Q (AU)	H
2015 GB46	Jupiter	2034-07-17	0.3499	6.805	0.775	5.307	1.528	12.082	19.23
2007 VU259	Mars	2036-05-07	0.2961	5.811	0.687	9.296	1.820	9.801	18.22
2017 UV43	Jupiter	2037-11-18	0.1714	6.734	0.261	5.199	4.977	8.491	13.75
2014 UF77	Mars	2041-04-01	0.2331	5.636	0.744	11.566	1.441	9.831	18.13
2010 LG61	Earth	2041-08-09	0.4530	6.281	0.784	123.812	1.360	11.203	19.3
2020 BZ12	Venus	2041-08-19	0.4292	7.694	0.921	165.557	0.604	14.784	18.12
2016 UG245	Mars	2041-11-17	0.1570	8.472	0.830	2.337	1.439	15.504	18.01
2019 QR60	Jupiter	2044-02-25	0.0541	5.590	0.202	1.736	4.460	6.72	15.6
2015 BQ311	Jupiter	2044-04-15	0.4506	7.088	0.293	24.495	5.011	9.164	12.28
2010 VC189	Earth	2045-02-09	0.3650	9.103	0.852	0.694	1.349	16.856	18.75
2019 QS3	Mars	2046-08-03	0.3079	5.678	0.774	13.599	1.281	10.075	21.2
2019 PR2	Earth	2047-10-27	0.2829	5.772	0.798	10.993	1.164	10.379	18.68
2019 QR6	Earth	2047-10-27	0.3012	5.771	0.798	10.978	1.165	10.376	20.05
2015 GB46	Jupiter	2049-10-06	0.4783	6.805	0.775	5.307	1.528	12.082	19.23
2021 YP	Jupiter	2050-11-30	0.4235	6.146	0.687	170.196	1.924	10.368	17.57
2015 RC41	Mars	2051-05-19	0.2962	6.906	0.813	6.339	1.293	12.519	19.16
2010 DG77	Venus	2055-11-04	0.2727	20.831	0.954	21.106	0.953	40.709	20.32
2023 RC49	Jupiter	2056-06-11	0.4444	10.186	0.522	98.489	4.872	15.501	13.92
2022 RT3	Jupiter	2056-12-08	0.4316	10.525	0.582	169.060	4.395	16.655	15.12
2010 KG12	Jupiter	2057-10-04	0.1919	6.219	0.290	23.050	4.418	8.019	14.26
2005 VD	Jupiter	2057-12-13	0.1490	6.685	0.254	172.195	4.990	8.379	14.28
2014 UG6	Mars	2058-11-18	0.2538	12.401	0.889	7.069	1.374	23.429	19.18
2020 JV3	Saturn	2059-01-17	0.2505	6.312	0.474	8.519	3.322	9.302	15.99
2013 YG48	Mars	2060-10-28	0.4421	8.182	0.752	61.323	2.029	14.336	17.2
2016 PW84	Jupiter	2061-09-13	0.1133	5.811	0.280	14.537	4.182	7.441	14.6
2016 UW222	Mars	2061-11-02	0.4554	6.099	0.722	1.446	1.694	10.505	19.42
2020 BZ12	Venus	2062-08-19	0.2388	7.694	0.921	165.557	0.604	14.784	18.12
2020 BZ12	Earth	2062-10-08	0.3792	7.694	0.921	165.557	0.604	14.784	18.12
2020 VS6	Mars	2064-02-10	0.4144	9.629	0.817	161.318	1.758	17.499	19.3
2010 DG77	Earth	2064-11-16	0.4906	20.831	0.954	21.106	0.953	40.709	20.32
2016 UP210	Mars	2066-10-07	0.2193	6.450	0.777	5.141	1.436	11.465	19.4
2023 FE12	Jupiter	2066-10-07	0.2585	7.617	0.495	18.974	3.844	11.391	15.39
2006 JG57	Jupiter	2066-11-06	0.4128	9.622	0.509	56.973	4.729	14.516	12.4
2019 SO48	Saturn	2067-02-14	0.2696	5.720	0.677	2.901	1.845	9.596	18.35
2015 RC41	Mars	2067-10-22	0.2787	6.906	0.813	6.339	1.293	12.519	19.16
2015 RC41	Earth	2067-12-21	0.3261	6.906	0.813	6.339	1.293	12.519	19.16
2015 VH105	Mars	2069-06-03	0.4643	5.913	0.752	29.501	1.469	10.357	17.6
2014 YO46	Mars	2069-09-11	0.4451	6.979	0.783	9.447	1.514	12.444	18.83
2014 EY247	Jupiter	2071-08-12	0.3838	6.079	0.282	6.136	4.362	7.796	15.0
2016 GE53	Uranus	2072-03-09	0.3520	10.768	0.875	0.582	1.347	20.19	16.77
2019 RZ16	Jupiter	2072-05-28	0.2894	6.676	0.651	4.588	2.331	11.021	16.38
2010 LG61	Mars	2073-02-22	0.1993	6.281	0.784	123.812	1.360	11.203	19.3
2010 DG77	Earth	2073-12-19	0.1112	20.831	0.954	21.106	0.953	40.709	20.32
1999 XS35	Earth	2074-12-04	0.3589	17.781	0.948	19.651	0.922	34.641	17.69
2019 PR2	Earth	2075-09-20	0.4962	5.772	0.798	10.993	1.164	10.379	18.68
2019 QR6	Earth	2075-09-20	0.4555	5.771	0.798	10.978	1.165	10.376	20.05
2018 RG39	Jupiter	2077-04-22	0.3139	5.845	0.529	15.852	2.755	8.935	15.1
2016 CM239	Mars	2082-02-15	0.1657	5.863	0.715	16.499	1.668	10.057	17.47
2010 DG77	Mars	2082-12-02	0.4661	20.831	0.954	21.106	0.953	40.709	20.32
2010 DG77	Earth	2083-03-02	0.4286	20.831	0.954	21.106	0.953	40.709	20.32
2020 BZ12	Venus	2083-07-20	0.2958	7.694	0.921	165.557	0.604	14.784	18.12
2020 BZ12	Earth	2083-09-08	0.2495	7.694	0.921	165.557	0.604	14.784	18.12
2016 UK219	Mars	2084-04-05	0.3312	5.647	0.735	10.683	1.496	9.798	18.41
2012 TN149	Jupiter	2085-02-09	0.2025	7.102	0.719	3.169	1.994	12.21	18.11
2016 GE53	Mars	2085-02-09	0.2614	10.768	0.875	0.582	1.347	20.19	16.77
2022 BG4	Mars	2085-02-09	0.4304	9.969	0.888	4.724	1.112	18.825	18.61
2024 JW	Mars	2085-07-19	0.1062	9.842	0.861	8.194	1.364	18.32	22.16
2015 HO176	Saturn	2088-10-11	0.3770	5.614	0.580	8.901	2.356	8.872	16.7
2019 QR115	Jupiter	2091-01-09	0.3802	5.624	0.237	6.522	4.289	6.96	16.36
2010 BA101	Mars	2092-10-20	0.3473	9.180	0.833	26.519	1.536	16.824	99.99
2011 SZ3	Mars	2093-05-28	0.1020	6.492	0.793	3.278	1.346	11.638	19.06
2010 VC189	Jupiter	2094-05-03	0.0967	9.103	0.852	0.694	1.349	16.856	18.75
2010 JO142	Jupiter	2094-06-12	0.2096	5.782	0.474	12.887	3.044	8.52	16.12
2011 SZ3	Jupiter	2094-11-29	0.4037	6.492	0.793	3.278	1.346	11.638	19.06
2010 HR68	Mars	2097-02-06	0.4791	14.984	0.896	21.719	1.563	28.405	99.99
2010 DG77	Mars	2097-02-16	0.4676	20.831	0.954	21.106	0.953	40.709	20.32
2013 RA96	Saturn	2098-08-10	0.4784	19.842	0.920	5.177	1.580	38.104	19.53

Table I. List of distant minor planet close passes to the planets of the Solar System. Distances belong to 00:00:00 UTC on the given dates of encounter, from JPL Horizons (JPL, 2024). Encounters with high perturbative accelerations are highlighted in bold. Keplerian orbital elements presented in the table (a, e, i, q, Q) belong to epochs no later than 2460400.5 JD and may change during close encounters.

ASTEROID-DEEPSKY APPULSES IN 2025

Brian D. Warner
Center for Solar System Studies
446 Sycamore Ave.
Eaton, CO 80615
brian@MinorPlanetObserver.com

(Received: 2024 June 2)

The following list is a *very small* subset of the results of a search for asteroid-deepsky appulses for 2024, presenting only the highlights for the year based on close approaches of brighter asteroids to brighter DSOs. For the complete set visit

<https://www.minorplanet.info/php/dsoappulses.php>

For any event not covered, the Minor Planet Center's web site at <https://www.minorplanetcenter.net/cgi-bin/checkmp.cgi> allows you to enter the location of a suspected asteroid or supernova and check if there are any known targets in the area.

The table gives the following data:

Date/Time	Universal Date (MM DD) and Time of closest approach.
#/Name	The number and name of the asteroid.
RA/Dec	The J2000 position of the asteroid.
AM	The approximate visual magnitude of the asteroid.
Sep/PA	The separation in arcseconds and the position angle from the DSO to the asteroid.
DSO	The DSO name or catalog designation.
DM	The approximate total magnitude of the DSO.
DT	DSO Type: OC = Open Cluster; GC = Globular Cluster; G = Galaxy.
SE/ME	The elongation in degrees from the sun and moon, respectively.
MP	The phase of the moon: 0 = New, 1.0 = Full. Positive = waxing; Negative = waning.

Date	UT	#	Name	RA	Dec	AM	Sep	PA	DSO	DM	DT	SE	ME	MP
01 23 15:45		79	Eurynome	07:27.11	+13:36.19	10.5	72	352	NGC 2395	8.0	OC	164	137	-0.21
02 02 06:08		135	Hertha	09:16.07	+17:36.06	12.3	118	168	NGC 2795	12.8	G	175	151	0.08
02 21 15:56		419	Aurelia	14:58.80	-19:16.18	12.8	11	177	NGC 5791	11.7	G	105	21	-0.45
02 21 22:15		526	Jena	10:08.42	+12:18.49	13.8	33	331	UGC 5470	10.2	G	175	121	-0.28
02 22 13:57		949	Hel	10:46.29	+01:51.15	13.2	129	2	NGC 3365	12.6	G	171	114	-0.24
02 23 02:48		1342	Brabantia	09:23.54	+02:09.94	13.0	126	23	NGC 2861	12.7	G	164	116	-0.35
02 25 14:54		345	Tercidina	11:36.42	-09:49.56	12.2	32	325	NGC 3763	13.0	G	157	147	-0.01
02 27 07:16		346	Hermentaria	11:15.30	+18:04.73	11.7	162	146	NGC 3599	11.9	G	167	169	0.00
02 28 03:23		144	Vibilia	11:00.37	+13:56.09	12.5	139	333	NGC 3489	10.3	G	173	165	0.01
03 02 03:00		313	Chaldaeia	11:58.15	-02:05.58	11.4	57	127	NGC 4006	12.6	G	161	168	0.07
03 02 05:03		481	Emita	12:34.12	+11:18.07	13.2	136	148	NGC 4528	12.1	G	155	160	0.09
03 03 03:21		740	Cantabria	10:17.71	+21:43.28	13.1	165	324	NGC 3185	12.2	G	163	127	0.11
03 03 14:02		135	Hertha	08:49.35	+19:06.89	13.0	178	346	NGC 2672	11.7	G	145	73	0.34
03 05 04:48		1318	Nerina	11:28.26	+16:53.25	14.0	118	209	NGC 3691	11.8	G	167	112	0.32
03 05 15:45		480	Hansa	12:10.18	-29:45.36	12.5	83	165	IC 764	12.2	G	142	120	0.48
03 24 10:02		481	Emita	12:15.90	+13:09.50	13.1	30	353	NGC 4216	10.0	G	165	136	-0.18
03 25 22:31		665	Sabine	17:38.21	-37:32.77	13.6	74	351	Cr 338	8.0	OC	100	67	-0.08
03 27 12:00		188	Menippe	17:17.98	-23:45.13	14.0	55	22	NGC 6325	10.7	GC	107	98	-0.01
03 27 16:55		674	Rachele	11:29.39	+24:05.75	11.5	45	6	NGC 3701	12.9	G	149	160	-0.02
04 18 05:51		165	Loreley	18:43.21	-32:17.17	12.4	50	354	NGC 6681	8.1	GC	144	122	-0.04
04 27 12:27		312	Pierretta	19:57.88	-31:53.26	13.4	136	171	NGC 6841	12.6	G	102	109	0.00
04 29 23:54		164	Eva	14:33.10	+10:29.01	13.8	1	27	NGC 5666	12.8	G	154	117	0.17
04 30 20:40		752	Sulamitis	13:33.21	-01:01.03	13.7	59	347	NGC 5211	12.3	G	161	126	0.09
05 01 02:58		769	Tatjana	12:47.87	-01:40.50	13.9	153	169	NGC 4690	12.9	G	150	88	0.26
05 01 21:22		906	Repsolda	17:01.16	-30:06.35	13.9	48	39	NGC 6266	6.6	GC	146	130	0.44
05 21 18:44		474	Prudentia	18:36.70	-08:13.04	13.9	4	126	NGC 6664	7.8	OC	142	123	-0.03
05 23 21:27		306	Unitas	10:42.09	+13:44.50	13.7	32	160	NGC 3338	11.1	G	93	111	-0.03
05 26 00:31		144	Vibilia	10:36.68	+14:12.20	14.0	151	330	NGC 3300	12.1	G	92	121	-0.07
05 26 18:48		117	Lomia	16:34.11	-44:03.23	12.8	14	199	NGC 6169	6.6	OC	157	156	-0.01
05 28 06:59		198	Ampella	12:53.27	-16:58.44	13.3	69	298	NGC 4763	12.6	G	130	98	0.08
05 28 17:58		424482	2008 DG5	14:17.65	-07:24.93	14.0	46	275	NGC 5534	12.3	G	147	123	0.04
05 31 17:16		1093	Freda	15:17.43	-21:02.10	12.8	70	201	NGC 5897	8.6	GC	161	87	0.36
06 01 05:08		776	Berbericia	11:43.42	+22:43.57	13.8	70	110	NGC 3832	13.0	G	97	43	0.22
06 29 20:17		198	Ampella	12:59.30	-15:02.36	13.7	21	178	NGC 4856	10.5	G	103	66	0.10
07 29 12:32		779	Nina	00:21.06	+22:21.75	11.6	124	70	NGC 80	12.1	G	112	164	0.31
08 18 15:39		1056	Azalea	22:03.16	-20:29.38	13.0	98	214	NGC 7185	12.6	G	172	106	-0.35
08 22 20:49		791	Ani	00:40.40	-13:52.57	13.3	94	75	NGC 210	10.9	G	141	120	-0.05
08 23 12:27		415	Palatia	02:43.30	+04:58.14	13.3	8	6	NGC 1070	11.9	G	109	101	-0.01
09 14 20:01		626	Notburga	01:07.45	+32:32.17	11.9	133	298	NGC 379	12.9	G	138	71	-0.35
09 14 21:46		375	Ursula	19:40.16	-30:58.28	12.4	125	263	NGC 6809	7.0	GC	120	151	-0.49
09 19 11:43		757	Portlandia	01:21.80	+05:16.84	13.0	50	357	NGC 488	10.3	G	155	126	-0.07
09 24 02:15		197	Arete	00:56.74	-09:51.29	12.7	114	26	NGC 309	12.5	G	164	141	0.12
10 17 10:17		444	Gyptis	23:36.50	+00:18.03	11.4	3	58	NGC 7716	12.1	G	149	173	-0.05
10 20 23:50		202	Chryseis	02:38.24	+02:08.55	12.2	107	30	NGC 1016	11.6	G	165	163	0.01
10 25 09:09		6	Hebe	22:20.73	-24:42.82	8.9	117	191	NGC 7252	12.1	G	114	57	0.23
10 26 01:57		943	Begonia	03:03.85	-01:07.87	14.0	179	196	NGC 1194	12.9	G	160	128	0.23
11 20 14:07		6	Hebe	22:47.86	-22:21.29	9.3	147	202	NGC 7377	11.1	G	96	84	0.01
12 24 12:31		925	Alphonsina	02:52.99	+42:11.41	12.8	132	258	NGC 1122	12.1	G	135	97	0.14
12 27 03:11		433	Eros	01:09.31	+32:45.20	10.7	13	332	NGC 403	12.5	G	112	37	0.44

TIMING LIGHTCURVE MINIMA TO LOOK FOR CANDIDATE CLOSE BINARY ASTEROIDS

W. Romanishin
1933 Whispering Pines Cir., Norman, OK 73072
wromanishin@ou.edu

(Received: 2024 April 23 Revised: 2024 August 14)

True detached binary asteroids are systems in which the components are connected only by gravity. Using only lightcurves, it can be difficult or impossible to determine if an asteroid is a true binary, a contact binary, or a single elongated object. However, if a true binary has an eccentric orbit, we might be able to use the time between lightcurve minima to provide a hint of its nature.

We now know of numerous binary asteroids. These have been discovered with several different techniques, including analysis of lightcurves. True detached binaries with small separations are difficult to find and study (unless your budget includes a spacecraft flyby!). Using only lightcurves, it is difficult or impossible to tell if an object is a single elongated object, a contact binary where two objects are in physical contact, or a true detached binary with a small separation. This is particularly true if the bodies in a close detached binary have exactly circular orbits around their common center of mass – the lightcurve can look just like an elongated single object (see e.g. Harris and Warner, 2020). However, if the orbits in a detached binary are even slightly non-circular, the true nature of the object might reveal itself in small lightcurve details.

Figure 1 shows a cartoon of a binary system with equal masses and non-circular orbits. The components orbit their common center of mass, indicated by the X. The line between the centers of the objects always crosses the X and for equal masses, the objects are equidistant from the center of mass at all times. The X lies at the common foci of the two elliptical paths traced by the components. Ellipses have a shape indicated by their eccentricity, e , which ranges from 0 for a circle to almost 1 for a very long flat ellipse. We assume the observer is in the plane of the orbits and observing along the direction indicated by the green arrow. The angle between the major axis of the orbit and the green arrow is θ .

As the components go through a complete period, which takes a time P , we would see two eclipses. If θ is zero, then the eclipses are separated in time by $0.5P$, no matter what e is. If e is zero, the eclipses are $0.5P$ apart no matter from which angle they are observed. But if $e > 0$ and $\theta \neq 0$ the times between eclipses are not the same. To get from the eclipse 1 (upper) configuration to the eclipse 2 (lower) configuration, each object must travel a longer, slower arc than to get from the lower configuration back to the upper configuration. A schematic lightcurve of the object is shown in Figure 2. We define Δ as the fraction of a period of the longer minima gap is compared to a half period. Thus, the longer minima gap is $P\Delta$ longer than $0.5P$.

Obviously, Δ must depend on both e and θ . To calculate Δ from e and θ , one must know how to calculate the time for an object to move between two arbitrary points on an elliptical orbit, taking into account a constantly varying orbital speed if $e > 0$. Of course, Kepler solved this problem over 400 years ago! Now, with a computer and a few dozen lines of code, one can numerically do the needed calculations in a few seconds. I calculated Δ for a grid of e and θ , and find that, at least for e less than 0.2 or so, the following formula provides a good approximation to Δ :

$$\Delta = 0.64 e \sin\theta$$

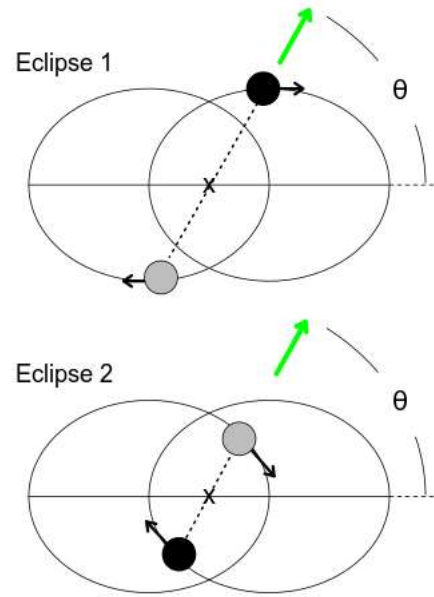


Figure 1. The components have different shading just to tell them apart. In an actual close binary, the bodies would be larger, relative to the size of the orbits, than shown here. The black arrows show the direction of motion. As plotted, the ellipses have $e \sim 0.6$.

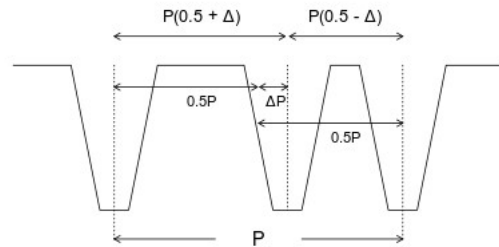


Figure 2. Schematic lightcurve.

Now, since we don't have detailed orbits for many close binaries, we don't know what kind of e values they might have. Of course, if they all have purely circular orbits, then all will have Δ of zero. But a numeric example shows that even a somewhat small eccentricity can give a readily observable effect. If P is 6 hours, a typical period for a close binary, and e is 0.05, the value of $P\Delta$ ranges from zero for θ of zero to 12 minutes for θ of 90° . The accuracy with which one can measure the time of minima in a real lightcurve depends on several factors: the observing cadence, the signal to noise of the magnitudes and the degree of symmetry of the minima. But, just as an astrometrist can measure the x,y coordinates of a star image to a fraction of a pixel, with high quality lightcurves one should be able to measure the time of a minimum to less than the length of one exposure, particularly for nice symmetric minima. Measurement of the time of minima to minute or less accuracy should be easy for exposures of several minutes. Thus, the 12-minute difference in the example would be very easily detected with good data.

I have done a cursory survey of lightcurves of objects with relatively sharp minima, using the thumbnail lightcurves provided by Behrend (2023web). For potentially interesting objects, I printed out full lightcurves and carefully measured (using a ruler) the phase difference between minima. Most lightcurves show $\Delta \sim 0.00$, as expected. However, I found some where Δ is almost certainly greater than zero. Of course, asteroids can have very strange shapes, and it may be some single objects have lightcurves that show $\Delta > 0.00$. These would presumably not change with observing epoch, if observed under similar solar lighting conditions and viewing geometry. But a system that has Δ significantly different from zero and also has Δ that changes from one epoch to another would be worth investigating as a possible non-circular binary. (Unfortunately, most of the objects only have a single lightcurve in the Behrend compilation.)

I did find one object, 1659 Pankaharju, that appears to have Δ significantly larger than zero and different Δ at three epochs. The lightcurve obtained in 2023 by Martin et al. (2023web) gives a period of 5.014 h, and the longer separation between the minima is 2.622 h ($\Delta = 0.023$). The 2011 lightcurve of Antonini (2011web) gives the same period (rounded to 0.001 h), with the longer separation equal to 2.780 h ($\Delta = 0.054$). A lightcurve from 2000 (Warner, 2011) gives a period of 5.01 h and longer minima separation of 2.75 h ($\Delta = 0.049$). A reviewer mentioned that the lightcurves for this object might be explained by a peculiarly shaped object, rather than the effect discussed here. It would be interesting to try to fit a shape model to the lightcurves for this object, to see if they could be fit with a single object.

Finding asteroids that definitely have Δ values indicating possible close non-circular binary orbits would be very interesting. Of course, the vast majority of asteroids will have $\Delta \sim 0.00$. So, is it worth the bother to measure Δ ? Once you have reduced your lightcurve data to magnitude-time pairs, it would take only a trivial amount of extra effort to carefully fit the times of minima and derive a Δ value to include in your lightcurve publications.

References

- Antonini, P. (2011web).
<http://obswww.unige.ch/~behrend/r001659-02a.png>
- Behrend, R. (2023web)
http://obswww.unige.ch/~behrend/page_cou.html
- Harris, A.; Warner, B.D. (2020). "Asteroid lightcurves: Can't tell a contact binary from a brick." *Icarus* **339**, 113602.
- Martin, A.; Nicollrat, R.; Behrend, R. (2023web).
<http://obswww.unige.ch/~behrend/r001659-01a.png>
- Warner, B.D. (2011). "Upon Further Review: V. An Examination of Previous Lightcurve Analysis from the Palmer Divide Observatory." *Minor Planet Bull.* **38**, 63-65.

LIGHTCURVE AND ROTATION PERIOD OF THE SLOW ROTATOR 12867 JOELOIC

Gerard Faure
 Lotissement Arzelier 2
 38650 Château-Bernard, FRANCE
 gpmfaure@club.internet.fr

Yves Jongen
 Chemin du Cyclotron 3
 1348 Louvain la Neuve, BELGIUM

Julian Oey
 Blue Mountains Observatory (MPC Q68)
 Leura - NSW, AUSTRALIA

(Received: 2024 July 7)

Minor planet 12867 Joeloic was estimated to have a long rotation period based on measurements during its 2016 opposition. To solve this period, we monitored the asteroid for five months during the 2023 opposition. A total of 3,708 measurements taken over 134 sessions made it possible to find a more reliable rotation period at $426.2 \text{ h} \pm 0.4 \text{ h}$, with a lightcurve amplitude of 0.53 ± 0.03 mag. The non-repetitiveness of the curve during the nine full periods led to suspicion that 12867 could be a tumbling object. This was confirmed by Dr. Petr Pravec, who assessed that 12867 is a tumbling object of $\text{PAR} = -2$ (secure tumbler but with and unresolved second period).

Minor planet 12867 Joeloic has an absolute magnitude (H) of 13.86 and is located in the inner main-belt with orbital elements $a = 2.3200$ au, $e = 0.2108$, and $i = 6.641^\circ$. It was discovered by Belgian professional astronomer Eric Elst on 1998 June 1 at the La Silla Observatory in Chile. The LCDB catalog (Warner et al., 2009; LCDB from hereon) as of 2023 October indicates an albedo of 0.2 and a G coefficient of 0.24.

As part of the PSABA (Photometric Survey for Asynchronous Binary Asteroids) project directed by Petr Pravec (Pravec, 2005), Julian Oey and Roger Groom estimated a rotation of 813 hours with an amplitude of 0.71 mag using 290 measurements of images taken between 2016 Sep 6 and Nov 24 (Oey and Groom, 2019), i.e., over two and a half months of monitoring.

The authors began to follow 12867 on 25 June 2023, well before its perihelion on 18 September 2023. The predicted magnitude of the asteroid increased from $V \sim 16.8$ to $V \sim 15.0$ before weakening to $V \sim 17.5$ on 2023 Nov 25. For our campaign, a total of 142 imaging sessions were done, but eight of them were not kept for the final curve, including four done in France with various telescopes, because the APN images were not manageable with the *MPO Canopus* software.

The successful tracking from France and Chile using unfiltered images (C) was carried out by Yves Jongen using his two Plane Wave CDK 420-mm telescopes on Plane Wave L500 Direct drive mounts and Moravian CCD G4-16000 CCD cameras at the Deep Sky Chile site and in France at Rasteau (Provence). The SNR was on average 139 (ranging from 61 to 216) in France from August to mid-September and 131 (ranging from 57 to 205) in Chile during the Southern winter, from August to the end of September. The SNR was low, decreasing from 120 to 30, and sometimes less during the months further from the perihelion date.

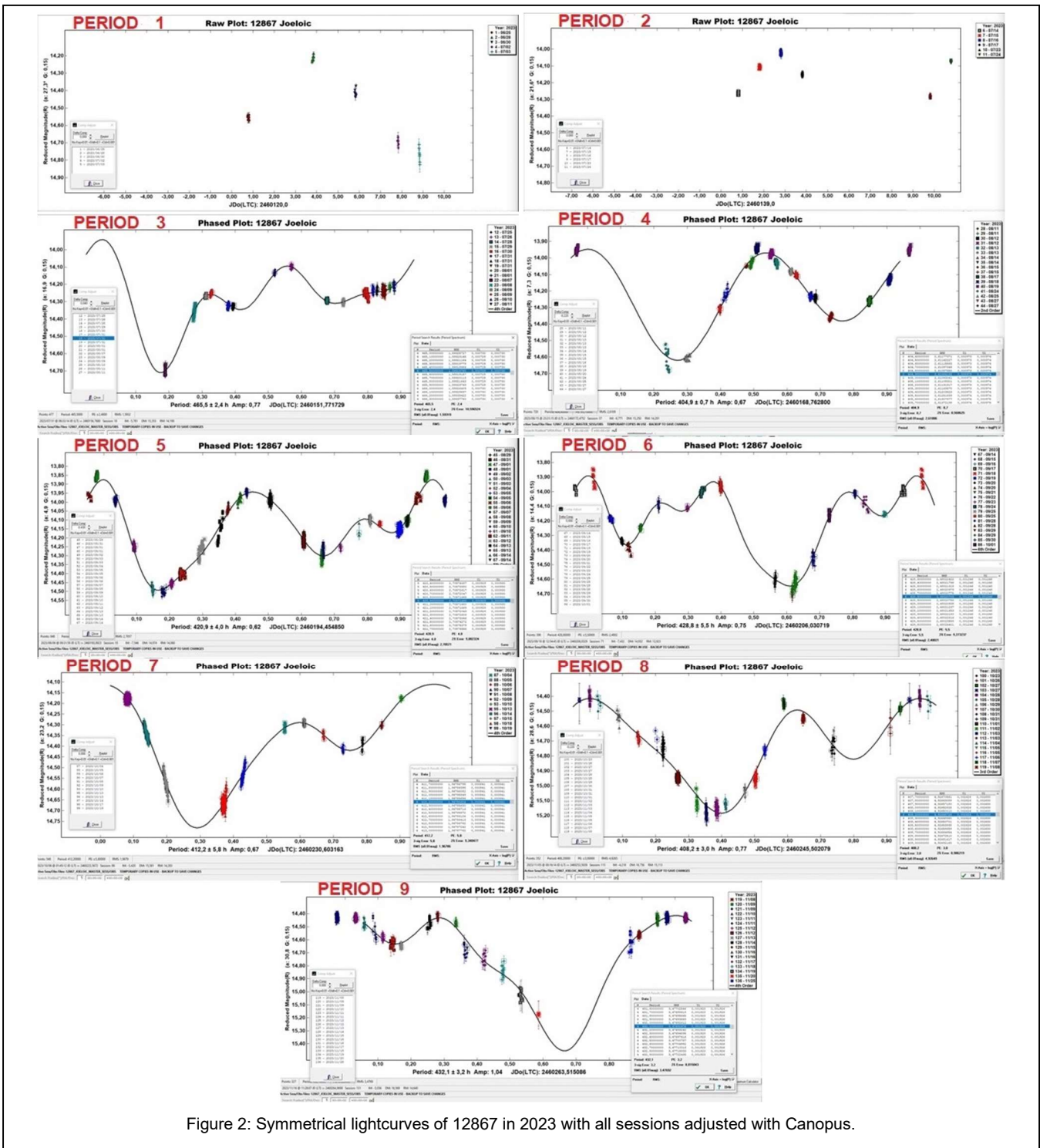


Figure 2: Symmetrical lightcurves of 12867 in 2023 with all sessions adjusted with Canopus.

On the Australian side, Julian Oey used a 35-cm telescope installed at the Blue Mountains Observatory in Leura (NSW) equipped with an SBIG STF-1603W CCD camera. A second 35-cm telescope and an SBIG ST-8XME CCD camera were used at a site located three hours further west in longitude.

The images were all calibrated following normal procedures (bias, darks and flats).

The analysis of unfiltered images in r' band data from France and Chile was carried out by Gerard Faure with *MPO Canopus* version 10.8.6.12 (Warner, 2022) and the CMC-14 catalog for comp star magnitudes. All measurements were light-time corrected. Those from Australia, also unfiltered, were measured in R band by Julian Oey using the CMC-15 (extension of the CMC 14) with the data subsequently transmitted to Gerard Faure, who then integrated them with an adjustment of -0.22 mag to connect them to other r' measurements from France and Chile.

TABLE OF THE PERIODS OF ROTATION AND SESSIONS - 12867 Joeloic Opposition 2023

Year: 2023			
P1	CHILI ● 1 - 06/26	FRAN ● 38 - 2023/08/18	AUST ● 85 - 2023/09/30
	CHILI ▲ 2 - 06/28	FRAN ● 39 - 2023/08/19	AUST ● 86 - 2023/10/01
	CHILI ▼ 3 - 06/30	FRAN ● 40 - 2023/08/20	CHILI ● 87 - 2023/10/04
	CHILI ◆ 4 - 07/02	AUST ● 41 - 2023/08/24	CHILI ● 88 - 2023/10/05
	CHILI + 5 - 07/03	AUST ● 42 - 2023/08/25	CHILI ● 89 - 2023/10/06
P2	CHILI ■ 6 - 07/14	CHILI ● 43 - 2023/08/27	CHILI ● 90 - 2023/10/07
	CHILI ✱ 7 - 07/15	AUST ● 44 - 2023/08/27	CHILI ● 91 - 2023/10/08
	CHILI ■ 8 - 07/16	AUST ● 45 - 2023/08/29	CHILI ● 92 - 2023/10/09
	CHILI ● 9 - 07/17	AUST ● 46 - 2023/08/31	CHILI ● 93 - 2023/10/10
	CHILI ▲ 10 - 07/23	AUST ● 47 - 2023/09/01	CHILI ● 94 - 2023/10/12
	CHILI ▼ 11 - 07/24	AUST ● 48 - 2023/09/01	CHILI ● 95 - 2023/10/13
	CHILI ◆ 12 - 07/25	AUST ● 49 - 2023/09/02	CHILI ● 96 - 2023/10/13
	CHILI + 13 - 07/26	AUST ● 50 - 2023/09/03	CHILI ● 97 - 2023/10/14
	CHILI ■ 14 - 07/28	FRAN ● 51 - 2023/09/03	CHILI ● 98 - 2023/10/17
	CHILI ✱ 15 - 07/29	AUST ● 52 - 2023/09/04	CHILI ● 99 - 2023/10/19
P3	AUST ■ 16 - 07/30	AUST ● 53 - 2023/09/05	AUST ■ 100 - 2023/10/23
	FRAN ● 17 - 07/31	FRAN ● 54 - 2023/09/05	AUST ● 101 - 2023/10/26
	CHILI ▲ 18 - 07/31	AUST ● 55 - 2023/09/06	CHILI ● 102 - 2023/10/27
	AUST ▼ 19 - 07/31	FRAN ● 56 - 2023/09/06	AUST ● 103 - 2023/10/27
	FRAN ◆ 20 - 08/01	FRAN ● 57 - 2023/09/07	CHILI ● 104 - 2023/10/28
	CHILI + 21 - 08/01	FRAN ● 58 - 2023/09/08	AUST ● 105 - 2023/10/28
	CHILI ■ 22 - 08/07	FRAN ● 59 - 2023/09/09	AUST ● 106 - 2023/10/29
	FRAN ✱ 23 - 08/08	AUST ● 60 - 2023/09/10	AUST ● 107 - 2023/10/30
	AUST ■ 24 - 08/09	FRAN ● 61 - 2023/09/10	AUST ● 108 - 2023/10/31
	FRAN ● 25 - 08/09	AUST ● 62 - 2023/09/11	FRAN ● 109 - 2023/10/31
P4	FRAN ▲ 26 - 08/10	AUST ● 63 - 2023/09/12	AUST ● 110 - 2023/11/01
	CHILI ▼ 27 - 08/11	AUST ● 64 - 2023/09/13	AUST ● 111 - 2023/11/02
	AUST ◆ 28 - 08/11	FRAN ● 65 - 2023/09/13	CHILI ● 112 - 2023/11/03
	FRAN + 29 - 08/11	AUST ● 66 - 2023/09/14	AUST ● 113 - 2023/11/03
	CHILI ■ 30 - 08/12	FRAN ● 67 - 2023/09/14	CHILI ● 114 - 2023/11/04
	FRAN ✱ 31 - 08/12	AUST ● 68 - 2023/09/15	CHILI ● 115 - 2023/11/05
	CHILI ■ 32 - 08/13	AUST ● 69 - 2023/09/16	AUST ● 116 - 2023/11/05
	FRAN ● 33 - 08/13	AUST ● 70 - 2023/09/17	CHILI ● 117 - 2023/11/06
	CHILI ▲ 34 - 08/14	AUST ● 71 - 2023/09/18	CHILI ● 118 - 2023/11/07
	FRAN ▼ 35 - 08/14	AUST ● 72 - 2023/09/19	CHILI ● 119 - 2023/11/08
P5	CHILI ◆ 36 - 08/15	CHILI ● 73 - 2023/09/20	CHILI ● 120 - 2023/11/09
	FRAN + 37 - 08/15	AUST ● 74 - 2023/09/20	AUST ● 121 - 2023/11/09
		CHILI ● 75 - 2023/09/21	AUST ● 122 - 2023/11/10
		CHILI ● 76 - 2023/09/22	CHILI ● 123 - 2023/11/11
		AUST ● 77 - 2023/09/23	AUST ● 124 - 2023/11/11
		AUST ● 78 - 2023/09/24	CHILI ● 125 - 2023/11/12
		AUST ● 79 - 2023/09/25	AUST ● 126 - 2023/11/12
		AUST ● 80 - 2023/09/25	CHILI ● 127 - 2023/11/13
		AUST ● 81 - 2023/09/28	AUST ● 128 - 2023/11/14
		AUST ● 82 - 2023/09/28	CHILI ● 129 - 2023/11/18
	AUST ● 83 - 2023/09/29	CHILI ● 130 - 2023/11/16	
	AUST ● 84 - 2023/09/29	AUST ● 131 - 2023/11/16	
		AUST ● 132 - 2023/11/17	
		AUST ● 133 - 2023/11/18	
		AUST ● 134 - 2023/11/19	
		AUST ● 135 - 2023/11/20	
		AUST ● 136 - 2023/11/25	

Table I. Table of legends of the 136 sessions measured for 12867 in 2023.

The lightcurve was developed using 3,708 image measurements from 134 sessions. Sessions 19 and 94 were removed due to poor quality. The image monitoring of 12867 was carried out from 2023 June 25, 06:00 UT, through 2023 Nov 25, 15:39 UT, i.e. over a total duration of 3681.6 hours (about 5 months, or 153.4 days). As the sessions progressed, the successive lightcurves did not seem to show very repetitive shapes; it was only after three months that a rotation period of between 420 and 428 hours began to be suspected.

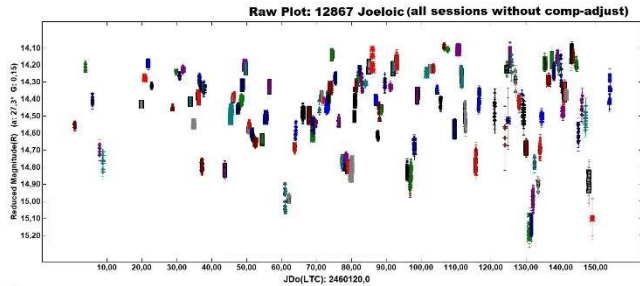


Figure 1: Raw global lightcurve of 12867 Joeloic in 2023 with its 136 measured sessions.

Using all available measurements through the end of November 2023, we adjusted all the sessions, starting with the session furthest from the curve, to the one closest to the curve. We obtained a low RMS and nine complete symmetrical periods which, without being real in their form, allowed us to confirm an approximate rotation period of 421.5h, included in the initial estimate of 420-428h.

After connecting each session to one of the nine complete periods, the analysis and detailed verification of the rotation periods using the periods numbered 3 to 9 began. Periods 1 and 2 were excluded because they had too few sessions. The zero-point adjustments, sometimes necessary given the problems of pollution of nearby stars, errors in the stellar catalogs used, measurements, climatic problems, etc. were kept to a minimum. This allowed establishing a complete lightcurve for periods 3 to 9. However, the lightcurves did not show clear correlations in terms of shapes, even if their curves connected quite well at their ends (see Figure 2).

We considered many causes for the unusual lightcurve results: evolution of the phase angle during the five months of observations, binarity, rotation on two axes (tumbling), and measurement errors, either as a single factor or as multiple factors. Before moving on to the study of these physical causes, the search for the best rotation period between 420 and 428 hours was made, using the Comp Adjust feature as little as possible, but also by excluding sessions 19 and 94, which deviated significantly from the curve, rather than keeping them with significant zero-point offsets. All global lightcurve searches resulted in rotation periods between 424.3 and 427.2 hours, with a preponderance of 424.334 h (3rd order) when using all nine periods and 134 sessions or 426.2 h (2nd order) when using periods 2 to 7 and 92 sessions, which excluded sessions at extreme phase angles and the largest lightcurve amplitudes at the start and end of tracking.

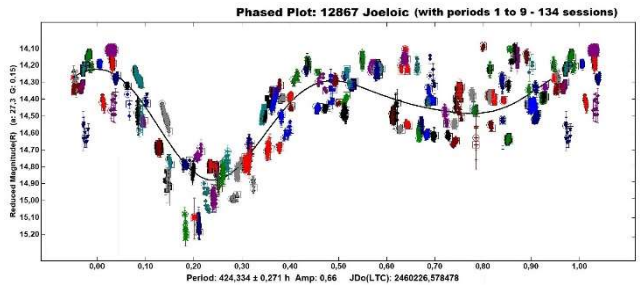


Figure 3: Lightcurve of 12867 in 2023 with 9 Periods (134 sessions - Order 3).

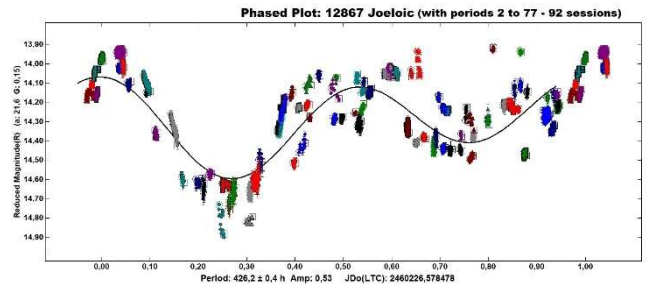


Figure 4: Lightcurve of 12867 in 2023 with Periods 2 to 77 (92 sessions - Order 2).

In Pilcher et al. (2017) it is discussed that for an object with a long period of rotation, one should not use high harmonic orders in the Fourier analysis due to the discordance of the curves from rotation to rotation, which is the case of 12867.

From all our analysis, the rotation period considered most reliable is 426.2 ± 0.4 h (*MPO Canopus* formal uncertainty), based on the complete periods No. 2 to 7, made with order 2 and excluding Sessions 19 and 94 as well as complete periods No. 1, 8 and 9. The lightcurve amplitude is 0.53 ± 0.03 mag.

We continued our analysis to check for the possibility of a satellite without success. With a maximum of 10 to 11% of total imaging time for the five-month follow-up period (around 400 hours out of a total of 3682 hours), we had only a 10 to 11% chance of capturing a possible companion. Moreover, binary asteroids are commonly found for very fast rotators and seldom for very slow rotators like 12867 Joeloic.

The lightcurves of the overall and nine complete periods, with sessions affected by clouds throughout, closely resemble those of 288 Glauke, which is a well-established tumbler, i.e., in non-principal axis rotation. The combination of the periods of rotation and precession result in chaotic lightcurves, both individually and combined (Pilcher et al., 2015).

Number	Name	yyyy mm/dd	Phase	L _{PAB}	B _{PAB}	Period (h)	P.E.	Amp	A.E.
12867	Joeloic	2023/06/25-11/25	*27.2, 31.7	331	+1	^T 426.2 290	0.4 5	0.53	0.03

Table II. Observing circumstances and results. The phase angle is given for the first and last date. If preceded by an asterisk, the phase angle reached a minimum during the period. L_{PAB} and B_{PAB} are the approximate phase angle bisector longitude/latitude at mid-date range (see Harris et al., 1984). ^T Dominant period of a tumbling asteroid. The second line is a possible second period.

We contacted Dr. Petr Pravec of the Czech Academy of Sciences, a specialist in tumbling asteroids, to submit the case of 12867. He replied that it is definitely a tumbler but he couldn't get a good solution for its both periods from the available data (Pravec, *private communications*). His analysis shows that there was a strong signal at 426 ± 5 h. It is likely the main period of the tumbler. For the second period, he found a possible solution of 289 h, again with an uncertainty of order of a few hours, but it was a somewhat weak solution because, for one, it is not far from a 2:3 commensurability with the main period of 426 h, and so it's possible that it is not a true second period of the tumbler, but rather a linear combination of its true second frequency with the main frequency of $1/426$ h. Pravec rates this tumbler as PAR = -2 (see Pravec et al., 2005 for definition of the PAR scale), with the likely main period of 426 h, but no good solution for its second period.

Pravec made a second attempt with only the French and Chilean measurements. The conclusion remained essentially unchanged, with the two period being only slightly different. The main period of the tumbler is 425 h and the candidate second period is 290 h, both with realistic uncertainties on the order of ± 5 h.

Acknowledgements

We warmly thank Dr Petr Pravec for his spontaneous help and his analysis of the tumbling aspect. We also thank Mr. Frederick Pilcher, ALPO Coordinator, for his various advice during the preparation of our article.

References

- ALCDEF (Asteroid Lightcurve Data Exchange Format) web site. (2023). <https://alcdef.org/>
- Harris, A.W.; Young, J.W.; Scaltriti, F.; Zappala, V. (1984). "Lightcurves and phase relations of the asteroids 82 Alkmene and 444 Gyptis." *Icarus* **57**, 251-258.
- Jongen, Y. (2021). "Les collaborations pro-am dans les mesures de transit d'exoplanètes - RCE 2021." <https://media.afastronomie.fr/RCE/PresentationsRCE2020/S2-19-JONGEN.pdf>
- MPCORB.dat (2023 Aug 15). <https://www.minorplanetcenter.net/iau/MPCORB.html>
- Oey, J.; Groom, R. (2019). "Lightcurve Analysis of asteroids from BMO and DRO in 2016: II." *Minor Planet Bulletin* **46**, 119-124.
- Pilcher, F.; Lorenzo, F.; Pravec, P. (2015). "A Nine Month Photometry Study of the Very Slowly Rotating Asteroid 288 Glauke." *Minor Planet Bulletin* **42**, 6-10.
- Pilcher, F.; Franco, L.; Pravec, P. (2017). "319 Leona and 341 California - Two very slowly rotating asteroids." *Minor Planet Bulletin* **44**, 86-89.
- Pravec, P. (2005). "Photometric Survey for Asynchronous Binary Asteroids" in *Proceedings of the Symposium on Telescope Science (The 24th Annual Conference of the Society for Astronomical Science)*, 61-67.
- Pravec, P.; Harris, A.W.; Scheirich, P.; Kušnirák, P.; Šarounová, L.; Hergenrother, C.W.; Mottola, S.; Hicks, M.D.; Masi, G.; Krugly, Yu.N.; Shevchenko, V.G.; Nolan, M.C.; Howell, E.S.; Kaasalainen, M.; Galád, A.; Brown, P.; Degraff, D.R.; Lambert, J.V.; Cooney, W.R.; Foglia, S. (2005). "Tumbling asteroids." *Icarus* **173**, 108-131.
- Warner, B.D. (2022). *MPO Canopus* software. <https://bdwpublishing.com>
- Warner, B.D.; Harris, A.W.; Pravec, P. (2009). "The Asteroid Lightcurve Database." *Icarus* **202**, 134-146. Updated 2023 June. <http://www.minorplanet.info/lightcurvedatabase.html>

LIGHTCURVE AND ROTATION PERIOD OF 32153 LAURENMCRAW

Gerard Faure
 Lotissement Arzelier 2
 38650 Château-Bernard, FRANCE
 gpmfaure@club.internet.fr

Yves Jongen
 Chemin du Cyclotron 3
 1348 Louvain la Neuve, BELGIUM

(Received: 2024 June 11)

The lightcurve, rotation period, and amplitude are determined for the asteroid 32153 Laurenmcgraw: 24.8082 ± 0.0007 hours, 0.54 ± 0.03 magnitudes.

During the tracking of the asteroid 12867 Joeloic with a long rotation period during the summer of 2023, we had the opportunity also to track 32153 Laurenmcgraw, which appeared in images with Joeloic for five nights from 2023 Jul 14-23. Images were then taken separately for 32153 Laurenmcgraw from 2023 Jul 24 to Sep 17 to finish defining its lightcurve.

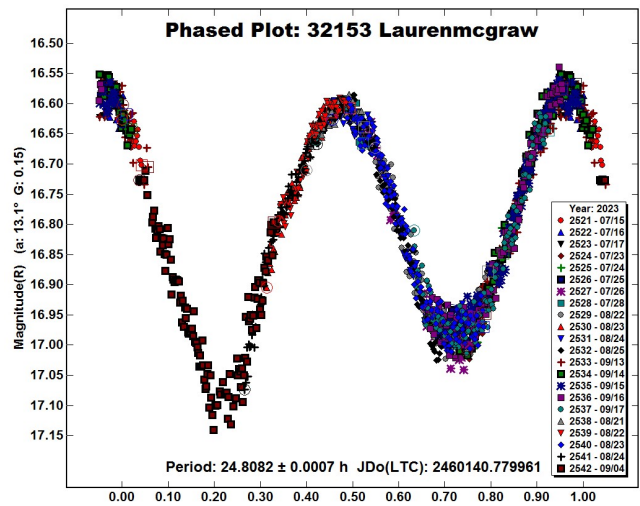
The acquisition of unfiltered images was entirely made by Yves Jongen using his two Plane Wave CDK 420-mm telescopes on Plane Wave L500 Direct drive mounts, with Moravian CCD G4-16000 cameras, one in Chile on site “Deep Sky Chile” and the other in France in Rasteau (Provence). The images were calibrated following normal procedures (bias, darks, and flats). The asteroid’s SNR averaged 46.4 with range 29-71.

The analysis of the images and data in unfiltered R band was carried out by Gerard Faure with the *MPO Canopus* software (Warner, 2022), version 10.8.6.12 and its MPOSC3 catalog. The date for each measurement was light-time corrected.

32153 Laurenmcgraw has absolute magnitude of $H = 13.87$; it is found in the middle main-belt with orbital parameters of $a = 2.7638$ au, $e = 0.1954$ and, $i = 10.759^\circ$. It was discovered by the LONEOS program at Anderson Mesa (USA) on 2000 June 3. The LCDB catalog (Warner et al., 2009) indicates an albedo of 0.057.

With a predicted magnitude of $V = 16.3$ to 17.1 during observations, this object passed perihelion on 2023 June 6, making the imaging carried out post-perihelion opposition.

The lightcurve was drawn using 22 imaging sessions. A secure rotation period of 24.8082 ± 0.001 hours and amplitude 0.54 ± 0.03 mag. No other rotation period appears for 32153 Laurenmcgraw in the LCDB catalog or on the ALCDEF (2023) website.



Acknowledgments

We thank Frederick Pilcher for agreeing to verify our data.

References

ALCDEF (2023). Asteroid Lightcurve Data Exchange Format website. <https://alcdef.org>

Harris, A.W.; Young, J.W.; Scaltriti, F.; Zappala, V. (1984). “Lightcurves and phase relations of the asteroids 82 Alkmene and 444 Gytis.” *Icarus* **57**, 251-258.

Jongen, Y. (2021). “Les collaborations pro-am dans les mesures de transit d’exoplanètes - RCE 2021.” <https://media.afastronomie.fr/RCE/PresentationsRCE2020/S2-19-JONGEN.pdf>

Minor Planet Center. “MPCORB.dat.” Accessed: 2023 Aug 15. <https://www.minorplanetcenter.net/iau/MPCORB.html>

Warner, B.D. (2022). *MPO Canopus* software. V version 10.8.6.12. <https://bdwpublishing.com>

Warner, B.D.; Harris, A.W.; Pravec, P. (2009). “The Asteroid Lightcurve Database.” *Icarus* **202**, 134-146. Updated 2023 June. <http://www.MinorPlanet.info/php/lcdb.php>

Number	Name	2023/mm/dd	Phase	L _{PAB}	B _{PAB}	Period (h)	P.E	Amp	A.E.
32153	Laurenmcgraw	07/15-09/17	*17.7, 12.9	328	+3	24.8082	0.0007	0.54	0.03

Table I. Observing circumstances and results. The phase angle is given for the first and last date. Preceded by an asterisk indicates the phase angle reached a minimum during the period. L_{PAB} and B_{PAB} are the approximate phase angle bisector longitude and latitude at mid-date range (see Harris et al., 1984).

LIGHTCURVE PHOTOMETRY OPPORTUNITIES: 2024 OCTOBER – 2025 JANUARY

Brian D. Warner
Center for Solar System Studies (CS3)
446 Sycamore Ave.
Eaton, CO 80615 USA
brian@MinPlanObs.org

Alan W. Harris
Center for Solar System Studies (CS3)
La Cañada, CA 91011-3364 USA

Josef Ďurech
Astronomical Institute
Charles University
18000 Prague, CZECH REPUBLIC
durech@sirrah.troja.mff.cuni.cz

Lance A.M. Benner
Jet Propulsion Laboratory
Pasadena, CA 91109-8099 USA
lance.benner@jpl.nasa.gov

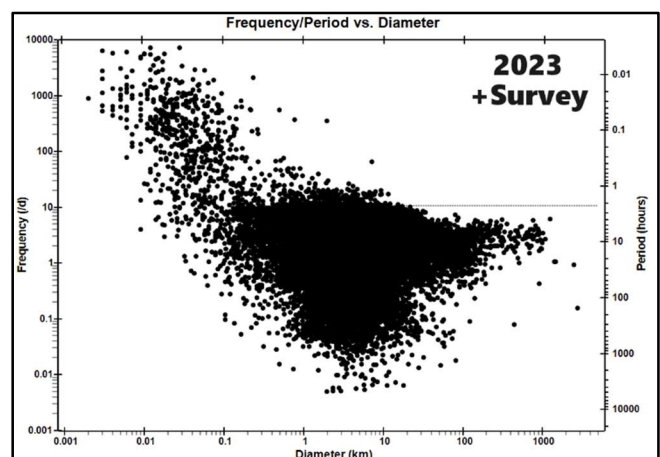
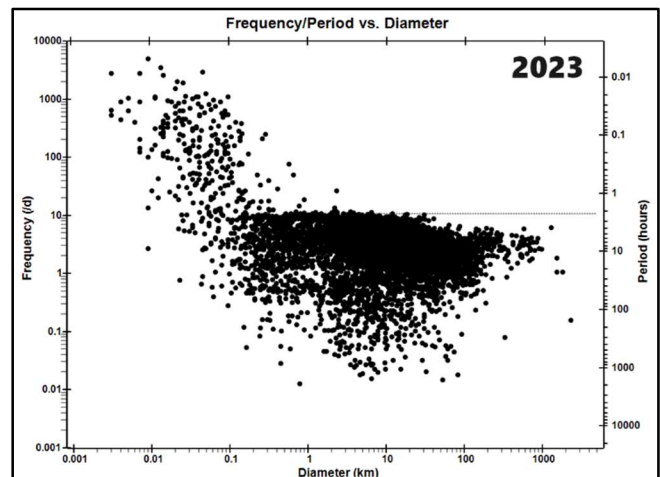
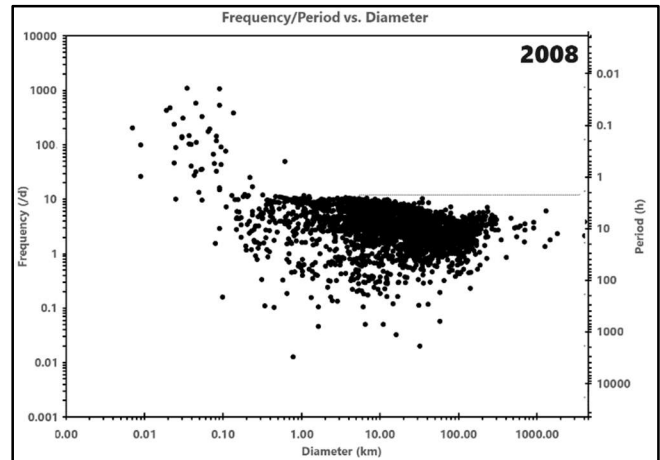
(Received: 2024 June 3 Revised: 2024 Aug 9)

We present lists of asteroid photometry opportunities for 2024 Oct – 2025 Jan, changing the long-standing format removing most boiler-plate text, resetting or adjusting the emphasis of each list, adding some new lists, and presenting those lists in tables with more information and larger, more easily-read text. Even when limiting the lists to objects that are generally $V \leq 15.5$ at brightest ($V \leq 17.0$ for NEAs), there remain dozens of candidates. The most important change is that the range of opportunities is now four months: the three months of the upcoming quarter year and the month immediately following. With each succeeding edition, that extra month will be repeated as part of next quarter year. This should allow better observation planning, especially for those working in wide-spread collaborations. With the massive input of survey photometry, even if mostly sparse data, the small telescope researcher's role is moving away from the medical equivalent of the family doctor and towards the well-versed specialist. With these changes, we hope to help make the transition easier, more fulfilling, and fruitful.

About 16 years ago, it would be possible to choose almost any asteroid brighter than $V \sim 16.0$ for observations and, if the lightcurve was not too complex, get a first-ever reported rotation period. The “2008” frequency-diameter plot shows summary table data from the asteroid lightcurve database (LCDB; Warner et al., 2009) that were thought to be statistically-valid ($U \geq 2-$). Almost every data point was the result of dense lightcurve observations, the kind typically done by small telescope researchers.

Move ahead to late 2023 and you see that “pick an asteroid, any asteroid” may no longer produce a fruitful contribution to rotation studies, especially after including the valid results based on wide-field surveys. Somewhere in that huge blob in the third plot is the asteroid you might choose at random. Unless you're just learning or want to refine your photometry and analysis techniques, the better contribution to new and improved science is to choose targets that are not as well studied as the vast majority. These include near-

Earth and long-period asteroids and those in want of additional dense data to determine or refine a rotation pole solution. There's always the somewhat rare chance that any one asteroid may be a previously unknown binary (or multiple) system or tumbling; those are more likely found by using the known or estimated size and/or rotation period to find the more likely candidates.



We present several lists of asteroids that are prime targets for photometry and/or astrometry during the period 2024 October through 2025 January. Frederick Pilcher, Coordinator for the Minor Planets Section of the Association of Lunar and Planetary Observers (ALPO), made the suggestion of extending the range of months from three to four so that observers can do better planning

when working long period or tumbling objects within or outside of a collaborative effort. Each subsequent issue in the *MPB* will repeat the overlap month as part of the upcoming quarter and extend one month into the next.

We refer the reader to earlier releases of this paper (e.g., Warner et al, 2023) for more detailed discussions about the requirements and considerations for the targets in the lists. For even more specific discussions, see also Warner et al. (2021a; 2021b).

An Improved Planning Tool

The ephemeris generator on the MinorPlanet.info web site allows creating custom lists for numbered objects reaching $V \leq 18.0$ during a given month from 2020 through 2035 by setting search parameters based on a number of parameters.

<https://www.minorplanet.info/php/callopplcdbquery.php>

The updated page added data for the minimum phase angle of any object included in the search: the date (0.001 d), the minimum phase angle (0.1°), and the declination. Searches can limit results to a phase angle range between $0-120^\circ$. Also new is limiting the results to a range of rotation periods and so, for example, one can look for only long, or especially short, period objects.

Important and Useful Web Sites

The dates and values given on the MinorPlanet.info site are very good estimates in most cases. NEAs are sometimes an important exception. Use the site for preliminary planning for objects and then confirm those plans using the Minor Planet Center or JPL Horizons web sites.

MPC: <http://www.minorplanetcenter.net/iau/MPEph/MPEph.html>

JPL: <https://ssd.jpl.nasa.gov/sb/orbits.html>

Those doing work for modeling should contact Josef Ďurech at the email address above. If looking to add lightcurves for objects with existing models, visit the Database of Asteroid Models from Inversion Techniques (DAMIT) web site.

<https://astro.troja.mff.cuni.cz/projects/damit/>

to see what, if any, information it has on a chosen target.

For near-Earth asteroids in particular, check the list found on the Goldstone planned targets schedule at

http://echo.jpl.nasa.gov/asteroids/goldstone_asteroid_schedule.html

and keep in touch with Lance Benner at the email above. The radar team often needs updated astrometry and photometry (rotation period) prior to observing. Keep in mind as well that the *MinorPlanet.info* site opposition database includes only numbered objects. Keep a close eye on the MPC NEA pages.

Once you've obtained and analyzed your data, it's important to publish your results. Papers appearing in the *Minor Planet Bulletin* are indexed in the Astrophysical Data System (ADS) and so can be referenced by others in subsequent papers. It's also important to make the data available at least on a personal website or upon request. We urge you to consider submitting your raw data to the ALCDEF database. This can be accessed for uploading and downloading data at

<http://www.alcdef.org>

The database contains about 10.69 million observations for 24,454 objects (as of 2024 May 27), making it one of the more useful sources for raw data of dense time-series asteroid photometry.

The Planning Lists

The lists, excluding the one for NEAs, are restricted to objects reaching $V \leq 15.5$ during the covered months. To include every object within a list that met this criterium alone resulted in far too many targets than the known community of asteroid photometrists could possibly handle, so only the "better" candidates are included. This is entirely subjective and the reader is encouraged to visit the MinorPlanet.info web site and use all the planning tools should our preferences don't necessarily match yours.

Don't presume that something rated $U \geq 3-$ doesn't need more work nor, at the other end, that something not rated at all or $1- < U < 2+$ or has a long period should be skipped in lieu of an "easier" project. The often-heard saying, "Past performance is not a guarantee of future results" should be part of your work ethic. Someone's "certain" result may not be so certain after all, especially if it's based on data that are minimal in quantity and/or quality.

Favorable Apparitions includes objects reaching one of the five brighter (favorable) apparitions from 1995 and 2050 and rated $U < 3-$ in the LCDB.

No Pole Solutions includes objects rated $U > 2+$ but do not have a pole indicated on the LCDB summary line. This list is the most likely needing further confirmation by checking the DAMIT web site, which grows in spurts large and small quite frequently and so the LCDB can lag considerably.

Poor Pole Solutions includes objects rated $U < 3-$ that have a pole solution on the summary line. In this case, the period is often based on using sparse survey data, with or without support of dense lightcurve data. An additional set of dense data may help elevate both the U rating and the quality of the pole solution.

Low Phase Angles includes objects, regardless of U rating or even having a period, that reach a solar phase angle $< 1^\circ$. You should refer to Warner et al. (2023) to review important information about low solar phase angle work.

Long Periods includes objects with $P \geq \sim 24$ hours. These are often overlooked because they are very difficult for a single-station campaign. However, they are ideal for collaborations, especially those with stations well-separated in longitude.

NEAs (aka Radar Target) is limited to *known* near-Earth asteroids that might be on the radar team's radar (pun intended). It is common for newly discovered objects to move into or out of the list. We recommend that you keep up with the latest discoveries by using the Minor Planet Center observing tools.

The List Data

If the list includes the "Fam" column, this is the orbital group (> 9000) using criteria from the LCDB or the collisional family (< 9000) based on Nesvorný et al. (2015) and Nesvorný (2015). To convert the number to a name, see the LCDB documentation on the LCDB web site or use the One Asteroid Lookup page on the site:

<https://www.minorplanet.info/php/lcdb.php>
<https://minorplanet.info/php/oneasteroidinfo.php>

Table Columns

Num	Asteroid number, if any.
Name	Name (or designation) assigned by the MPC.
Fam	Orbital group or collisional family.
BMD	Date of maximum brightness (to 0.1 d precision).
BMg	Approximate V magnitude at brightest.
BDC	Approximate declination at brightest.
PD	Date of minimum phase angle (to 0.001 d precision).
PMn	Phase angle at minimum (solar elongation > 90°).
PDC	Approximate declination at minimum phase angle.

P (h)	Synodic rotation period from summary line in the LCDB summary table. An * indicates a sidereal period.
U	LCDB solution quality (U) from 1 (probably wrong) to 3 (secure).
Notes	Comments about the object.

Some asteroids may appear in more than one list. The reader is referred to the latest LCDB release and, where and when necessary, the original reference source should be used. The Notes column is rarely used, for now, except for the NEAs list.

Favorable Apparitions (U < 3-)											
Num	Name	Fam	BMD	BMg	BDC	PD	PMn	PDC	P (h)	U	Notes
2794	Kulik	9104	10 03.5	15.1	+13	10 02.666	4.8	+13	8	2	
2565	Grogler	2004	10 04.0	15.4	+6	10 04.041	1.1	+6	2.15	2	
13836	1999 XF24	502	10 09.7	15.5	-9	10 10.049	7.6	+9	4.857	2	
1752	van Herk	402	10 10.2	14.7	+11	10 10.818	2.5	+11	*88.45	2	
363027	1998 ST27	9101	10 10.7	13.0	+1	10 09.321	17.9	+23	3	2	
5110	Belgirate	9104	10 10.9	15.4	+13	10 10.884	3.0	+13	8.26	2	
4339	Almater	9104	10 16.7	15.4	+14	10 16.968	2.6	+14	30.84	2	
5287	Heishu	9105	10 16.9	15.4	+0	10 16.282	4.3	+0	15.731	2	
18960	2000 QE130	9104	10 17.8	15.4	+11	10 17.957	0.6	+11	47.358	2	
6153	Hershey	9106	10 20.0	15.2	+6	10 19.977	2.6	+6	6.094	2-	
3843	OISCA	9107	10 20.5	15.4	+9	10 18.178	0.1	+9	19.089	2+	
5934	Mats	2004	10 21.4	15.3	+8	10 21.532	1.6	+8	5.184	2	
14379	1989 UM4	502	10 23.3	15.2	+15	10 23.303	1.6	+15	2.72	2	
450649	2006 UY64	9101	10 23.9	14.1	+19	10 24.242	10.5	+19	2.824	2+	
2046	Leningrad	602	10 31.4	14.9	+12	10 31.435	0.9	+12	5.296	2+	
3987	Wujek	9106	10 31.4	15.2	+13	11 01.011	0.6	+13	8.037	2+	
3509	Sanshui	9104	11 02.4	14.8	+15	11 03.778	0.3	+15	13.68	2	
8823	1987 WS3	531	11 03.3	14.7	+25	11 03.151	5.7	+25	110.88	2	
7291	Hyakutake	9106	11 03.7	15.2	+6	11 04.206	3.9	+6	198.743	2	
43028	1999 VE23	9104	11 05.1	15.5	+9	11 05.296	3.4	+9	3.94	2	
1808	Bellerophon	9106	11 05.5	14.4	+17	11 05.127	0.8	+17	3.82	2	
3220	Murayama	9104	11 08.0	14.5	+21	11 08.072	2.6	+21	4.86	2	
4566	Chaokuangpiu	633	11 09.3	15.2	+25	11 10.085	3.5	+25	*16.382	2	
69315	1992 UR2	701	11 09.5	15.1	+18	11 09.945	0.7	+18	105.757	2	
7067	Kiyose	606	11 14.4	15.3	+18	11 15.900	0.2	+18	67.787	2	
7870	1987 UP2	9103	11 15.4	14.2	+20	11 15.405	0.7	+20	12	1	
3771	Alexejtolstoj	2009	11 27.4	15.4	+22	11 28.124	0.3	+22	11.094	1	
2266	Tchaikovsky	9106	11 28.0	14.6	+15	11 28.031	2.1	+15	37.7	2	
2803	Vilho	602	11 30.4	15.1	+23	12 01.342	0.6	+23	12.5	2-	
5193	Tanakawataru	602	11 30.5	15.5	+20	11 30.099	0.6	+20	5.336	2	
163899	2003 SD220	9101	12 01.0	15.1	+43	11 28.729	78.0	+46	285	2+	
15243	1989 TU1	9105	12 01.9	15.1	+24	12 02.008	1.3	+24	*215.05	2	
3935	Toatenmongakkai	9104	12 02.9	14.1	+35	12 04.218	6.4	+35	106.3	2	
2208	Pushkin	9106	12 03.6	15.3	+21	12 04.071	0.2	+21	8.405	2	
6821	Ranevskaya	9104	12 11.5	15.2	+22	12 10.312	0.3	+22	2.81	2+	
11441	Anadiego	9104	12 13.9	15.1	+5	12 15.818	9.2	+5	3.179	2	
13521	1991 BK	2006	12 16.6	15.4	+27	12 16.352	1.8	+27	*126.14	2	
32385	2000 QU191	9106	12 18.8	15.3	+21	12 18.637	1.3	+21	5.317	2	
3134	Kostinsky	001	12 19.4	14.8	+21	12 20.489	0.7	+21	14.7	2	
691	Lehigh	9106	12 23.4	12.8	+25	12 24.058	0.6	+25	12.891	2+	
4207	Chernova	606	12 23.5	15.5	+21	12 22.874	0.8	+21	10.288	2	
5202	Charleseliot	9104	12 28.1	15.3	+17	12 28.579	3.0	+17	183	2	
18513	1996 TS5	701	01 12.6	15.5	+27	01 12.226	2.8	+27	9.749	2	
7186	Tomiooka	9104	01 14.5	15.2	+22	01 14.017	0.2	+22	7.309	2	
4176	Sudek	602	01 17.5	15.4	+21	01 18.356	0.2	+21	8.164	2	
4683	Veratar	602	01 20.4	15.5	+19	01 21.076	0.5	+19	29.391	2	
2843	Yeti	9104	01 25.4	15.2	+11	01 25.063	3.9	+11	156.718	2	

Table I. A partial list of numbered asteroids reaching a favorable apparition and with an LCDB rating U < 3-. Objects in bold text are near-Earth asteroids.

Spin Axis and Modeling (Favorable Apparition, $U > 2+$, No LCDB pole, not in DAMIT)

Num	Name	Fam	BMD	BMg	BDC	PD	PMn	PDC	P (h)	U	Notes
1229	Tilia	602	10 01.4	14.7	+4	10 02.328	0.2	+4	7.035	3	
1416	Renauxa	606	10 03.2	14.4	+8	10 03.118	1.7	+8	8.7	3	
5402	Kejosmith	9104	10 07.6	15.3	+28	10 08.368	14.7	+28	2.695	3	
1242	Zambesia	9106	10 11.6	13.2	+16	10 11.295	3.9	+16	17.315	3	
547	Praxedis	541	10 12.4	12.1	+4	10 12.426	1.8	+4	9.105	3	
2262	Mitidika	9104	10 18.1	14.3	+23	10 20.254	6.4	+23	28.53	3	
66146	1998 TU3	9101	10 30.3	11.6	-46	10 16.562	46.3	-17	2.375	3	
8116	Jeanperrin	402	11 03.4	15.4	+14	11 03.783	0.8	+14	3.617	3	
24029	1999 RT198	9103	11 05.2	15.0	-3	10 31.950	11.2	-1	5.491	3	
2179	Platzeck	606	11 10.0	15.0	+26	11 09.947	3.3	+26	5.995	3	
5175	Ables	9102	11 17.5	15.0	+19	11 16.891	0.1	+19	2.686	3	
465	Alekto	9106	11 18.7	15.1	+25	11 18.676	1.5	+25	10.936	3	
3106	Morabito	604	11 20.7	14.9	-2	11 21.436	9.1	-2	6.26	3	
3951	Zichichi	9104	11 27.1	14.7	+26	11 27.244	2.4	+26	3.394	3	
2195	Tengstrom	9104	11 28.1	14.5	+16	11 28.343	2.5	+16	2.821	3	
3672	Stevedberg	402	11 29.0	15.1	+32	11 29.635	5.5	+32	2.778	3-	
2647	Sova	402	12 03.9	14.5	+27	12 04.130	2.5	+27	9.366	3	
16959	1998 QE17	9105	12 09.1	15.2	+45	12 12.945	11.1	+44	3.227	3	
5598	Carlmurray	9104	12 27.5	14.5	+25	12 27.580	0.7	+25	2.923	3	
1302	Werra	602	01 02.4	14.1	+24	01 03.961	0.4	+24	8.183	3-	
3335	Quanzhou	502	01 13.1	15.0	+15	01 13.284	2.7	+15	6.156	3	
3048	Guangzhou	2004	01 14.0	15.2	+18	01 14.054	1.8	+18	3.811	3-	
862	Franzia	9106	01 17.4	13.2	+21	01 18.685	0.3	+21	7.523	3	
4440	Tchantches	9102	01 20.3	15.3	+4	01 19.827	8.6	+4	2.788	3	

Table II. A partial list of numbered asteroids reaching a favorable apparition that have high-quality periods solutions but do not have a pole solution in the LCDB or DAMIT databases. Objects in bold text are near-Earth asteroids.

Spin Axis and Modeling (Any Apparition, $U < 3-$, Pole in LCDB/DAMIT)

Num	Name	Fam	BMD	BMg	BDC	PD	PMn	PDC	P (h)	U	Notes
3093	Bergholz	502	10 02.9	14.5	+26	10 05.825	10.3	+26	25.245	2	
1128	Astrid	515	10 07.4	14.6	+5	10 09.040	0.4	+5	10.228	2+	
12193	1979 EL	502	10 09.2	15.5	-18	10 07.234	10.8	-18	7.577	2+	
13836	1999 XF24*	502	10 09.7	15.5	-9	10 10.049	7.6	-9	4.857	2	
1594	Danjon	9104	10 14.2	14.6	-2	10 16.352	5.4	-2	121.6	2	
2086	Newell	401	10 16.3	15.1	-1	10 15.825	4.9	-1	78.2	2	
3860	Plovdiv	9106	10 16.4	15.1	+22	10 17.775	5.3	+22	6.114	2+	
5287	Heishu*	9105	10 16.9	15.4	+0	10 16.282	4.3	+0	15.731	2	
630	Euphemia	502	10 18.2	15.3	-11	10 16.877	7.6	-11	350	2	
3167	Babcock	9104	10 19.6	14.7	+14	10 19.854	1.6	+14	15.398	2+	
856	Backlunda	9104	10 23.0	14.9	-9	10 22.856	8.0	-9	12.08	2	
4614	Masamura	402	10 27.7	15.4	+8	10 28.630	2.7	+8	199.774	2	
3987	Wujek*	9106	10 31.4	15.2	+13	11 01.011	0.6	+13	8.037	2+	
1479	Inkeri	9105	11 04.4	14.6	+20	11 03.989	2.2	+20	660	2+	
1064	Aethusa	9104	11 05.0	14.3	+28	11 06.774	5.0	+28	8.621	2	
946	Poesia	602	11 23.5	14.1	+20	11 21.891	0.2	+20	108.5	2+	
2832	Lada	9104	11 30.3	15.4	+15	11 29.989	2.8	+15	8.357	2+	
3935	Toatenmongakkai*	9104	12 02.9	14.1	+35	12 04.218	6.4	+35	106.3	2	
1337	Gerarda	9106	12 08.1	15.5	-4	12 10.374	9.2	-4	12.52	2	
4558	Janesick	9103	12 08.8	14.2	+21	12 09.422	1.3	+21	173.4	2	
1237	Genevieve	9105	12 12.6	14.4	+29	12 12.936	2.5	+29	16.37	2	
3134	Kostinsky*	001	12 19.4	14.8	+21	12 20.489	0.7	+21	14.7	2	
5202	Charleseliot*	9104	12 28.1	15.3	+17	12 28.579	3.0	+17	183	2	
1502	Arenda	9106	12 28.7	14.7	+17	12 28.670	2.5	+17	45.8	2	
2248	Kanda	602	01 01.5	15.3	+25	12 31.751	0.7	+25	16.308	2	
2546	Libitina	9105	01 07.4	15.1	+31	01 06.432	3.3	+31	132.71	2+	
3233	Krisbarons	9104	01 11.6	15.3	+27	01 12.007	2.6	+27	888	2	
4176	Sudek*	602	01 17.5	15.4	+21	01 18.356	0.2	+21	8.164	2	
1332	Marconia	636	01 18.0	15.0	+24	01 18.216	1.1	+24	19.16	2	
2165	Young	602	01 24.4	15.3	+20	01 25.359	0.5	+20	6.389	2	
2843	Yeti*	9104	01 25.4	15.2	+11	01 25.063	3.9	+11	156.718	2	
3811	Karma	534	01 28.8	15.2	+26	01 29.443	3.3	+26	13.23	2+	
1684	Iguassu	602	01 30.5	15.5	+20	01 29.406	0.6	+20	6.416	2	

Table III. A partial list of numbered asteroids reaching brightest magnitude that have a reported pole position but the LCDB rating is $U < 3-$. An * indicates a favorable apparition.

Low Phase Angle ($V \leq 15.0$, phase angle $\alpha \leq 1.0^\circ$)

Num	Name	Fam	BMD	BMg	BDC	PD	PMn	PDC	P (h)	U	Notes
1229	Tilia	602	10 01.4	14.7	+4	10 02.328	0.2	+04	7.035	3	
1691	Oort	602	10 03.5	14.2	+3	10 02.648	0.2	+03	10.2705	3	
875	Nymphe	506	10 05.4	13.6	+7	10 06.345	0.6	+06	12.618	3-	
3481	Xianglupeak	402	10 08.5	15.0	+4	10 08.166	0.8	+05	5.3193	3	
1814	Bach	9104	10 14.5	14.7	+8	10 13.576	0.2	+08	7.2408	3	
2239	Paracelsus	9106	10 14.8	14.6	+9	10 15.748	0.3	+09	6.101	3-	
19	Fortuna	9104	10 18.1	9.2	+10	10 17.527	0.3	+10	7.4432	3	
10064	Hirosetamotsu	9106	10 28.4	14.9	+15	10 28.955	0.6	+15	8.052	3	
2046	Leningrad	602	10 31.4	14.9	+12	10 31.435	0.9	+12	5.296	2+	
3509	Sanshui	9104	11 02.4	14.8	+15	11 03.778	0.3	+15	13.68	2	
1808	Bellerophon	9106	11 05.5	14.4	+17	11 05.127	0.8	+17	3.82	2	
959	Arne	9106	11 09.4	13.6	+16	11 10.029	0.6	+16	123.7	3-	
979	Ilsewa	9106	11 09.4	13.6	+18	11 10.647	0.2	+18	42.61	3	
3722	Urata	9104	11 13.4	14.0	+19	11 14.288	0.2	+18	5.567	3	
7870	1987 UP2	9103	11 15.4	14.2	+20	11 15.405	0.7	+20	12	1	
22412	1995 UQ4	9104	11 15.4	14.8	+19	11 15.922	0.3	+19	4.487	3-	
5175	Ables	9102	11 17.5	15.0	+19	11 16.891	0.1	+19	2.6862	3	
1223	Neckar	605	11 30.4	13.9	+24	11 30.846	0.7	+24	7.81	3	
534	Nassovia	605	11 30.8	13.1	+20	12 01.220	0.8	+20	9.382	3	
977	Philippa	9106	12 09.8	14.0	+23	12 09.097	0.2	+23	15.405	3	
3134	Kostinsky	001	12 19.4	14.8	+21	12 20.489	0.7	+21	14.7	2	
691	Lehigh	9106	12 23.4	12.8	+25	12 24.058	0.6	+25	12.891	2+	
5598	Carlmurray	9104	12 27.5	14.5	+25	12 27.580	0.7	+25	2.9226	3	
1411	Brauna	9106	12 28.4	14.9	+25	12 29.867	0.4	+24	4.9	3	
1302	Werra	602	01 02.4	14.1	+24	01 03.961	0.4	+24	8.183	3-	
1254	Erfordia	9106	01 05.0	14.8	+24	01 03.864	0.3	+24	12.287	3	
1067	Lunaria	633	01 10.4	13.9	+21	01 11.688	0.3	+21	6.057	3	
556	Phyllis	401	01 13.4	11.7	+20	01 13.617	0.6	+20	4.293	3	
364	Isara	9104	01 15.0	11.5	+23	01 15.314	1.0	+23	9.156	3	
862	Franzia	9106	01 17.4	13.2	+21	01 18.685	0.3	+21	7.523	3	
2380	Heilongjiang	9104	01 28.4	14.9	+19	01 28.604	0.5	+19	11.237	3	

Table IV. A partial list of numbered asteroids reaching a minimum phase angle $\alpha \leq 1.0^\circ$.**Long Period (Favorable Apparition, $P \geq 24$ h)**

Num	Name	Fam	BMD	BMg	BDC	PD	PMn	PDC	P (h)	U	Notes
4339	Almamater	9104	10 16.7	15.4	+14	10 16.968	2.6	+14	30.84	2	
18960	2000 QE130	9104	10 17.8	15.4	+11	10 17.957	0.6	+11	47.36	2	
8823	1987 WS3	531	11 03.3	14.7	+25	11 03.151	5.7	+25	110.88	2	
7291	Hyakutake	9106	11 03.7	15.2	+6	11 04.206	4.0	+6	198.74	2	
69315	1992 UR2	701	11 09.5	15.1	+18	11 09.945	0.7	+18	105.76	2	
7067	Kiyose	606	11 14.4	15.3	+18	11 15.900	0.2	+18	67.78	2	
2266	Tchaikovsky	9106	11 28.0	14.6	+15	11 28.031	2.1	+15	37.7	2	
163899	2003 SD220	9101	12 01.0	15.1	+43	11 28.729	78.0	+46	285.	2+	
15243	1989 TU1	9105	12 01.9	15.1	+24	12 02.008	1.3	+24	215.05	2	
3935	Toatenmongakkai	9104	12 02.9	14.1	+35	12 04.218	6.4	+35	106.3	2	
13521	1991 BK	9105	12 16.6	15.4	+27	12 16.352	1.8	+27	126.14	2	
5202	Charleseliot	9104	12 28.1	15.3	+17	12 28.579	3.0	+17	183.	2	
4683	Veratar	602	01 20.4	15.5	+19	01 21.076	0.5	+19	29.39	2	
2843	Yeti	9104	01 25.4	15.2	+11	01 25.063	3.9	+11	156.72	2	

Table V. A partial list of numbered asteroids reaching a favorable apparition and with a reported period $P \geq 24$ hours.

NEAs (aka Radar) Reaching Brightest for Year (Any Apparition, $V \leq 17.0$, $\alpha \leq 90^\circ$)												
Num	Name	Fam	BMD	BMg	BDC	PD	PMn	PDC	P (h)	U	Notes	
154807	2004 PP97*	9101	10 08.5	16.7	-5	09 30.133	11.0	-11	161.	2		
363027	1998 ST27*	9101	10 10.7	13.0	+1	10 09.321	17.9	+23	3.	2	PHA	
	2014 FP47*	9101	10 11.1	17.0	-35	02 17.341	10.0	+26	0.44	3-		
65679	1989 UQ	9101	10 13.5	16.2	+4	10 13.482	3.2	+5	7.746	3		
	1036 Ganymed*	9101	10 17.8	9.1	+27	01 01.	14.0	-16	10.297	3		
87684	2000 SY2	9101	10 23.6	16.6	-29	10 21.948	29.8	-28	2.5712	2		
450649	2006 UY64*	9101	10 23.9	14.1	+19	10 24.242	10.5	+19	2.824	2+		
219071	1997 US9*	9101	10 25.9	15.5	+12	10 25.970	0.6	+12	3.319	3-		
503941	2003 UV11*	9101	10 28.1	16.6	-1	10 19.454	2.8	+7	18.25	3-		
154589	2003 MX2*	9101	10 29.2	15.6	+5	11 05.576	5.9	+8	1.611	1+		
	66146 1998 TU3*	9101	10 30.3	11.6	-46	10 16.562	46.3	-17	2.375	3		
	88710 2001 SL9*	9101	10 30.9	16.3	-16	10 23.858	28.0	-4	2.4004	3		
363305	2002 NV16*	9101	11 02.1	16.9	-52	06 01.301	12.5	-7	0.9067	2	NHATS	
	88263 2001 KQ1*	9101	11 16.2	16.3	+27	11 06.458	17.2	+37	13.170	3		
	36183 1999 TX16*	9101	11 16.7	12.7	+16	11 17.047	3.7	+16	5.613	3		
	2201 Oljato	9101	11 22.0	16.4	+9	01 01.	16.3	-4	>26.	2-		
98943	2001 CC21	9101	11 24.5	16.7	+16	11 24.826	4.1	+16	5.0159	3		
163899	2003 SD220*	9101	12 01.0	15.1	+43	11 28.729	78.0	+46	285.	2+	NHATS	
	3200 Phaethon	9101	12 01.4	16.3	+37	11 25.090	8.9	+38	3.604	3		
	6611 1993 VW*	9101	12 05.7	16.5	-9	01 01.	14.8	-8	2.5568	3		
143678	2003 SA224*	9101	12 14.3	16.6	+63	11 13.295	24.8	+54	35.	2		
	1866 Sisyphus	9101	12 18.6	14.1	-26	05 11.646	10.8	+4	2.400	3	PHA	
377097	2002 WQ4*	9101	12 21.9	16.4	+8	11 29.999	25.6	+27	36.	1+		
	1980 Tezcatlipoca	9101	12 23.8	15.8	-18	01 01.	15.4	-27	7.2461	3		
99935	2002 AV4	9101	12 26.4	16.9	+22	03 23.385	2.2	+4	5.532	1		
175706	1996 FG3	9101	12 28.2	16.0	+27	02 01.846	1.0	+16	3.5942	3	PHA BA NHATS 137805	
1999 YK5		9101	01 19.9	16.7	+73	01 10.837	36.9	+70	3.930	3-		
103067	1999 XA143	9101	01 20.6	15.9	+31	01 17.633	5.5	+26	9.8490	3		
	6239 Minos*	9101	01 22.7	15.9	+48	11 01.189	5.0	+22	3.5558	3		
265196	2004 BW58*	9101	01 28.4	15.3	-4	02 20.648	27.6	+39	6.479	3	PHA	
	1627 Ivar	9101	01 29.5	15.9	+17	01 28.900	0.4	+17	4.795	3		

Table VI. A list of near-Earth asteroids known as of 2024 May 28. Green bar lines are on the Goldstone list of planned targets. An * indicates a favorable apparition. A date of "12 31." indicates that the object is moving towards but has not yet reach a minimum in 2024. A date of "01 01." indicates that the object is moving away from its most immediate minimum for all of 2025. PHA: Potentially Hazardous Asteroid. NHATS: Near-Earth Object Human Space Flight Accessible Targets Study. BA: Binary asteroid.

References

Warner, B.D.; Harris, A.W.; Pravec, P. (2009). "The Asteroid Lightcurve Database." *Icarus* **202**, 134-146. Updated 2023 Oct. <http://www.minorplanet.info/lightcurvedatabase.html>

Warner, B.D.; Harris, A.W.; Durech, J.; Benner, L.A.M. (2021a). "Lightcurve Photometry Opportunities: 2021 January-March." *Minor Planet Bull.* **48**, 89-97.

Warner, B.D.; Harris, A.W.; Durech, J.; Benner, L.A.M. (2021b). "Lightcurve Photometry Opportunities: 2021 October-December." *Minor Planet Bull.* **48**, 406-410.

Warner, B.D.; Harris, A.W.; Durech, J.; Benner, L.A.M. (2023). "Lightcurve Photometry Opportunities: 2024 April-June." *Minor Planet Bull.* **48**, 406-410.

INDEX TO VOLUME 51

- Benishek, V. "Lightcurves and Synodic Rotation Periods for 30 Asteroids from Sopot Astronomical Observatory: 2023 April – December" 151-158.
- Benishek, V. "Photometry of 18 Asteroids from Sopot Astronomical Observatory: 2023 December – 2024 April" 239-243.
- Bentz, M.C.; Alahakone, R.; Albin, E.; Brown, R.; Featherstone, C.; Hung, D.; Kane, C.; LaFountain, M.; Lange, R.; Miles, L.; Shah, Y.; Sharifi, K.; Sulaiman, A.Y.; Tipton, B.; Whyte, C. "V-Band Monitoring of 1083 Salvia" 224-225.
- Binzel, R.P. "Call for Observations of the Patroclus and Menoetius Mutual Events: Support for the NASA Lucy Mission to the Trojan Asteroids" 212.
- Birtwhistle, P. "Lightcurve Analysis for Six Near-Earth Asteroids Observed in 2009, 2017 and 2023" 66-72.
- Birtwhistle, P. "Lightcurve Analysis for Nine Near-Earth Asteroids Observed Between 2009 – 2023" 184-191.
- Birtwhistle, P. "Lightcurve Analysis for 17 Near-Earth Asteroids Observed Between 2009 and 2024" 277-289.
- Birtwhistle, P. "Lightcurve Analysis for 6 Near-Earth Asteroids Observed Between 2010 and 2024" 363-368.
- Bramardi, N.; Mascherpa, S.; Raviola, A.; Bonamico, R. "Determining the Rotation Period of Main-Belt Asteroid 19633 Rusjan" 230.
- Brincat, S.M.; Bucek, M.; Galdies, C.; Mifsud, M.; Grech, W. "Lightcurves and Rotation Period Determination of Seven Main-Belt Asteroids Observed from Malta and Slovakia" 12-15.
- Brincat, S.M.; Bucek, M.; Galdies, C.; Mifsud, M.; Grech, W.; Eenmäe, T. "Photometric Observations and Analysis of Eight Asteroids from Malta, Slovakia and Estonia" 161-166.
- Brincat, S.M.; Bucek, M.; Galdies, C.; Mifsud, M.; Rivard, N.; Grech, W.; Zammit, V.; Richmond, M.; Demers, D.; Harrison, M.; Montes, S.; Segio, J.; Stanek, V. "Photometric Investigation and Rotational Characterization of Seven Main-Belt Asteroids" 333-337.
- Clark, M. "Asteroid Photometry from the Dunwurkin Observatory" 31-32.
- Colazo, M.; Fornari, C.; Suárez, N.; Morales, M.; Garcí, A.; Scotta, D.; Melia, R.; Speranza, T.; Stechina, A.; Monteleone, B.; Cianci, G.; Wilberge, A.; Suligoy, M.; Ortiz, A.; Santos, F.; Colazo, C. "Asteroid Photometry and Lightcurves for Twelve Asteroids - September 2023" 39-41.
- Colazo, M.; Monteleone, B.; Santos, F.; García, A.; Ciancia, G.; Morales, M.; Melia, R.; Speranza, T.; Ortiz, A.; Scotta, D.; Suárez, N.; Aldinucci, P.; Montecchiari, N.; Wilberger, A.; Anzola, M.; Colazo, C. "Asteroid Photometry of Eight Asteroids" 143-146.
- Colazo, M.; Santos, F.; Monteleone, B.; Aldinucci, P.; Ciancia, G.; Scotta, D.; Suárez, N.; García, A.; Melia, R.; Morales, M.; Montecchiari, N.; Speranza, T.; Colazo, C. "Asteroid Photometry and Lightcurves of Nine Asteroids" 272-274.
- Colazo, M.; Ciancia, G.; Montecchiari, N.; Melia, R.; Aldinucci, P.; García, A.; Monteleone, B.; Suárez, N.; Morales, M.; Moreschi, A.; Santos, F.; Anzola, M.; Amelotti, V.; Wilberg, A.; Stechina, A.; Colazo, C. "Asteroid Lightcurves for Six Asteroids" 316-318.
- Das, N.; Wilkin, F.P.; Zora, D.-V. "Lightcurves for L5 Trojan Asteroid (884) Priamus and Koronis Family Member (1443) Ruppina" 221-222.
- Dose, E.V. "Lightcurves of Eighteen Asteroids" 42-49.
- Dose, E.V. "Lightcurves of Eighteen Asteroids" 117-125.
- Dose, E.V. "Lightcurves of Ten Asteroids" 251-256.
- Dose, E.V. "Lightcurves of Eleven Asteroids" 324-330.
- Faure, G.; Jongen, Y. "Lightcurve and Rotation Period of 32153 Laurenmcgraw" 378.
- Faure, G.; Jongen, Y.; Oey, J. "Lightcurve and Rotation Period of the Slow-Rotator 12867 Joeloic" 373-377.
- Fekete, P.; Porter, J.J.; Willis, J.P. "Space-Rocky Road to Observatory Automation and Lightcures" 1-3.
- Fornas, G.; Huet, F.; Barberá, R.; Fornas, Á.; Mas, V. "Lightcurve Analysis for Twelve Main-Belt and One PHA Asteroids" 33-38.
- Fornas, G.; Huet, F.; Arce, E.; Barberá, R.; Fornas, Á.; Gornas Jr. G.; Mas, V. "Lightcurve Analysis for Eight Main-Belt and Three Near-Earth Asteroids" 169-174.
- Fornas, G.; Fornas, Á.; Huet, F.; Arce, E.; Barberá, R.; Mas, V. "Lightcurve Analysis for Three Main-Belt, Three Near-Earth, and Two Mars-Crosser Asteroids" 244-247.
- Fornas, G.; Huet, F.; Fornas, Á.; Fornas Jr., G. "Lightcurve Analysis for Five Main Belt Asteroids" 319-324.
- Foylan, M. "Lightcurve and Rotation Period for Minor Planets 2090 Mizuho (1978 EA) and 4164 Shilov (1969 UR)" 64-65.
- Franco, L.; Licchelli, D. "Lightcurves Analysis of 1677 Tycho Brahe, 1802 Zhang Heng, and 18151 Licchelli" 146-147.
- Franco, L.; Scarfí, G.; Baj, G.; Iozzi, M.; Lombardo, M.; Marchini, A.; Papini, R.; Falco, C.; Nastasi, A.; Fini, P.; Betti, G.; Arangio, J.; Bacci, P.; Maestripieri, M.; Montigiani, N.; Mannucci, M.; Coffano, A.; Marinello, W.; Aceti, P.; Banfi, M.; Galli, G.; Ruocco, N.; Tinelli, L. "Collaborative Asteroid Photometry for UAI: 2023 July - September" 56-61.
- Franco, L.; Pilcher, F.; Oey, J.; Marchini, A.; Papini, R.; Scarfí, G.; Iozzi, M.; Ruocco, N.; Bacci, P.; Maestripieri, M.; Montigiani, N.; Mannucci, M. "Spin-Shape Model for 357 Ninina" 100-102.
- Franco, L.; Marchini, A.; Iozzi, M.; Baj, G.; Tinelli, L.; Scarfí, G.; Carbognani, A.; Galli, G.; Aceti, P.; Banfi, M.; Fini, P.; Betti, G.; Ruocco, N.; Lombardo, M. "Collaborative Asteroid Photometry from UAI: 2023 October-December" 148-150.
- Franco, L.; Pravec, P.; Benishek, V.; Durkee, R.; Buzzi, L.; Calabrò, M.; Galli, G.; Bacci, P.; Maestripieri, M.; Montigiani, N.; Mannucci, M.; Marchini, A.; Papini, R.; Ruocco, N.; Tombelli, M.; Iozzi, M.; Lombardo, M.; Scarfí, G.; Baj, G. "Binary System 6086 Vrchlicky" 232-233.

- Franco, L.; Marchini, A.; Papini, R.; Ruocco, N.; Fini, P.; Betti, G.; Bacci, P.; Maestripieri, M.; Scarfi, G.; Baj, G.; Montigiani, N.; Mannucci, M.; Casalnuovo, G.B.; Iozzi, M.; Galli, M. "Collaborative Asteroid Photometry from UAI: January-March" 289-293.
- Franco, L.; Scarfi, G.; Marchini, A.; Iozzi, M. "Collaborative Asteroid Photometry from UAI: April-June" 309-311.
- Franco, L.; Carbognani, A.; Scarfi, G.; Montigiani, N.; Mannucci, M.; Iozzi, M.; Baj, G.; Coffano, A.; Marinello, W. "Lightcurve Analysis of (415029) 2011 UL21" 312-313.
- Galdies, C.; Brincat, S.M.; Buček, M.; Mifsud, M. "Photometric Observations of Main-Belt Asteroids 784 Pickeringia, 1465 Autonoma, 1477 Bonsdorffia, 3057 Malaren, 5708 Melancholia, and 8548 Sumizihara" 16-19.
- Galdies, C.; Brincat, S.M.; Bucek, M.; Grech, W. "Photometric Observations and Analysis of Eight Asteroids" 268-271.
- González Farfán, R.; García de la Cuesta, F.; González Carballo, J.-L.; Fernández, J.M.; Reina, E.; Podlowska-Gaca, E.; de Elias Cantalapiedra, J. "Lightcurve Analysis of 5780 Lafontaine" 10-11.
- González Farfán, R.; Benarque Fonseca, F.J.; Fernández Mañanes, E.; Graciá Ribes, N. "Lightcurve Analysis of 1485 Isa" 99.
- González Farfán, R.; García de la Cuesta, F.; Reina Lorenz, E.; Fernández Mañanes, E.; Fernández Andújar, J.M.; Ruiz Fernández, J.; Delgado Casal, J.; de Elías Cantalapiedra, J.; de la Fuente, P.; Collada, J. "Photometry and Lightcurve Analysis of 26 Asteroids" 133-138.
- González Farfán, R.; García de la Cuesta, F.; Limón Martínez, F.; Reina Lorenz, E.; Botana Albá, C.; Delgado Casal, J.; De Elías Cantalapiedra, J.; Martín Saura, A.; Fernández Mañanes, E.; Ruiz Fernández, J.; Fernández Andújar, J.M.; Naves Nogue, R.; Santos Álamo, F.M. "Aanalysis and Lightcurves of 22 Asteroids" 259-263.
- Güler, H.A. "An Investigation of Close Passes of Distant Minor Planets Throughout the Solar System" 369-370.
- Hawley, W.; Miles, R.; Wiggins, P.; McCormick J.; Dawson, M.; Pilcher, F. "Lightcurve and Rotation Period Analysis of 4226 Damiaan and (25242) 1998 UH15" 54-55.
- Hawley, W.; Miles, R.; Wiggins, P.; McCormick, J.; Watkins, A.; Armstrong, J.D. Kardasis, E.; Pilcher, F.; Arnold, S. "Lightcurve and Rotation Period Analysis of 1887 Virton and 4099 Wiggins" 166-168.
- Hawley, W.; Miles, R.; Wiggins, P.; McCormick, J.; Watkins, A.; Armstrong, J.D.; Kardasis, E.; Pilcher, F.; Arnold, S.; Haymes, T.; Privett, G.J.; Moss, S. "Lightcurve and Rotational Period Analysis of 1429 Pemba and 14835 Holdridge" 227-229.
- Hawley, W.; Scott, B.; Wiggins, P.; McCormick, J.; Armstrong, J.D.; Kardasis, E.; Pilcher, F.; Haymes, T.; Privett, G.J.; Leyland, P.C.; Genebriera, J. "Lightcurve and Rotation Period Analysis of 1532 Inari" 306-307.
- Hayes-Gehrke, M.; Placido-Reyes, J.; Villano-Herrera, D.; Lombardo, A.; Coil, K.; Kitching, J.; Bauer, B.; van Doorn, J.; Bravo-Palacio, D.; Jordanel, C.; Mazzone, A.; Jiang, E.; Bonilla, E. "Lightcurve and Rotation Period for 1417 Walinskia" 300-301.
- Hayes-Gehrke, M.; Wallace, B.; Luo, D.; Parrott, C.; Phillips, Z.; Bellevue, J.; Rzomp, A.; Henrikson, R.; Ator, J.; Herrera, J.; Kumar, A.; Needham, L. "Lightcurve Analysis and Period Determination for Asteroid 16405 Testudo" 311-312.
- Hayes-Gehrke, M.; Gray, R.; Linico, S.; Ng, P.; Thota, H.; Akintoye, O.; Brown, M.; Egan, C.; Xie, A.; Keenan, J.; Marinez, R.; Tang, E.; Yang, D. "Lightcurve Photometry and Analysis of 5167 Joeharms" 314.
- Hayes-Gehrke, M.; Brownfield, J.; Cleary, S.; El Kochta, R.; Gardner, D.; Kumar, V.; Mai, V.; Matheson, J.; Mitchell, T.; Roviera, H.; Smith, D.; Tung, J.; Welinder, L.M. "Lightcurve Analysis of 7851 Azumino and Estimated Rotation Period" 315.
- Huet, F.; Fornas, G., Fornas, A. "Lightcurve Analysis for Eight Main-Belt Asteroids and One Mars Crosser" 106-112.
- Hutton, L.J.; Fieber-Beyer, S. "Photometry of PHA (349507) 2008 QY" 231.
- Kalisek, K.; Montgomery, K. "Determining the Lightcurves and Rotation Periods of Four Main-Belt Asteroids" 91-92.
- Kikwaya Eluo, J.-B.; Hergenrother, C.W. "Lightcurves and Colors of Seven Small Near-Earth Asteroids: 2023 LQ1, 2023 LT1, 2023 MC, 2023 VQ5, 2023 VE6, 2023 VF6, 2023 VV7" 192-196.
- Lang, K. "Lightcurves of 3 Small Main-Belt Asteroids from February to April 2023" 237-238.
- Marchini, A.; Papini, R. "Lightcurve Analysis of Asteroids 6108 Glebov, 6991 Chichibu and 10039 Keet Seel" 62-63.
- Marchini, A.; Papini, R. "Photometric Observations of Asteroids 1631 Kopff, 2244 Tesla, 2967 Vladisvyat and 9628 Sendaiotsuna" 158-160.
- Marchini, A.; Papini, R.; Pierguidi, L. "Photometric Observations of Asteroids 347 Pariana, 632 Pyrrha, 3067 Akhmatova, and 8602 Oedicnemus" 256-258.
- Marchini, A.; Papini, R.; Savino, J.P.; Schintu, S.; Scali, S.; Atiyha, A.; Hanania, M. "Photometric Observations of Asteroid 1602 Indiana" 308-309.
- Mathias, B.; Samuele, R.; Sofia, G.; Micol, T.; Bonamico, R. "Determining the Rotational Period of Main-Belt Asteroids 3704 Gaoshiqi and (16905) 1998 DT21" 234-235.
- Miftah, M.A.; Ferrais, M.; Moulane, Y.; Jehin, E.; Jabiri, A.; Benkhaldoun, Z. "Rotation Periods for Five Near-Earth Asteroids with the TRAPPIST Telescopes: (17188) 1999 WC2, (242450) 2004 QY2, (503871) 2000 SL, 2023 DZ2 and 2023 CM" 76-78.
- Mohoto, M.; Montgomery, K. "Lightcurve and Rotation Periods of Four Asteroids" 93-95.
- Pereira, W.; Arcoverde, P.; Evangelista-Santana, M.; Michimani, J.; Rondón, E.; Monteiro, F.; Mesquita, W.; Córrea, T.; Souza, R.; Rodrigues, T.; Lazzaro, D. "Photometry and Lightcurve Analysis of Eight Near-Earth Asteroids" 72-76.
- Pilcher, F. "Minor Planets at Unusually Favorable Elongations in 2024" 79-81.
- Pilcher, F. "Call for Observations" 97.

- Pilcher, F. "General Report of Position Observations by the ALPO Minor Planets Section for the Year 2023" 210-211.
- Pilcher, F. "An Appeal for Photometric Observations of 887 Alinda" 303.
- Pilcher, F. "Lightcurves and Rotation Periods of 903 Nealley, 1051 Merope, and 1187 Afra" 19-21.
- Pilcher, F. "The Rotation Period of 717 Wisibada Could Not Be Found" 95-97.
- Pilcher, F. "Lightcurves and Rotation Periods of 738 Alagasta and 1011 Laodamia, and a Note on 991 McDonalda" 104-106.
- Pilcher, F. "Lightcurves and Rotational Periods of 57 Mnemosyne, 58 Concordia, and 78 Diana" 235-236.
- Pilcher, F. "Lightcurves and Rotation Periods of 49 Pales, 62 Erato, 901 Brunzia, 995 Sternberga, and 1114 Lorraine" 338-341.
- Pilcher, F.; Stephens, R.D. "The Rotation Period of 740 Cantabria is Re-Examined" 217-218.
- Pilcher, F.; Delgado Casal, J. "Lightcurve and Rotation Period of 358 Apollonia" 98.
- Pilcher, F.; Franco, L.; Aceti, P.; Banfi, M.; Baj, G.; Marchini, A. "A Photometric Investigation of 526 Jena" 103-104.
- Pilcher, F.; Hawley, W.; Wiggins, P.; Leyland, P.C.; McCormick, J.; Genebriera, J.; Armstrong, J.D.; Kardasis, E.; Arnold, S.; Haymes, T.; Privett, G.J.; Noschese, A.; Catapano, A.; Di Dato, A.; D'Avino, L. "Lightcurve and Rotation Period of 703 Noemi" 215-216.
- Pilcher, F.; Benishek, V.; Oey, J.; Franco, L.; Ruocco, N.; Marchini, A. "The Ambiguous Rotation Period of 805 Hormuthia is Solved by a Global Collaboration of Observers" 219-220.
- Pilcher, F.; Delgado Casal, J.; Oey, J. "Lightcurve and Rotation Period of 1238 Predappia" 302-303.
- Polakis, T. "Photometric Results for Ten Minor Planets" 49-53.
- Polakis, T. "Photometric Observations of Thirteen Minor Planets" 264-268.
- Polakis, T. "Photometric Observations of Ten Minor Planets" 341-344.
- Polakis, T.; Wiles, M. "Photometric Results for Twenty Minor Planets" 126-132.
- Romanishin, W. "300 Geraldina: Possibly a Binary with a Tilted Rotational Axis" 213-214.
- Romanishin, W. "Timing Lightcurve Minima to Look for Candidate Close Binary Asteroids" 372-373.
- Slivan, S.M.; Barrera, K.; Colclasure, A.M.; Cusson, E.M.; Larsen, S.S.; McLellan-Cassivi, C.J.; Moulder, S.A.; Nair, P.R.; Namphy, P.D.; Neto, O.S.; Noto, M.I.; Redden, M.S.; Rhodes, S.J.; Youssef, S.A. "Lightcurves and Derived Results for Koronis Family Member (5139) Rumoi, Including a Discussion of Measurements for Epochs Analysis" 6-10.
- Slivan, S.M.; Barrera, K.; Colclasure, A.M.; Cusson, E.M.; Larsen, S.S.; McLellan-Cassivi, C.J.; Moulder, S.A.; Nair, P.R.; Namphy, P.D.; Neto, O.S.; Noto, M.I.; Redden, M.S.; Rhodes, S.J.; Youssef, S.A. "Lightcurves and Derived Results for Koronis Family Member (452) Hamiltonia" 176-179.
- Slivan, S.M.; Sindoni, J.; Wilkin, F.P. "Lightcurves and Solar Phase Coefficients for Koronis Family Member (1725) CrAO from Union College Observatory" 225-226.
- Slivan, S.M.; Berne, A.D.; Brennan, M.P.; Ekelmann, J.R.; Gray, L.C.; Jackson, E.H.; Rajesh, P.A.; Sheffield, E.M. "Rotation Period of Koronis Family Member (2811) Štřemchovi, Including a Discussion of Period Error Estimation" 304-305.
- Stone, G. "Lightcurves and Rotation Periods of 1292 Luce, 1340 Yvette, 2738 Viracocha, 2841 Puijo, 4362 Carlisle, and 9911 Quantz" 3-5.
- Stone, G. "Lightcurves and Rotation Periods of Asteroids 1861 Komensky, 2096 Vaino, 3127 Bagration, 3289 Mitani, 3582 Cyrano, 3589 Loyola, 3811 Karma, 4226 Damiaan, 4458 Oizumi, 6086 Vrchlicky, 6875 Golgi, (18118) 2000 NB24 and 29185 Reich" 112-116.
- Stone, G. "Lightcurves and Rotation Periods of Asteroids 1033 Simona, 3100 Zimmerman, 4026 Beet, 10707 Prunariu, 13039 Awashima, 15817 Lucianotesi, 17855 Geffert, and (29826) 1999 DW6" 248-250.
- Warner, B.D. "Asteroid-Deepsky Appulses in 2024" 82.
- Warner, B.D. "Asteroid-Deepsky Appulses in 2025" 371.
- Warner, B.D. "A New Optional Table and Updated MS WORD© Templates for MPB Papers" 209-210.
- Warner, B.D. "Hungaria Asteroid 6859 Datemasamune: A Split Decision" 356-363.
- Warner, B.D. "Asteroid Lightcurve Analysis at the Center for Solar System Studies Palmer Divide Station:"
- | | |
|--------------------------|----------|
| 2023 July – October | 22- 30. |
| 2023 September – October | 182-184. |
| 2024 January | 275-276. |
| 2024 April – June | 345-355. |
- Warner, B.D.; Harris, A.W.; Ďurech, J.; Benner, L.A.M. "Lightcurve Photometry Opportunities:"
- | | |
|-----------------------------|----------|
| 2024 January – March | 83- 86. |
| 2024 April – June | 202-205. |
| 2024 July – September | 293-297. |
| 2024 October – 2025 January | 379-384. |
- Weber, C.; Mánek, J.; Dramonis, S.; Meister, S.; Schweizer, A.; Antuszewicz, D.; Kubánek, J.; Rottenborn, M. "Satellite of 5457 Queen's Discovery and Confirmation by Two Stellar Occultations" 197-201.
- Wiles, M. "Photometric Observations and Rotation Period Determination for 14 Minor Planets" 138-142.
- Wiles, M. "Rotational Period and Lightcurve Determination for Seven Minor Planets" 330-332.
- Wilkin, F.P.; Maier, J.J. "Synodic Rotation Period for Koronis Family Object (452) Hamiltonia" 174-175.

Wilkin, F.P.; Castro, E.; Magno, M.; Petruskas, R., Zora, D.V. "Lightcurves for Three Koronis Family Asteroids" 180-181.

Wright, G.; Doud, H.; Crowley, E.M.; Wilkin, F.P. "Photometric Analysis for Koronis Family Asteroid (993) Moultona" 223.

Zari, S.; Montgomery, K. "Rotation Periods of Three Asteroids Through Differential Photometry" 89-90.

Zora, D.-V.; Ramos, D.; Wilkin, F.P. "Lightcurve for Koronis Family Member (1482) Sebastiana" 299-300.

IN THIS ISSUE

This list gives those asteroids in this issue for which physical observations (excluding astrometric only) were made. This includes lightcurves, color index, and H-G determinations, etc. In some cases, no specific results are reported due to a lack of or poor-quality data. The page number is for the first page of the paper mentioning the asteroid. EP is the "go to page" value in the electronic version.

NumberName	Page	EP
49 Pales	40	338
57 Mnemosyne	18	316
62 Erato	40	338
191 Kolga	18	316
236 Honoria	18	316
435 Ella	21	319
470 Kilia	43	341
477 Italia	11	309
612 Veronika	35	333
625 Xenia	43	341
793 Arizona	43	341
796 Sarita	43	341
858 El Djezair	26	324
858 El Djezair	43	341
887 Alinda	5	303
901 Brunsia	40	338
904 Rockefellia	43	341
995 Sternberga	40	338
1105 Fragaria	21	319
1114 Lorraine	40	338
1238 Predappia	4	302
1248 Jugurtha	21	319

NumberName	Page	EP
1243 Pamela	43	341
1285 Julietta	26	324
1285 Julietta	32	330
1417 Walinska	2	300
1428 Mombasa	18	316
1482 Sebastiana	1	299
1532 Inari	8	306
1532 Inari	18	316
1532 Inari	35	333
1556 Wingolfia	26	324
1600 Vysotsky	47	345
1602 Indiana	10	308
1614 Goldschmidt	18	316
1727 Mette	47	345
1911 Schubart	26	324
1920 Sarmiento	47	345
1965 van de Kamp	26	324
1965 van de Kamp	32	330
2049 Grietje	47	345
2085 Henan	26	324
2150 Nyctimene	47	345
2240 Tsai	35	333
2343 Siding Spring	21	319
2383 Bradley	43	341
2410 Morrison	26	324
2811 Stremchovi	6	304
2830 Greenwich	43	341
3089 Oujianquan	26	324
3761 Romanskaya	43	341
4288 Tokyotech	35	333
4297 Eichhorn	26	324
4446 Carolyn	47	345
4460 Bihoro	32	330
4764 Joneberhart	47	345
4765 Wasserburg	47	345
4868 Knushevia	47	345

NumberName	Page	EP
5167 Joe harms	16	314
5430 Luu	32	330
5627 Short	47	345
5947 Bonnie	32	330
5967 Edithlevy	47	345
6296 Cleveland	47	345
6663 Tatabayashi	26	324
6663 Tatabayashi	32	330
6859 Datemasamune	58	356
7055 Fabiopagan	21	319
7309 Shinkawakami	26	324
7851 Azumino	17	315
8024 Robertwhite	47	345
9333 Hiraimasa	35	333
12867 Joeloic	75	373
13042 1990 QE	35	333
16405 Testudo	13	311
18890 2000 EV26	47	345
20936 Nemrut Dagi	47	345
21374 1997 WS22	11	309
26187 1996 XA27	35	333
32153 Laurenmcgraw	80	378
40203 1998 SP27	47	345
52316 Daveslater	47	345
55964 1998 KB2	47	345
78857 2003 QO70	47	345
381677 2009 BJ81	32	330
415029 2011 UL21	14	312
2010 QG2	65	363
2018 XS4	65	363
2024 KP	65	363
2024 HK1	65	363
2024 LZ4	65	363
2024 GZ5	65	363

THE MINOR PLANET BULLETIN (ISSN 1052-8091) is the quarterly journal of the Minor Planets Section of the Association of Lunar and Planetary Observers (ALPO, <http://www.alpo-astronomy.org>). Current and most recent issues of the *MPB* are available on line, free of charge from:

<https://mpbulletin.org/>

The Minor Planets Section is directed by its Coordinator, Prof. Frederick Pilcher, 4438 Organ Mesa Loop, Las Cruces, NM 88011 USA (fpilcher35@gmail.com). Robert Stephens (rstephens@foxandstephens.com) serves as Associate Coordinator. Dr. Alan W. Harris (MoreData! Inc.; harrisaw@colorado.edu), and Dr. Petr Pravec (Ondrejov Observatory; ppravec@asu.cas.cz) serve as Scientific Advisors. The Asteroid Photometry Coordinator is Brian D. Warner (Center for Solar System Studies), Palmer Divide Observatory, 446 Sycamore Ave., Eaton, CO 80615 USA (brian@MinorPlanetObserver.com).

The *Minor Planet Bulletin* is edited by Professor Richard P. Binzel, MIT 54-410, 77 Massachusetts Ave, Cambridge, MA 02139 USA (rpb@mit.edu). Brian D. Warner (address above) is Associate Editor. Assistant Editors are Dr. David Polishook, Department of Earth and Planetary Sciences, Weizmann Institute of Science (david.polishook@weizmann.ac.il) and Dr. Melissa Hayes-Gehrke, Department of Astronomy, University of Maryland (mhayesge@umd.edu). The *MPB* is produced by Dr. Pedro A. Valdés Sada (psada2@ix.netcom.com).

Effective with Volume 50, the *Minor Planet Bulletin* is an electronic-only journal; print subscriptions are no longer available. In addition to the free electronic download of the *MPB* as noted above, electronic retrieval of all *Minor Planet Bulletin* articles (back to Volume 1, Issue Number 1) is available through the Astrophysical Data System:

<http://www.adsabs.harvard.edu/>

Authors should submit their manuscripts by electronic mail (rpb@mit.edu). Author instructions and a Microsoft Word template document are available at the web page given above. All materials must arrive by the deadline for each issue. Visual photometry observations, positional observations, any type of observation not covered above, and general information requests should be sent to the Coordinator.

* * * * *

The deadline for the next issue (52-1) is October 15, 2024. The deadline for issue 52-2 is January 15, 2025.